STUDY ON PHYSICAL AND CHEMICAL CLOGGING PHENOMENA DURING ARTIFICIAL RECHARGE OF GROUNDWATER

Claudia HARTWIG

September, 2013

Graduate School of Environmental Science

OKAYAMA UNIVERSITY

STUDY ON PHYSICAL AND CHEMICAL CLOGGING PHENOMENA DURING ARTIFICIAL RECHARGE OF GROUNDWATER

By

Dipl.-Ing. Claudia HARTWIG (# 74422352)

A thesis submitted in partial fulfillment of the requirements for

DOCTOR OF PHILOSOPHY DEGREE

at the

GRADUATE SCHOOL OF ENVIRONMENTAL SCIENCE

of the

OKAYAMA UNIVERSITY, JAPAN

September, 2013

Approvals of Thesis Committee Members:

_____

Professor Makoto NISHIGAKI (Chairman)

_____

Associate Professor Mitsuru KOMATSU

_____

Associate Professor Shigeyuki SUZUKI

SUMMARY

For more than half of the world`s population, groundwater is the main water supply. Groundwater is a renewable resource but its natural recharge strongly dependents on local climate and soil-aquifer characteristics. Human interference with groundwater causes serious problems such as overexploitation, salt-water intrusion, or land-subsidence. In order to augment the groundwater resources, artificial recharge is a general practice. Furthermore, because the aquifer temperature is almost constant over the year, groundwater is a good resource for open loop groundwater heat pumps. Groundwater heat pumps consist of two wells, one pumping well and one injection well. The pumped water can be used for heating or cooling of a building and is then injected back into the aquifer. Nevertheless, clogging is the primary problem for the injection of water into an aquifer. Clogging can be understood as the blockage of the flow pathways due to chemical, biological and/or physical processes. The focuses of this study rely on chemical and physical clogging. Chemical clogging can be caused by precipitated metabolic products of bacteria including iron hydroxide, ferrous bicarbonate, manganese, metallic sulfide, or calcium carbonate reaction of high sodium water with soil particles causing de-flocculation and swelling of the soil (clay) particles. Physical clogging can be separated into two groups. One, is clogging because of suspended particles contained in the injection water, and the other one is considering fine particles in the aquifer getting mobilized during the injection process. The latter is rarely investigated because of the difficulty of the processes. The mobilization of small particles depends mainly on the infiltration velocity, thus on the hydraulic gradient.

Literature review has shown that many artificial recharge projects are successfully in practice, but most of them are recharge basins. In case of deep injection wells, clogging occurrence has often reported as a main disadvantage. In the United States and Europe, groundwater heat pump systems are mainly in practice. Great Britain already has developed an online available system, were appropriate places for closed or open loop systems can be investigated with information on the geology and aquifers.

To date, studies on physical clogging were conducted almost considering suspended particles in the recharge water. However, research on particle mobilization of soil particles initially present in the aquifer should not be neglected, especially its influence it is not well known. During recharge, these particles getting mobilized due to injection velocity and will plug the flow pathways. In order to combat the physical clogging because of particle mobilization, characterization of a critical hydraulic gradient or rather to say a critical velocity should be determined which can be found in the

literature considering piping effect of earth fill dams. Regarding chemical clogging techniques for iron removal are widely available. Nevertheless, these methods are expensive and also including oxygenation of the water, what can also lead to clogging during injection because of precipitation of iron in the aquifer due to high oxygen concentrations in the injecting water. Because open-loop heat pump systems have a high advantage because of the higher efficiency comparing to closed loop systems, and also deep injection wells are more efficient than recharge basins, injecting groundwater under low-cost and easy maintenance has to be investigated, therefore, clogging is depicted as a worldwide issue under maintaining groundwater.

In this research, investigations in physical and chemical clogging were carried out. Regarding to physical clogging, one- dimensional column experiments were conducted in order to clarify the particle mobilization under different hydraulic gradients. Furthermore, a previous two- dimensional study on particle movement conducted by Takuya Tanaka, was used for comparison with one- dimensional results and also the applicability of research regarding piping and field conditions was evaluated.

Regarding to chemical clogging, the adsorption ability of dissolved iron ions for cheap and eco-friendly filter materials: charcoal, fine sand (Yamasuna) and volcanic ash was investigated. In an additional field test, with wooden charcoal and layers of gravel, middle and fine sand at the inlet and the outlet, filled pilot filter was tested under realistic operational conditions. The treated water was then used to lower the temperature in a room of 18.9 m^2 and was re-injected into the aquifer.

In addition, wooden charcoal is thought to be a good fertilizer for agricultural usage; however, the survival of plants is firstly strongly depending on phosphate availability in the soil. In order to investigate the plant survival strategies, a study was carried out using different *Brassica* cultivars, which are known to survive even in low-P soils. Phosphate (Pi) influences virtually all developmental and biochemical processes in plants; however, its availability and distribution are widely heterogeneous. However, even total P is abundant in the lithosphere; elusive soil chemistry of Pi renders the element the most dilute and the least mobile in natural and agricultural ecosystems, resulting in P deprivation due to its low mobility and high fixation capacity in the soil. Using a soil low in P (Mehlich 3–extractable P) with or without P fertilization, the P-utilization efficiency (PUE), P efficiency (PE), P-efficiency ratio (PER), and P-stress factor (PSF) were investigated.

In this study the following results were obtained:

(1) Wooden charcoal showed the best adsorption capacity and thus, is applicable for dissolved iron ion removal from groundwater.

(2) In the one-dimensional experiments, the results showed, that not only fine particles are (≦0.106 mm) mobilized during injection, but also particles between 0.25 – 2 mm showed a movement. Especially for the higher hydraulic gradient (i = 0.3) bigger particle sizes were mobilized.

(3) From the two-dimensional aquifer model, it was obtained that it is possible to apply research on piping effect to physical clogging due to particle mobilization problems.

(4) Two dimensional experiments give more realistic results and are more capable for field application.

(5) In comparison to the Ferrolite MC3 filter, which was able to adsorb dissolved iron from 1890 m^3 of groundwater and the wooden charcoal on-site filter, the Ferrolite MC3 filter showed an adsorption capacity of 6.17 g/L material, whereas the wooden charcoal showed a higher performance in the field experiment than in the column studies and thus if the field wooden charcoal filter is taken into account, an adsorption capacity of 2.2 – 3.3 g/L material is possible, which means a 36 % – 53 % efficiency of the Ferrolite MC3 filter.

(6) *Brassica* cultivars presented considerable genetic variability and differential growth potential in accessing, mobilizing, acquiring, and efficiently using P in a low-P environment.

Conclusions drawn from the research have shown that it is possible to connect different research areas together in order to conduct sustainable environmental development. A relation between studies on piping and physical clogging regarding particle mobilization could be testified. A new efficient eco- friendly and cost efficient filter material for iron removal was proposed, which may be applicable in developing countries, as well. In order to investigate the charcoal being efficient as fertilizer after iron adsorption, different conditions according to plant analysis have to be taken into account for basic knowledge. Since the most problems occur in developing countries, cost efficient, easy in maintenance, and eco-friendly techniques are required for artificial recharge techniques and also open-loop groundwater heat pump applications.

ACKNOWLEDGEMENT

"A person who never made a mistake never tried anything new."

–Albert Einstein

It is 6 years ago, when I came the first time to Japan as an exchange student from Dresden University of Technology. When somebody would have told me at that time what I would do 6 years later and where I would be and whom I would be, I probably would have called him crazy. I entered the Geo-environmental evaluation Laboratory at Okayama University and met Professor Nishigaki right after my landing on the 2nd of October in 2007 and from then on he was always being so kind supporting me when I had problems helping with getting along to Japanese life, get the opportunity to try really delicious Japanese food and sake, and also discussions with him about his projects and deep knowledge and experience was very exciting and enjoying. During my year as an exchange student I had the opportunity to learn Japanese language, get to know Japanese culture and the country. Besides that, I could stay in this laboratory, and for the first time I got in contact with real research work since in Germany, we don't have laboratories for students, and we just go to lectures every day. I got so many interested in doing research that I forced myself to use the opportunity to do some own research. The first steps were quite difficult and hard, and I don't remember how many times I was furious about something, what didn't work out how I wanted. But I met some really helpful people here in Japan.

Every time when I don't know what is coming next, and when I think there is a wall I can't go through, I think about my grandfather, who died some years ago; he always treated me very hard, was angry when I had bad grades in school, that time I didn't like him very much because of that. But at the time he died I already entered university, and I struggled hard to get my degree and fulfill the requirements of passing the examinations. But the imagination of my grandfather being there, somewhere around me, make me feel that I want to make him proud of me, I want to show him that, despite everything happened, I will fight for my dreams to become true, and go through good and bad times along may way, without giving up. So, every time when I think there is no way through, I remember him and somehow from somewhere I can get the power to fight. Because when I something learned in my life, nothing is for free, you always have to say and sometimes also to fight for that what you want. So my first special thanks are going to my grandfather for always being there and watching me, and giving me the power I need some time. I hope I could make you proud by coming this way.

A person who always was there for me and treated me like a father is the man without his help I would not be here now, Professor Makoto Nishigaki. I owe him so much for supporting me from the first day on, here in Japan and always being kind and patient to me. And I'm pretty sure that it was not easy with me all the time. He was also very helpful every time with my studies and taught me how do scientific work and how to present it.

I'm also thankful to Associate Professor Komatsu and Associate Professor Suzuki who were my co-supervisors, as well as a member of the thesis committee, for their constructive criticism.

I also wish to thank the Japanese Government for awarding me the Monbukagakusho scholarship, which was a great honor to me, to support my studies at Okayama University, Japan. I also acknowledge the scholarship from the Yakumo Foundation for Environmental Science for supporting my staying in Canada at the 39th IAH Congress in Niagara Falls.

Also, my special thanks go to John Apambilla Akudago and Larry Pax Chegbeleh, whom I met during my stay from 2007 until 2008. They were very good "senpais" in the lab and were always there for me like big brothers. They showed me what it is to be a researcher and infected me with their ambition.

Many thanks also go to Ray Ruemenapp, who accompanied me and my research for one year, he supported me so much, and discussions with him were always very effective.

I also would like to thank Yoshida-san, who helped and supported me so many in the field. I appreciate his help so much, I profited from his extraordinary knowledge and experience in field work. He was also showing me the beautiful countryside of Okayama prefecture. Thank you so much!

To my laboratory mates such as Kazuki Hagiwara, Keita Imanishi, Keiji Jyoujima, Tomoko Ninomiya and Ryuta Hamamoto thanks for being my friends helping me in the laboratory and having a great time. I hope we will meet sometimes somewhere again. To Abe-san, you have been always there helping me with the paperwork and preparing the staying of the new German exchange students. I enjoyed my time in total 4 and a half years staying in this lab, studying, doing experiments, having parties, sleeping, eating, cooking, and drinking, and so on. I will never forget this important time in my life, and I hope to see you again somewhere and sometime. 皆様本当にありがとうございました。

I also wish to thank my family; I know that my decision going to Japan was not very comfortable for you all. But I thank you so much for supporting me choosing may way

and always caring about me when I came home. Even when thousands of kilometers are between us, with my heart and thoughts I'm always there, and today's technology makes it possible to see and hear each other any time.

The last very special thanks are going to the most important person to me, my fiancé. Thank you for your support, advices and also just being there, at my side, every time. You were always my bridge over troubled waters. Thank you so much, without you I truly can say, I wouldn't have been able to come this far. 過去は過去だ, 後ろを振り返らないで前を見て一緒に進もう!

TABLE OF CONTENTS

LIST OF FIGURES

LIST OF TABLES

CHAPTER 1

RESEARCH BACKGROUND

1.1 INTRODUCTION

Water is the world`s and its residents most essential resource. However, only 35 million km^3 freshwater (2.5 % of total water on earth) is available, of which 30 % are stored as groundwater in the subsurface (UNEP). Ambient readily available groundwater is the safest source for domestic, agricultural and industrial utilization.Groundwater is less vulnerable to environmental influences because of its location in the subsurface. Nevertheless, groundwater availability is of high influence of natural recharge rates, population growth, soil contamination and/ or agricultural production. Hence, two upcoming global problems: climate change and population growth are the primary causes for groundwater depletion.

Climate change is variation of climate over time in local and global scale. For example, seasons may vary in their occurrence during the year; experts agree in regional growing tendency of high intense precipitation events and longer dry seasons (Kundzewicz et al. 2007). However, it has to be considered that not every region will experience the same changes, depending on the climate zone and conditions, the changes also differ. However, the trend set on precipitation changes whether decrease or increase, the increasing number of disasters (Wilhelmi and Morss 2013, Yu et al. 2010) during the past years due to precipitation changes have shown that water management is of high importance for a future sustainable environment. Precipitation is a main part of the water cycle next to run-off and evaporation. Being an input to the cycle, its formations will have an impact on local groundwater resources. After precipitation reached the ground surface, it infiltrates into the subsurface. Water which cannot infiltrate due to the slope or exceeded infiltration capacity flows as overland flow to surface water basins. Water that infiltrates into the underground can either flow through the unsaturated zone, parallel to the ground surface as interflow, from where it may reach the surface, move directly to surface water basins, or reach the groundwater table and recharge the aquifer. Hence, if the input source precipitation changes in its quality and / or quantity, natural groundwater recharge may also change.

In 2012, the world counted over 7 billion people who are living on earth, and it is expected that the world's population will grow up to 9.6 billion until the year 2050 (Population Reference Bureau 2012). Figure 1.1 shows the growing population until 2100 compared to 1950 for different continents. As it is evident from Figure 1, the

highest population growth will occur in developing countries. The population increase will result in urbanization and water demand increase. This may have tremendous impacts on the groundwater resource. Available areas for water infiltration into the subsurface will decrease,due to urbanization ; thus, natural groundwater decreases more and more.

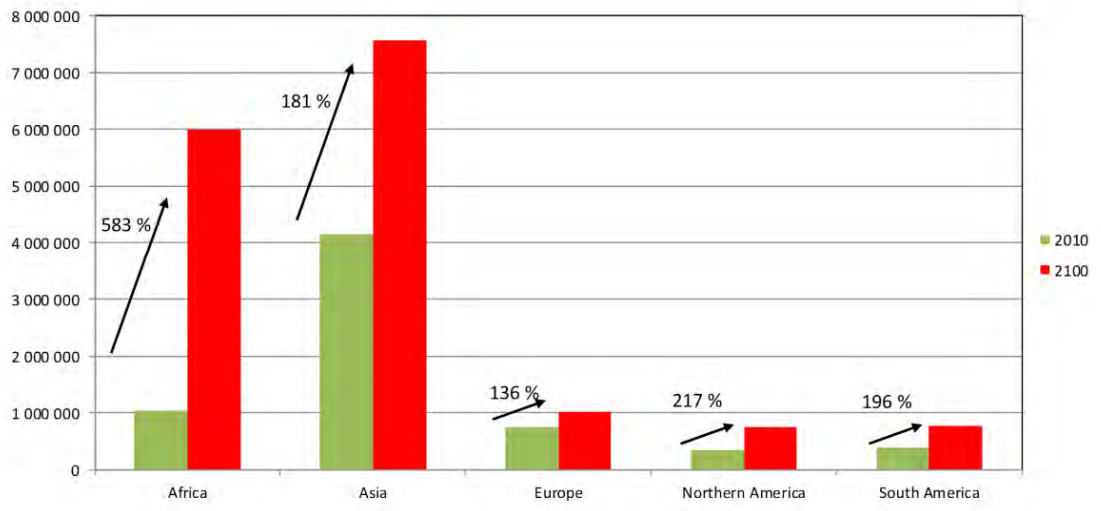

Figure 1.1－Total population by primary area for 2010 and 2100 (thousands) under high fertility scenario (source: United Nations 2013).

When population is increasing, therefore, the energy demand also increases. However, as the energy demand increases, the current available energy resources decreases. The primary usage grew by 45 % over the past 20 years, and is expected to increase by 39 % over the next 20 years (BP Statistical Review of World Energy 2009). At the moment, about 95 % of thermal heat is made of fossil fuel burning. To reduce the primary energy demand, a heat pump system can be used. Such a system uses three quarters of energy from the underground, groundwater, or air. Only one quarter of electric energy is used for operating power. For installing, such a groundwater heat pump two wells are needed; one is for water pumping and the other one for reinjecting of the water. Referring to the sources of energy production, petroleum (34.8 %), natural gas (24.1 %), and coal (29.2 %) are mainly used. Nuclear energy has a proportion of 5.5 %. Regarding to fossil fuel the problem is one, that the resources are limited, and two, in times of global warming, environmental problems have to be considered. Because of making efforts in CO_2 mitigation, renewable energy (wind power, hydro power, solar, etc.) and recycling energy (biomass) should be considered for the future.

Nevertheless, every type comes with problems, such as unstable supply, changes in the environment or pollution. In case of Japan, heat power and nuclear power are the most important energy sources. As useful nuclear power is, it implicates a lot of problems like safety, treatment of nuclear waste, and also social acceptance problems. The Fukushima disaster in Japan in 2011, and also former disasters, for example, Chernobyl in 1986, have shown that nuclear power is under eligible criticism. On the other hand, there are advantages such as the possibility to generate a large amount of energy, no CO_2 emission and reuse of fuel.

1.1.1 Geothermal Heat Pump Systems

Geothermal heat is thermal energy stored in the upper parts of the earth crust. In general, this heat is influenced by the sun, which influences until a depth of about 15 m, or by the heat flow from the earth core to the surface. Depending on the area, below the influence area of the sun, the temperature increases with depth, for instance in for Japan the geothermal gradient is shown in Figure 1.2.

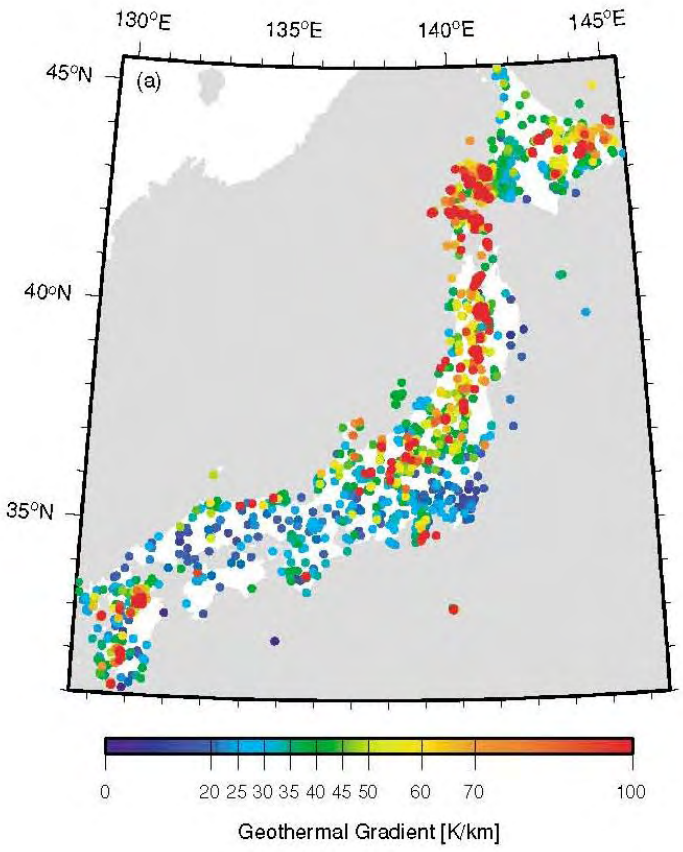

Figure 1.2－Geothermal gradient for Japan after Tanaka et al. (2004).

Geothermal systems are applied in order to use the heat source for cooling, heating or also to produce energy. Geothermal heat pump systems can be divided into two Categories: open-loop and closed systems. In every case, the carrier fluid with the absorbed heat or the direct water source is connected to a heat pump (Figure 1.3) from where the heat will be distributed through the object intended for heating or cooling. Figure 1.3 shows a heat pump in warming mode. The heat will be transferred through the refrigerant (in case of open loop: groundwater) to the heat pump cycle (① in Figure 1.3). The warm fluid passes the compressor (③in Figure 1.3) which is driven by a motor. The motor is the only apparatus which needs electrical energy supply. In the compressor, mechanical work is applied to the fluid resulting in pressure increase (from around 5 bar up til 17 bar), temperature rise and the condition of aggregation turns into the gas phase. The heated steam continues the cycle until point ⑤ in Figure 1.3. There, the thermal energy enters the next cycle, the heating circuit. Usually water is used as a carrier fluid. The water absorbs the thermal energy from the heat pump circuit and carries it through the circle. The Contributor (⑨ in Figure 1.3) finally delivers the hot water in the rooms were the heating devices (⑩ in Figure 1.3) releases the thermal energy into the rooms for heating. Because the thermal energy is released to air, the water temperature decreases (⑪ in Figure 1.3) and the fluid enters the circle again. In summer, the heat pump operates in reversible direction for cooling mode. In this case, the higher temperatures in the rooms will be absorbed and carried into the ground and cool temperatures from the ground distributed into the rooms.

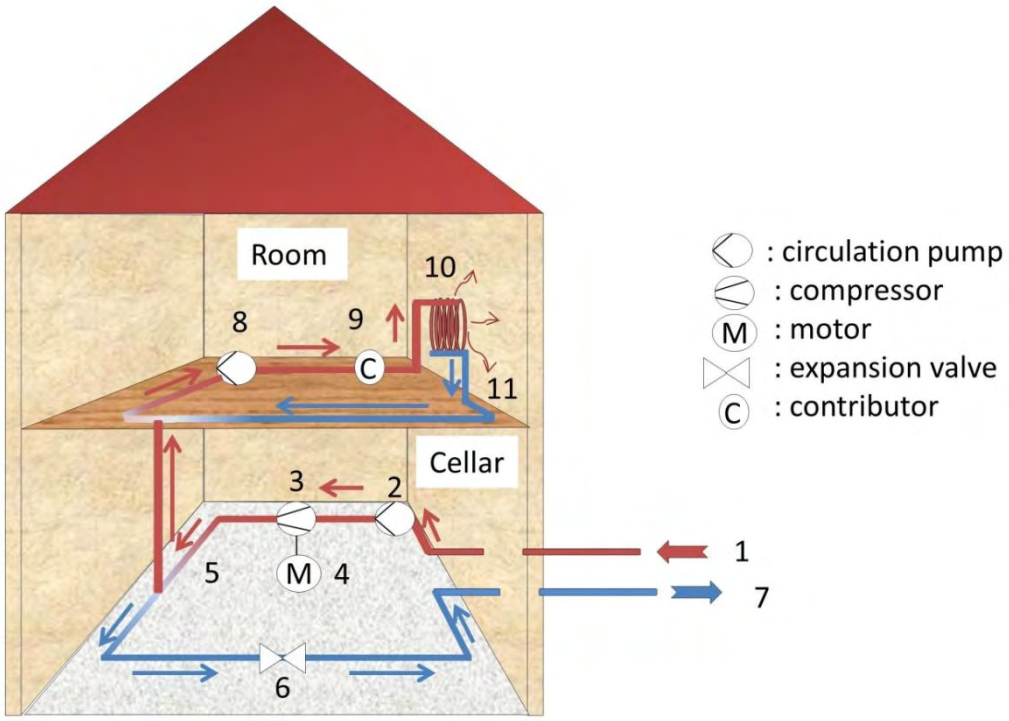

① Thermal heat comes from the ground source

② A circulation pump, distributes the fluid through the cycle

③ In the compressor, the fluid will be turned into the gas phase by means of mechanical work

④ The motor drives the compressor with electrical energy

⑤ The warm steam crosses over to the next cycle, from where the heat will be distributed to the rooms

⑥ The expansion valve takes the pressure, which was added in (3); thus, the steam turns back in fluid condition and is cooled down

⑦ The cooled down fluid will be distributed to the ground

⑧ In the second cycle water for heating cycles through the pipes, this water uses the thermal energy which crosses over at point 5 and is distributed through the cycle by a circulation pump

⑨ The contributor contributes the warm water to the various heating devices in the rooms

⑩ The heating device distributes thermal energy into the room

⑪ The cold down water goes back into the cycle

Figure 1.2－Schematic view of the heat pump cycle.

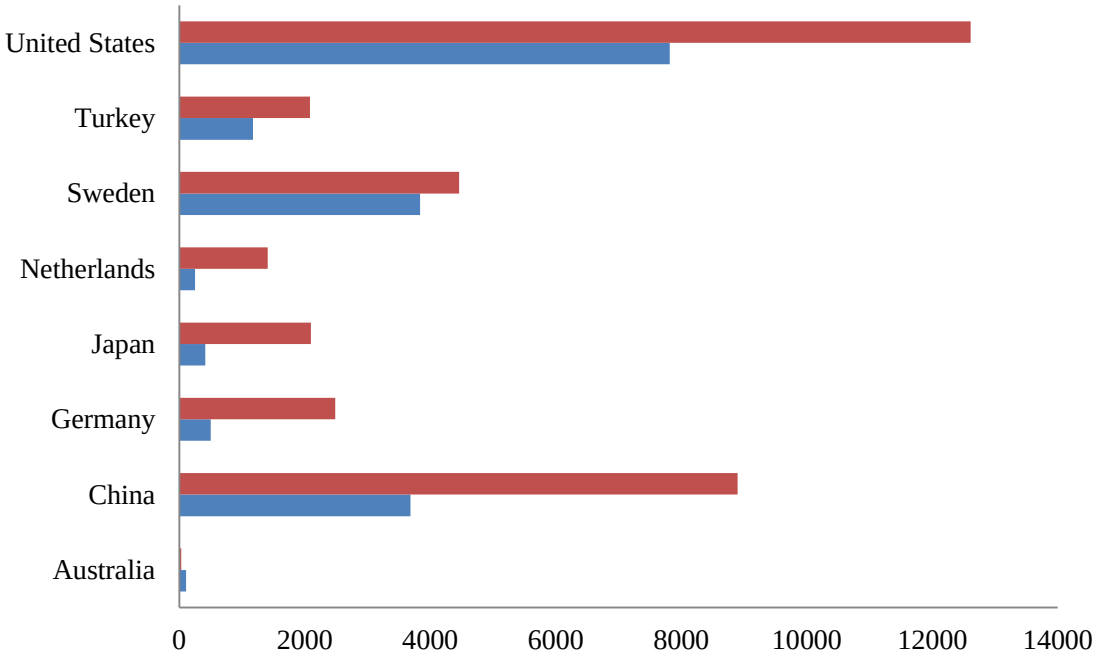

	Australia	China	Germany	Japan	Netherlands	Sweden	Turkey	United States
2010	33.33	8898	2485.4	2099.53	1410.26	4460	2084	12611.46
2005	109.5	3687	504.6	413.4	253.5	3840	1177	7817.4

Figure 1.4 Global installations of geothermal heat pumps, a comparison between 2005 and 2010. In 2005 worldwide 27825 geothermal energy plants were installed and in 2010 48483 plants (Lund et al. 2005, Lund et al. 2011)

1.1.1.1 Closed-loop systems

In closed-loop heat pump systems, a heat transfer fluid (refrigerant) (Huttrer 1997) circulates in horizontal or vertical high density polyethylene pipes and carries the absorbed heat to a heat pump. A vertical closed-loop heat pump is applied when the space is small. The depth of the boreholes ranges between 30 and 100 m (Huttrer 1997, Zeng et al. 2003, Hecht-Méndez et al. 2013). A schematic view of the vertical pipes is shown in Figure 1.5. As it is shown in Figure 1.5, the refrigerant circulates in a U-form pipe. In summer, time (Figure 1.5 (a)) the heat from the house will be distributed into the underground and cold temperatures will be extracted from the underground and used for cooling the house. In winter season, the thermal energy will be absorbed from the ground, passed through the heat pump and used for heating of the house.

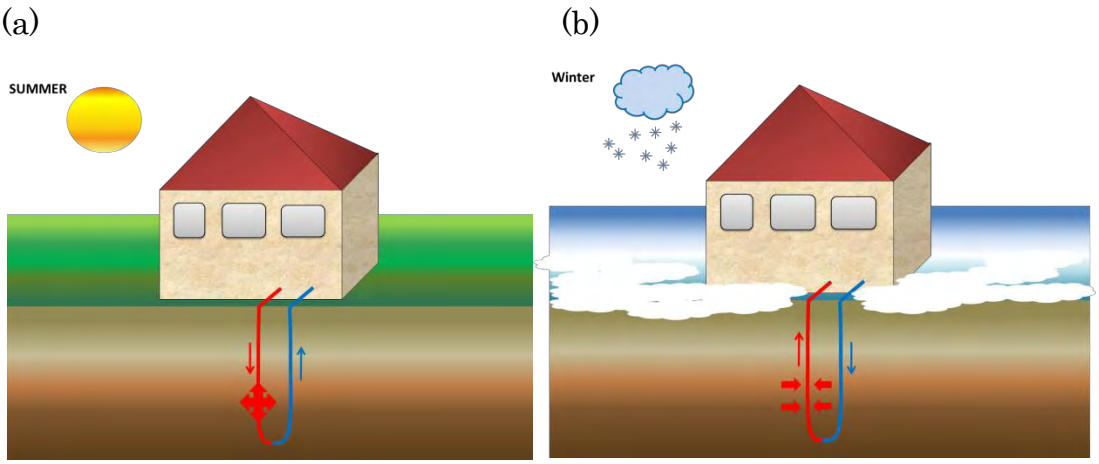

Figure 1.5－Vertical closed heat pump system (a) cooling in summer season; (b) heating in winter season.

The horizontal closed-loop systems require more space than the vertical system. For example in order to heat a house with 200 m^2 living space an area of 150 m^2 will be needed (Tarnawski et al. 2009). Depending on the area, burying of 1 or 2 m depth can be enough (Huttrer 1997, Lund et al. 2004). In many cases, this type of ground source heat pump is installed in public institutions, such as schools, where the property has enough space. It can be also considered for farmlands. Figure 1.6 shows such a vertical closed-loop system.

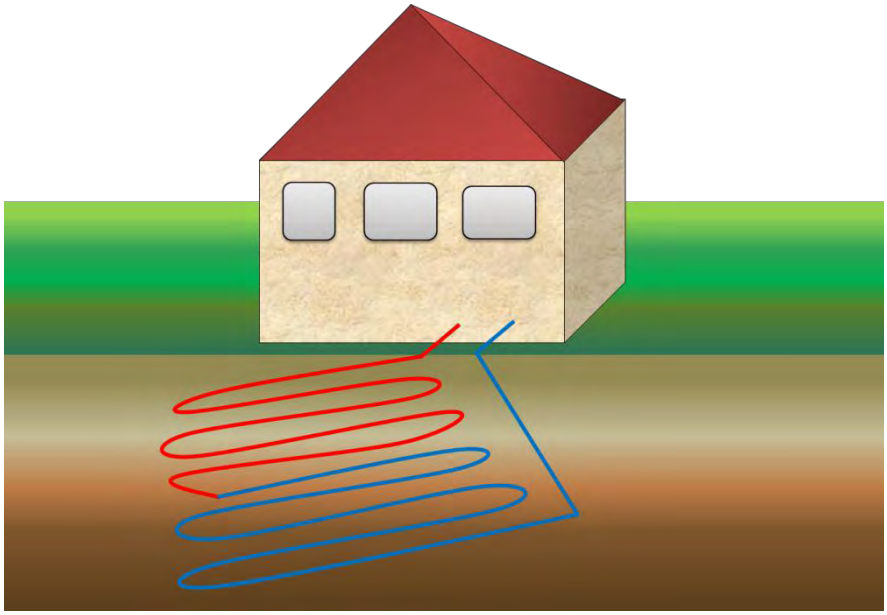

Figure 1.6－Horizontal closed heat pump system.

1.1.1.2 Open- loop system

For open- loop ground source, heat pumps no refrigerant is required for thermal energy absorption, here, the extracted groundwater will be the carrier fluid and thermal energy source at the same time. Groundwater has an almost constant temperature over the year (Figure 1.7) which makes the efficiency of this system high efficient.

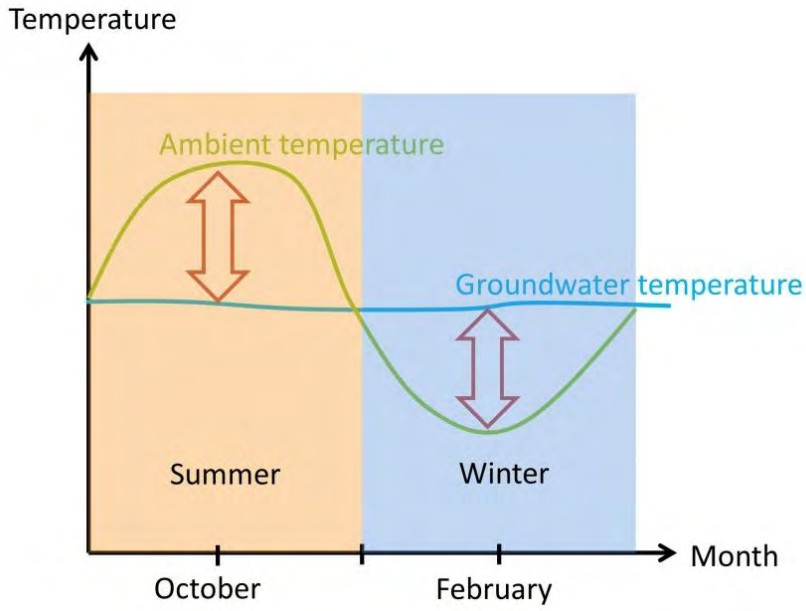

Figure 1.7－Relationship between groundwater temperature and ambient temperature over the year. In summer time, the groundwater temperature is appropriate for cooling and in winter time for heating.

The aim is to store the excess heat energy from the summer months that can then be used for heating buildings in the winter and vice versa. For the system, a cold well and a warm well will be created. In the summer months, water is extracted from the cold well and passed through a heat exchanger to provide direct cooling to the building. This process warms the water and will be rejected into the warm water well. The water will be stored in the aquifer until winter months; then water will be extracted from the warm water well. Here, the water will pass through the heat exchanger and to a heat pump in order to use it for the heating system of the building. In this case, the water temperature falls and will then returned through the cold well. Figure 1.8 (a) and (b) show the open-loop system for cooling and heating mode, respectively.

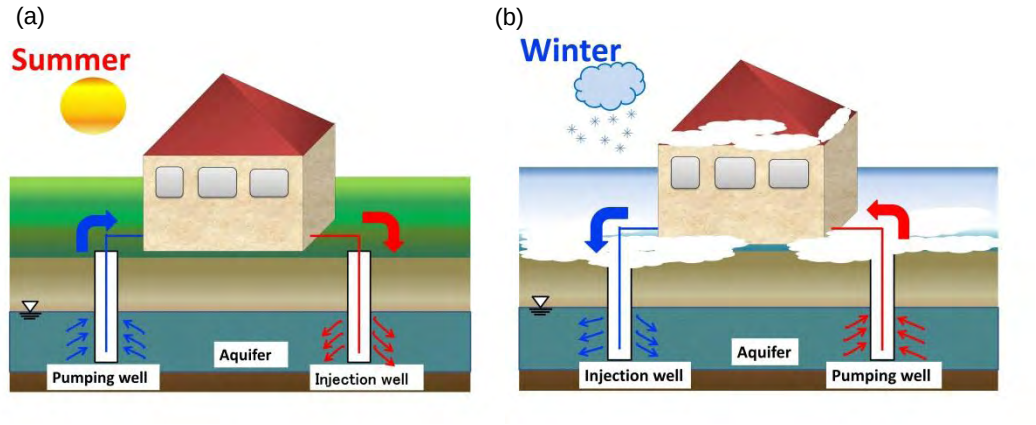

Figure 1.8－schematic view of the open-loop heat pump system for (a) the cooling mode in summer season, and (b) the heating mode in winter season.

However, when injecting water into an aquifer, clogging occurs. Clogging can be understood as the blockage of the flow pathways due to chemical, physical or biological processes. Clogging results in reduction of the permeability; thus, reduction in injection rate eventually makes the system ineffective, expensive and complicated in maintenance. The three clogging mechanisms are defined as follows:

(1) Biological clogging: clogging because of bacteria attach to the solid particle, cells grow, and the entire deposit is termed the biofilm (Trulear and Characklis 1982).

(2) Chemical clogging: clogging because of (i) precipitated metabolic products of bacteria including iron hydroxide, ferrous bicarbonate, metallic sulfide, or calcium carbonate; (ii)chemical interactions of the dissolved chemicals in the injected water and (iii) in the aquifer formation yielding precipitates, or solution and redeposition of soluble compounds (Appelo et al. 1999, Saaltink et al. 2003).

(3) Physical clogging: clogging because of the deposition and detachment of small particles during transport through the aquifer (Ahfir et al. 2009).

In this research, investigations were done in order to make open-loop groundwater heat pump systems and also aquifer recharge systems (deep well injection) more applicable, cost efficient, and less complex in maintenance. This study focuses on chemical and physical problem, whereas chemical clogging is related to anaerobe dissolved iron ion removal with a cheap and eco-friendly filter material, and physical clogging is concerned to the particle mobilization initially present in the aquifer during water injection. The biological clogging is neglected in this research because it is minimized when the injection water is on a “well-to-well” basis (Roscoe Moss

Company 1990). Furthermore, it is considered that the presence of high iron concentration is a major cause of both, chemical and biological clogging. Hence, a cost efficient filter material for dissolved iron removal without oxygen contact is the main purpose of this study.

1.2 THESIS LAYOUT

This thesis is divided into 5 chapters. Chapter 1 provides a brief introduction and objective of the research. Chapter 2 includes a literature review regarding mainly to physical and chemical clogging problems and methods of combating clogging. In this connection, the clogging issues are reviewed regarding aquifer recharge, open-loop heat pump systems, as well as physical and biological clogging mechanism.

Chapter 3 discusses experimental results regarding physical and chemical clogging. Here regarding physical clogging, one-dimensional experiments were carried out and compared to two-dimensional experiments conducted in a previous work in order to define a critical hydraulic gradient. Regarding chemical clogging charcoal was proposed as a new cheap filter material in order to remove iron from groundwater. The laboratory experimental results were tested in a field open-loop heat pump system at Okayama University, Japan.

Chapter 4 contains a study on Solubilization and Acquisition of Phosphorus from Sparingly Soluble Phosphorus Sources and Differential Growth Response of Brassica Cultivars Exposed to Phosphorus-Stress Environment. This study was conducted in order to understand the behavior of special cultivars under low phosphate conditions because the chemistry of phosphorus in the soil is known to be very elusive and is necessary for thinking of a sustainable environment, such as eco-friendly fertilizers for agricultural use.

The last chapter, Chapter 5, gives concluding remarks and recommendations and also deals with the designing of a charcoal filter.

REFERENCES

Ahfir, N.D., Benamar, A., Alem, A., and Wang, H.Q., 2009. Influence of Internal Structure and Medium Length on Transport and Deposition of Suspended Particles: A Laboratory Study. Transport in Porous Media 76, (2): 289–307.

Appelo, C.A.J., Drijver, B., Hekkenberg, R., and de Jonge, M., 1999. Modeling in situ iron removal from ground water. Ground Water 37, (6): 811–817.

BP Energy Outlook, 2030, URL: http://www.bp.com/liveassets/bp_internet/globalbp/globalbp_uk_english/reports_and_publications/statistical_energy_review_2008/STAGING/local_assets/2010_downloads/2030_energy_outlook_booklet.pdf: last access 2013.07.04.

Hecht-M., J., de Paly, M., Beck, M., and Bayer, P., 2013. Optimization of Energy Extraction for Vertical Closed-loop Geothermal Systems Considering Groundwater Flow. Energy Conversion and Management, 66: 1–10.

Huttrer, G.W., 1997. Geothermal Heat Pumps: An Increasingly Successful Technology. Renewable Energy , 10, (2–3): 481–488.

Kundzewicz, Z.W., Mata, L.J., Arnell, N.W., Döll, P., Kabat, P., Jiménez, B., Miller, K.A., Oki, T., Sen Z., and Shiklomanov, I.A., 2007. Freshwater resources and their management. Climate Change 2007: Impacts, Adaptation and Vulnerability, Contribution of Working Group II to the Fourth Assessment Report of the Intergovernmental Panel on Climate Change, M.L. Parry, O.F. Canziani, J.P. Palutikof, P.J. van der Linden and C.E. Hanson, Eds., Cambridge University Press, Cambridge, UK: 173-210.

Lund. J., Sanner, B., Rybach, L., Curtis, R., and Hellström, G., 2004. Geothermal (Ground-Source) Heat Pumps—A World Overview. Geo-Heat Center Bulletin, September.

Lund, J., Derek, W., Freeston, H., and Boyd, T.L., 2005. Direct Application of Geothermal Energy: 2005 Worldwide Review. Geothermics 34, (6): 691–727.

Lund, J., Derek, W., Freeston, H., and Boyd, T.L., 2011. Direct Utilization of Geothermal Energy 2010 Worldwide Review. Geothermics 40, (3): 159–180.

Population Reference Bureau, 2012, World Population Data Sheet, URL: http://www.prb.org/Publications/Datasheets/2012/world-population-data-sheet/data-sheet.aspx: last access 2013.06.17.

Roscoe Moss Company, 1990. Handbook of Ground Water Development. Wiley.

Saaltink, M.W., Ayora, C., Stuyfzand, P.J., and Timmer, H., 2003. Analysis of a deep well recharge experiment by calibrating a reactive transport model with field data. Journal of Contaminant Hydrology 65, (1–2): 1–18.

Tarnawski, V.R., Leong, W.H., Momose, T., and Hamada, Y., 2009. Analysis of Ground Source Heat Pumps with Horizontal Ground Heat Exchangers for Northern Japan. Renewable Energy 34, (1): 127–134.

Tanaka, A., Yamano, M., Yano, Y., and Sasada, M., 2004. Geothermal gradient and heat flow data in and around Japan (I): Appraisal of heat flow from geothermal gradient data. Earth Planets Space 56: 1191–1194.

Trulear, M.G. and Characklis, W.G., 1982. Dynamics of biofilm processes. Journal of the Water Pollution Control Federation 54, (9): 1288–1301.

United Nations, 2013, Department of Economic and Social Affairs, Population Division, World Population Prospects: The 2012 Revision, CD-ROM Edition.

UNEP － United Nations Environment Programme, URL: http://www.unwater.org/statistics_res.html: last access: 2013.06.17

Wilhelmi, O.V., and Morss, R.E., 2013. Integrated Analysis of Societal Vulnerability in an Extreme Precipitation Event: A Fort Collins Case Study, Environmental Science & Policy: 49–62.

Yu, W.H., Zhang, Y.J., Sun, M.P., and Wang, Y., 2010. Impact of Annual Precipitation and Rainy Days with Different Grades Variation on Drought Disaster in Shandong Province. Journal of Arid Meteorology 28, (1): 35-40.

Zeng, H., Diao, N., and Fang, Z., 2003. Efficiency of Vertical Geothermal Heat Exchangers in the Ground Source Heat Pump System. Journal of Thermal Science 12, (1): 77–81.

CHAPTER 2

LITERATURE REVIEW

2.1 CLOGGING MECHANISMS

2.1.1 Chemical clogging

Natural groundwater is considered being of persistent quality and hygienically safe; however, the groundwater composition varies immensely and is influenced by a complex of factors, such as, the quality of infiltrating water, the interaction soil layers, redox conditions, temperature, and microbial activity (De Vet 2011). Geochemical reactions due to incompatibility between the recharge water and the native groundwater and aquifer material results in the formation of various chemical precipitates resulting in chemical clogging, chemical precipitation due to the role of some ions, for example, iron (Fe) and manganese (Mn), is extremely significant. Fe and Mn, which compromise 5 % and 0.1 %, respectively, of the earth's crust, are found widely distributed in both, surface and ground waters, in nearly all geographic areas. During weathering and circulation of water in rocks and soils, ions leach out and dissolve in groundwater. The abundance of primary ions mainly depends upon the nature of bed rocks, climatic conditions and mobility. The presence of nitrate, nitrite and ammonia is regarded as an indicator of potential sewage and animal waste pollution in phreatic groundwater (WHO 2008). In anaerobic groundwater, however, inorganic compounds are related to the decomposition of natural organic matter (De Vet 2011). The oxidative decay of organic matter 'enriches' the groundwater with ammonium but also with other inorganic compounds, such as iron, manganese and trace metals from the reductive dissolution of soil minerals. The oxidation of natural organic matter is paired with, in typical order, the reduction of oxygen, nitrate, and sulfate and fermentation alongside with reductive dissolution of iron and manganese, acidification, dissolution of calcium carbonate and mineralization of ammonium (Styfzand 1989, De Vet 2011).

In ground waters, iron and manganese are usually present in soluble form because of anerobic conditions. When the water, containing these ions, gets in contact with oxygen, redox reactions take place. Nevertheless, these reactions are based on electron transfer, thus, an elusive chemistry depending on many different circumstances. The following equations are presenting the redox reaction for iron:

$$\text{Reduction: } O_2 + 4H^+ + 4e^- = 2H_2O \quad (2.1)$$

$$\text{Oxidation: } 4Fe^{2+} = 4Fe^{3+} + 4e^- \quad (2.2)$$

$$\text{Redox reaction: } O_2 + 4Fe^{2+} + 4H^+ = 4Fe^{3+} + 2H_2O \quad (2.3)$$

Accordingly the redox reaction for manganese is as shown below:

$$\text{Reduction: } O_2 + 4H^+ + 4e^- = 2H_2O \quad (2.4)$$

$$\text{Oxidation: } 2Mn^{2+} + 4H_2O = 2MnO_2 + 8H^+ + 4e^- \quad (2.5)$$

$$\text{Redox reaction: } O_2 + 2Mn^{2+} + 4H^+ + 2H_2O = 2MnO_2 + 8H^+ \quad (2.6)$$

Considering the atomic weight of iron, manganese (55.8 and 54.9, respectively) and oxygen (31.9) and also the number of molecule, which are involved in the reaction, the necessary oxygen amount for each 1 mg/L Fe^{2+} and 1 mg/L Mn^{2+} manganese will be 0.14 mg/L and 0.29 mg/L, respectively.

Figure 2.1 shows the development of equilibrium concentrations as a function of pε at a pH of 7.0.

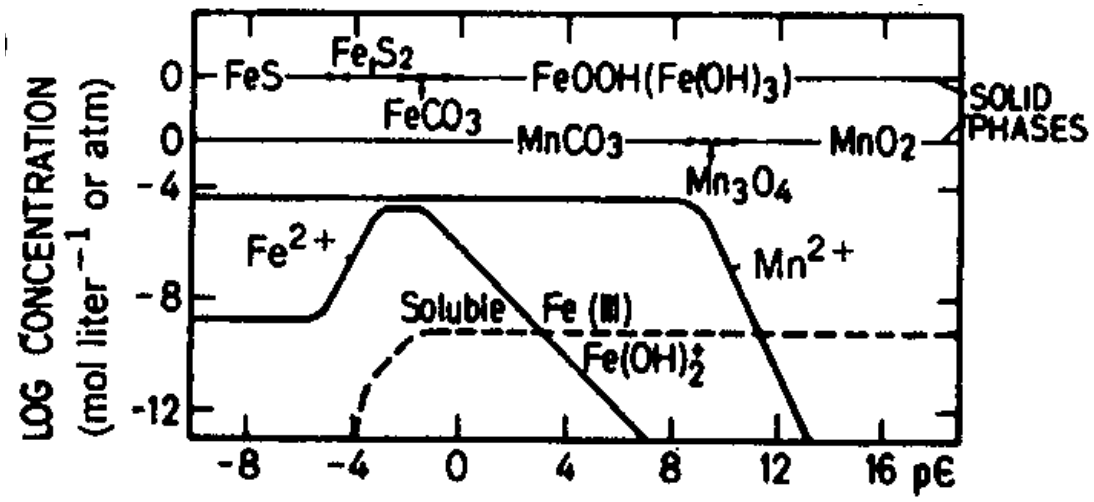

Figure 2.1—change of equilibrium concentrations as a function of pε at a pH of 7.0. (Adopted from Stumm and Morgan 1996)

Figure 2.1 shows, that if oxygen is present and the pε is below 11, the equilibrium for iron and manganese is reached only in solid phase. Furthermore, the solubility of Fe^{2+} and Mn^{2+} increases with decreasing pε (Stumm and Morgan 1996).

Redox reactions are strongly dependent on pH and pε in soil and water systems. The two parameters are coupled with each other, such that with a decrease of pH, pε increases. Redox reactions always taking place under equilibrium conditions; thus, oxidation and a reduction, since there are no free electrons present in aquatic solutions, electron transfer takes places were one element has the function of electron-acceptor and one element has the function of electron-donator. pH and pε play here an important role because pH is the measure of the relative tendency either a solution accepts or transfers protons and pε are a measure for the redox intensity what means the relative tendency of a solution to accept or transfer electrons. For example, when the pH is low the tendency of a solution to transfer protons is very low and vice versa. Furthermore, a high value of pε designates a high tendency for oxidation (Stumm and Morgan 1996). Figure 2.2 shows the different ranges for redox intensity in soil and water. Range 1 is for waters containing oxygen; range 2 is for soils where organic matter degradation takes place accompanied with oxygen consummation, range 3 mainly includes the equilibrium of sulfate ions and range 4 is related to sediments and sludge under anoxic conditions. It can be seen that under lower pε, the concentrations of Mn^{2+} and Fe^{2+} further increases.

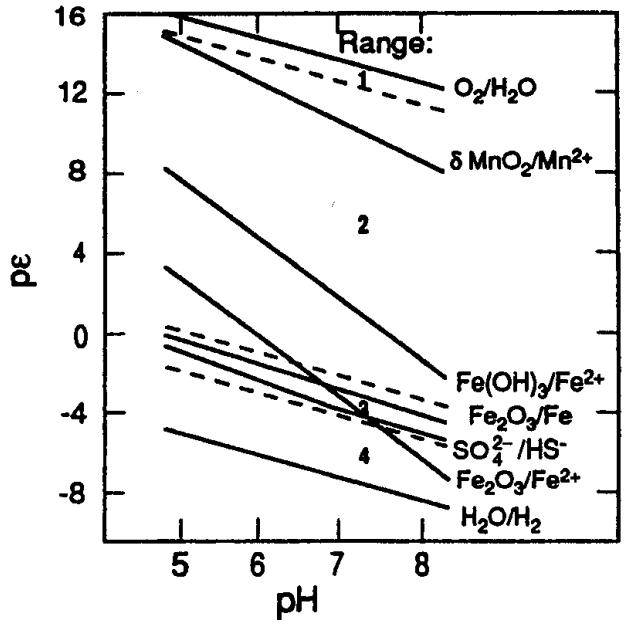

Figure 2.2—Different ranges for redox intensity in soil and water. Range 1 is for waters containing oxygen; range 2 is for soils where organic matter degradation takes place accompanied with oxygen consummation; range 3 mainly includes the equilibrium of sulfate ions and range 4 is related to sediments and sludge under anoxic conditions. (taken from Stumm and Morgan 1996)

Fe^{3+} easily forms iron hydroxide flocks. These flocks form particles and are visible in the water. Conversion of Fe^{2+} to Fe^{3+} resulting in the formation of iron hydroxide is represented as below:

Mn-concentration (Mn) occurs less than 1 mg/L, but it can be as high as 5 mg/L. Occasionally, even much higher Mn is present. Fe may range from less than 1 mg/L to over 40 mg/L, though the majority of well waters contain less than 5 mg/L of iron (John and Harold 1983).

Fe and Mn are problematic in water due to their tendency to oxidize and precipitate as insoluble oxides under a variety of conditions, causing both aesthetic and process water problems. Even very low levels of iron may cause environment conducive for the growth of iron bacteria that utilize energy from the oxidation of ferrous to ferric iron to 'fix' dissolved CO_2 into organic molecules necessary for their existence. The growth of these organisms at phenomenal rates can result in the formation of an existence. The growth of these organisms at phenomenal rates can result in the formation of a gelatinous mat which may cause pipe encrustations and corrosion due to the creation of a galvanic cell and the formation of corrosive by-products (e.g. sulfuric acid and hydrogen sulfide) from associated organisms.

Dissolution of these elements occurs by various processes and results in a variety of conditions regarding the concentrations and chemical forms in which they are found in water. For example, formation and precipitation from iron of native ground water due to recharge of water with a pH and oxidation reduction potential (Eh) in the range of ferric iron. The Eh of the recharge water will, therefore, differ significantly from native groundwater. In humid areas, due to an abundant amount of organic compounds, the oxygen content and Eh is different from arid regions because oxygen consumption during the oxidation process resulting in reduced condition at a shallower depth in humid regions. In artificial recharge system, usually surface recharge water is saturated with oxygen, and even, the deeper layers of the aquifer are more anaerobic. The most significant reaction follows the blending of anaerobic groundwater containing ferrous iron with aerobic recharge water, producing insoluble ferric oxide hydrates.

Hydrochemical species such as Fe, Mn, and other metallic ions, as well as nitrogen and sulphur compounds, will be in the reduced form. Well recharge can lead to precipitation of iron and manganese oxides or hydroxides as dissolved oxygen levels change and to a solution or precipitation of calcium carbonates due to changes in pH and carbon dioxide levels (Bouwer 2002). Developmental mechanisms of chemical clogging are complex, diverse and influenced by a large number of factors such as the chemical components of recharge and native groundwater, the mineral gradients of

aquifer (aquifer mineralogy), and the environmental conditions or physical variables (temperature and pressure, etc.) that control precipitation and deposition. Sometimes, the kinds of reactions are mostly microbial mediated processes; therefore, in many real situations it is difficult to uncouple biological and chemical processes. The rate of precipitation or dissolution is indicated by the reactive surface area of a mineral. Furthermore, addition or depletion of oxygen and carbon dioxide, bacterial metabolism, as well as the presence of catalysts, affect mineral precipitation and dissolution (Perez-Paricio 2001). In the presence of iron oxidizing bacteria, biological oxidation will take place, why it is considered, that one of the main causes of biological and chemical clogging is iron, especially in areas with the presence of high iron concentrations.

2.1.2 Physical clogging

Physical clogging occurs because of deposition and detachment of small particles during transport through an aquifer. Hereby it has to be differentiated between two types like shown in Figure 2.3; one is clogging because of suspended particles initially present in the water considered for injection Figure 2.3 (a). The second type refers to the fine soil particles initially present in the aquifer where the water will be injected into Figure 2.3 (b).

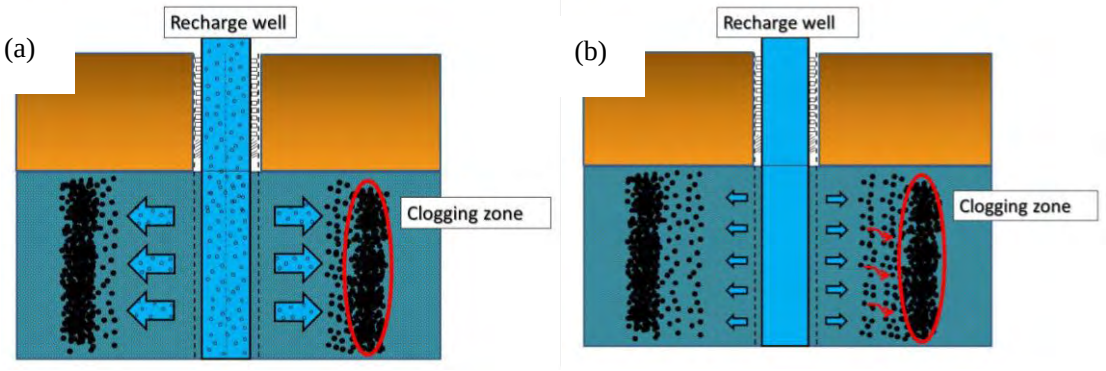

Figure 2.3－Two kinds of physical clogging. (a) Clogging because of suspended particles and (b) clogging because of fine particles initially present in the aquifer.

Many authors agreed, that physical clogging leads to about 70% reduction in permeability in artificial recharge systems (Bichara 1988, Reddi et al. 2000, Holländer et al. 2005). The primary factors affecting the particle deposition are suspended solids concentrations of the recharging water, soil size and distribution, and porosity.

In order to develop mathematical models, efforts were performed to describe the movement of suspended particles in the aquifer (Vigneswaran and Thiyagaram 1984, Vigneswaren et al. 1985, Ahfir et al. 2009). Nevertheless, all these mathematical models include constants and their definitions vary from author to author. Although, the models in these studies could be verified with the experimental data from the respective study site; however, these are not appropriate for different recharge areas with different soil and environmental conditions.

Since 1940, infiltration of surface water into an aquifer is successfully practiced in the Netherlands. To avoid clogging periodic back washing is used. In order to manage clogging, three main parameters are used for prediction of clogging (Bouwer 2002). (a) The Membrane Filtration Index (MFI) is determined by using membrane filtrations, and shows the slope of inverse filtered flow versus cumulative filtered volume. In some reports, the MFI is also termed as the Modified Fouling Index (Olsthoorn 1982, Pérez Paricio 2001). (b) The Assimilable Organic Carbon Content (AOC) that investigates a water sample for growth of bacteria. (c) The third parameter is the Parallel Filter Index (PFI). This parameter is determined via laboratory experiments, passing recharge water through columns filled with aquifer material. It is assumed that clogging in the columns occurs faster than in the field, and thus an early warning factor can be defined (Bouwer (2002). Olsthoorn (1982) has shown that there is a relation between the MFI and the clogging rate of a recharge well. However, still there have been no investigations on a quantitative relation because costly field tests are necessary. However, a quantitative relation between clogging rate and MFI was not available. Buik and Willemsen (2002) described a quantitative, theoretically correct relation between the MFI and the clogging rate of recharge wells due to suspended matter. The theory makes it possible to predict the rate when clogging occurs, but it cannot predict whether clogging occurs or not.

To date most research has been done on suspended solids contained in the injection water (McDowell-Boyer et al. 1986, Herzig et al. 1970, Moghadasi et al. 2004, Ahfir et al. 2009, Ye et al. 2010). Moghadasi et al. (2004) investigated the movement of fine particles in the aquifer. They applied a porous bed made of glass beads filled with alumina particles. The experiment showed that, during injection, the pressure drop increases rapidly after some time, thus, the pores become plugged because of particle mobilization. After some time, plugs and bridges present in the water flow path break and wider path becomes available for water flow. The pressure drop decreases and the cycle start again from the beginning. Unfortunately, this study is outstanding considering particle mobilization during injection practice. Nevertheless, it shows the influence of injection rate or rather to say velocity and hydraulic gradient on the particle

movement in the aquifer. Searching the literature regarding to particle mobilization multiple reports can be found regarding the piping effect of earth fill dams.

Studies on critical hydraulic gradient or critical velocity have already conducted regarding the piping effect of earth fill dams, and an overview is shown in Table 2.1 (Sugii et al. 2009, Jones 2010). For instance, Terzaghi (1922) (in Terzaghi et al. 1996) proposed a critical hydraulic gradient, saying that, when the effective stress in a test specimen where water flows through, approaches to near zero, then, the flow pressure ($i \times \gamma_w$) is quite the same as the submerged (buoyant) unit weight of the soil. Sichardt (1928) derived an equation for critical hydraulic gradient from observed groundwater lowering data. He assumed that erosion may not occur, when the hydraulic gradient is kept below the equation result. For critical velocity regarding movement of soil particles, Justin (1924) carried out an equation for critical velocity depending on the effective particle size of the corresponding soil, whereas, the determination of the mean grain diameter of an existing soil is known to be difficult.

Table 2.1－Summary of previous studies on critical hydraulic gradient and critical velocity regarding particle movement.

Author	Equation	Parameter
Terzaghi (1922)	$i_c=\frac{\gamma'}{\gamma_w}=\frac{G_s-1}{1+e}$	i_c: critical hydraulic gradient [-] γ': submerged unit weight of the soil [N/cm3] γ_w: unit weight of water [N/cm3] G_s: specific gravity of the soil [g/cm3] e: void ratio [-]
Sichardt (1928)	$i_c\leq\frac{1}{15\sqrt{K}}$	i_c: hydraulic gradient [-] K: darcy coefficient [m/s]
Koslova	$v\geq 2.6d^2\left(1+1000\frac{d^2}{D^2}\right)$	v: percolation velocity at which the fine particles begin to move [cm/s] d: diameter of fine particle, which exists between the mean particles of the soil [mm] D: mean particle diameter [mm]
Justin (1924)	$v_c=\sqrt{\frac{2}{3}g(G_s-1)d}$	v_c: critical velocity [cm/s^1] g: acceleration of gravity [m/s^2] d: particle size with central impact on permeability [mm] G_s: specific gravity of the soil [g/cm^3]
Ohno et al. (1984)	$V_p=2.25d^{1.94}$	V_p: critical velocity [cm/s^1] d: particle size [mm]

Keeping in view the above scenario, almost every study considers the suspended particles present in the recharge water. However, regarding the physical clogging, fine particles initially present in the aquifer must also have to be considered. During the recharge process, these particles will be mobilized due to injection velocity and will plug the flow path ways. In order to combat the physical clogging because of particle mobilization, characterization of a critical hydraulic gradient or rather to say a critical velocity should be determined.

2.2 CLOGGING PREVENTION

In order to make injection of water more practicable, investigations were also made in order to prevent clogging.

It has been concluded that clogging can be avoided by proper aquifer exploration, optimal well design, construction and operation, adequate pre-treatment and early regeneration by appropriate methods (Olsthoorn 1982, Peters 1995). Stuyfzand et al. (2002) showed that, after two years of deep well injection practice in the Netherlands, oxygen, contained in the injected water was increasing in the aquifer. Hence, sufficient distance should be maintained between injection and recovery well, in order to raise the redox buffer capacity of the usually anoxic target aquifer.

In almost every applied construction referring to water injection into the aquifer, the water considered for injection is pre-treated in different ways depending on the purpose for re-use. In general, it should be considered that the composition differs not too much to the quality of the ambient groundwater.

Back flushing by extracting water through the recharge well is until now the most applied method in order to unclog the aquifer. This refers mostly to physical clogging problems. Bichara (1988) reproduced field conditions in a 2-D laboratory experiment in order to investigate on pumping, over pumping and back washing of a clogged recharge well. He concluded that the most efficient method is the multiple reversals of flow. The intermittent pumping following the first reversal of flow and neither the usage of back washing tubes had no mentionable effect. It was also found out that the recovery of the initial flow rates of a gravel-packed recharge well depends on the size of the suspended solids as well as their concentration in the flow. Compared to that, Jenne, et al. (1992) found rapid filtration and frequent (twice a day) back flushing to be efficient.

For the chemical clogging investigations were made by using the Vyredox method (Hallberg and Martinell 1976). The purpose using this method is to accomplish around the well a high degree of oxidation in the underground. When the groundwater goes through this oxygen zone, the ferrous will react to the ferric state and precipitate in the underground. This method also works for other metals, like manganese. To setup the system two wells have to installed, one for discharge and one for recharge. To achieve a better oxygen zone, additional injection wells are installed around supply well. The water will be discharged from one well, degassed, enriched with oxygen and injected back to the aquifer through the injection wells. It will take some time until the oxygen zone is build. This principle is successfully used since 30 years in the Switzerland for drinking water treatment (Mengis 2010). Calculations and simulations showed that the system has duration of life of about more than 100 years without clogging occurrence.

Ebermann et al. (2010) developed a mobile unit, based on the Vyredox method, for pilot tests in order to investigate on the applicability of the iron removal in the underground. With this mobile unit, aquifer conditions can be determined and decided, whether subsurface iron removal can successfully be applied.
In Table, 2.2 different methods for redevelopment of deep injection wells after Olsthoorn (1982) are presented.

Table 2.2－Mechanical and Chemical redevelopment methods after Olsthoorn (1982).

Mechanical methods	Flushing pumping	Removes the clogged material and can redevelop up to 70 %; is depending on flow rate, material, pumping time
	Juttering with compressed air	Air will be compressed into the closed injection well what forces the water level down, then the well will be opened and the water shoots upwards. Continuing this process, the material will be loosen and removed
	High-pressure jetting	A water jet with a pressure of about 80 bar is used. The removed material will be extracted by following pumping.
Chemical methods	Chlorine	Used to break up organic deposits, such as slime, and to remove bacteria.
	Acid	Removes deposits of iron and aluminium hydroxides and also other soluble materials.
	Polyphosphates	Removing clay particles, sludge, silt and air bubbles.

From the quite long experience of artificial recharge and also aquifer storage in the Netherlands, Stuyfzand et al. (2005) published some guidelines for preventing clogging (Table 2.3).

Table 2.3－Guideline values for clogging prevention and aquifer requirements after Stuyfzand et al. (2005).

Clogging potential	Suspended matter <0,1 mg/l
	Turbidity < 1 NTU
	Iron < 0,01 mg/l
	Sodium Adsorption Ratio (SAR; = Na/S (Ca+Mg) mmol/L); SAR< 6 if EC 40-100 mS/m
	DOC< 2 mg/l
	AOC (Assimilable Organic Carbon) < 10 μg acetate-C/L
	MFI (Modified Fouling Index) < 3-5 s/L^2
Preservation of aerobicity	Oxygen concentration such that water at surface level > 90% saturated
	Addition of extra oxygen seems desirable
	If necessary, increase of pH by the addition of e.g. NaOH, to keep pH> 7.1
	Infiltrated water should be as cold as possible
Aquifer requirements- hydrological	Relatively thin in comparison to bubble diameter L (height< 3 L)
	Sufficiently permeable (KH >10 m/day) and sufficiently porous (> 0.2)
	Underlying and overlying strata sufficiently confining (impermeable)
	Regional changes in groundwater head < 3 m/8km
	Fully penetrating well screen is possible
Aquifer requirements- hydrochemical	No gypsum ($CaSO_4$,$2H_2O$), anhydrite ($CaSO_4$) and halite (NaCl)
	As inert as possible with regard to iron- and manganese minerals, fluoride
	And arsenic

2.3 CONCLUSIONS

There have been carried out lots of research according clogging mechanisms and their prevention or redevelopment methods. What was obtained from this literature review is that clogging occurrence is depending on many influencing factors, like aquifer composition, chemical composition of the underground, groundwater and also of the water considered for injection. The following points were derived:

(1) Iron and manganese are the most causes for chemical clogging occurrence.
(2) The oxidation of iron and manganese already occurs at very low oxygen amounts.
(3) The composition of the groundwater has a high influence on the chemical reactions and bacterial growth taking place during pumping and injection of groundwater.
(4) The chemistry of injecting water should be too many different compared to the ambient groundwater, primarily temperature and gaseous phase, hence oxygen amount.
(5) Studies regarding clogging because of fine particles initially present in the aquifer are rare.
(6) Mathematical models describing particle movement in the aquifer are site-specific and not applicable in other areas.
(7) There have been studies regarding particle movement in the saturated zone regarding piping occurrence in earth fill dams.
(8) Critical velocity and critical hydraulic gradients are mainly depending on the main particle diameter of the soil.
(9) Determining the mean particle diameter is difficult.
(10) *In-situ* field test methods are missing; thus, application of conducted study is still unknown.
(11) In almost every case, injecting water is pre-treated in order to avoid clogging.
(12) Frequently back washing is needed in order to redevelop the recharge system.
(13) Guidelines are obtained from experienced application systems.
(14) For prevention of clogging or redevelopment after clogging occurred, general construction, treatment and operation instructions are needed.

REFERENCES

Ahfir, N.D., A. Benamar, A. A., and Wang, H.Q., 2009. Influence of internal structure and medium length on transport and deposition of suspended particles: A laboratory study. Transport in Porous Media, 76(29): 289–307.

Appelo, C.A.J., Drijver, B., Hekkenberg, R., and de Jonge, M., 1999. Modeling in situ iron removal from ground water. Ground Water 37, (6): 811–817.

Beek, C. G. E. M. van., 2011. Cause and Prevention of Clogging of Wells Abstracting Groundwater from Unconsolidated Aquifers. IWA Publishing.

Bichara, A. 1988. Redevelopment of clogged recharge wells. Journal of Irrigation and Drainage Engineering 114, (2): 343–350.

Bouwer, H., 2002. Artificial Recharge of Groundwater: Hydrogeology and Engineering. Hydrogeology Journal 10, (1): 121–142.

Buik, N. A., Willemsen, G., 2002. Clogging Rates in Re charge Wells in Porous Media. Pro ceedings (Ed. P. J. Dillon), 4th In ternational Symposium on Artificial Recharge, Adelaide, Australia: 195-198

Crosta, G., and di Prisco, C., 1999. Onslope instability induced by seepage erosion. Canadian Geotechnical Journal 36, (6): 1056–1073.

De Vet, W.W.J.M., 2011. Biological Drinking Water Treatment of Anaerobic Groundwater in Trickling Filters. PhD Thesis, Delft University of Technology, The Netherlands.

Ebermann J, Eichorn D., Macheleidt W., Grischek T., 2010. Groundwater quality sustainbility. Edited by Zuber A, Kania J, Kmiecik E.: 895-901

Hallberg, R.O., and Martinell, R., 1976. Vyredox — In Situ Purification of Ground Water. Ground Water 14, (2): 88–93.

Herzig, J.P., Leclerc, D.M., and Goff, P.L., 1970. Flow of suspensions through porous media-Application to deep filtration. Industrial and Engineering Chemistry 62, (5): 8–35.

Holländer, H.M., Boochs, P.W., Billib, M., and Panda, S.N., 2005. Labor-Säulenversuche zur Untersuchung von Clogging-Effekten im Grundwasserleiter—Einfluss von physikalischen An- und Ablagerungen, Gasblasen und biologischer Aktivität. Grundwasser 10, (4): 205–215. (in German)

Japanese Geotechnical Society, 1965. Handbook of soil mechanics and foundation engineering, Tokyo, Japanese Geotechnical Society: 93. (in Japanese)

Jenne, E.A., Andersson, O., and Willemsen, A., 1992. Well, Hydrology, and Geochemistry Problems Encountered in ATES Systems and Their Solutions. SAE

Technical Paper 929153. Warrendale, PA: SAE International. http://papers.sae.org/929153/.

Jobin, R., and Ghosh, M. M., 1972. Effect of buffer intensity and organic matter on the oxygenation of ferrous iron. Journal American Water Works Association 64, (9): 540-595.

John, F. M., and Harold, L. A., 1983. Iron in Water and Processes for its Removal. In: 21st Annual Liberty Bell Corrosion Course: 1-17, Philadelphia, Pennsylvania, USA.

Jones, J.A.A., 2010. Soil piping and catchment response. Hydrological Processes 24, (12): 1548–1566.

Justin, J.D., 1924. The design of earth dams. Transactions of the American Society of Civil Engineers 88, (1): 1–61.

McDowell-Boyer, L.M., Hunt, J.R., and Sitar, N., 1986. Particle transport through porous media. Water Resources Research 22, (13): 1901–1921.

Mengis Gebr. AG – Bohrunternehmung, 2010, URL: http://www.mengis-gebr.ch/VDX.htm: last access: 2013.07.02.

Moghadasi, J., Müller-Steinhagen, H., Jamialahmadi, M., and Sharif, A., 2004. Theoretical and experimental study of particle movement and deposition in porous media during water injection. Journal of Petroleum Science and Engineering 43, (3–4): 163–181.

Mulqueen, J. 2005. The flow of water through gravels. Irish Journal of Agricultural and Food Research 44, (1): 83–94.

Nakashima, H., Matsubara M., and Iijima, J., 1986. Observation of the piping phenomenon by x-ray radiography. In Proceedings of the 21st Annual Conference of Japanese Society of Soil Mechanics and Foundation Engineering (JSSMFE), Sapporo, Japan: 1479-1482. (in Japanese)

Ohno, M., Yamazaki, H., and Tran-Duc, P.O., 1984. Experimental study of piping property of sand. Report of Hazama: 33-40. (in Japanese)

Okajima, K., and Tanaka, T., 2008. Evaluation of analyses of downstream piping of weirs by model experiments and elasto-plastic FEM. Proceedings of Fourth International Conference on Scour and Erosion (ICSE), November 5-7, Tokyo: 460-567. (in Japanese)

Olsthoorn, T.N. 1982. The clogging of recharge wells: Main subjects. Rijswijk, The Netherlands, KeuringsinstituutvoorWaterleidingArtikelen (KIWA).

Pérez P., A., 2001. Integrated Modelling of Clogging Processes in Artificial Groundwater Recharge. PhD Thesis, Technical University of Catalonia (UPC).

Peters, J.H., 1995. Artificial recharge and water supply in the Netherlands, state of the arts and future trends. In Johnson, A.I. and Pyne, R.D.G., 1995. Artificial recharge of ground water. II. Proceedings of the Second International Symposium on Artificial Recharge of Ground Water.

Stumm, W., and Morgan, J.J., 1996. Aquatic Chemistry: Chemical Equilibria and Rates in Natural Waters. Wiley.

Stuyfzand, P.J. 1989. Hydrology and Water Quality Aspects of Rhine Bank Groundwater in The Netherlands. Journal of Hydrology 106, (3–4): 341–363.

Stuyfzand, P.J., Vogelaar, A.J., and Wakker, J., 2002. Hydrogeochemistry of prolonged deep well injection and subsequent aquifer storage in pyritiferous sands; DIZON pilot, Netherlands. In Dillon, P. J. (ed), Management of Aquifer Recharge for Sustainability, Proc. 4th Internat. Symp. on Artificial Recharge, Adelaide, Australia, 22-26 Sept. 2002, Balkema: 107-110.

Stuyfzand, P.J., Wakker, J.C., and Beckers, R.J.S..M., 2005. Water quality changes during Aquifer Storage and Recovery (ASR): results from pilot Herten (Netherlands), and their implications for modeling. ISMAR-5, Berlin, 12-17 June 2005, in prep.

Pavelic, P., Dillon, P.J., Mucha, M., Nakai, T., Barry, K.E., and Bestland, E., 2011. Laboratory assessment of factors affecting soil clogging of soil aquifer treatment systems. Water Research 45, (10): 3153–3163.

Pérez Paricio, A. 2001. Integrated modelling of clogging processes in artificial groundwater recharge.Ph.D. thesis, Technical University of Catalonia (UPC).

Reddi, L.N., Ming, X., Hajra, M.G., and Lee, I.M., 2000. Permeability reduction of soil filters due to physical clogging. Journal of Geotechnical and Geoenvironmental Engineering 126, (3): 236–246.

Saaltink, M.W., Ayora, C., Stuyfzand, P.J., and Timmer, H., 2003. Analysis of a deep well recharge experiment by calibrating a reactive transport model with field data. Journal of Contaminant Hydrology 65, (1–2): 1–18.

Shindo, K. 1967. Rock Mechanics, Morikita, Tokyo. (Japanese translation of :Talobre, J.,and D. O. Martin. 1957.La mécanique des roches:appliqué aux travaux publics. Dunod.)

Sichardt, W. 1928.Das Fassungsvermögen von Rohrbrunnen und seine Bedeutung für die Grundwasserabsenkung, insbesondere für größere Absenkungstiefen. Springer. (in German)

Sugii, T., Yamada, K., and Nagura, S., 2009. Critical velocity for progressive seepage failure and change in permeability. Geotecnical Engineering Magazine Japan 57, (9): 26–29. (in Japanese)

Terzaghi, K., Peck, R.B., and Mesri, G., 1996. Soil Mechanics in Engineering Practice. John Wiley and Sons.

Vigneswaran, S., and Thiyagaram, M., 1984. Application of filtration theories to ground water recharge problems. Water, Air, and Soil Pollution 22, (4): 417–428.

Vigneswaren, S., Jeyaseelan, S., and Gupta, A. D., 1985. A pilot-scale investigation of particle retention during artificial recharge. Water, Air and Soil Pollution 25, (1): 1–13.

WHO- World Health Organisation, 2008. Guidelines for Drinking Water Quality, 3rd edition, Geneva.

Ye, X., Du, X., Li, S., and Yang, Y., 2010. Study on clogging mechanism and control methods of artificial recharge. In Proceedings of the2010 International Conference on Challenges in Environmental Science and Computer Engineering (CESCE), March 6-7, Wuhan, China, Institute of Electrical and Electronics Engineers (IEEE) 2:29–32.

CHAPTER 3

EXPERIMENTAL WORK ON CLOGGING PREVENTION

3.1 EXPERIMENTAL STUDY FOR PREDICTING PARTICLE MOBILIZATION RESULTING IN PHYSICAL CLOGGING

3.1.1 Introduction

Due to water injection into an aquifer, the hydraulic gradient decreases with radial distance from the injection well. When soil particles near the well are moving, permeability decreases with moving distance resulting in accumulation of the soil particles and clogging occurs (Figure 3.1). Thus, determination of the critical hydraulic gradient and also the critical velocity are of great importance.

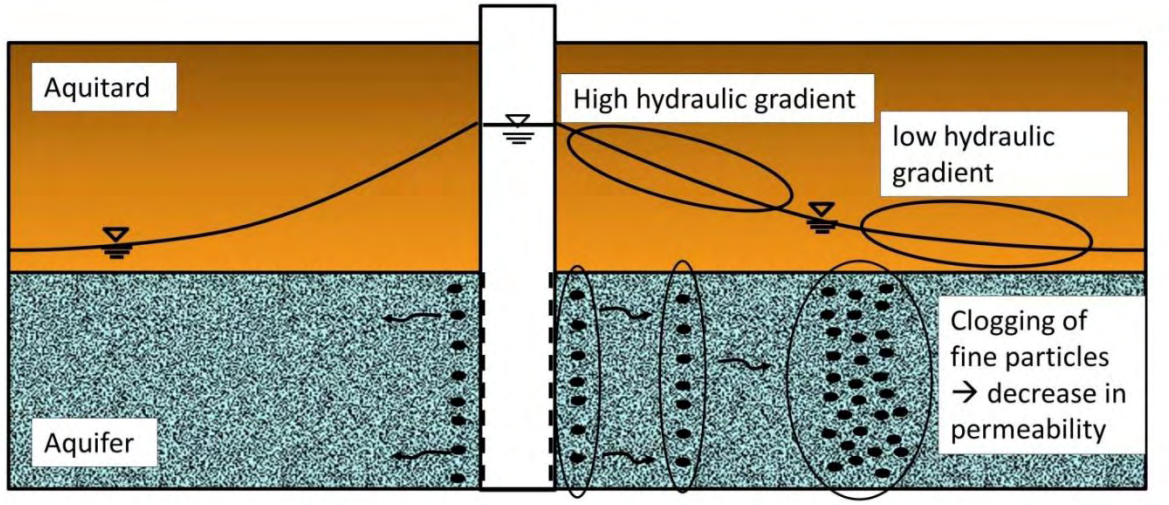

Figure 3.1－Clogging because of fine particle movement in the aquifer.

To date, studies on physical clogging were conducted almost considering suspended particles in the recharge water. However, research on particle mobilization of soil particles initially present in the aquifer should not be neglected, especially its influence it is not well known. During the recharge process these particles will be mobilized due to injection velocity and will plug the flow path ways. In order to combat the physical clogging because of particle mobilization, characterization of a critical hydraulic gradient or rather to say a critical velocity should be determined which can be found in the literature considering piping effect of earth fill dams.

The objective of this study is to determine the critical hydraulic gradient in order to avoid particle mobilization as well as to understand the physical processes occurring during the injection process. Although, it is to prove how the theories of particle mobilization regarding the piping effect is adoptable for clogging problems. One- and two-dimensional experiments were conducted in order to determine the critical hydraulic gradient, whereas the two- dimensional experiment was carried out by Tanaka (1992). During water injection

into the aquifer, the hydraulic gradient is decreasing because of the particle clogging near the injection well. Thus, determination of the critical hydraulic gradient as well as the critical velocity are of great importance for understanding this clogging phenomenon. From the one-dimensional experiment it is expected, that the process of particle movement under different hydraulic gradients will give a deeper understanding. From the two-dimensional (axisymmetric) experiments, a critical hydraulic gradient will be determined and a comparison with different theories on critical velocity and critical hydraulic gradient can be given and what it is obtained for perspective work.

3.1.2 Materials and Methods

3.1.2.1 Experiment 1: One Dimensional Groundwater Model

When fine particles move due to velocity forces, voids are getting clogged, and thus permeability decreases with time. For water injection methods, it is important to operate with a flow rate where clogging does not occur for a preferably long time.

3.1.2.1.1 Experimental Setup and Procedure

A cylindrical column of 100 cm length and 10 cm diameter (for test A and B, 50 cm column length with 10 cm diameter) were used in order to analyze the particle movement in every 10 cm soil layer. The columns were densely packed with Masa soil, which is a weathered granite soil typically found in Okayama Prefecture (western Japan). Before the soil was packed into the column, every 10 cm layer was sieved in order to compare the sieve curves before and after the experiment. The experiments were performed with different chosen hydraulic gradients (i) of 0.02, 0.10, 0.20 and 0.30 by using a constant pressure head difference Δh, and considering the Darcy flow:

$$Q=-K\frac{\Delta h}{\Delta l}A \tag{3.1}$$

where Q is the flow rate [cm^3/s], k is the permeability coefficient [cm/s], Δh is the pressure head difference [cm], Δl is the length of the soil sample [cm] and A is the surface area [cm^2].

In order to observe the permeability during the experiment, the outflow volume of water was recorded by a mass balance and a manometer was installed on the column to observe the water head changes along the column. The experimental setup and the soil characteristics are shown in Figure 3.2 and Table 3.1, respectively.

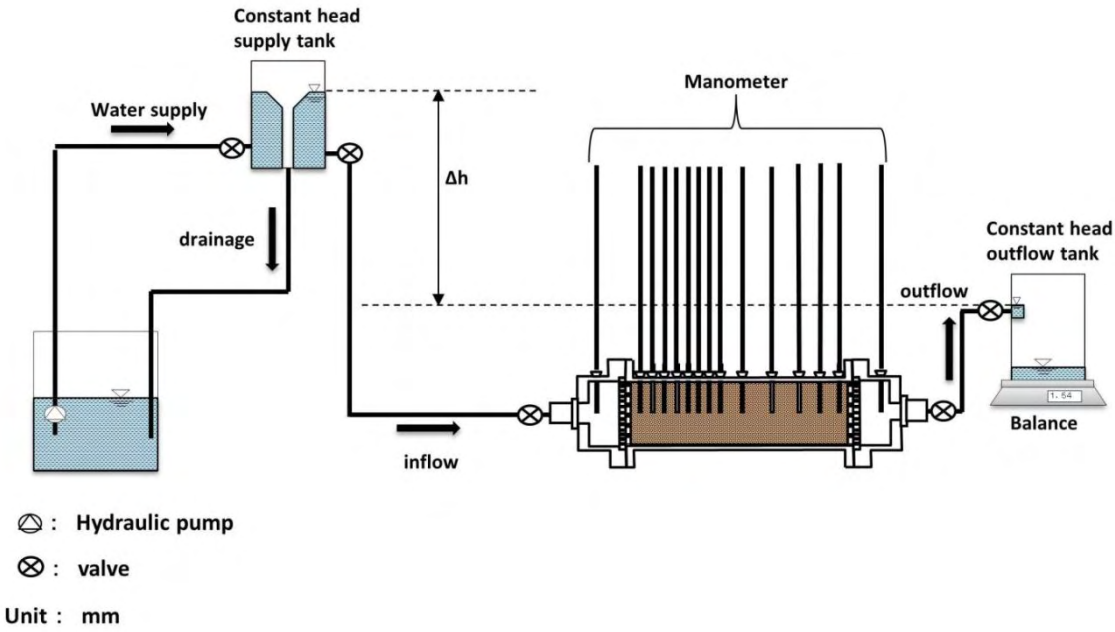

Figure 3.2－Experimental setup of the one- dimensional column experiment investigating particle mobilization. A picture from the experimental setup is shown in the Appendix A 39.

Table 3.1－Experimental characteristics of test specimen for one-dimensional experiments

	A	**B**	**C**	**D**
Hydraulic gradient i [-]	0.02	0.10	0.20	0.30
Saturated permeability coefficient k_s [cm/s]	2.8×10^{-3}			
Void ratio e [-]	0.254	0.262	0.265	0.273
Specific gravity G_s [g/cm^3]	2.46			
Column size (diameter×length) [cm]	10×50	10×50	10×100	10×100
Manometer placement [cm]	2, 4, 6, 8, 10, 20, 30, 46, 48	10, 20, 30, 40	5, 10, 20, 50, 90, 95	5, 10, 13, 17, 20, 30, 40, 50, 70, 90, 95

3.1.2.1.2 Experimental Results and Discussion

Due to the movement of fine particles by velocity forces, voids are started to be clogged and hence permeability decreased with time. The experiments were conducted until a decrease in permeability was observed. When almost no flow was observed, the experiment was stopped and the soil was taken out and separated into the same 10 cm layers as were taken at the start of experiment. After drying the soil in an oven at 105 °C for 24 hrs., each soil layer was sieved in order to compare the sieve curves to the original ones. For the lowest hydraulic gradient of i= 0.02 (test A), the comparison of sieve curves showed almost no change except at 20-40 cm soil layer. As shown in Figure 3, the particles

below 2 mm clearly deposited between 30 and 40 cm layer. The same trend was observed in case of test B. For i= 0.02, it was also observed that until 40 cm, particles below 0.045 mm size were accumulated. The same trend was observed for i= 0.1 which can be explained by the effect that the bigger particles have more surface area, thus these particles can be moved by the velocity forces and the fine particles displaced these bigger particles. For test C, the particle movement and a clear difference in the particle distribution curves was observed within the first 50 cm of the column length. Compared to test C, test D showed more differences up to 30 cm column length. Thus, with increasing hydraulic gradient, clogging occurs more and more near the injection point. Two examples of the particle distribution curves obtained from experimental results are shown in Figures 3.3 and 3.4, all distribution curves are illustrated in the Appendix (A 1 - A 30)

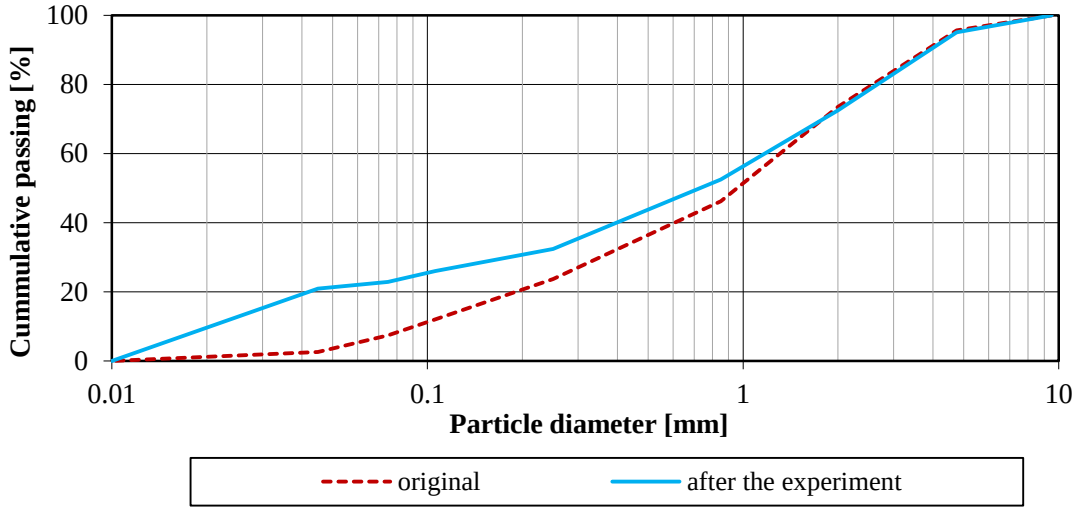

Figure 3.3—Comparison of soil distribution curves for test A with i= 0.02 (30-40 cm). Deposition of particles below 2 mm size was observed, especially high accumulation of particles below 0.045 mm.

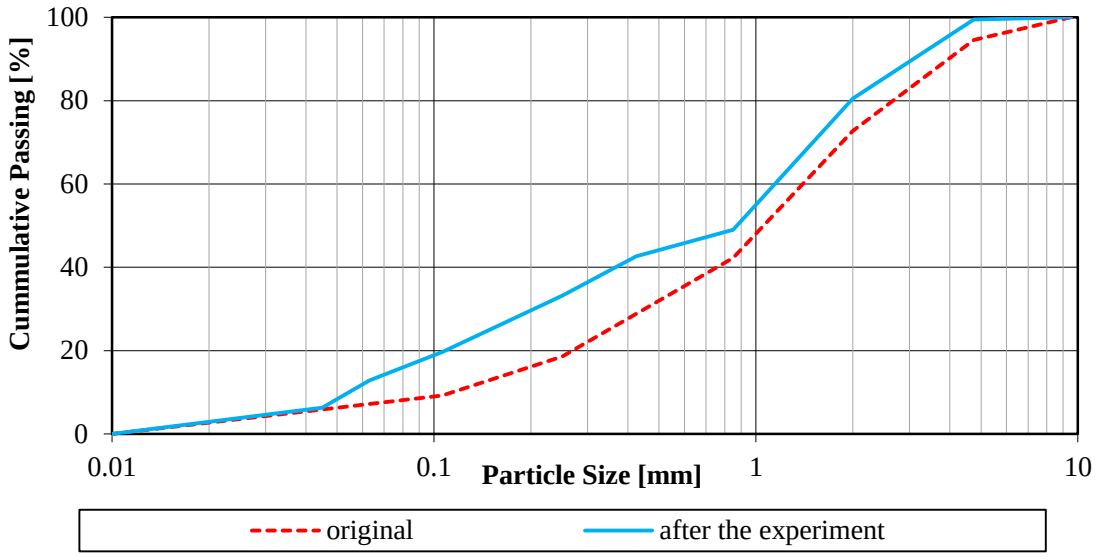

Figure 3.4—Comparison of soil distribution curves for test D with i=0.3 (10-20 cm). Within the first 30 cm column length, particle movement between 0.85 and 2 mm was observed.

Hydraulic head changes for i= 0.2 are represented in Figure 3.5. For i= 0.02, 0.1 and 0.3 the graphs can be found in the Appendix (A 31 - A 33). The curves indicated that after half of the time, the heads showed a maximum decrease in each manometer up to 50 cm column length. The highest decrease was observed at of 20 cm column length, which highlights that the flow path ways got blocked. However, the decrease did not continue showing that the settled particles in that zone mobilized again, confirming Moghadasi's results (Moghadasi et al., 2004).

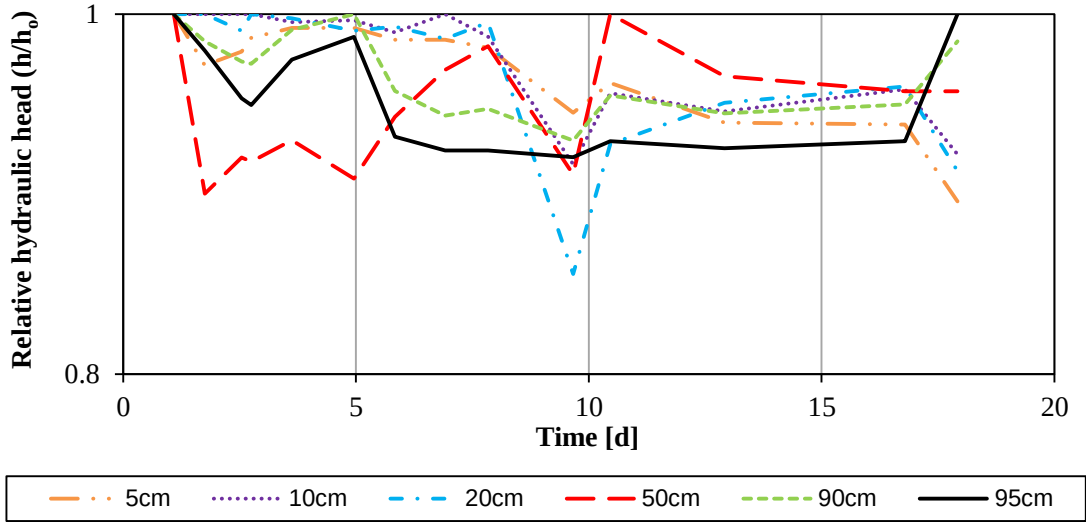

Figure 3.5—Change of the pressure heads over time at different points of the column length, measured by manometer for i= 0.2 (test C). The same behavior was observed for all other tests at different hydraulic gradients. Even for long experimental time about 48 days, the decrease followed by an increase at the middle of experiment time was observed.

When Terzaghi's equation (Table 3.4) for the critical hydraulic gradient (i_c) was applied to experimental data, for test A i_c= 1.16 and for B, C and D a gradient of 1.15, respectively were obtained. By comparing these values utilized in the experiments with gradients of i= 0.02, i= 0.1, i= 0.2 and i= 0.3, it is concluded, that values obtained by using Terzaghi's equation are not applicable for clogging prevention when using presented experimental data. This phenomenon is because Terzaghi's theory is based on upward flow, but here, horizontal groundwater flow was simulated. The same conclusion was obtained by applying Sichardt's equation where the i_c for Masa soil was 1.26. Comparing obtained results with the critical velocity values documented in literature (Table3.4), it is difficult to evaluate the critical velocity because the velocity decreased with time. Hence, it is difficult to predict which particle moved at what time and with which velocity. Regarding the size of the particles moved during the experiments, following results were obtained.

(1) Masa soil includes a high amount of particles between 0.85 mm and 4.75 mm.
(2) 10-30 cm (i= 0.02): particles between 2 and 4.75 mm moved away from the injection point.
(3) 0-10 cm (i= 0.02): movement of particles between 0.106 and 0.25 cm was observed.
(4) 40-50 cm (i= 0.02 and i= 0.1): no change observed in the particle distribution curves.
(5) 10-40 cm (i= 0.02): deposition of particles below 0.045 mm (Figure 3.3).
(6) 0-30 cm (i= 0.1): particles between 2 and 4.75 mm moved away from the injection point.
(7) 20-40 cm (i= 0.1): particles between 0.85 and 2 mm moved from the 30-40 cm layer into the 20-30 cm layer.
(8) 10-20 cm (i= 0.2): particle sizes between 0.106 mm and 0.25 mm deposited, and between 0.25 mm and 0.85 mm moved away from the injection point.
(9) 30-40 cm (i= 0.2): particles below 0.85 mm settled down, and particles below 0.106 mm doubled in this zone.
(10) 50-80 cm (i= 0.2): deposition of particles between 0.25 and 4.75 mm.
(11) 80-100 cm (i= 0.2, i-0.3): almost no change in the particle distribution was observed.
(12) 0-30 cm (i= 0.3): movement of particles between 0.85 mm and 2 mm was observed (Figure 3.4).
(13) 40-50 cm (i= 0.3): particle between 0.25 and 0.85 mm moved into the next layer.

For test A (i=0.02) and test B (i= 0.1) it is concluded, that particles between 0.25 and 2 mm contrasting to predictions showed the highest moving capacity.

In general it was obtained, that the mass balance in these experiments is not valid. It is concluded, comparing the particle size distribution curves before and after the experiments, fine particles increased. The reason for that is because of errors in the method, especially using this type of soil. Masa soil has a wide range particle sizes; hence, clayey particles easily act as a binding agent between soil particles, which may cause a different particle size distribution after drying and sieving after the experiments. Furthermore the packing of the column is considered of great influence on the results.

3.1.2.2 Experiment 2: Two-Dimensional Axisymmetric Groundwater Model (Tanaka ,1992)

One dimensional groundwater models can only give information about flow in x-direction. A 2-dimensional axisymmetric aquifer model gives information in radial flow direction, thus it gives more realistic results. An axisymmetric model was constructed to simulate radial groundwater flow away from an injection well.

3.1.2.2.1 Experimental Setup and Procedure

In order to evaluate the relationship between grain distribution curve and injection flow rate due to clogging, an axisymmetric confined groundwater model was applied. The purpose of this study is to investigate the problem of fine particle movement and to determine the critical water level rise in an injection well. The experimental setup is shown in Figure 3.6.

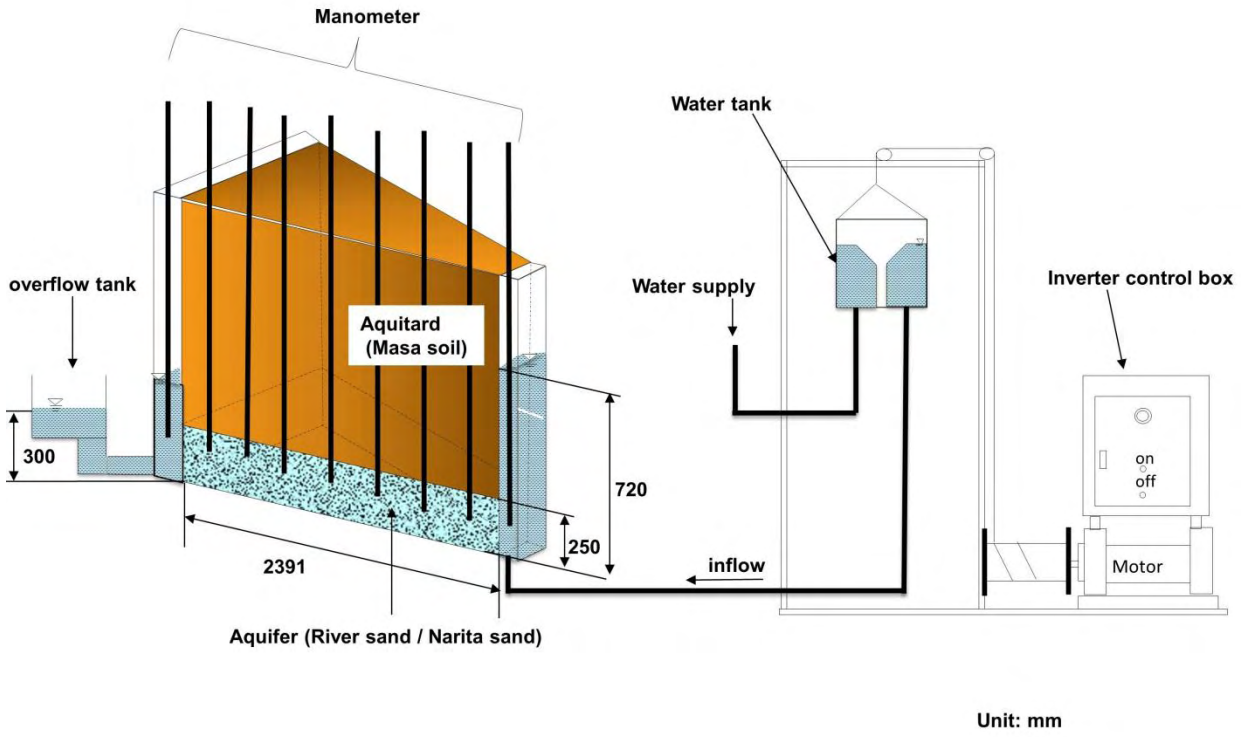

Figure 3.6—Experimental Setup of the two-dimensional axisymmetric confined groundwater model.

River sand and Narita sand (from the Narita region in Tokyo) were used as aquifer materials, and for the aquitard Masa soil was utilized. The physical properties of the sands are shown in Table 3.2. The grain size distribution curves for the aquifer material were changed as shown in Figure 6, where also the grain size distribution curve of Masa soil is presented. The water level in the injection well-tank was gradually increased up until 72 cm. This water level was kept constant using a mariotte tank. In order to control the

injection flow rate, a mariotte syphon was applied. The experiment was conducted with a constant flow rate of 0.025 cm/s.

Table 3.2— Physical properties of each soil type used for two-dimensional experiments

Soil type		Specific gravity [g/cm^3]	Porosity [-]	Permeability [cm/s]
River sand	No. 1	2.69	0.50	7.46×10^{-2}
	No. 2	2.69	0.50	4.50×10^{-2}
	No. 3	2.69	0.50	3.08×10^{-2}
	No. 4	2.69	0.50	4.50×10^{-1}
Narita sand	No. 1	2.72	0.70	2.25×10^{-2}
	No. 2	2.72	0.70	3.02×10^{-2}
Masa soil		2.65	0.42	4.83×10^{-6}

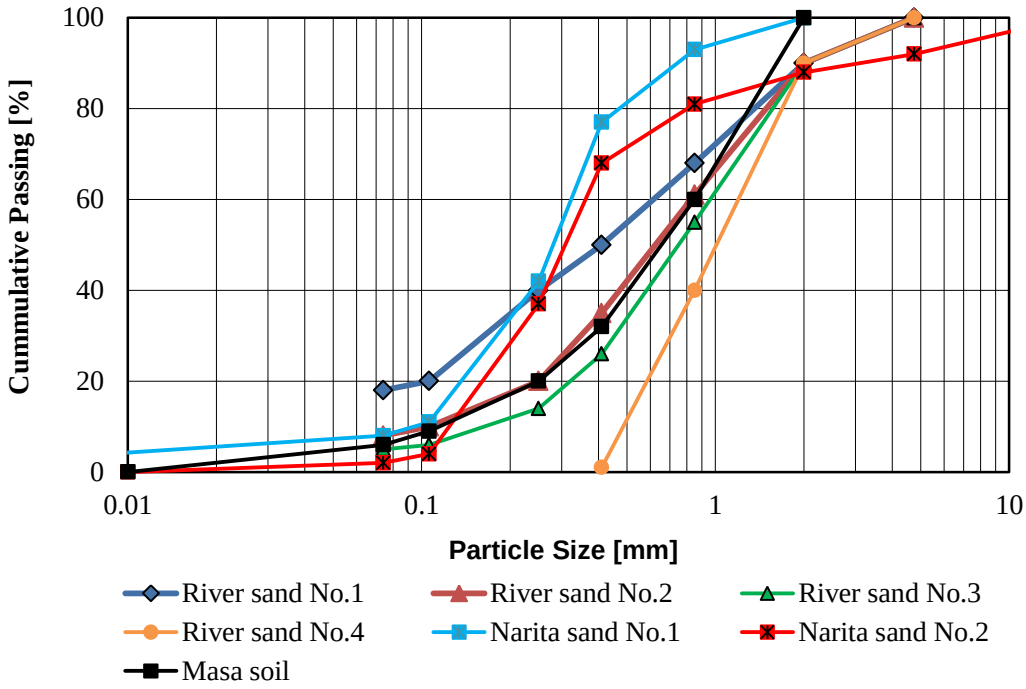

Figure 3.7—Particle size distribution curves of each material used in these experiments.

3.1.2.2.2 Permeability and hydrological gradient calculation

The fundamental equation of groundwater movement in a confined aquifer can be expressed as given below:

$$Q_r = -2\pi rDK \tag{3.2}$$

where Q_r is the injection flow rate [L^3/T]; D is the aquifer thickness [L]; K is the hydraulic conductivity [L/T]; and r is the range of influence in radial direction [L].

Regarding to the flow between two points (Figure 3.8) ($r_1 \leqq r \leqq r_2$), equation (3.2) can be written as

$$\ln\left(\frac{r_2}{r_1}\right) = -\frac{2\pi DK}{Qr}\left(h_2-h_1\right) \tag{3.3}$$

where, h is the total head [L].

By solving equation (3.3) for hydraulic conductivity (K), K will be:

$$K = \frac{-Qr}{2\pi D}\frac{\ln\left(\frac{r_2}{r_1}\right)}{\left(h_2-h_1\right)} \tag{3.4}$$

or by solving the flow rate (Q_r), Q_r will be as below:

$$Q_r = \frac{-2\pi DK\left(h_2-h_1\right)}{\ln\left(\frac{r_2}{r_1}\right)} \tag{3.5}$$

By substituting equation (3.4) in equation (3.2), it follows

$$i = \left(\frac{\partial h}{\partial r}\right) = \frac{-\left(h_2-h_1\right)}{\ln\left(\frac{r_2}{r_1}\right)}\left(\frac{1}{r}\right) \tag{3.6}$$

Figure 3.8 shows a 2-dimensional axisymmetric confined aquifer model profile and its presentation of equation (3.2) relevant parameters for groundwater movement in a confined aquifer system.

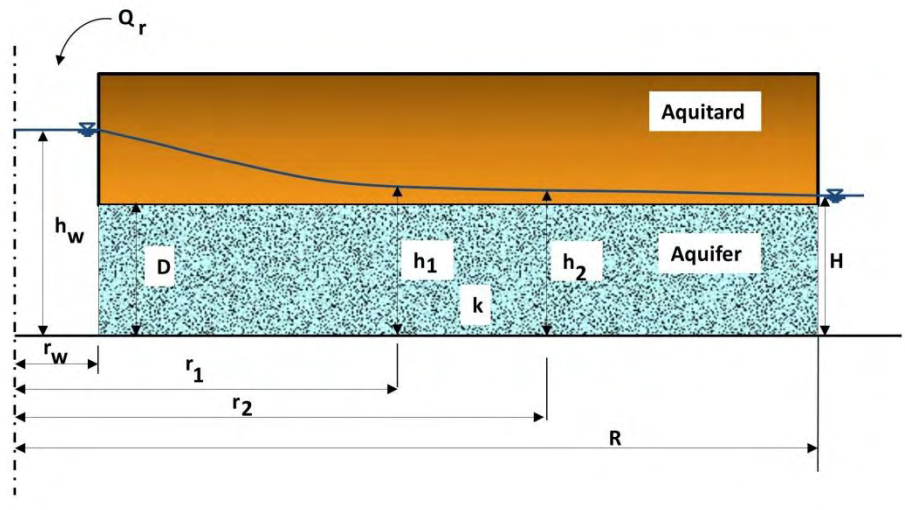

Figure 3.8—Two-dimensional axisymmetric confined aquifer model profile and its presentation of equation 2 relevant parameters for groundwater movement in a confined aquifer system.

3.1.2.2.3 Experimental results and discussion

During the experiment, the flow rate was decreased about 17%, when the experimental material included fine particles below 0.42 mm (Riversand No.4) is used in experiment. These results state that no clogging occurs by using this material. When the material included 20% of fine particles below 0.104 mm (Riversand No.3) was used, the injection flow rate decreased about 80%. With regard to Narita-sand, it was observed that if the amount of fine particles increases, the rate of diminution of flow rate also increases.

When permeability reduction occurs, relationships between hydraulic gradient and permeability were obtained like shown in Figure 3.9 for river sand No. 1 (river sand No. 2 - 4 and Narita sand No.1 - 2 are illustrated in the Appendix (A 34 – A 38) and also tabulated in Table 3.3.

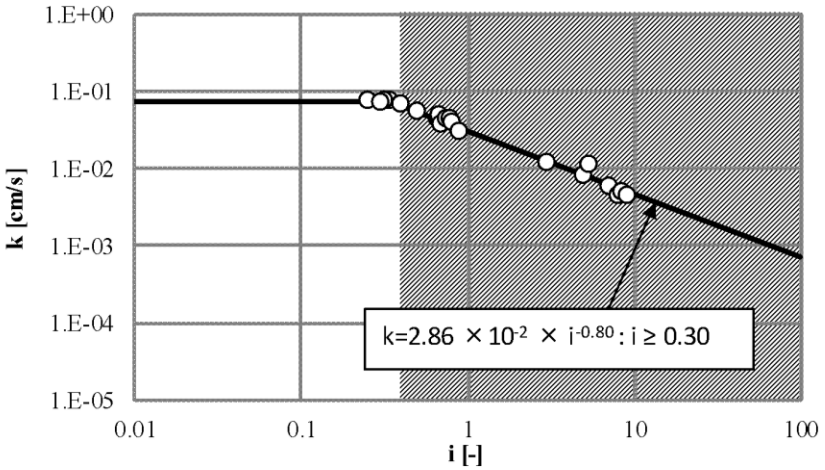

Figure 3.9—Relationship between permeability (k) and hydraulic gradient (i) for River sand No. 1.

The shaded parts in the graph indicate the above mentioned relation between hydraulic gradient and permeability in the areas of flow rate reduction. The non-shaded area in the graph represent the relation between hydraulic gradient and permeability outside the area of permeability reduction at the termination of the experiment.

From the graphs, like presented in Figure 3.9 and also from those of the other experiments, a relationship between hydraulic gradient (i) and permeability (k) was found (also described by Mulqueen (2005)).

$$k=ai^{-b} \tag{3.7}$$

where a and b are constants.

Experimental data values and the coefficients a and b obtained from equation (3.7) for each sample, correlation coefficients (R^2) between the measured values, and the smallest hydraulic gradient (i_{min}) at the starting point of the permeability reduction (e.g. Figure 3.9) are summarized in Table 3.3. From Table 3.3 it can be confirmed that a minimum hydraulic gradient exists at the starting point of permeability reduction.

Table 3.3－Experimental results and determined values for Equation (3.7)

Soil type	a [cm/s]	b	R^2	k_0 [cm/s]	i_{min}
River sand					
No. 1	2.86×10^{-2}	0.80	0.97	7.46×10^{-2}	0.30
No. 2	5.02×10^{-3}	0.95	0.98	4.50×10^{-2}	0.10
No. 3	3.08×10^{-3}	1.01	0.87	3.08×10^{-2}	0.07
No. 4	2.50×10^{-1}	0.70	0.96	4.50×10^{-1}	0.50
Narita sand					
No. 1	7.50×10^{-3}	0.91	0.99	2.25×10^{-2}	0.30
No. 2	6.59×10^{-3}	0.94	0.99	3.02×10^{-2}	0.20

Figure 3.10 shows the relationship between hydraulic gradient and the materials which include grain sizes below 0.104 mm. From this graph it can be concluded that clogging occurs because of fine particle movement when the hydraulic gradient is below 0.3.

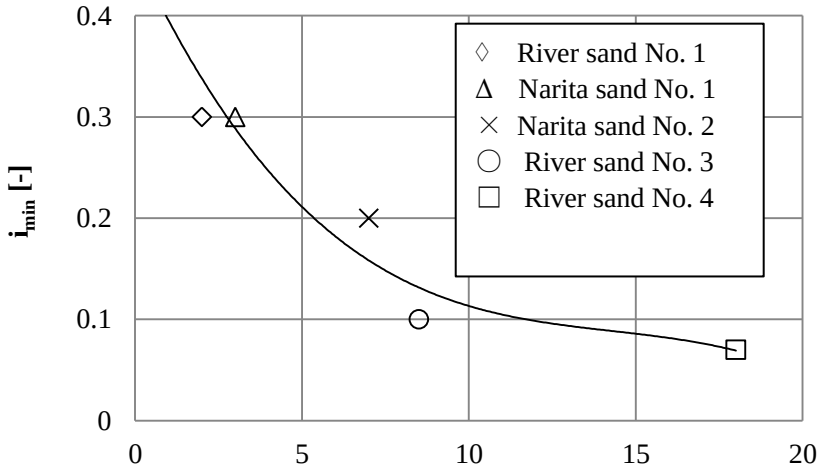

Figure 3.10－Relationship between minimal hydraulic gradient and soil content finer than 0.104 mm

For application regarding the studies of the piping effect, the following theories shown in Table 3.4 were applied to the present experimental data.

Table 3.4－Summary of previous studies on critical hydraulic gradient and critical velocity regarding particle movement.

author	equation	parameter
Terzaghi (1922)	$i_c=\frac{\gamma'}{\gamma_w}=\frac{G_s-1}{1+e}$	i_c: critical hydraulic gradient [-] γ': submerged unit weight of the soil [N/cm3] γ_w: unit weight of water [N/cm3] G_s: specific gravity of the soil [g/cm3] e: void ratio [-]
Sichardt (1928)	$i_c \leq \frac{1}{15\sqrt{K}}$	i_c: hydraulic gradient [-] K: darcy coefficient [m/s]
Koslova	$v_p \geq 2.6d^2\left(1+1000\frac{d^2}{D^2}\right)$	v_p: percolation velocity at which the fine particles begin to move [cm/s] d: diameter of fine particle which exists between the mean particles of the soil [mm] D: mean particle diameter [mm]
Justin (1924)	$v_c=\sqrt{\frac{2}{3}g(G_s-1)d}$	v_c: critical velocity [cm/s^1] g: acceleration of gravity [m/s^2] d: particle size with main impact on permeability [mm] G_s: specific gravity of the soil [g/cm^3]
Ohno et al. (1984)	$V_p=2.25d^{1.94}$	V_p: critical velocity [cm/s^1] d: particle size [mm]

If Terzaghi's law is applied to the data, then the critical hydraulic gradient is 1.01 for Narita-sand and 1.13 for the River sand. These values confirmed that Terzaghi's equation gives a too high critical hydraulic gradient for clogging issues. Compared to that when Sichardt's equation was applied to the data, the critical hydraulic gradient for River sand No.1, No.2, No.3, and No.4 will be 0.24, 0.31, 0.8, and 0.01, respectively. For Narita Sand No.1 and No.2 is i=0.44 and 0.38, respectively. From these results it can be concluded that Sichardt's assumption seems to be applicable in field injection systems.

For determining critical velocity, Koslova carried out an equation by using experiments with well graded soil (Shindo 1967, Okajima and Tanaka 2008). Koslova's equation represents for which velocity a small particle of diameter `d`, that exists between the particles of diameter `D`, starts moving (Figure 3.11).

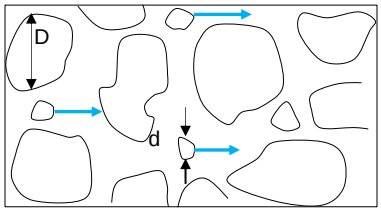

Figure 3.11－Representation of d and D of the Koslova equation. Koslova's equation represents at which velocity a small particle of diameter `d` that exists between the particles of diameter `D` starts moving.

Because the effective size of a soil sample is difficult to determine, Justin (1924) recommended that a safety factor of 4 to the theoretical critical velocity value can be applied for practical utilization. Kubota (Japanese Geotechnical Society, 1965) published critical velocities regarding the particle sizes of a narrow range calculated from experimental results. Unfortunately, neither experimental method nor the calculation method was explained. Ohno et al. (1984) obtained an empirical equation for critical velocity from experimental data with uniform particle sizes and shapes. In case of a wide range of particle sizes, they found that the movement of particles below the size of 25 - 32 mm are to be considered for piping; thus, D_{25} should be used for determining the critical velocity. Nakashima et al. (1986) obtained the experimental data by observing the movement of particles with x-ray radiography. The results showed that the data are nearly approaching to that obtained by Ohno et al. (1984). There are some other reports in the pertinent literature referring to critical velocity or critical hydraulic gradient with experimental data results. One point is evident in each of these studies that the theoretical critical hydraulic gradient introduced by Justin is greater than the value obtained from experimental data of each study. Another question arises to which extent the study on piping can be applied to clogging phenomena because piping describes an expansion of the flow path way, whereas clogging has the opposite effect.

A comparison of the critical hydraulic velocities between the axisymmetric experimental data and previous studies is shown in Figure 3.12.

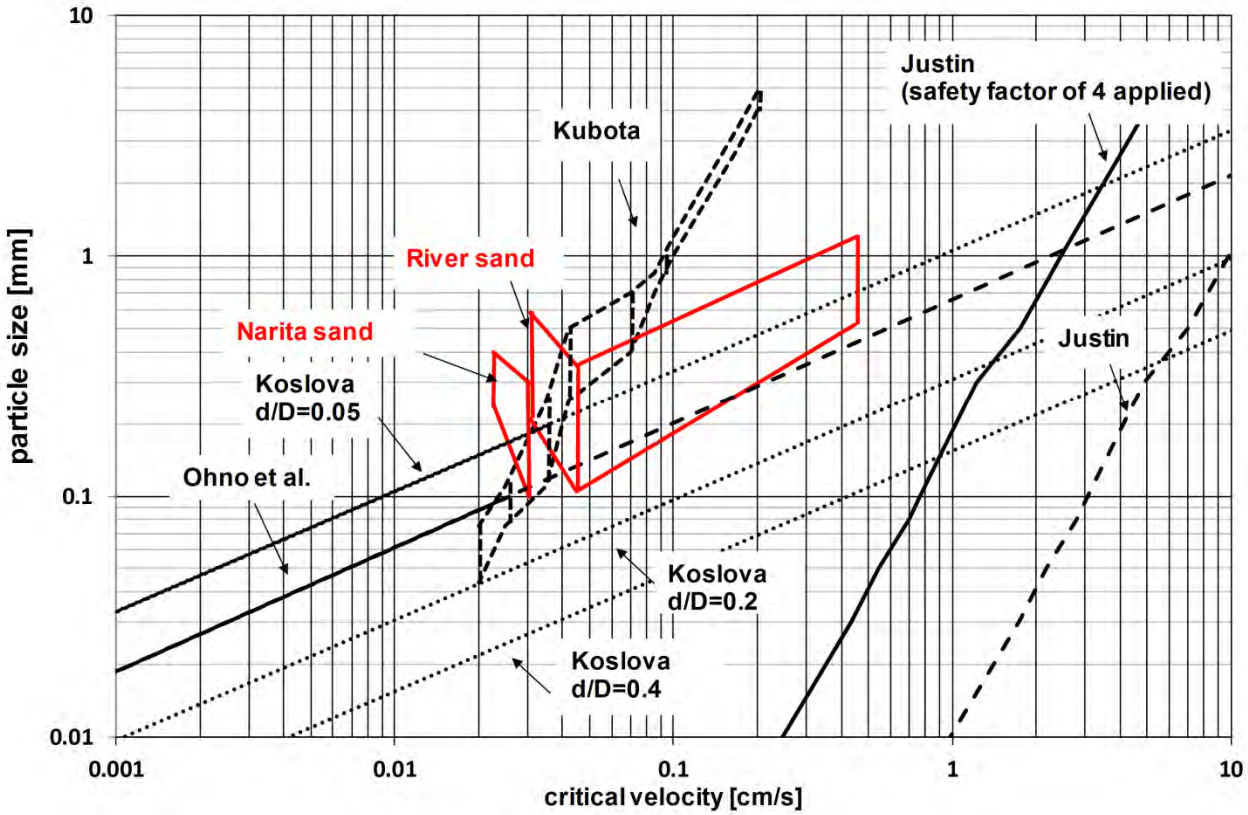

Figure 3.12－Comparison of experimental results and previous studies on critical velocity regarding to particle size.

From Figure 3.12, it can be concluded that the experimental results are in agreement with other studies except Justin's equation. Thus, Justin's equation leads to an overestimation of the critical velocity, even when the safety factor of 4 will be applied. In contrast to Justin's equation, Ohno's equation seems to be more applicable for physical clogging problems despite its application for piping effect.

3.1.3 Conclusions

In the present study, a one dimensional and a two-dimensional axisymmetric aquifer models were constructed in order to define the critical hydraulic gradient during injection of water. The following conclusions were obtained:

(1) The experimental results showed that mobilization of fine particles initially present in the aquifer should also taken into account for physical clogging.

(2) The mobilization velocity or critical hydraulic gradient should be used as a guidance for reverse pumping in order to unclog the aquifer.

(3) In the one-dimensional experiments, the results show that not only fine particles ($\leqq$ 0.106 mm) are mobilized during injection, but also the particles ranging between 0.25-2 mm presented their movement.

(4) Particularly for the higher hydraulic gradient (i=0.3), particles of bigger sizes were mobilized.
(5) Furthermore, after Darcy`s law (Equation 3.1), with increasing hydraulic gradient, the velocity of injected water will increase.
(6) Thus, when the hydraulic gradient will be too high then the following high velocity causes a fast movement of particles what finally results in a accumulation of particles near the injection point. This was also observed in present experiments.
(7) In the axisymmetric experiments, a critical hydraulic gradient of 0.3 was determined when the soil included the particle having sizes below 0.104 mm.
(8) When comparing the results from axisymmetric groundwater model with the previous studies on critical velocity (Figure 3.12), a good agreement with the data of Ohno and Koslova was obtained.
(9) A comparison of the critical hydraulic gradient approaches from Terzaghi and Sichardt showed that for the one-dimensional experimental data both equations do not agree with the results.
(10) For the two- dimensional axisymmetric groundwater model, Terzaghi's equation again results in too high value of hydraulic gradients.
(11) But for Sichardt's equation, the resulting hydraulic gradients agree with the experimental data.
(12) The two models showed different results and it can be concluded that one dimensional laboratory experimental results have to be confirmed in the field tests.
(13) The one-dimensional groundwater model provided information about the processes during injection, it was obtained that particles of bigger sizes were mobilized and pushed smaller particles aside, thus smaller particles start to accumulate and a clogging zone is build.
(14) When the hydraulic gradient is too low, the bridges of the accumulated fine particles become difficult to break, thus permeability continuous to decrease.
(15) From the two-dimensional (axisymmetric) aquifer model it was obtained that it is possible to apply research on piping effect to physical clogging due to particle mobilization problems.
(16) The critical hydraulic gradient, carried out by Sichardt fitted best with experimental data, what indicates that the two dimensional experiment gives more realistic results and is more capable for field application.

3.2 STUDY ON CLOGGING PREVENTION IN OPEN LOOP HEAT PUMP SYSTEMS DUE TO IRON REMOVAL FROM GROUNDWATER

3.2.1 Introduction

Readily available groundwater with constant water temperatures allows for techniques relying on groundwater acting as a heat pump to be employed cost effectively and efficiently. Open loop heat pump systems (OLHPS) uses pumped groundwater for cooling or heating of a building and re-inject it into the aquifer. The aim is to store the excess heat energy in the summer months that can be reused for heating in the winter season and vice versa. The system is constructed by using two wells, a cold well and a warm well. In the summer months water is extracted from the cold well (ambient native groundwater or previously stored water by injection in the winter months) and passed through a heat exchanger to provide direct cooling to the building. This process warms the water that will be re-injected into the warm water well. The injected water is stored in the aquifer until the winter months, then water will be extracted from the warm water well. However, re-injection of groundwater involves a significant problem: i.e. clogging. Clogging can be distinguished between three major causes: biological, chemical and physical clogging. Iron removal methods from groundwater like ion exchange (Hódi et al., 1995), oxidation and microfiltration (Ellis et al., 2000) and biological treatment methods (Pacini et al., 2005; Seppánen, 1992) are in practice; however, these methods are expensive in terms of economics and maintenance and difficult in operation. Moreno et al. (2010) tested cow bone charcoal for its adsorption capacity for metal ions from wastewater and showed that it has ability for removal of metals. Ahmad and Jawed (2010) carried out batch and column experiments in downward flow mode by using wooden charcoal in order to estimate its adsorption capacity. They concluded that the adsorption is depending on temperature, flow rates and bed depth. However, these experiments were conducted on a small-scale and in downward flow mode without minimizing oxygen contact with water.

Generally an aquifer is under anaerobic conditions; hence, iron exists as dilute ferrous (Fe^{2+}) form. When groundwater is extracted, it gets in contact with oxygen and reacts primarily to ferric ion (Fe^{3+}) (Equation (3.8)) and secondly to iron (III)-hydroxide ($Fe(OH)_3$ (Equation (3.9)). The redox reaction can be summarized as shown in Equation (3.10).

$$4Fe^{2+}+O_2+2H_2O \leftrightarrows 4Fe^{3+}+4OH^- \quad (3.8)$$

$$4Fe^{3+}+4OH^-+8H_2O \leftrightarrows Fe(OH)_3+8H^+ \quad (3.9)$$

$$4Fe^{2+}+O_2+10H_2O \leftrightarrows 4Fe(OH)_3+8H^+ \quad (3.10)$$

The reactions are strongly dependent on parameters like pH, amount of oxygen, and temperature. For example, the oxidation of ferrous into ferric state needs a minimum

amount of oxygen of 0.15 mg O_2/mg Fe^{2+} (Mutschmann and Stimmelmayr, 1991). Iron (III)-hydroxide has a low water solubility and precipitates at low concentrations. These precipitations are commonly known as `rust`. Precipitated flakes are serious cause for clogging problems. When the extracted groundwater will be re-injected into the aquifer, these flakes may plug the voids and can decrease permeability that can cause clogging.

In order to keep the OLHPS cost efficient, an eco-friendly open loop heat pump system is required in order to make the system applicable in developing countries. Furthermore, to avoid clogging during injection of the water, iron has to be removed without oxygenation of the groundwater, whereas existing methods with aeration are not applicable and effective. In present study, wooden charcoal was tested for its ability of iron removal and compared to fine sand and volcanic ash filter materials. The experiments were conducted in an upward flow mode by avoiding oxygen contact of the groundwater by introducing nitrogen gas in experimental setup.

3.2.2 Materials and methods

The study site was located at the University of Okayama, Okayama city, Chūgoku region in Japan. The used groundwater had an average temperature of 18 ºC and contained 10.85 mg/L ferrous ions having a pH of 6.61 and electronic conductivity (EC) of 43 mS/m.

Vertical columns of 30 cm height and 10 cm diameter were prepared in the laboratory. Each column had total 6 ports, each port is 5 cm apart from each other for water sampling as shown in Figure 3.13. The pump (TERAL THP-V150S) from the well was directly connected with an enclosed tube and the constant head water supply tank. The water supply tank was sealed in order to minimize oxygen intrusion. In addition, nitrogen gas was connected in order to displace oxygen in the tank. The overflow water from the supply tank was controlled by leading into a second (drainage) tank in order to keep the pressure in the supply tank constant. Tubes from the supply tank were connected to the bottom of the columns and each outflow of the columns was connected to a constant head outflow tank.

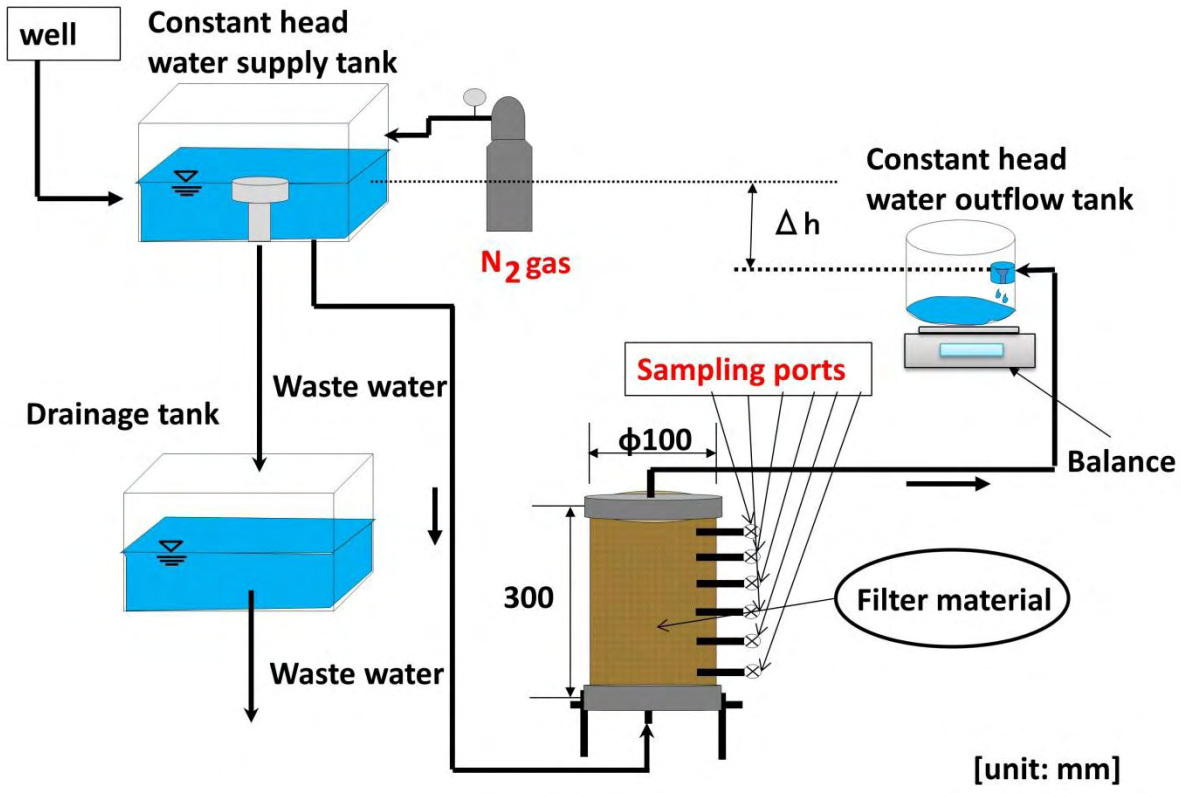

Figure 3.13－Experimental setup. The flow was controlled by a constant head supply tank and a constant head outflow tank. Each column was prepared with total 6 sampling ports. In order to minimize contact with oxygen, N_2 gas was introduced.

The columns were filled with oven dried charcoal material free from debris and inert materials. In separate columns fine sand and volcanic ash were also used for comparison. The first experiments were conducted with constant pressure head (Δh), later on the pressure head was changed in order to keep the velocity constant.

3.2.2.1 Charcoal as filter material

A well-known material for iron removal is activated carbon (Siemens Water Technologies, H2O Remediation Engineering, Ampac USA). This study aims to investigate the adsorption ability for dissolved iron ions of three cheap and easily available materials in Japan: wooden charcoal, Yamasuna sand (Igarashi and Saito, 2005), and volcanic ash (Oba et al., 1967). Especially the used wooden charcoal (2.76 YEN/kg) is compared to activated carbon particles (1.65 - 9.90 US$/kg (Marsh and Rodríguez-Reinoso, 2006)) about 50 to

320 times cheaper and may serve, due to its large surface area and various functional groups as appropriate and efficient adsorbent for the removal of dissolved iron from groundwater. The advantage in using wooden charcoal to other incombustible solid filter materials lays in its possible usage as fertilizer after incineration or decomposition of the material. Besides, Japan has a lot of unused forests and excess wood, thus, producing charcoal for water treatment may have a beneficial effect to the country. The reason why activated carbon is so effective for filtering harmful substances from water is the quite high surface area of the material. Activated carbon has about 500 – 2000 m^2/g surface area where substances can be adsorbed. Figure 3.14 shows a comparison of the surface areas of the wooden charcoal and activated carbon. The wooden charcoal was tested to have about 139- 154 m^2/g surface area which is about 1/4 of the surface area of activated carbon. However, adsorption, retention and bacteria residence is enough efficient. Figures 3.15 and 3.16 show the wooden charcoal under electron microscope, Figure 3.15 shows a picture 25 times enlarged and Figure 3.16 was 5000 times enlarged. As it can be seen in Figures 3.15 and 3.16, many pores are available for high potential for adsorption, water retention and accumulation of bacteria. Further characteristics on the wooden charcoal used in this study were prepared by 'JFE Recycling Management Japan' and are listed in Table 3.5 - 3.7.

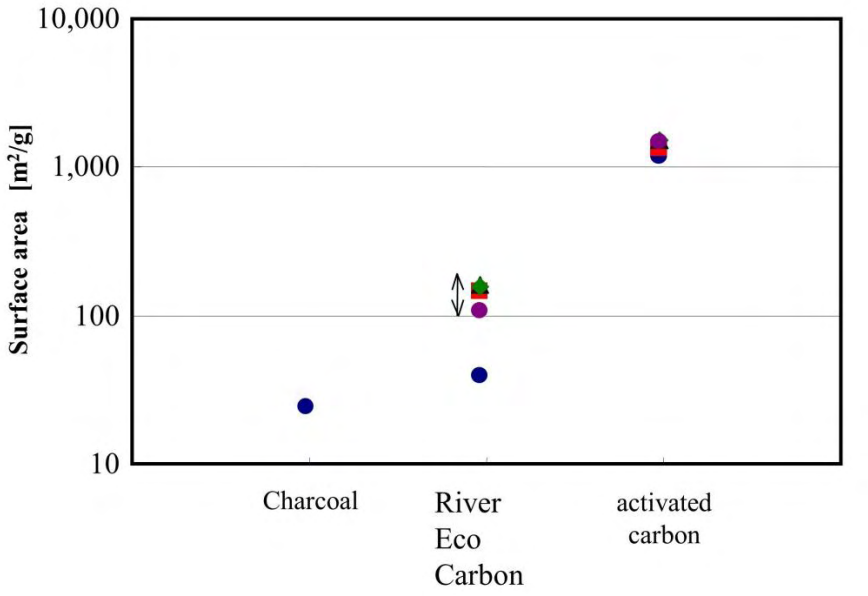

Figure 3.14—Comparison of the surface areas of wooden charcoal (River eco carbon) and activated carbon. [JFE Recycling Management Japan]

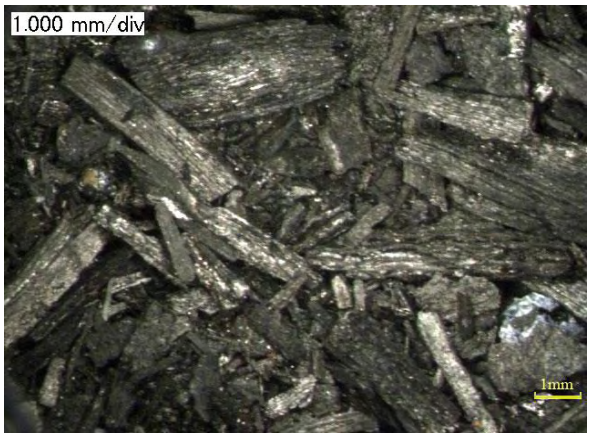

Figure 3.15－Microscope enlarged picture of used wooden charcoal (25 times enlarged).

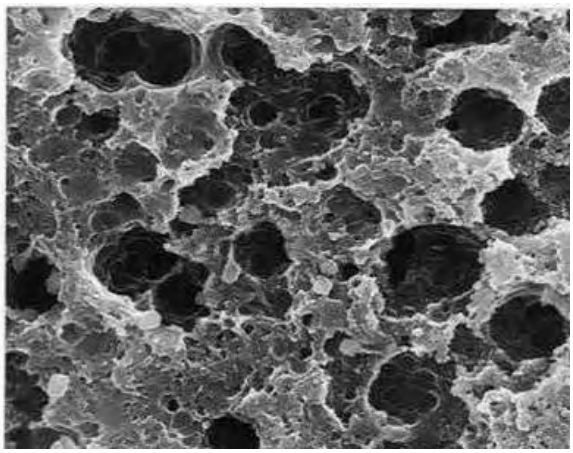

Figure 3.16－Microscope enlarged picture of used wooden charcoal (5000 times enlarged). [JFE Recycling Management Japan]

Table 3.5－Characteristics of the wooden charcoal tested for dry matter (except moisture).

Items		Unit	Result	Detection limit
Moisture		%	9.1	0.1
Ash	(Ash)	%	9.8	0.1
Volatile matter	(VM)	%	3.4	0.1
Fixed carbon	(FC)	%	86.8	0.1
Higher calorific value		kJ/kg	36,100	150

Table 3.6－Content test result of the wooden charcoal tested for dry matter (except moisture).

Element			Result	Detection limit	Standard
Arsenic	(As)	mg/kg	3.4	0.15	50
Cadmium	(Cd)	mg/kg	< 0.50	0.50	5
Total mercury	(Hg)	mg/kg	< 0.05	0.05	2

Table 3.7－Leaching test result of the wooden charcoal tested for dry matter (except moisture).

Element			Result	Detection limit	Standard
cadmium	(Cd)	mg/ℓ	ND	0.01	0.3
lead	(Pb)	mg/ℓ	ND	0.005	0.3
chromium VI	(Cr^{6+})	mg/ℓ	ND	0.03	1.5
total mercury	(T-Hg)	mg/ℓ	ND	0.0005	0.005
alkyl mercury		mg/ℓ	ND	0.0005	ND
selenium	(Se)	mg/ℓ	0.006	0.003	0.3
total cyanide	(CN)	mg/ℓ	ND	0.02	1.0
organic phosphorous		mg/ℓ	ND	0.1	1.0
polychlorinated biphenyl	(PCB)	mg/ℓ	ND	0.0005	0.003
arsenic	(As)	mg/ℓ	0.0049	0.0025	0.3
pH	(at 18.3℃)	—	10.0		

3.2.2.2 Constant pressure head experiments

For the experiments conducted under constant pressure head, three materials were tested for their filtering capacity in order to remove iron from pumped groundwater. Table 3.8 represents a summary of the soil characteristics that were used in the experiments.

Table 3.8－Characteristics of the materials used for experiments under constant pressure head

	Unit	Charcoal (0)	Fine sand (0)	Volcanic ash
Specific surface area	[m^2/g]	139 – 154	—	—
Permeability	[cm/s]	$1.0x10^{-1}$	$4.7x10^{-2}$	$4.9x10^{-2}$
Porosity	[-]	0.67	0.39	0.90
Specific gravity	[g/cm^3]	1.45	2.74	2.29
D_{10}	[mm]	0.12	0.14	0.11
D_{60}	[mm]	0.70	0.70	0.38

Yamasuna (fine sand) collected in the Chiba prefecture, and Shirasu, a fine white pumiceous, fine grained volcanic ash typically found in Kyushu, south western part of Japan were used in experiments. The particle size distribution curves are shown for charcoal, fine sand and volcanic ash in Figure 3.17.

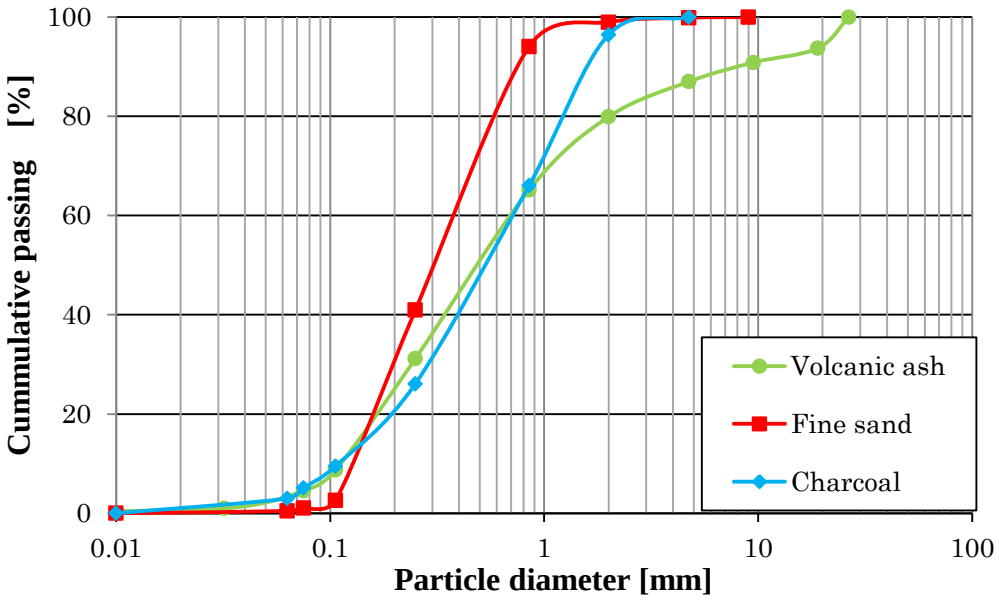

Figure 3.17—Particle size distribution curves of the three tested filter materials charcoal, fine sand, and volcanic ash.

3.2.2.3 Constant velocity experiments

In order to determine the adsorption capacity of filtering materials under constant velocities, the materials charcoal and sand (volcanic ash was not considered any further because of its non-applicability due to low filtering ability) were tested in a second series by changing the pressure head in order to keep the velocity constant throughout the experiments. When iron concentration was detected in the outflow tank, the experiments were stopped and the filter material was taken out in 2-3 cm layers in order to measure the total iron contents. The experiments were conducted by determining the porosity of iron columns and calculating the velocity by using different retention times of the contaminated water in the filter medium. The experimental characteristics are listed in Table 3.9.

Table 3.9—Experimental characteristics of the experiments under constant velocity.

		Fine sand (A)	Fine sand (B)	Charcoal (A)	Charcoal (B)	Charcoal (C)
Dry mass	[g]	3586.7	4293.8	813.9	532.1	766.6
Porosity	[-]	0.38	0.40	0.61	0.59	0.85
Retention time	[min]	15.0	15.0	15.0	30.0	45.0
Velocity (margin of error)	[cm/s]	1.8E-2 (±7%)	1.6E-2 (±20%)	1.7E-2 (±9.8%)	8.4E-3 (±10%)	4.2E-3 (±10%)

3.2.3 Results and discussion

3.2.3.1 Experiments under constant pressure head

During the operation of the experiments system conditions, oxygen level at the well and in front of the column inlet, temperature, electronic conductivity (EC) and flow rate were recorded. The oxygen level at the well could be obtained constant at 0.5 ppm. Table 3.10 shows the measured parameters during the experiment. A slight increase of the room temperature due to increase of air temperature could be noted. The changes in EC from the inlet of the column until the outlet occurred from reactions and adsorption in the filter medium and are negligibly low.

Table 3.10－Measured system conditions during the experiments under constant pressure head.

Dissolved oxygen at the well (DO) [ppm]	0.5
Room temperature（laboratory）[℃]	23.7 (±1.8) Max: 26.7 ; Min: 20.3
pH （charcoal filter columns）[-]	Column inlet： 6.74 (±0.04) Column outflow： 6.95 (±0.09)
Electronic conductivity (EC) (charcoal filter columns）[mS/cm]	Column inlet： 0.44 (±0.01) Column outlet： 0.45 (±0.03)

The flow rate of each column was also measured during the experiments, thus the filter velocity over experiment time could be determined, shown in Figure 3.18. Point A in Figure 3.18 indicates the point until the pressure was unstable due to entrapped air remained in the column after packing. B in Figure 3.18 indicates back flushing with resulting recover of the flow rate. When back flushing was conducted, small particles (iron flakes) were observed (Figure 3.18). These flakes are thought to occur during pumping because the oxygen level right after the pump was 0.5 mg/L and the chemical reaction starts already when 0.15 mg oxygen per mg ferrous (Fe^{2+}) ion are available. Thus, it is unpreventable that iron precipitates before filtering.

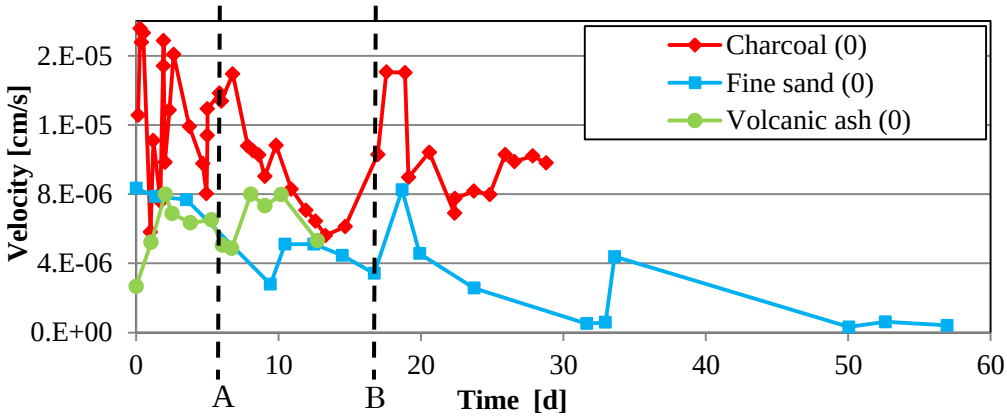

Figure 3.18—Changing of velocity of the experiments under constant pressure head. Until point A :fluctuation of velocity because of pressure variances in the water supply tank and also because of possible air in the micro pores of the filter medium at the beginning of the experiments. At point B: the velocity could be recovered by back flushing of the filter columns.

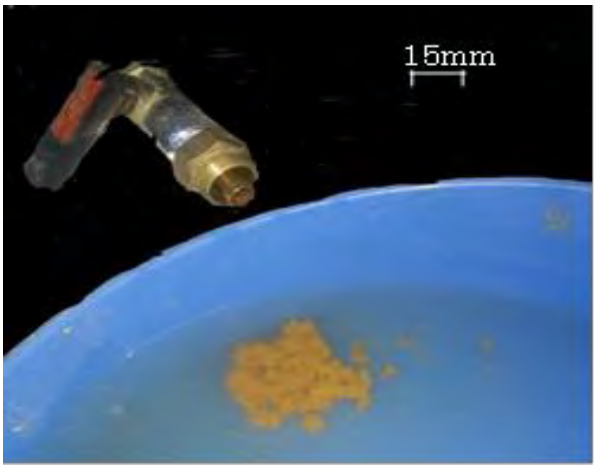

Figure 3.19—Picture of the outflowing iron precipitates during back flushing.

After a breakthrough of dissolved iron concentration at the outlet tank was observed, the experiments were stopped. For volcanic ash the breakthrough was the fastest within 13 days, hence, the material is not considered to be an appropriate filter material, and therefore, was not considered in any further experiments. Charcoal (0) and fine sand (0) showed adsorption potential for dissolved iron and thus were chosen for further investigations. The breakthrough curves of relative dissolved iron concentration in the columns after a breakthrough in the outlet tank could be observed and depicted in Figures 3.20 - 3.22. The curves are plotted according to various filtered water volumes. The fine sand (0) column filtered iron contaminated water for 66 days, whereas the charcoal (0) column only filtered for 35 days. But when the filtered volume of water will be considered,

the charcoal (0) column filtered 2.8 times more water (2471.7 L) than the fine sand (0) column (867.9 L).

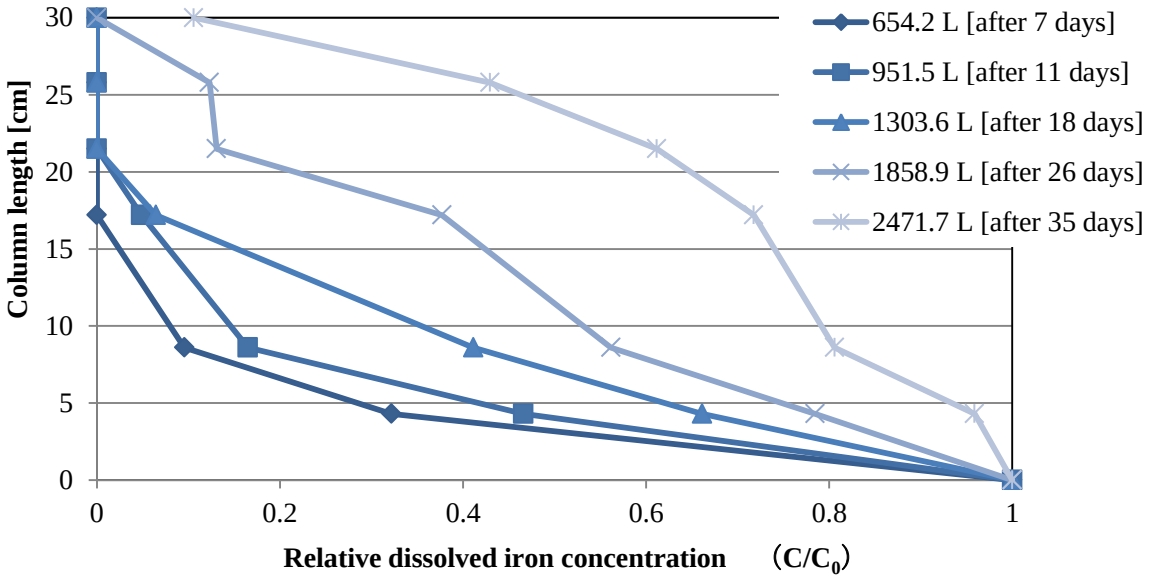

Figure 3.20－Breakthrough curves of the charcoal (0) filter column under constant pressure head condition, plotted according to various filtered water volumes.

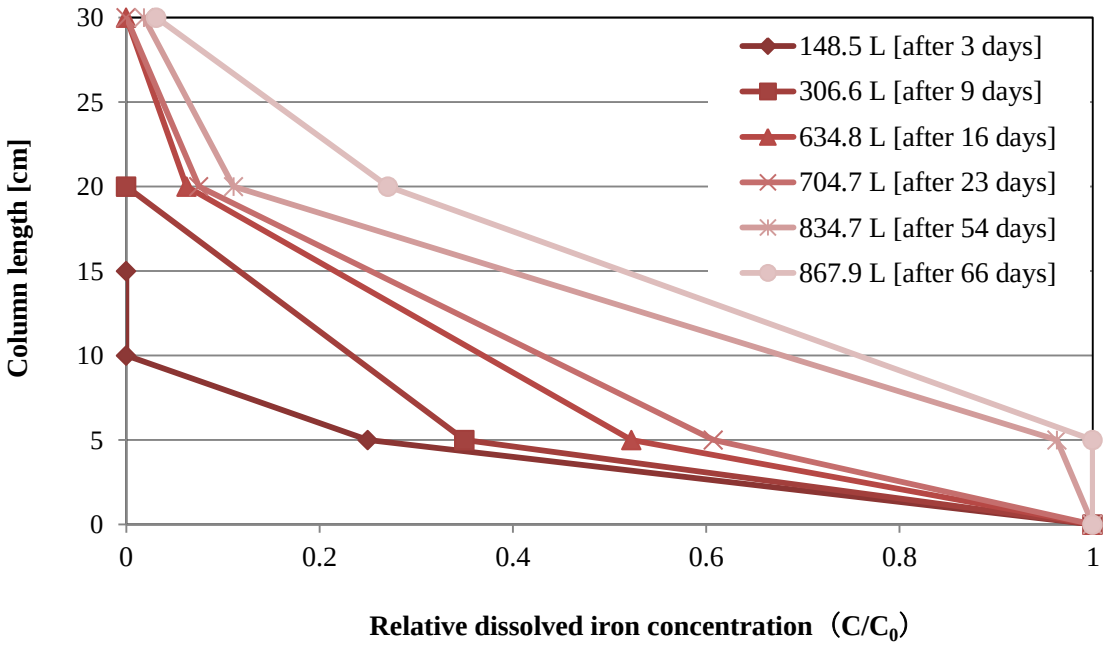

Figure 3.21－Breakthrough curves of the fine sand (0) filter column, plotted according to various filtered water volumes under constant pressure head condition.

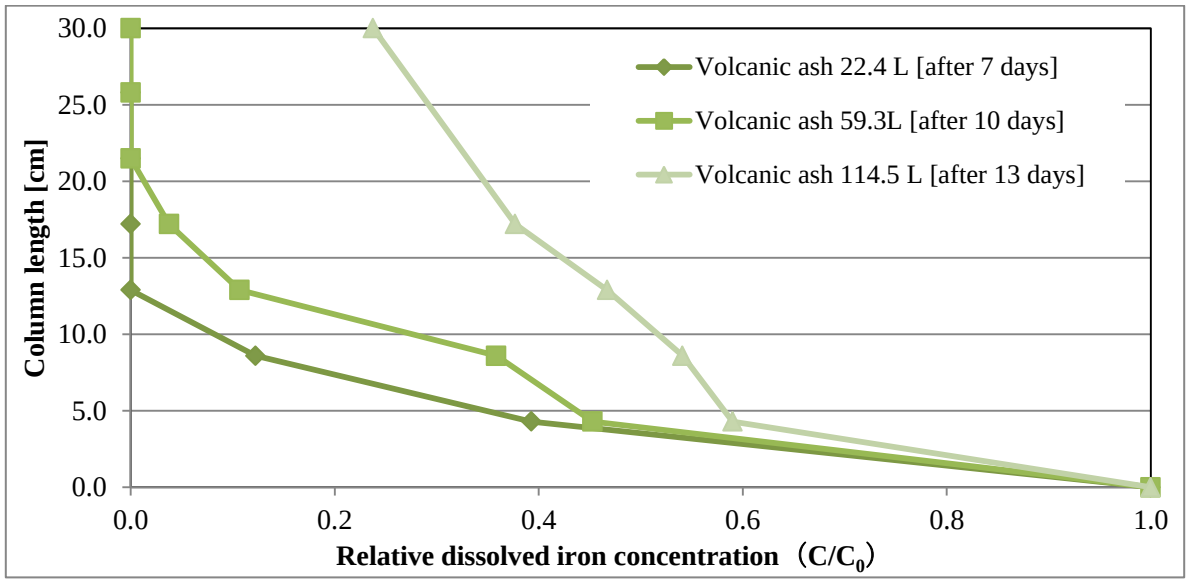

Figure 3.22－Breakthrough curves of the volcanic ash filter column, plotted according to various filtered water volumes under constant pressure head condition.

3.2.3.2 Experiments under constant velocity

By considering the porosity and residence times (15, 30 and 45 minutes) of the groundwater in the filter medium, the experiments were conducted with constant velocity. During the operation, the velocity, outflow rate and permeability of the filter were recorded. The velocity changes over experimental time are shown in Figure 3.23. For every column the permeability curve goes down during the first two days of operation time. Nevertheless, because of iron precipitates which could not be avoided due to pumping, the inlet connection of the columns got blocked during experiments. To remove the blockage of these precipitates the columns were back flushed from time to time, which can be seen in the small increases in permeability indicated by the vertical dotted lines with the letter 'B' in Figure 3.23. The fluctuations at the beginning of the charcoal (C) filter with 45 minutes residence time and the maximum increase in permeability at the end of the charcoal (B) with 30 minutes residence time indicating removal of trapped air bubbles in the filter medium which was also observed visually in the tubes during the experiments.

Regarding sand, the material proved to be inappropriate as a filter material. The fine sand column occurred to be blocked as it was observed in velocity decrease. Even removal of the precipitates from the inlet through back flushing did not increase the velocity. It is assumed, that as a consequence of fine particle movement, the flow path ways got blocked and thus velocity decreases with time. A second sand column was prepared (fine sand (B)) with washed sand material by using sieve size of 0.2 mm opening to clarify the influence of suspended matter on the clogging phenomenon. But even the washed sand filter column

resulted in rapid velocity decrease without any possibility to recover. This problem is due to physical clogging, hence, it was concluded that sand is not practicable as a filter material for large amounts of water for iron removal from groundwater.

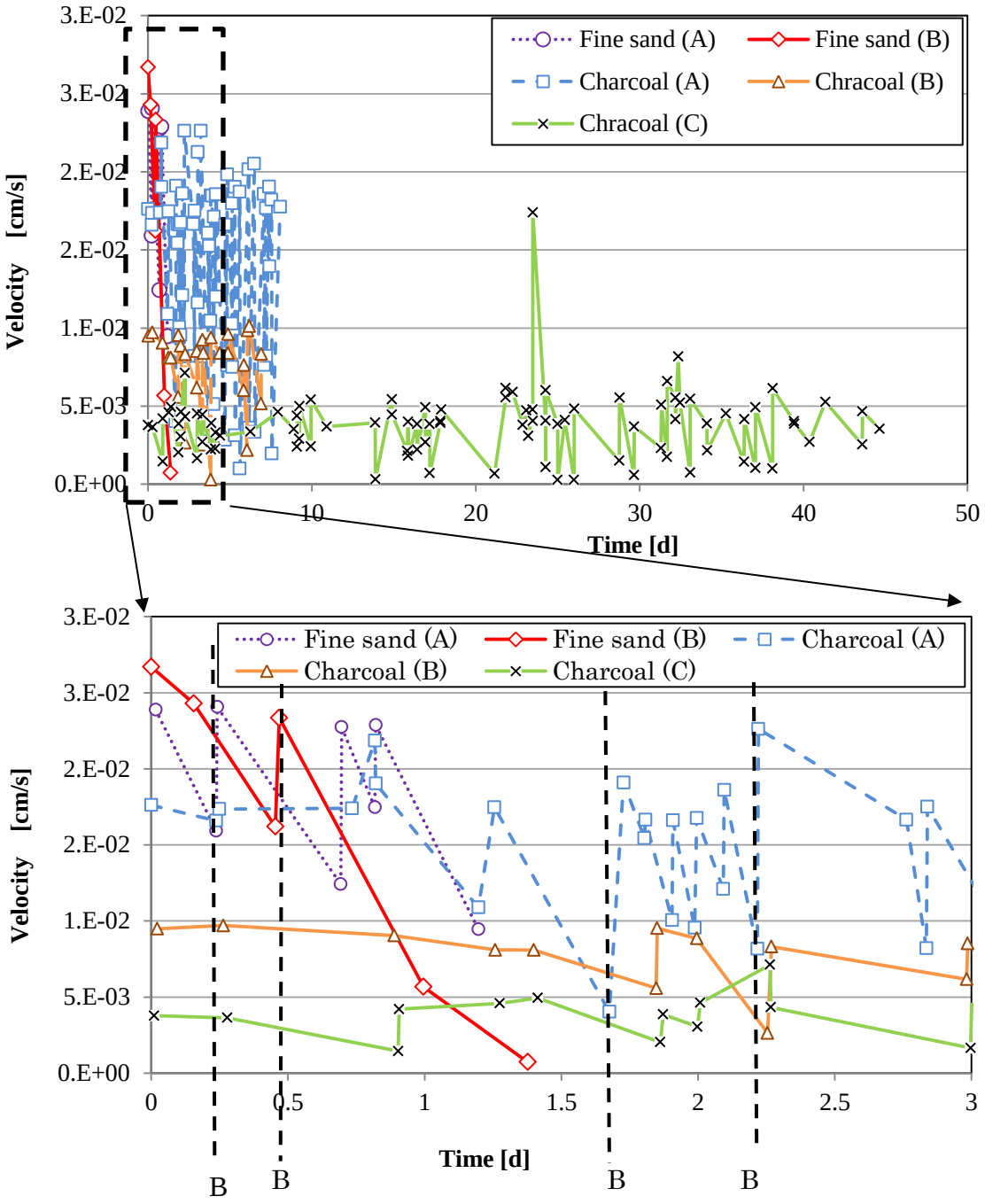

Figure 3.23－a) Velocity changes for full experimental time. b) Plotted for the first three days, and their recover through changing pressure head and back flushing. Some back flushing times are indicated by the vertical dotted lines and the letter 'B'.

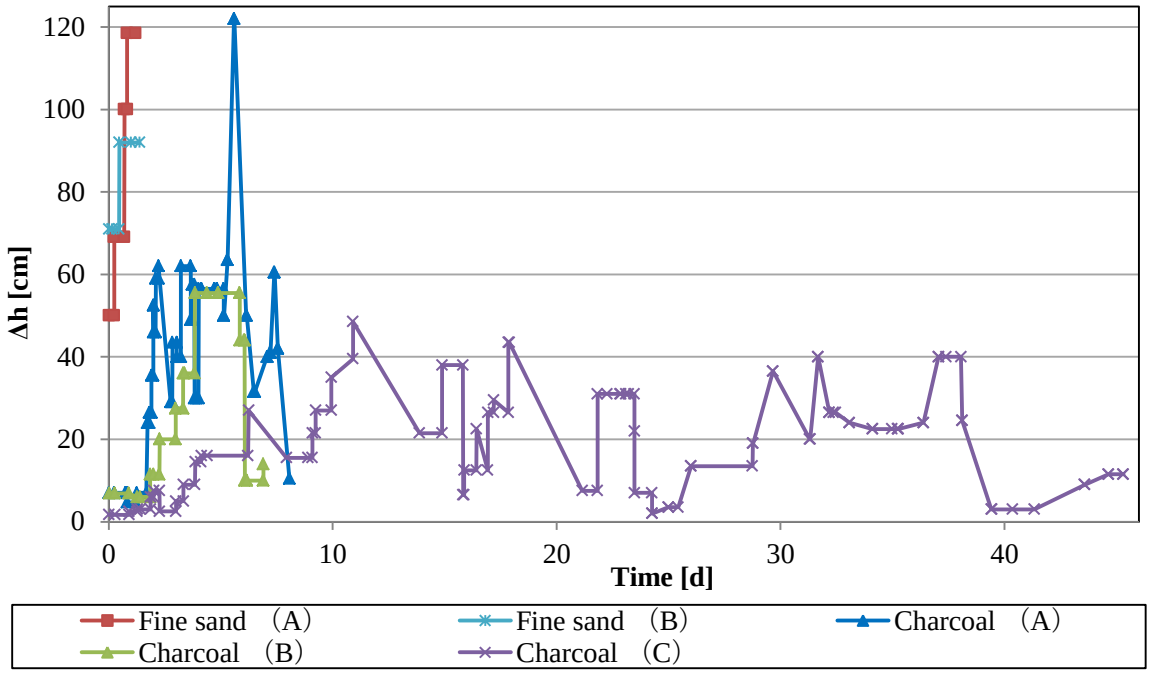

Figure 3.24－Pressure head changes during the experiment in order to adjust the velocity of each column. For the sand column, soon the maximum pressure head difference was reached due to physical clogging occurrence.

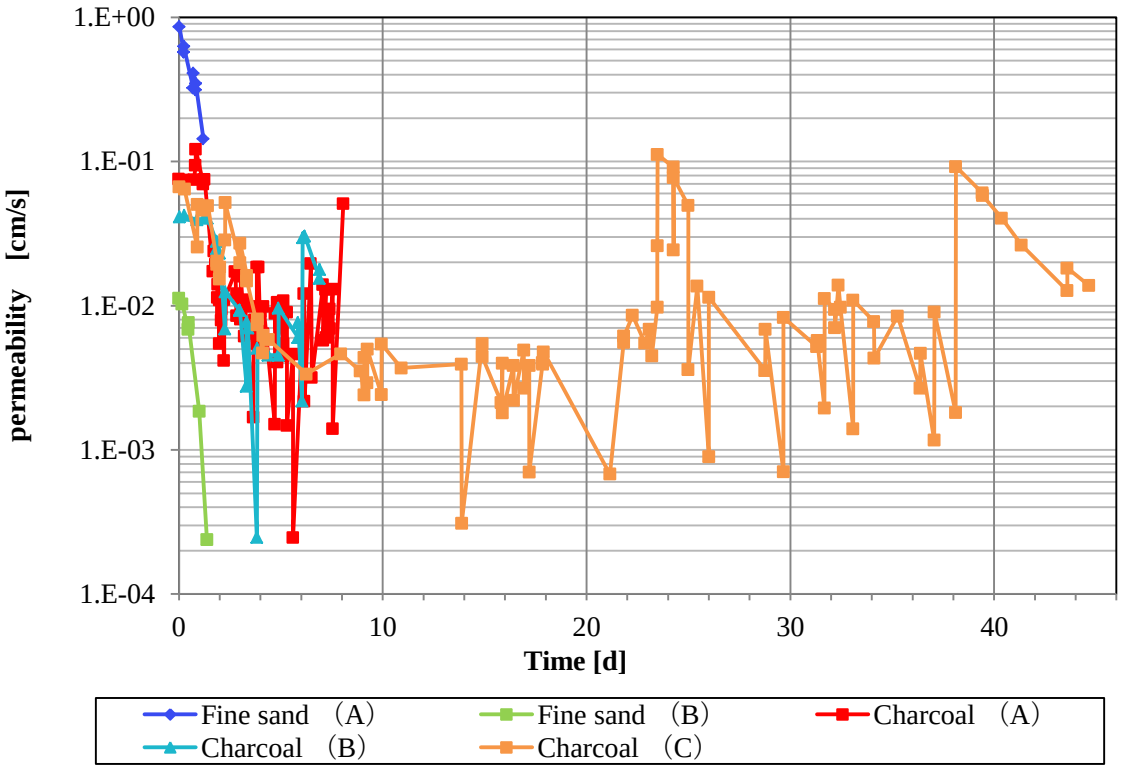

Figure 3.25－Permeability change over experimental time.

The breakthrough curves of relative dissolved iron concentrations in the columns after a breakthrough in the outlet tank were observed and are shown in Figs. 3.26 - 3.30. The obtained curves are plotted according to various filtered water volumes. The volume of water which passed the column until the breakthrough of iron concentration was 891 L for charcoal (A), 541 L for charcoal (B) and 1007 L for charcoal (C) column.

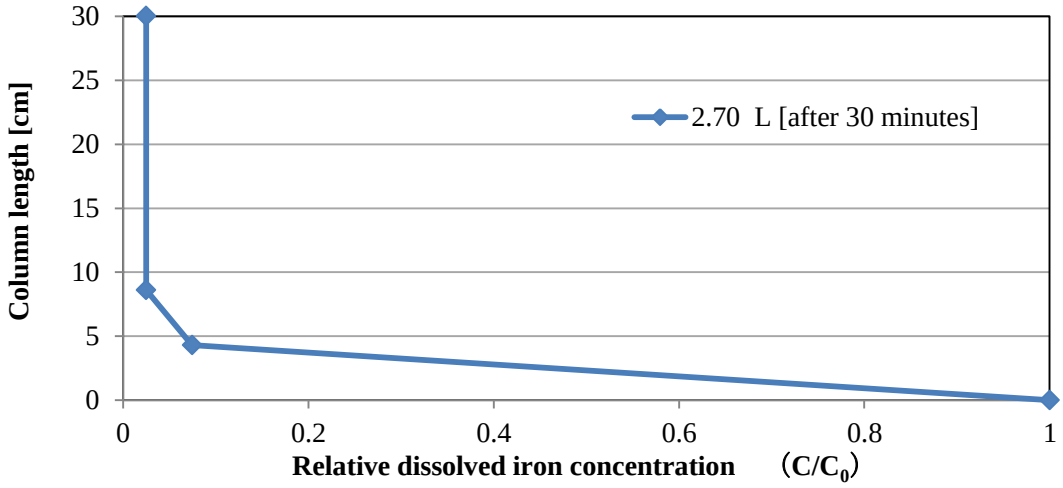

Figure 3.26－Breakthrough curves of relative dissolved iron concentration in column Fine sand (A) after various filtered water volumes. Stop of column after 106 L filtered water due to decrease in flow rate caused by clogging.

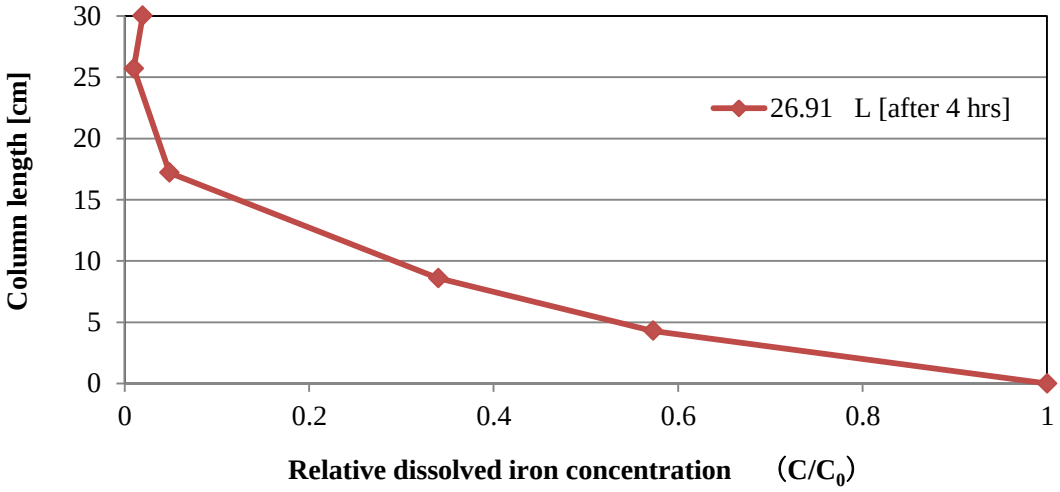

Figure 3.27－Breakthrough curves of relative dissolved iron concentration in column Fine sand (B) after various filtered water volumes. Stop of column after 130 L filtered water due to decrease in flow rate caused by clogging.

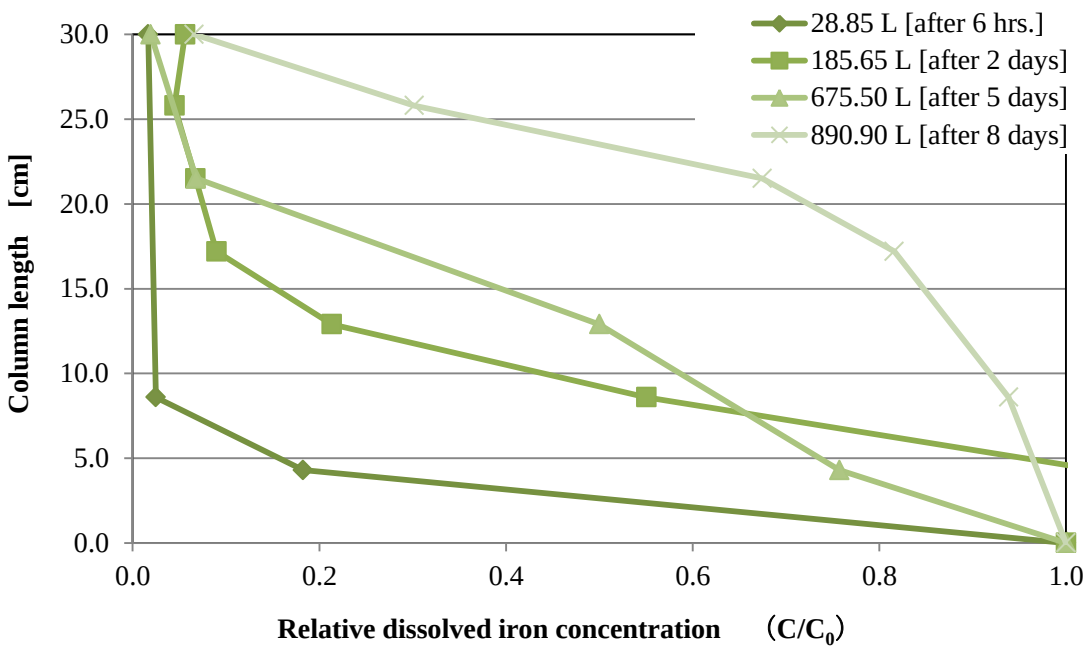

Figure 3.28－Breakthrough curves of relative dissolved iron concentration in column charcoal (A) after various filtered water volumes. Stop of column after 891 L filtered water due to breakthrough at outlet.

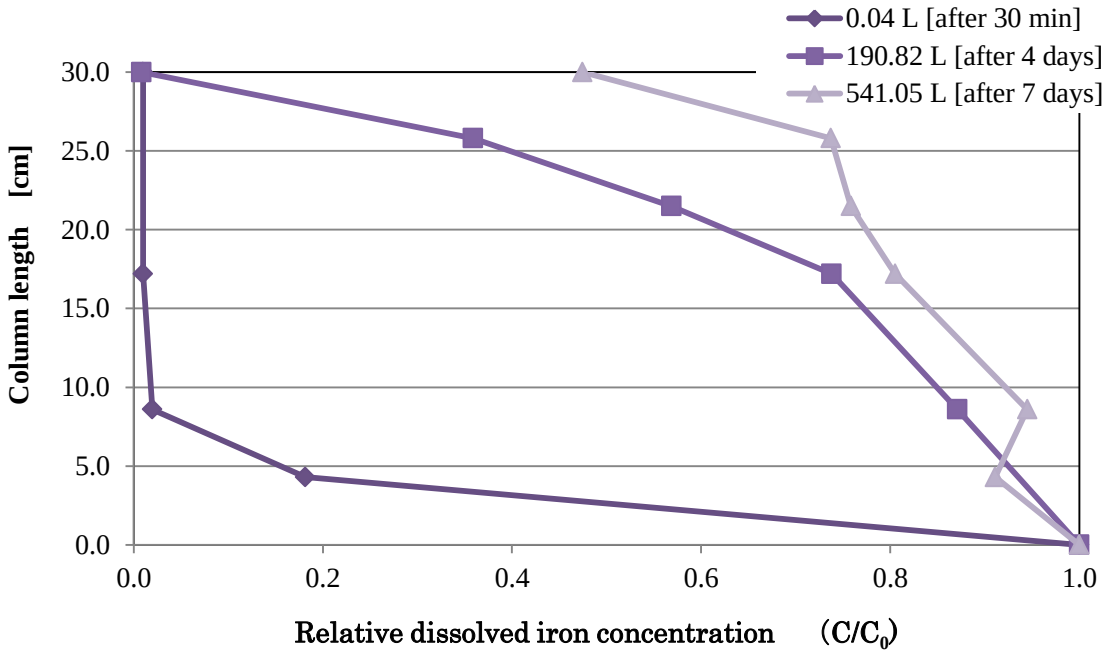

Figure 3.29－ Breakthrough curves of relative dissolved iron concentration in column charcoal (B) after various filtered water volumes. Stop of column after 541 L filtered water due to breakthrough at outlet.

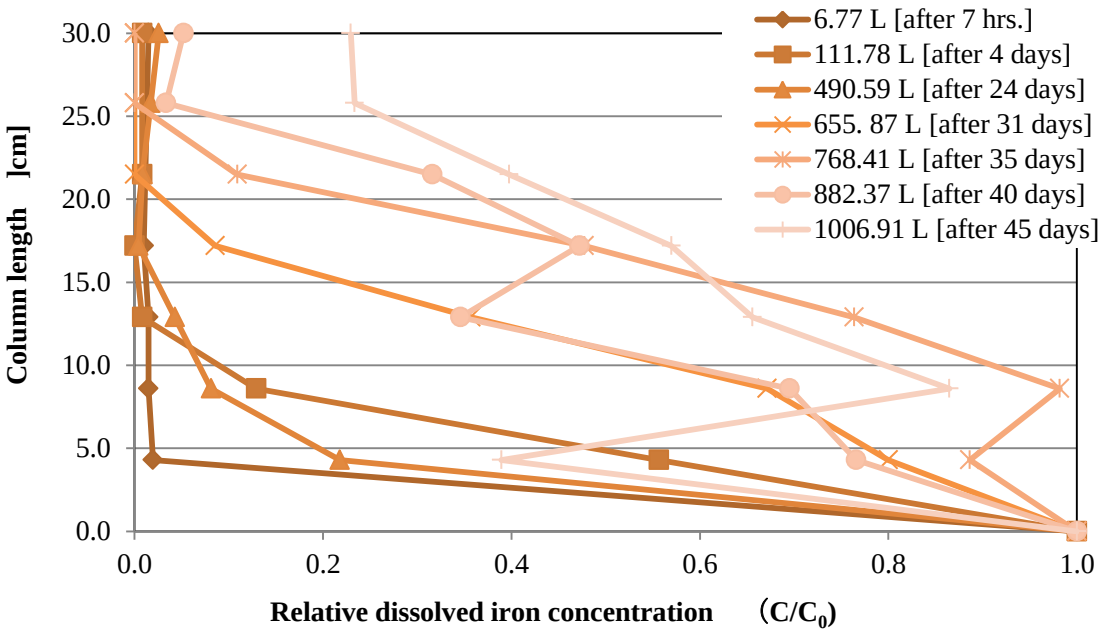

Figure 3.30－Breakthrough curves of relative dissolved iron concentration in column charcoal (C) after various filtered water volumes. Stop of column after 1007 L filtered water due to breakthrough at outlet.

In order to determine the retained amount of total iron in the charcoal material, the filter material was separated into 2-3 cm layers, dried in the oven for 24 hours and the total iron content for each layer was determined (pictures in Appendix A 40 – A 41). Due to iron precipitates, the first 5 cm of the columns showed extremely high total iron contents in the charcoal material. Hence, these values were neglected for retention capacity calculation. Furthermore, charcoal has an average blank total iron concentration of 1.5 g iron per kg dry coal mass. Figures 3.31 - 3.34 show the measured iron content of the filter materials for each charcoal column experiment. For the charcoal (0) column experiment conducted under constant pressure head condition, average total iron content of the middle part of the column (15 - 20 cm) has been observed to be 2.3 g iron per kg dry charcoal indicating an iron uptake of 1.3 g iron per kg dry charcoal. Hence, this column under its conditions had a retention of 1.3 g iron per kg dry charcoal in the charcoal material, which was low compared to other experiments. For the columns under constant head velocity conditions, different results were obtained. For column charcoal (A) with a retention time of 15 minutes of the contaminated water, the total iron content was observed at the initial two-third of the column length to be 4.6 g iron per kg dry charcoal which means an iron retention of 3.55 g iron per kg dry charcoal compared to the initial iron content of 0.85 g iron per kg dry charcoal. Compared to that the retention capacity of charcoal (B) and (C) was also obtained to be 3.5 g iron per kg dry charcoal.

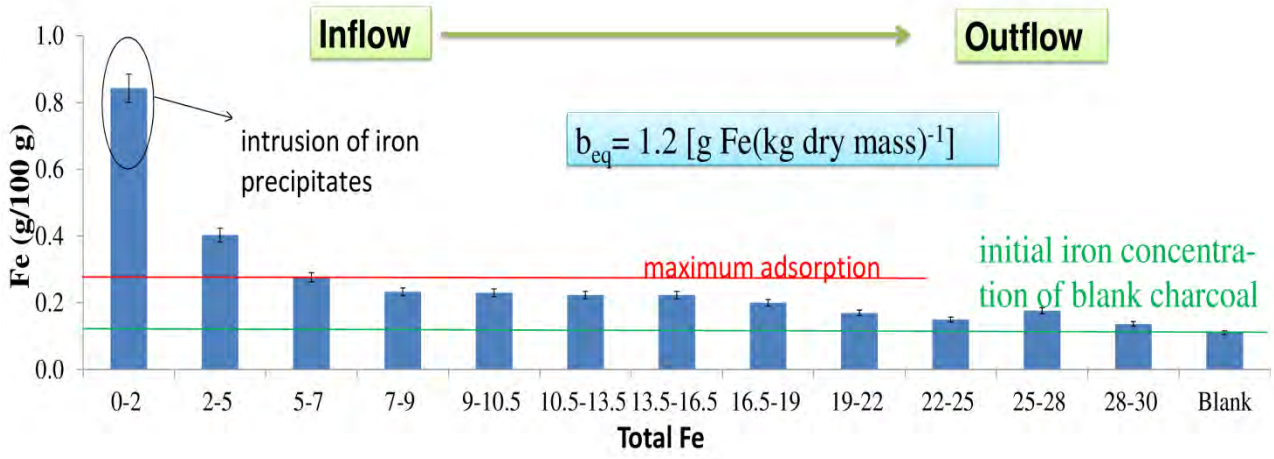

Figure 3.31－Iron content per 100 g dry mass of charcoal for various column lengths from the outlet of column under constant pressure head condition (charcoal (0)).

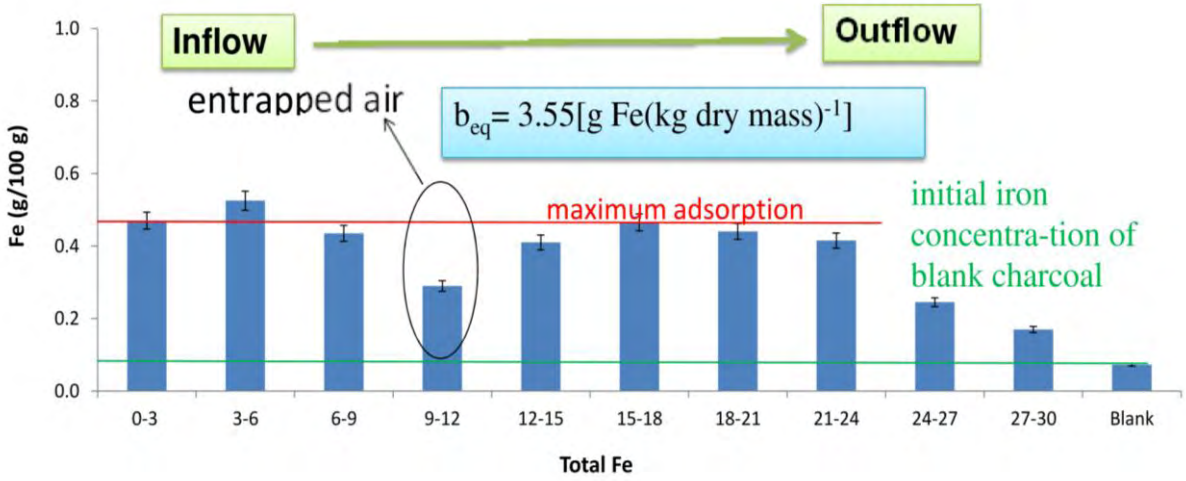

Figure 3.32－Iron content per 100 g dry mass of charcoal for various column lengths from the outlet of column charcoal (A) under constant velocity condition.

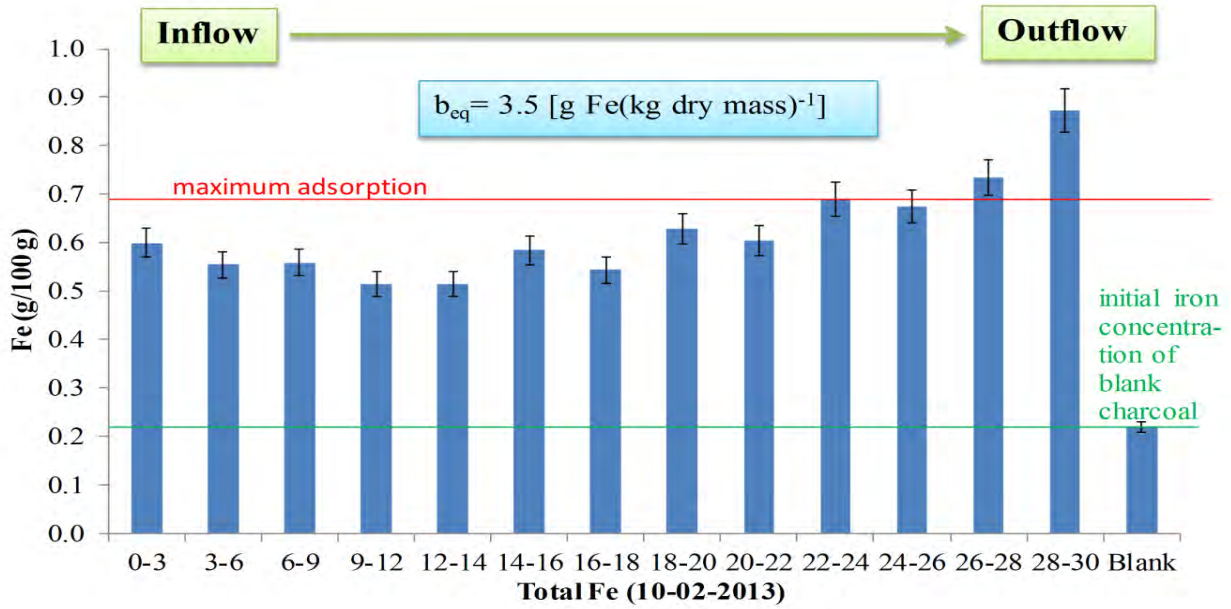

Figure 3.33— Iron content per 100 g dry mass of charcoal for various column lengths from the outlet of column charcoal (B) under constant velocity condition.

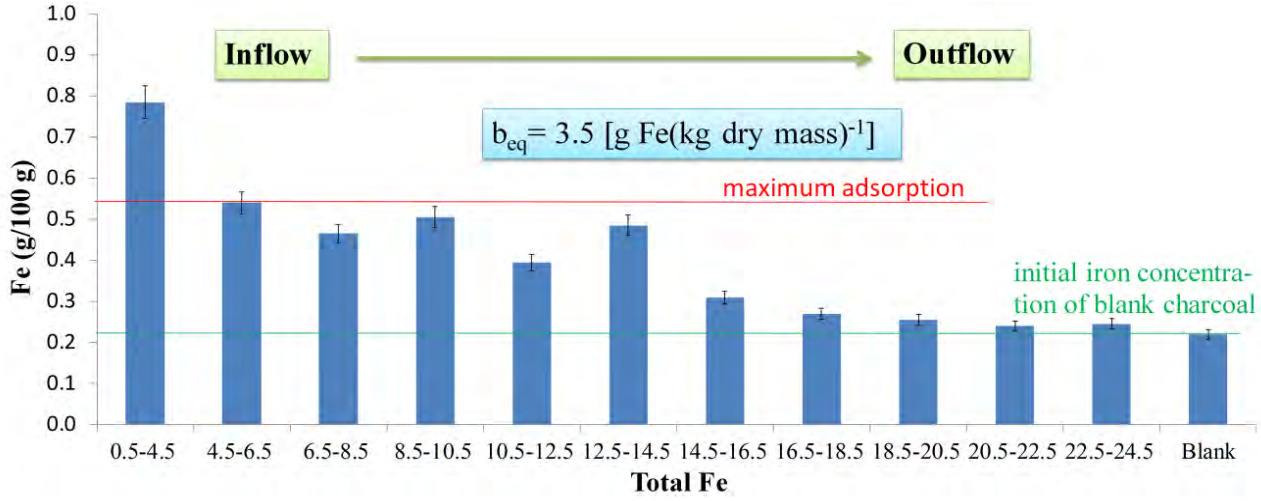

Figure 3.34—Iron content per 100 g dry mas of charcoal for various column lengths from the outlet of column charcoal (C) under constant velocity condition.

The experiments with charcoal under different velocities or rather retention times of iron contaminated groundwater showed that if a high amount in a short times is focused then the charcoal (A) with 15 min retention time and a velocity of 0.08 L/min showed a high potential with 891 L filtered water within 8 days. But for a long time use, the filter construction needs more filter volume. The column with 30 min retention time (charcoal (B)) did not filtered much water, only 541 L were filtered within 7 days, which makes only 60 % compared to the filtered water amount of charcoal (A) column. The charcoal (C) column filtered under a retention time of 45 min and a velocity of 0.02 L/min the most amount of iron contaminated groundwater, however, it took 45 days because of its low velocity

3.1.1 Conclusions

In this study charcoal was proposed as a new filter material in order to remove dissolved iron from groundwater and also compared to fine sand and volcanic ash. The following conclusions were obtained:

(1) Experimental results showed that wooden charcoal can be an appropriate material for the removal of iron from groundwater.

(2) Out of three tested filtering materials (charcoal, fine sand and volcanic ash), charcoal remarkably showed the best retention capacity for iron.

(3) Volcanic ash was not able to significantly retain iron, whereas, fine sand showed retention capacities; however, because of easy blocking and high velocity reduction, it can be suggested only for slow velocity filters.

(4) The experiments under constant velocity showed that charcoal (A), (B) and (C), had the same retention capacity of 3.5 g iron per kg dry charcoal. From these results it can be concluded that the retention capacity of the charcoal material does not strongly depend on the retention time or rather the velocity of the contaminated water.

(5) However, considering the filtered water volumes, charcoal (B) only filtered 60 % compared to charcoal (A), despite the lower retention time in charcoal (B) column, hence it can be concluded that a velocity of 0.04 L/min or rather a retention time of 30 min cannot be considered as an effective operation for filter application.

(6) Nevertheless, for practical application, a constant flow rate and other influencing factors on retention capacity such as temperature, pH, and/or initial iron concentration of the groundwater should be considered (Worch 2012).

(7) From the obtained experimental data it is possible to calculate the necessary dry mass of charcoal and the filter dimensions for practical use by using the retained amount by material (g iron per kg dry charcoal), the velocity and the utilization time of the filter.

(8) It is also suggested to apply a safety factor of about 30 % to consider the high dependency of retention on various factors.

(9) Nevertheless, it is highly recommended to conduct column experiments in order to determine the retained iron content for effective filter design.

(10) Because the groundwater composition is site specific and the retention behavior might be different under different conditions.

3.2 CHARCOAL WASHING

3.2.1 Introduction

When using charcoal as filter material, it has to be clarified that no turbid water will be injected into the aquifer. In order to estimate the time necessary to flush the filter material before usage, the charcoal was washed with tab water in column experiments for various filter velocities. During the experiments the outflowing water was tested according to turbidity, because it is considered as a good measure of the quality of water.

Turbidity is a measure of the degree to which the water loses its transparency due to the presence of suspended particulate matter. The more total suspended solids in the water, the cloudier it seems and the higher the turbidity. The suspended particles also help the attachment of heavy metals and many other toxic organic compounds and pesticides. Turbidity is measured in NTU: **N**ephelometric **T**urbidity **U**nits. The instrument used for measuring it is called nephelometer or turbidimeter, which measures the intensity of light scattered at 90 degrees as a beam of light passes through a water sample.

The main impact is merely esthetic; nobody likes the look of dirty water. But also, it is essential to eliminate the turbidity of water in order to effectively disinfect it for drinking purposes. The World Health Organization (WHO) provides guidelines for drinking-water quality and defines a critical value of 5 NTU, but ideally turbidity should be kept under 1 NTU.

This research shows the turbidity change over discharge volume, depending on the darcy velocity in order to investigate the water quality according to the elution of suspended solids from the charcoal.

3.2.2 Materials and Method

A cylindrical column of 30 cm height and 10 cm diameter was prepared and packed with charcoal. The column filled with charcoal was saturated and set into a pan and a constant head tank was installed at an appropriate height. The experimental setup is shown in Figure 3.35. The experiments were done by choosing nine different filter velocities (v_f). The following table (Table 3.11) shows the experimental conditions for each run.

Table 3.11－ Experimental conditions

Filter velocity v_f [cm/s]	Dry mass of charcoal m_d [g]	Turbidity after 5 seconds T_5 [NTU]	Filtered water volume until a turbidity of 2 NTU was reached $V_{w,2}$ [mL]	Equivalent filter pore volume until 2 NTU was reached $V_{n,eq}$ [-]
0.04	510.7	30.9	408-816	0.3-0.61
0.05	527.6	36.8	221	0.15
0.07	503.4	54.2	664-1329	0.50-1.00
0.07	600.0	104.7	2749	2.12
0.18	601.9	56.7	432-864	0.29-0.58
0.23	588.9	36.4	2147	1.52
0.24	481.8	90.9	2306	1.80
0.28	584.2	72.6	1299-2598	0.84-1.70

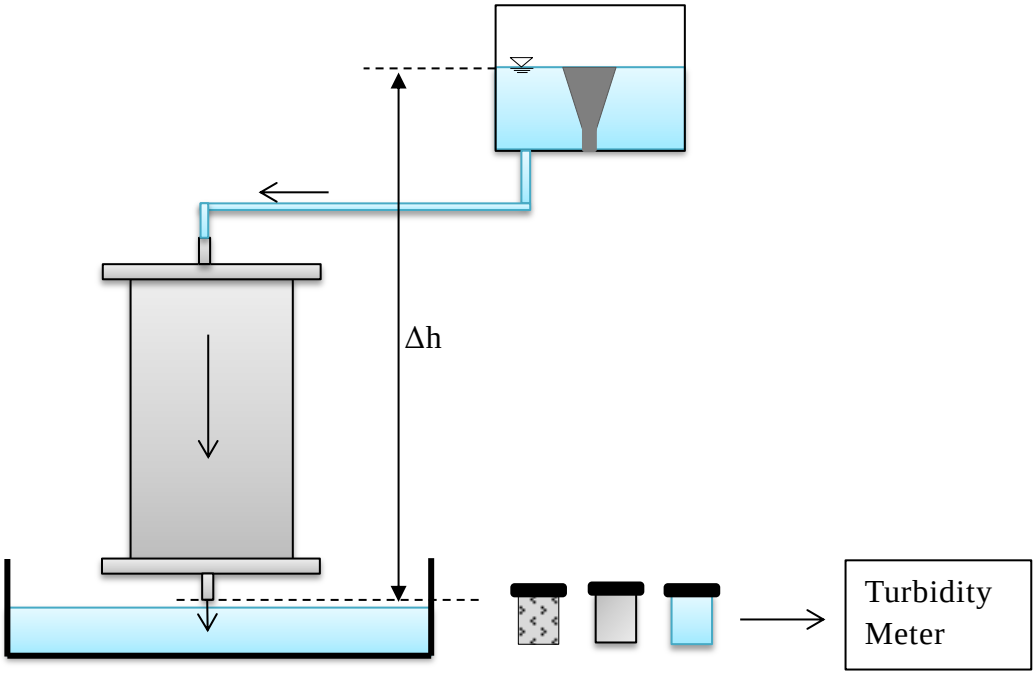

Figure 3.35－Experimental setup of the charcoal wash-experiment.

3.2.3 Results

The turbidity was measured right after the sampling, the sampling vessels were cleaned and the surface polished. Because of particulate matter in the sample, the vessel was stirred in order to avoid settling and one measurement was done three times. The outflow was collected in a pan under the column, so the flow rate could be determined and the turbidity of the outflow was compared to the amount of outflow (Figure 3.36). Average tab water turbidity was measured to be 0.179 NTU (± 0.004 NTU) which is represented as the light blue line in Figure 3.36. In all eight experiments the initial turbidity of the tab water could not be reached within 8 minutes. However for filter velocities lower than 0.2 cm/s a turbidity of 2 NTU could be reached after at least one pore volume flushing ($V_{n,eq}$). For filter velocities from 0.2 to 0.3 cm/s at least two filter pore volumes were necessary. The result of the experiment with v_f = 0.07 cm/s and a coal input dry mass of m_d = 600.0 g is outstanding, since 2.12 $V_{n,eq}$ were necessary. The results in Figure 3.36 show that the turbidity of charcoal reach values below 5 NTU and also below 1 NTU after one complete pass of about 2.5 L.

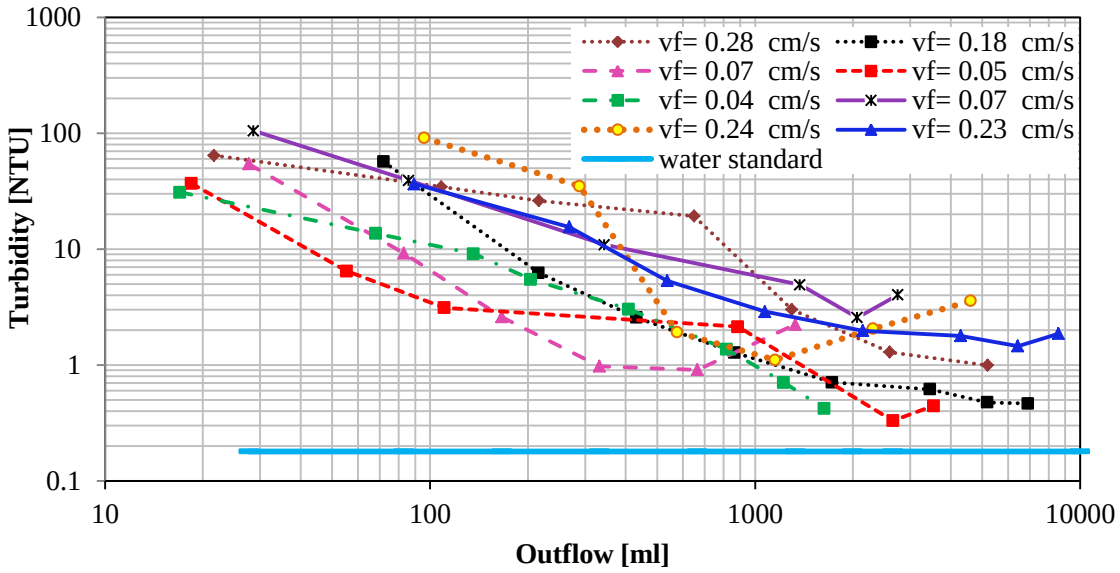

Figure 3.36－Results of the charcoal adsorbent washing experiment for various filter velocities (v_f) from 0.04 cm/s to 0.28 cm/s.

3.2.4 Conclusions

In order to clarify that no harmful substances will be included in the effluent from the charcoal filtration, experiments were done to measure the turbidity of the charcoal material after passing normal water through it. The following conclusions were obtained:

(1). The turbidity values for each experiment are under the suggested turbidity of 5 NTU for drinking water by WHO.

(2). No problems are expected regarding to possible deficites in water quality through the charcoal filter material.

(3). For filter velocities from 0.2 to 0.3 cm/s at least two filter pore volumes were necessary to reach 2 NTU.

3.4 OPEN LOOP HEAT PUMP UTILIZATION AT OKAYAMA UNIVERSITY, JAPAN

3.4.1 Introduction

In this study the examination of the potentially domestic geothermal usage of ambient groundwater in Okayama, Japan for cooling and heating. For this purpose a field study was conducted under the here presented conditions in order to estimate the cooling potential of a PVC-U heat exchanger in a single room. Furthermore, the potential to remove dissolved iron from groundwater due to the usage of an anaerobe charcoal filter was evaluated and compared to commercial Ferrolite MC3 filter.

Okayama city is located in Okayama prefecture in the western part of Japan. On Tsushima Campus of Okayama University, (Figure 3.37) 7 wells were installed (pictures and boring logs are illustrated in the Appendix A 42 – A 46), one pumping well (No 2), one injection well (No 1) and five observation wells (No 1', 2', 3', 4' and 5') (Figure 3.38). Figure 3.38 shows the position plan of the wells at the biotope side at Tsushima campus, Okayama University.

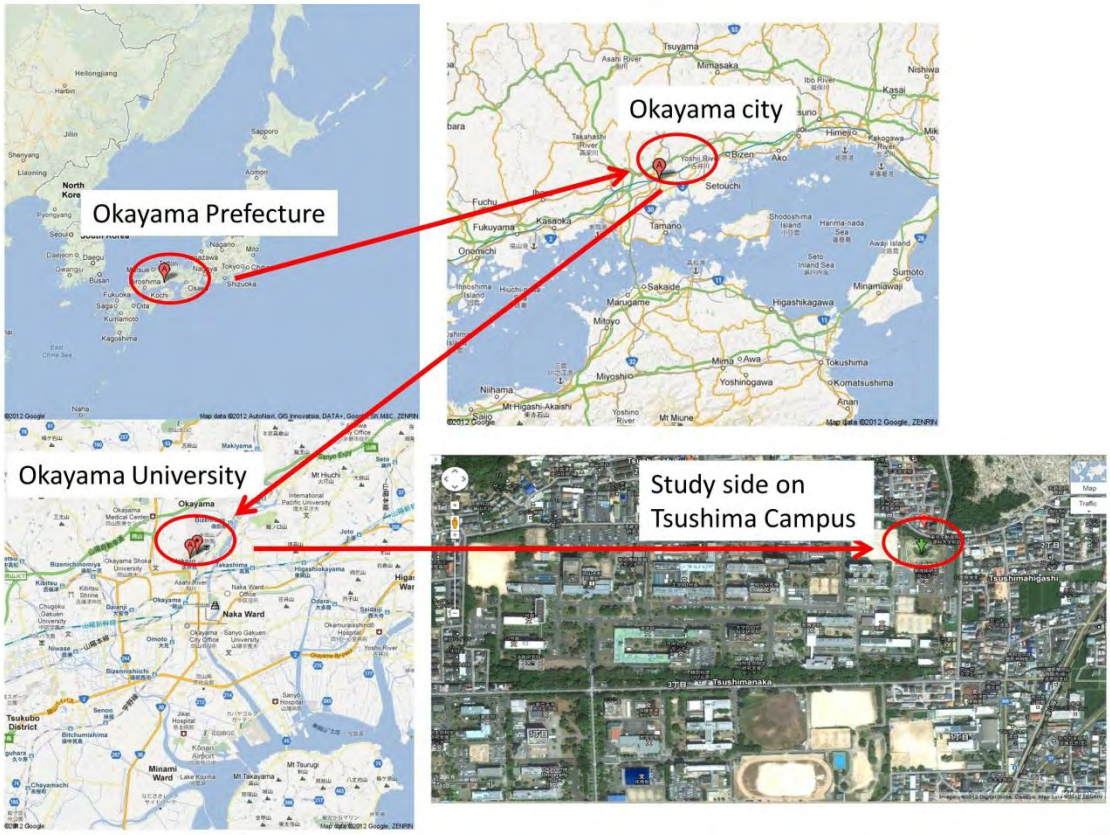

Figure 3.37－ Location of Okayama University and the study side on Tsushima Campus, Okayama, Japan. [Google Inc., 2013]

The pumped water was injected in a charcoal filled filter in order to remove dissolved iron from the ambient groundwater before injecting it into the heat exchanger to prevent scaling and clogging of the pipe network and further clogging in the injection well due to precipitation of iron minerals.

The site consists of two main wells for injection or extraction of groundwater of a secondary Aquifer from about 10 m depth. The distance between both wells is about 50 m in southern

direction. Furthermore, five observation wells were installed. Four of these observation wells were constructed on an axial line between both main wells. Observation well No 2’ is located one meter south from the main pumping well (No 2). Observation well No 1’ was constructed one meter north of the injection well (No 1). Observation well No 3’ lays 1.5 m south of the injection well. The last two observation wells No 4’ and No 5’ were constructed in the middle (about 20 m south from well No 2) between No. 1 and 2 and 2.20 south from well No 1 respectively. The Position map of the installed wells can be seen in Figure 3.35. Groundwater for the field experiment was delivered from Aquifer II from well No. 2 (Pumping well). The well was sealed with an inflatable packer MD-3.4 BASK I, in order to prevent air mixing with groundwater.

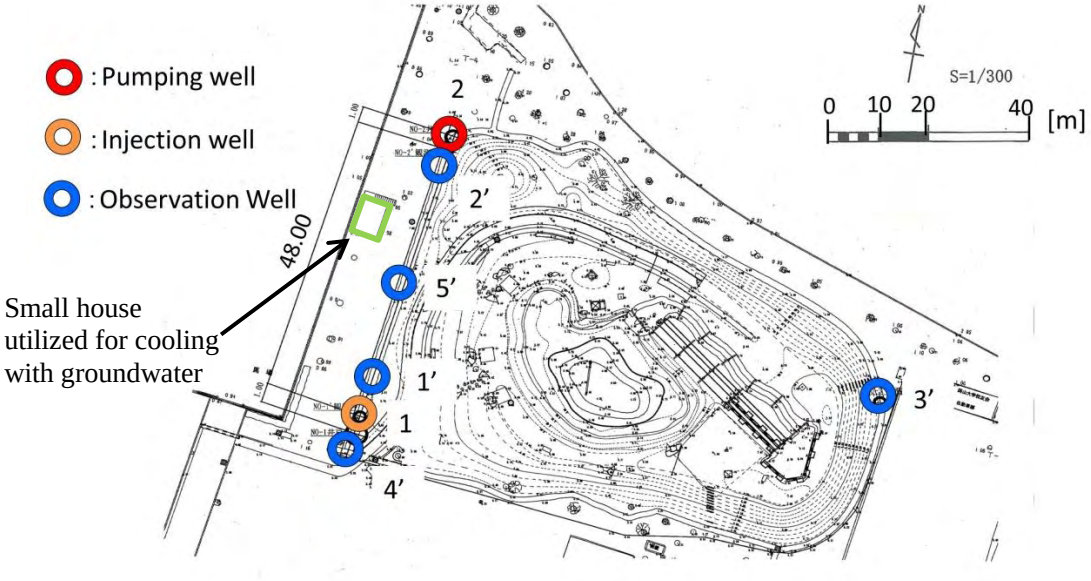

Figure 3.38－ Position map of the installed wells at the biotope site on Tsushima campus, Okayama University, Japan.

The Aquifer consists of unconsolidated sediments of gravel, sand, and clay at a former flood land area (NLID 2011) (Figure 3.39 and 3.40). The test site consists out of two aquifers: (1) Aquifer one is a shallow clay-sand aquifer (0-6 m below ground surface), and (2) Aquifer II: A confined Aquifer starting 6 m below GL. The second Aquifer consists of gravel-sand with a high hydraulic conductivity of 0.16 cm/s. Therefore, Aquifer two was chosen for the recovery of groundwater.

The chemical and physical parameter of the used groundwater is summarized in Table 3.12.

Table 3.12－ Physical and chemical parameters for Aquifer II (column experiment) with average temperature (T), initial dissolved iron and manganese ion concentration, pH, electric conductivity, dissolved oxygen level and hydraulic conductivity.

Parameter	Unit	Aquifer II
T	°C	17.6
$C_{[Fe^{2+}]}$	Mg/L	3.71 (±0.09)
$C_{[Mn^{2+}]}$	Mg/L	2.98 (±0.11)
pH	-	6.8
EC	mS/cm	0.22
DO	mg/L	0.5
k	m/s	$1.6x10^{-3}$
T	m^2/s	$1.6x10^{-2}$

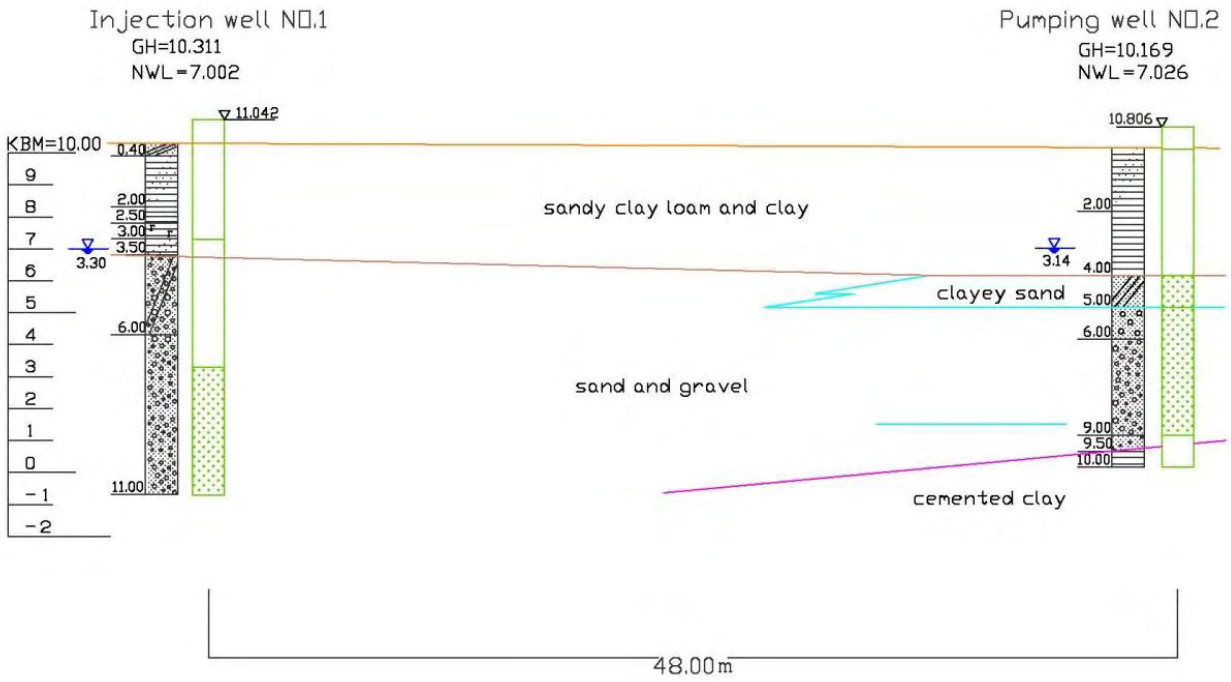

Figure 3.39－ Geological profile between the injection well No. 1 and the pumping well No. 2.

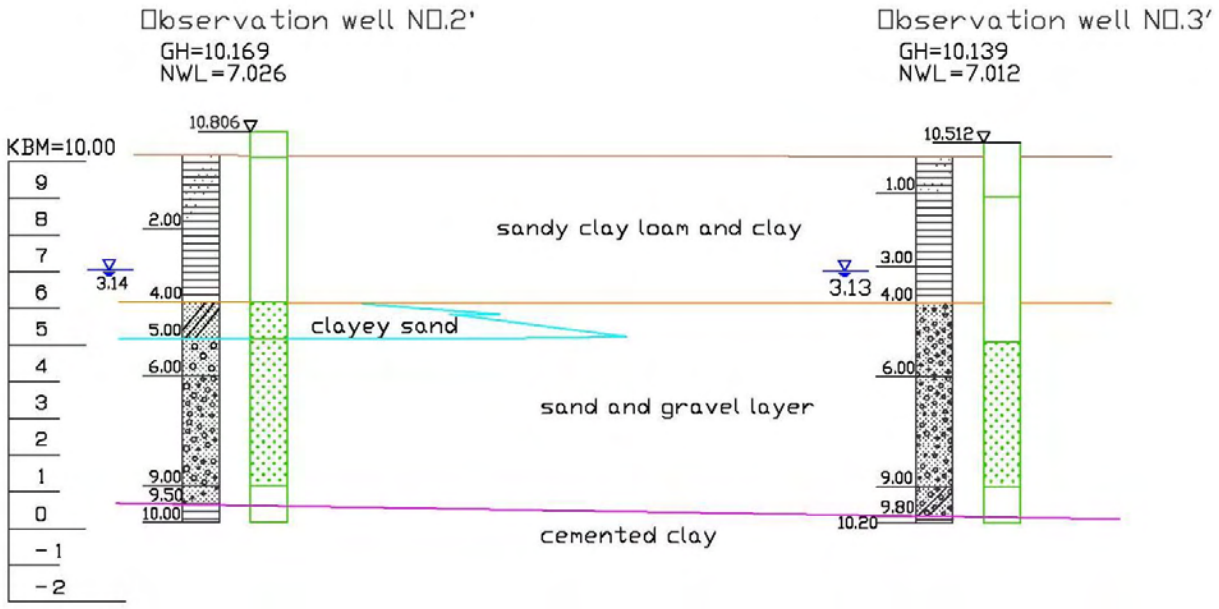

Figure 3.40－ Geological profile between the observation well No. 2' and the observation well No. 3'.

3.42 Materials and Method

3.4.2.1 Charcoal filter

As filter material wooden charcoal was used in a cylindrical acryl casing. The inlet of the filter was set-up with a rough mesh, followed by layers of gravel, coarse sand and middle sand. 25.3 kg dry mass of wooden charcoal were pact as filter material. On the top of the charcoal a layer of gravel was placed in order to avoid swelling of the charcoal. The filter is schematically shown in Figure 3.41 and pictures are illustrated in the Appendix (A 47 – A 53). Three sampling ports at a height of 30, 60 and 90 cm from the bottom of the filter were used for sampling in order to control the effective operation of the charcoal filter. From the sampling ports a stainless steel pipe of 5 mm diameter lead to the center of the filter, in order to take samples from the middle of the adsorbent material body. At the bottom of the filter a perforated acryl plate was used to distribute the inflow evenly through the filter cross-area, as shown in Figure 3.41. From the inlet a layer of 8 cm gravel, middle sand and fine sand were given each into the filter, followed by a layer of 68 cm wooden charcoal. Finally, a 4 cm layer of gravel prevented the transport of charcoal from of the filter. The filter casing was insulated with a 1.0 cm thick porous foam blanket with outer aluminum insulation; in order minimize the effect of solar insulation on the water temperature.

The charcoal porosity was about 60-70%. The flow through the filter was controlled by a flow meter placed before the filter inlet. The filter was located close to the east wall of the used house (Figure 3.42). Groundwater was pumped from a recovery well to the filter and entered the filter from the bottom. The pressure in the filter was controlled with a manometer and the flow was adjusted accordingly, in order to not exceed a pressure of 200 kPa to avoid damage at the filter casing. The flow was regulated by a MAEZAWA© 13 mm flow meter. The filtered water was then re-injected into a heat exchanger, in order to heat (winter time) or cool (summer time) a room of 5.25 m length, 3.6 m width, and a height of 2.55 m. The groundwater that was filtered by the wooden charcoal filter was not re-injected back into the aquifer, but rather disposed in the drain.

This was done to prevent damage to the aquifer due to clogging as long as the practicability of the adsorbent was unconfirmed.

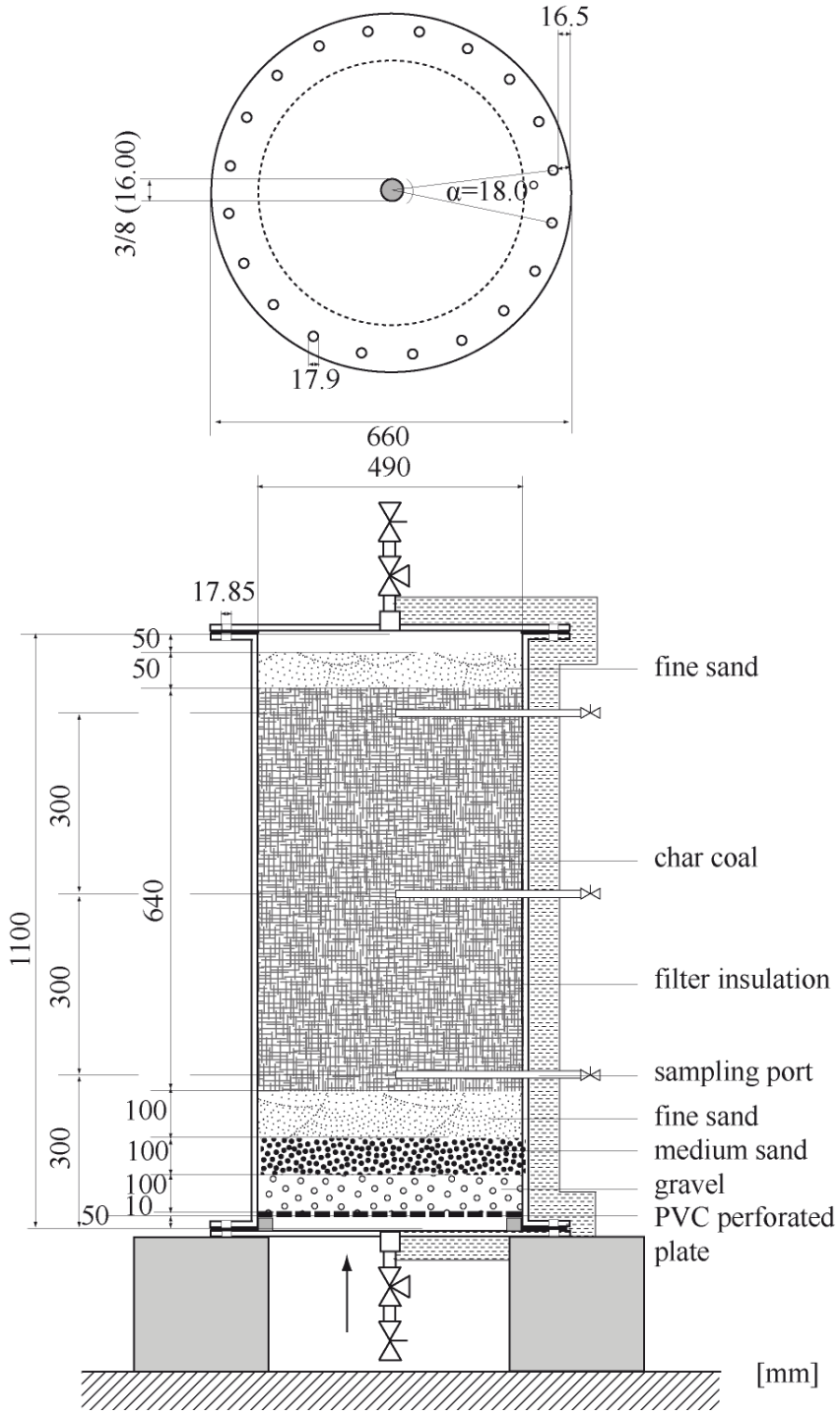

Figure 3.41－ Filter set-up and dimensions, with gravel and sand layers at the inlet and outlet.

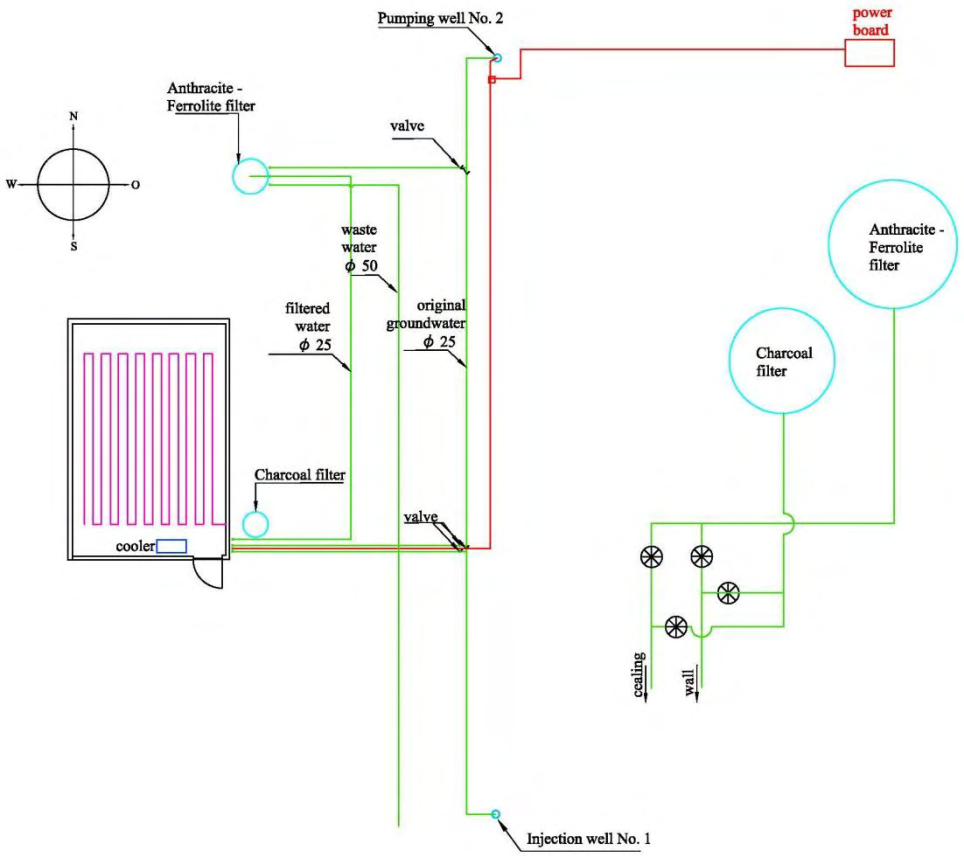

Figure 3.42－ pipe network plan of the study side on Tsushima campus, Okayama University.

3.4.2.2 Ferrolite MC3 filter

To estimate whether clogging may occur in the aquifer due to inner-aquifer particle movement rather than precipitation of ferric or ferrous mineral phases, a Ferrolite MC3 TOHKEMY© granulate filled filter was used, in order to remove dissolved iron and manganese from groundwater. The price for the Ferrolite MC3 filter was 350,000 japanese YEN. The cylindrical stainless steel filter casing had a height of 2.5 m, and diameter of 0.8 m (Figure 3.43, A 54)). The filter was filled from the bottom to the top with four layer, each of 10 cm thickness, of 12-20 mm, 6-12 mm, 3-6 mm, and 2-4 mm sand, followed by a 1.55 m layer of Ferrolite MC3 material (ø = 0.3-0.65 mm) and a final layer of 15 cm Anthracite sand. The flow from the top to the bottom was adjusted in order to not exceed a water pressure of more than 0.22 MPa, resulting in an average flow rate of 25 L/min. The treatment with ferrolite of iron and manganese removal by use of these media is contact-oxidation with chlorine dosing. The particular chemicals coating the surface of media act as catalysts to make the target substance adhere to the surface of media and remove them. It is not adsorption method such as activated carbon but continuously regenerated. So it is not needed to replace the media in short intervals but can be used in long intervals (Tohkemy Corporation, 2013).

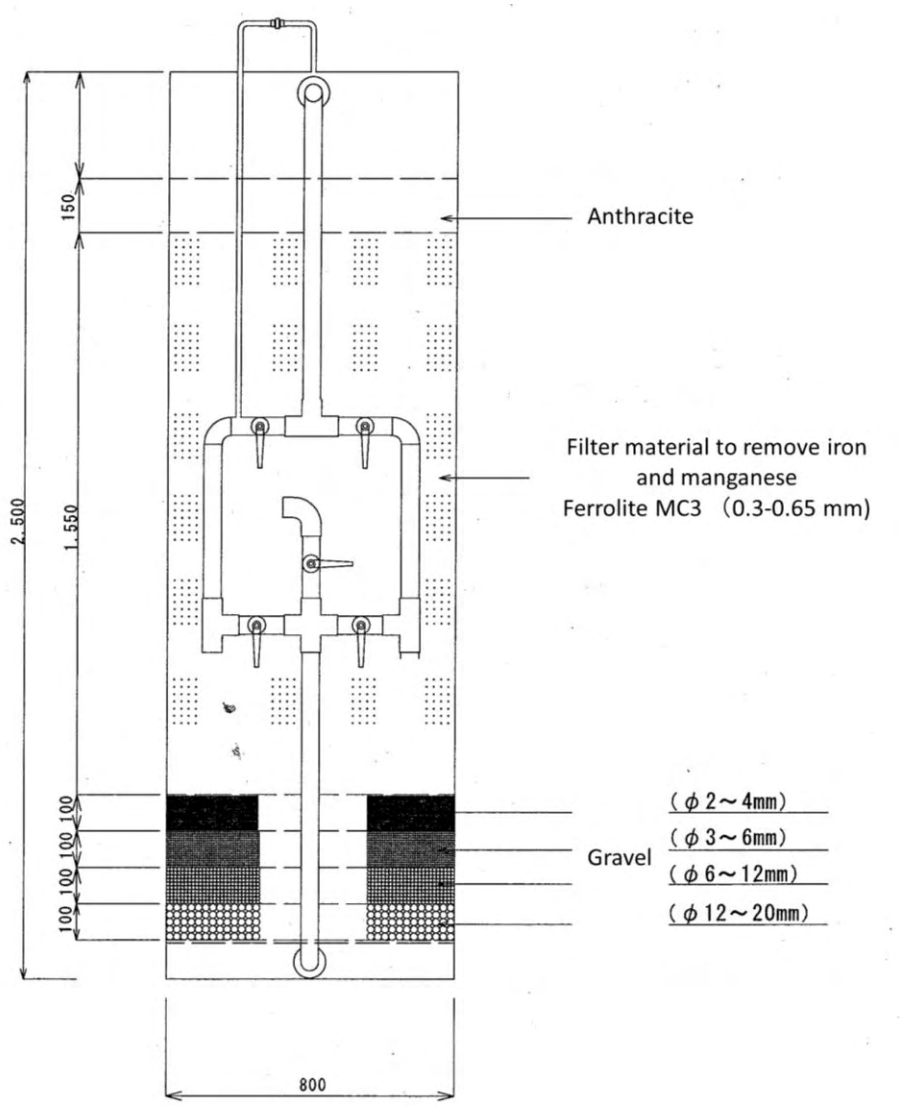

Figure 3.43－ Dimensions and composition of the Ferrolite MC3 filter at the study side on Tsushima campus, Okayama University.

4.2.3 Cooling and Injection

The heat exchanger is a room constructed on the study site. PVC-U pipes were laid along the walls and ceiling of the room to establish a long retention time of the water in the pipe network and to maximise the surface area of the network. The room has an inside dimension of 5.25 m length, 3.60 m width, and a height of 2.55 m. The PVC-U pipes have an inner radius of 10 mm and a wall thickness of 3 mm. The geometrical properties of the network are summarised in Table 3.13 and Figure 3.44 shows the top-view of the room in north-south direction. Pictures of piping network in the room are presented in the Appendix A 55 - 56.

Table 3.13－ Summary of geometrical properties of the pipe network, as heat exchanger within the room.

	Pipe wall	Pipe Ceiling	Total
Length [m]	137.3	79.0	216.3
Volume [dm³]	43.13	24.82	67.95
Inner surface [m²]	8.63	4.96	13.59
Outer surface [m²]	9.92	5.71	15.63

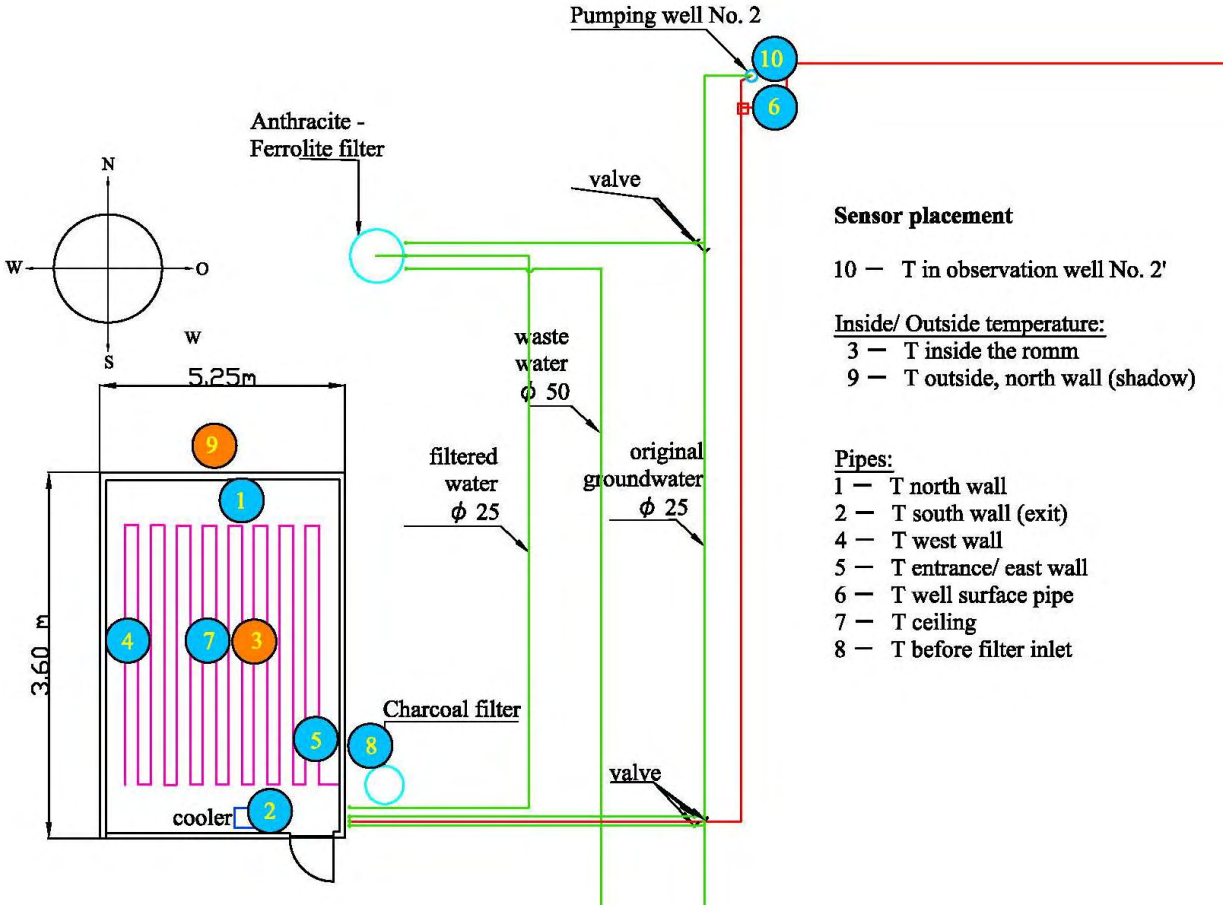

Figure 3.44－ Sensor placement for temperature measurement at the study site on Tsushima campus, Okayama University.

As sensors to measure the temperature in the room and of the used groundwater were temperature sensors used. The sensors were connected to a GRAPHTEC MIDI LOGGER GL200 Data Logger (A 58) for automatically collecting the temperature data of 10 sensors distributed in the room and the field (Figure 3.44, A 57). According to the purpose of the measurement two installations were done: (1) The first installation was used to estimate and monitor the daily distribution of temperature around the house and in the room. Four sensors were installed at each sites of the house, covered by an opaque shield to minimize the effect of direct isolation. This installation was thought to help estimating the surface temperature of the wall for a better understanding the inner heat distribution. The average outside temperature (shadow) was estimated from the minimum temperature of these four sensors. The other six sensors were installed in the room. One in the centre (No. 3), about 1.3 m from the ground, and further more at the ceiling pipe, pipe exit at the south wall, at the pipe entrance at the east wall, pipe at the north wall, and pipe at

the west wall. The average room temperature was estimated from all six sensors. (2) For the second installation only the location of the outside sensors from the east, west and south wall were changed. One sensor was placed in observation Well No. 2' at a depth of about 6 m from the well end; another one was placed at the exit of the well, attached to the pipe; the last one was attached to the entrance of the filter, in order to estimate the heat lose in the filter. The outside and room-inside temperatures were estimated from sensor No. 3 and No. 9. The sensors couldn't be placed directly in the pipe, they were attached to the PVC-U pipes surface or, if possible, to metal parts that were in contact with groundwater, such as the flow meter, to measure the pipe surface temperature. Each sensor was insulated by several layer of air-foliage and aluminium foliage to minimise the effect on the temperature measurement due to the surrounding air temperature. Table 3.14 summarises the sensor placement with sensor number, place of set-up and attached surface material.

Table 3.14－ Placement of the sensor (number) in Installation I and II and attached surface material.

Sensor No.	Installation I place	Attached material	Installation II place	Attached material
1	Room/pipe north wall	PVC-U		
2	Room/pipe exit (south wall)	PVC-U		
3	Room centre	Air		
4	Room/pipe west wall	PVC-U		
5	Room/pipe entrance (east wall)	PVC-U		
6	East-out-wall	White gypsum	Observation well No. 2' (-6 m)	Groundwater
7	Room/pipe ceiling	PVC-U		
8	South-out-wall	White gypsum	Filter Entrance	Stainless steel
9	North-out-wall	White gypsum	North-out-wall	PVC
10	West-out-wall	White gypsum	Well-pipe	Stainless steel

The Experiment field equipment was operated according to the following scenarios that are displayed in Table 3.15, in order to estimate the performance of the geothermal usage of groundwater for cooling the onsite-room during the summer period.

Table 3.15－ Scenario (set-up) A - D that was used to operate the cooler (MITSUBISHI© MSZ-GXV22P-W from 2004) and pump-system in order to cool the onsite room and to estimate the performance of the geothermal system.

Scenario Name	Description	Date
Scenario A-1	Flow of 4.3 L/min in wall	2012/08/22－23 (1 day)
Scenario A-2	Flow of 7.3 L/min in ceiling	2012/08/30－31 (1 day)
Scenario B-1	Flow of 2.5 L/min in ceiling	2012/08/31－09/01 (1 day)
Scenario B-2	Flow of 0.5 L/min in ceiling	2012/09/03－05 (2 days)
Scenario C	Usage of Cooler in most energy efficient mode	2012/09/06－07 (1 day)
Scenario D	Flow of 3.2 L min^{-1} in wall and ceiling with fan utilization in room	2012/09/10－12 (2 days)

3.4.3 Results and Discussion

3.4.3.1 Charcoal filter

The wooden charcoal filled pilot filter was tested in the field on Tsushima campus Okayama University for in total 9 days. During this time 44.6 m³ groundwater were filtered with a weighted average flow rate of 5.52 L/min (v_f = 2.93 cm/min), but not re-injected into the aquifer, as it could initially not be ensured that dissolved iron adsorption takes place. The flow rate at the beginning was set to 5 L/min and after 1 day increased uptil 10 L/min. This increase in flow rate resulted in an enormous pressure increase like shown in Figure 3.45 und 3.46. Because of too high pressure at the column outlet (measured with a pressure gauge), the lid of the charcoal column broke. After repairing the lid and a second start, the flow rate was regulated down to 2 L/min (pressure drop after 2 days in Figure 3.46. After 9 days the lid again broke due to pressure increase, hence the experiment was stopped. It is suggested for filter design, that a pressure relief valve should be installed, so that the exceeding pressure can be released through this valve.

However, during this time no dissolved iron break-through was detectable neither at the outlet of the filter nor at the middle of the filter length (Port at 60 cm column length). Based on the maximum adsorption capacity (b_{eq} ≈ 3.5 g/(kg dry coal)) of the wooden charcoal from the laboratory column experiments, the 25.27 kg dry mass of wooden charcoal would have been able to adsorb 88.4 g of dissolved iron, with a groundwater dissolved iron concentration of 3.71 mg/L (± 0.09 mg/L) resulting in a total of 23.8 m³ filtered groundwater. The measured relative dissolved iron ion concentrations measured during the experiment at the ports is shown for various filtered water volumes [L] according to the column heights 30, 60 and 90 cm is shown in Figure 3.47.

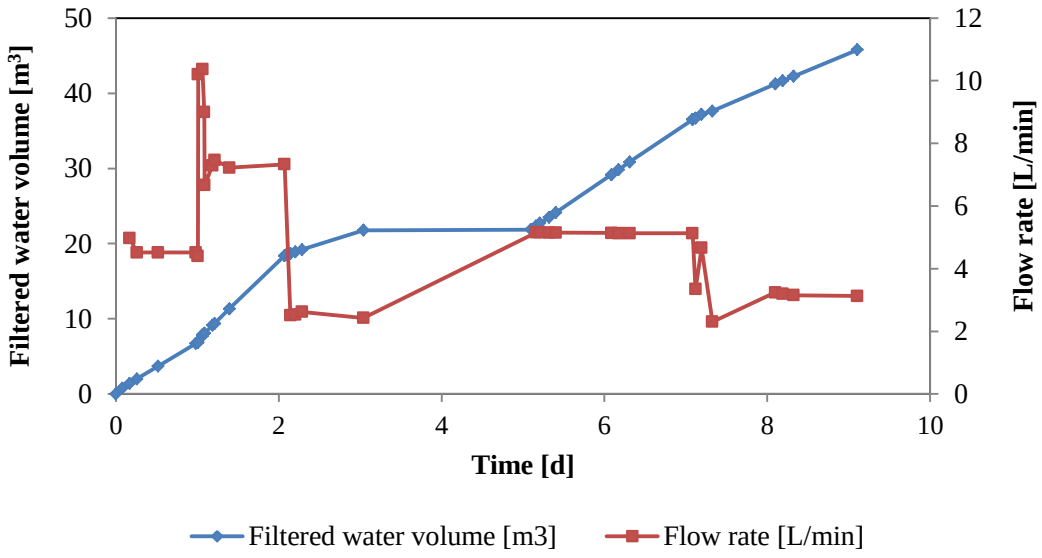

Figure 3.45— Filtered water volume and flow rate plotted over experimental time of the charcoal filter in field experiment.

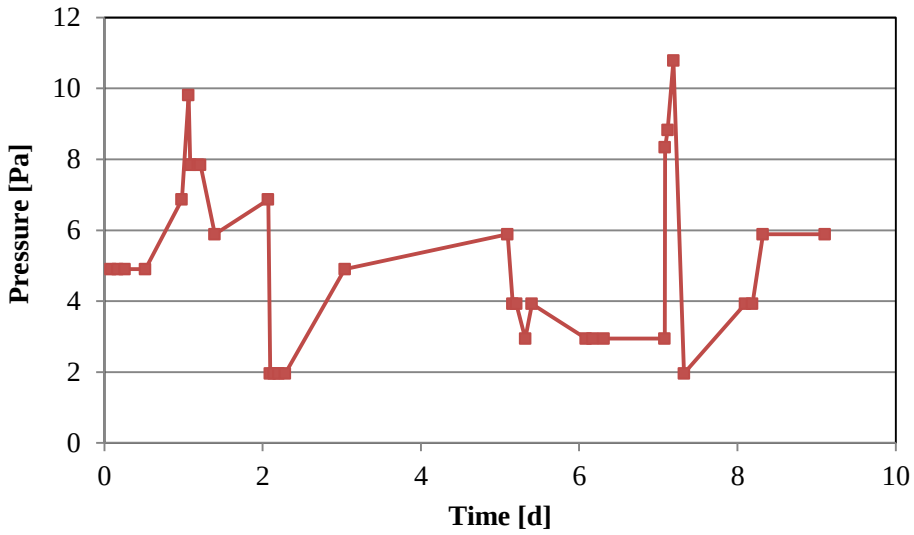

Figure 3.46－ Pressure at the filter outlet plotted over experimental time of the charcoal filter in field experiment.

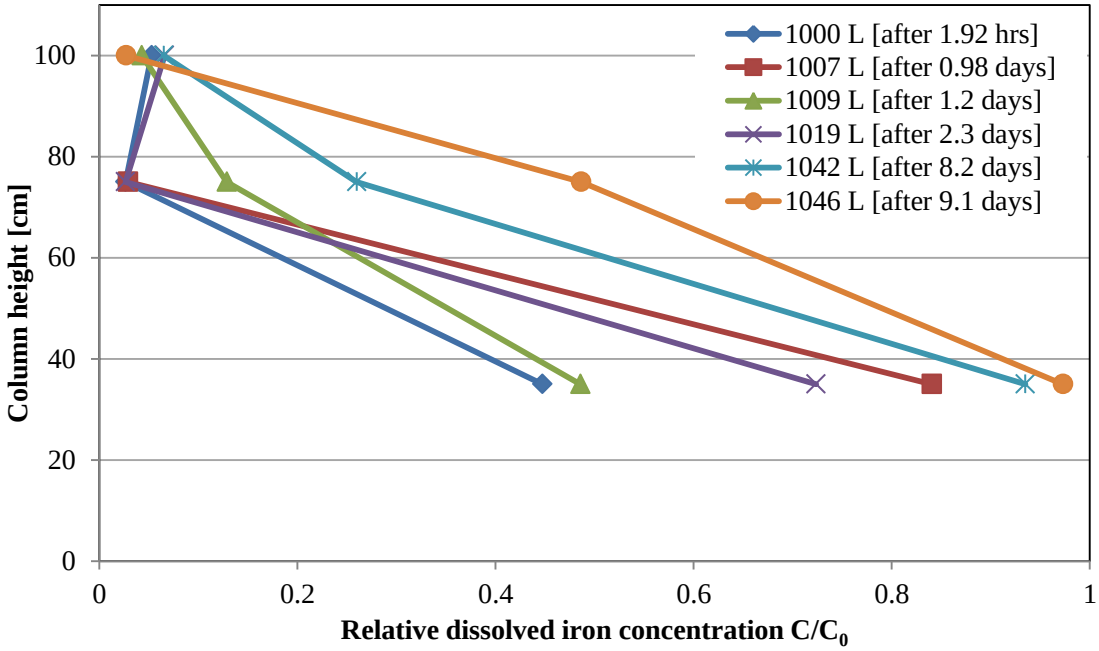

Figure 3.47－ Breakthrough curves of the pilot charcoal filter at the field side, plotted according to various filtered water volumes. In 9 days 45.8 m³ groundwater from the well during the experiment were filtered. After 9 days the experiment had to be stopped because of too high pressure damage.

3.4.3.2 Ferrolite MC3 filter and injection

For the estimation of the potential usage of ambient groundwater heat (17.6 °C) to cool and heat a facility on-site, groundwater was previously filtered through a Ferrolite filter and re-injected back into the aquifer after utilization. The groundwater table (interval: 30 min) and temperature (interval: 30 s) were continuously observed during the re-injection period of 55 d (from 15th of November

2012 to 8th of January 2013) in the injection well and an observation well one meter in north direction from the injection well.

The difference in hydraulic head between the observation and the injection well during the injection is shown in Figure 3.48. While the FerroliteMC3 filter removed dissolved iron (C_0 = 3.71 mg/L (± 0.09 mg/L)) from the groundwater for the initial 36 days the head difference was stable between 0.2 – 0.7 cm. The dissolved oxygen level of the injected water was 0.7 mg/L, respectively. However, as soon as the groundwater was injected into the well it got in contact with oxygen through mixing with air. At the time the dissolved iron broke through, after 1296 m³ filtered groundwater had been injected into the Aquifer, the head difference decreased rapidly until the shutdown of the pump after 55 days of continues operation. At the moment of shutdown a total of 1899 m³ groundwater had been re-injected into the Aquifer and the absolute head difference between the observation well and the injection well was 24.4 cm.

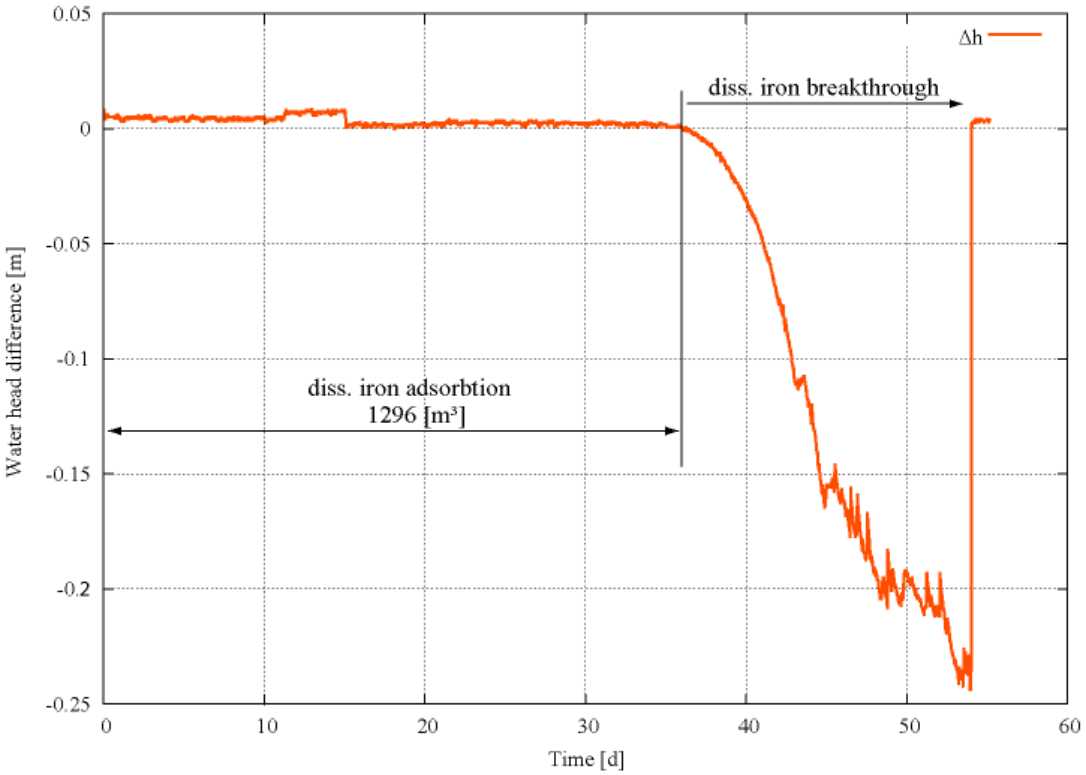

Figure 3.48— Water head difference between the observation well No 1' (one meter north of injection well) and the injection well. Breakthrough of dissolved iron occurred 36 days after the start of the injection and caused an immediate increase in head difference due to clogging.

The general groundwater fluctuation during the re-injection period can be seen from the bottom graph of Figure 3.49. The groundwater head of observation well No 5', which is located between the recovery and injection well, was assumed to have not been influenced by draw down or up-coning effects of these wells. It can be seen, that the groundwater table highly fluctuated from 6.4 m above mean sea level (AMSL) to 7.1 m AMSL. If compared to precipitation data (JMA, 2012) of that period, a general trend of increasing groundwater level after a precipitation event becomes obvious. This indicates a high influence of surface water on the second Aquifer.

(a)

(b)

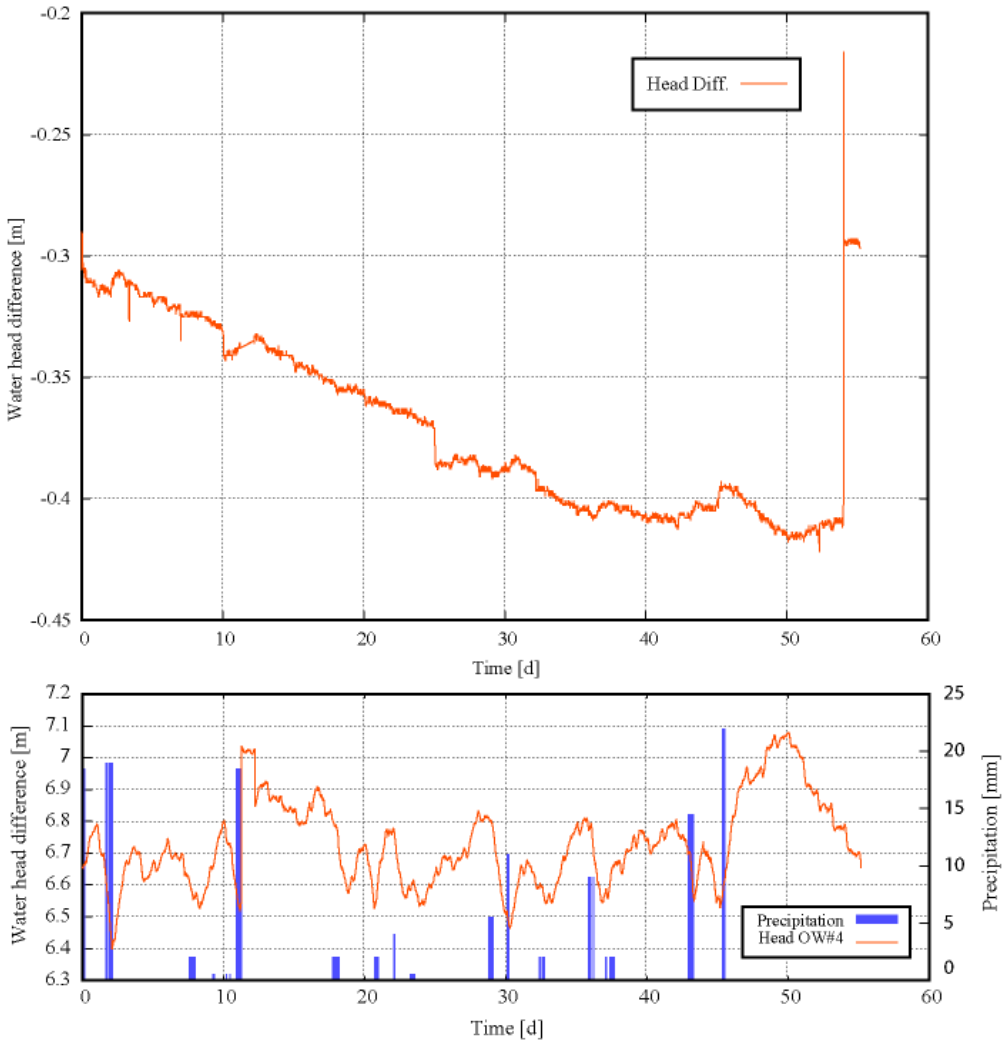

Figure 3.49—(a): Head difference between observation well No. 2' (1 meter south of pumping well) and No. 5' during the injection period (top). (b): Water table in observation well No 5' (25 m south of pumping well (No. 2) and 25 m north of injection well) with precipitation data [mm] [JMA].

3.4.3.3 Cooling and temperature measurements

3.4.3.3.1 Average Room temperature – Installation I

During the observation period the average outside temperature varied from 23°C in the morning, with sunrise at about 6 o'clock, to a peak temperature of 35-36°C in the early afternoon at 14 o'clock. The typical day-curve for the inside and outside temperature is displayed in Figure 3.50 for a sunny day at the 8th of August 2012. The mean inside temperature was estimated from six sensors placed in the room. The red area indicated the variation of the inside temperature according to its 5 %-quintile of the student distribution. It can be seen that the inside temperature rises according to the outside temperature with sunrise and the variation in the room increases, respectively. The room temperature peaks with, or shortly after, the outside temperature maximum temperature in the early afternoon, but keeps the temperature for about two hours longer. The inside temperature falls with sunset, according to the outside temperature, whereas the variation in the

room decreases. The minimum temperature of the room at sunrise is about 26°C and therefore higher than the outside temperature. The isolation of the walls from direct sunlight causes this high variation as it can be seen during the noon, as clouds blocked the sunlight and the variation rapidly decreased. It has to be concluded that the room insulation is far from perfect. Further typical inside and outside temperature curves can be seen in Figure 3.51 to Figure 3.53. They all follow the same characteristic pattern, explained above. It has to be noted that the inside temperature is never remarkably lower than the outside temperature.

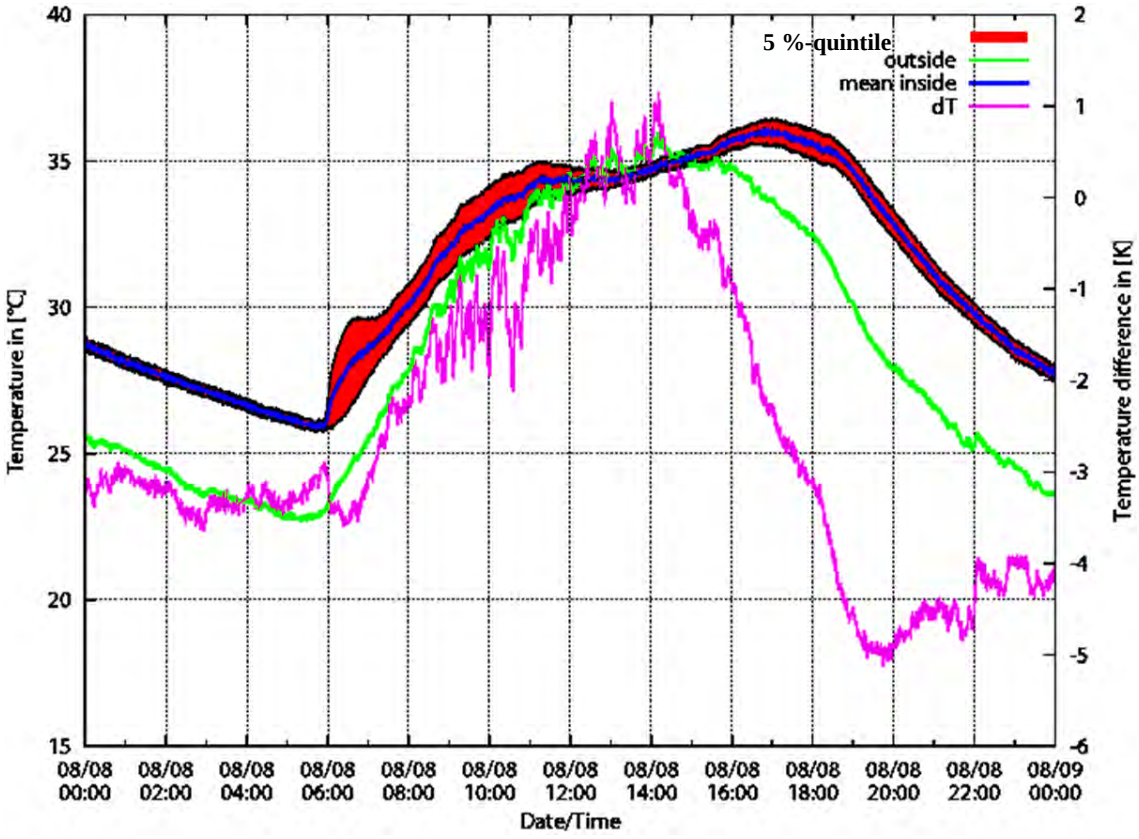

Figure 3.50—Mean inside and Outside temperature for the onsite room and site for the 8th of August 2012. The red area indicates the 5%-quintile of five temperature measurements in the room.

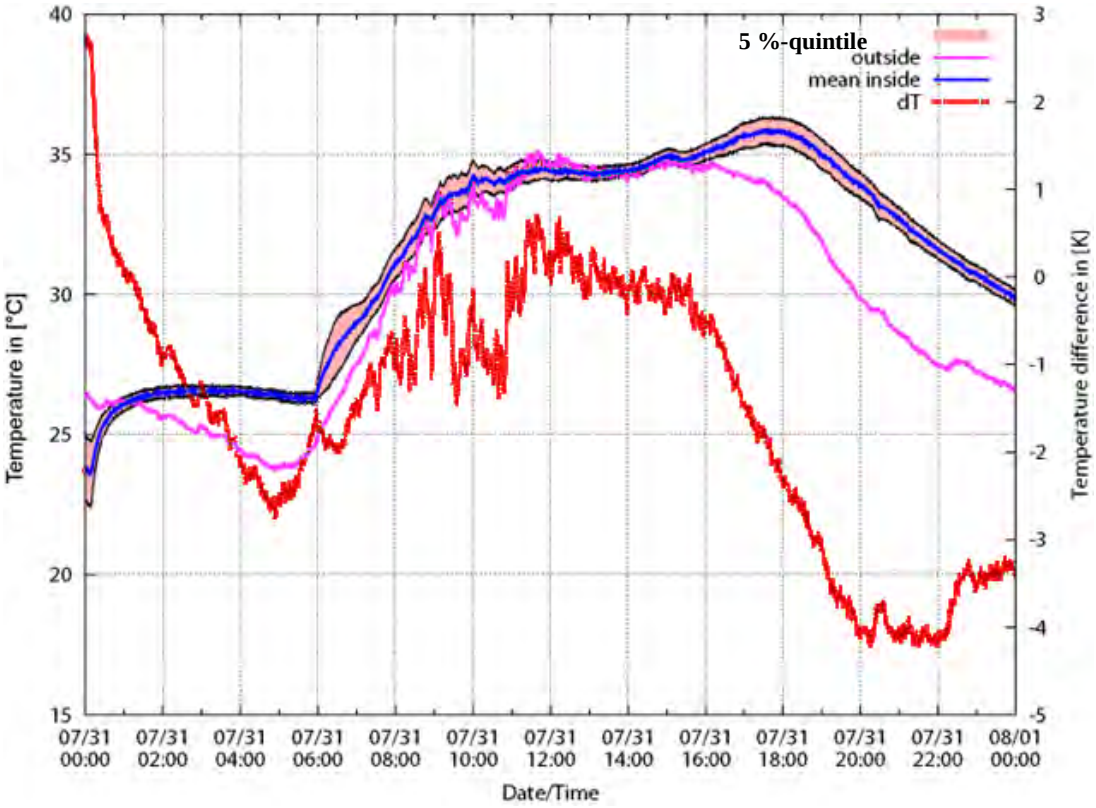

Figure 3.51－Mean inside and outside temperature for the onsite room and site for the 31st of July 2012. The light red area indicates the 5%-quintile of five temperature measurements in the room.

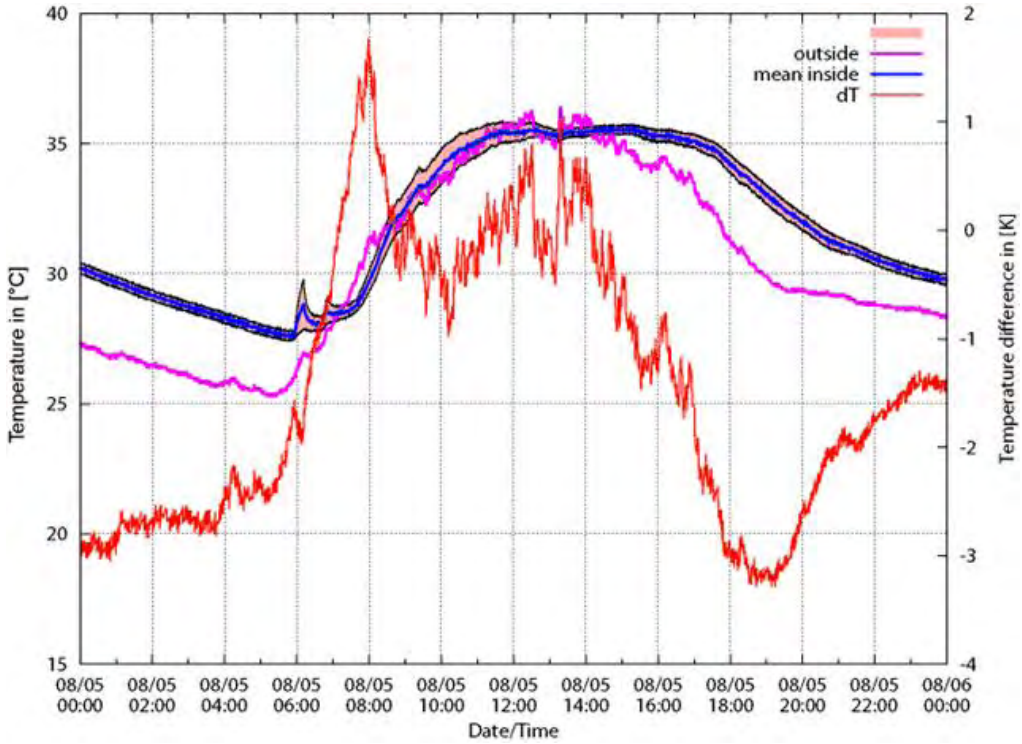

Figure 3.52－Mean inside and outside temperature for the onsite room and site for the 5th of August 2012. The light red area indicates the 5%-quintile of five temperature measurements in the room.

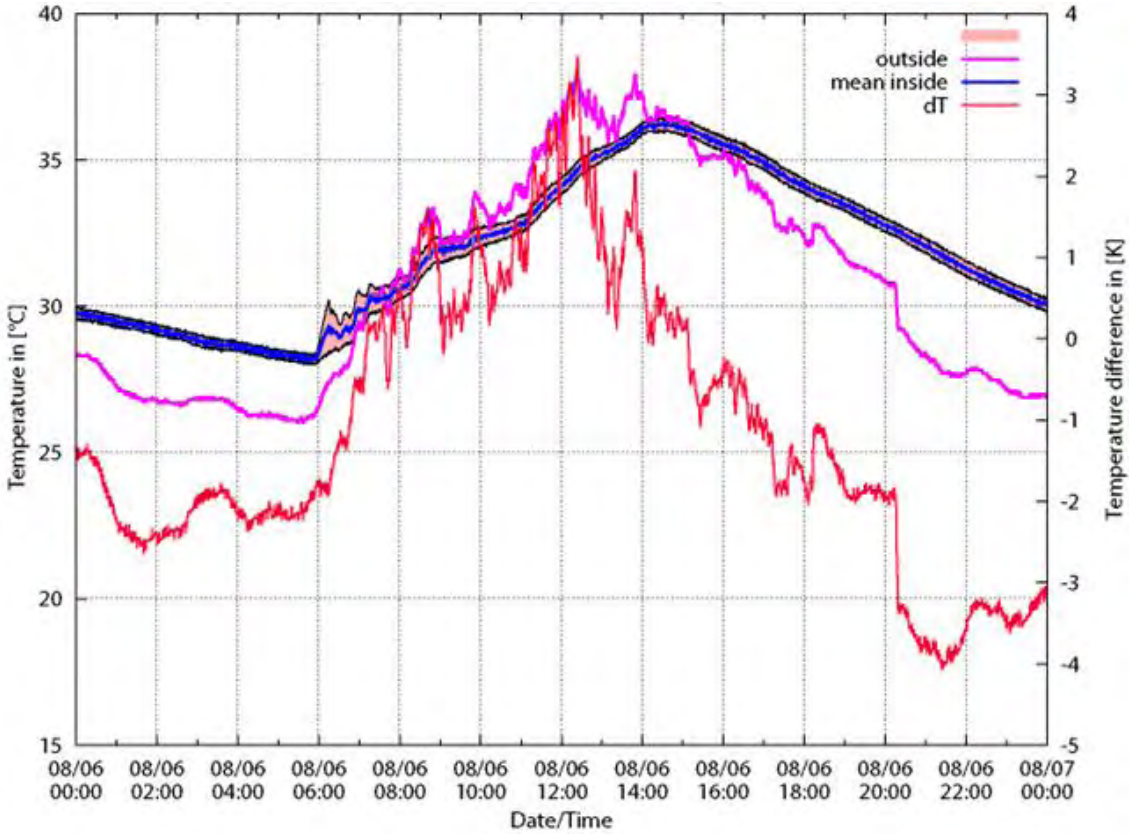

Figure 3.53－Mean inside and outside temperature for the onsite room and site for the 6th of August 2012. The light red area indicates the 5%-quintile of five temperature measurements in the room. Scenario A-1: Wall flow with 4.36 L/min.

In the first scenario the wall pipes of the room were flushed with groundwater with an average flow rate of 4.36 L/min. This flow rate was chosen, as the pressure in the filter did not exceed 50 kPa and was estimated to be safe for the acryl filter case material and the lid. The total operation time was 1394 min. The weather at this day was sunny with small clouds. As it can be seen from Figure 3.54, the mean inside temperature was always below the outside temperature. The difference was highest when the outside temperature peaked around noon with about 5 °C difference between outside and inside temperature. The pipe temperature, as shown in Figure 3.55 at the entrance of the house was about 23 °C and 22 °C at night, whereas the groundwater temperature was constant at 19.5 °C. The water therefore increased its temperature on its way to the house of about 2 °C, probably more as a slight error might have occurred by measuring the temperature in the observation well at a depth of 6 m, as the temperature in the well seems to be layered with 18°C (-10 m from the well end) at the bottom and 21 °C at the top (- 3.5 m from the well end). However, in the house the temperature rose about 2 °C as the exit water had a temperature of about 25 °C in the afternoon and at night only 23 °C; therefore a temperature difference to the entrance of only 1 °C during the night. The temperature difference of the exit pipe surface area to the room temperature ranged from 6 °C during the noon and early afternoon time to about 1.5 °C in the night.

The mean energy usage to operate the pump was 390 W. The relatively humidity in the room reached 90 % due to the cooling of the air. Since an appropriate system is missing that dries the air, the felt temperature in the room, compared to outside, was much higher, even though the mean temperature was below the outside temperature.

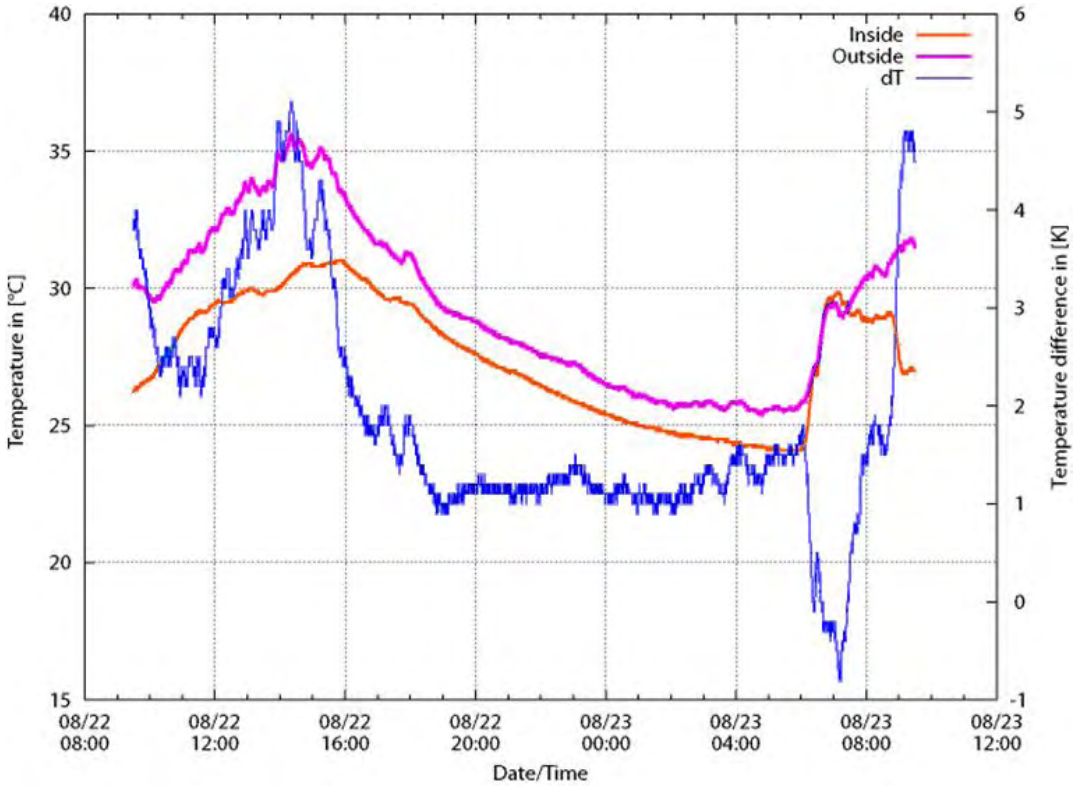

Figure 3.54－Inside and Outside temperature during the operation time (in °C) as well as temperature difference (blue, in K) for Scenario A-1.

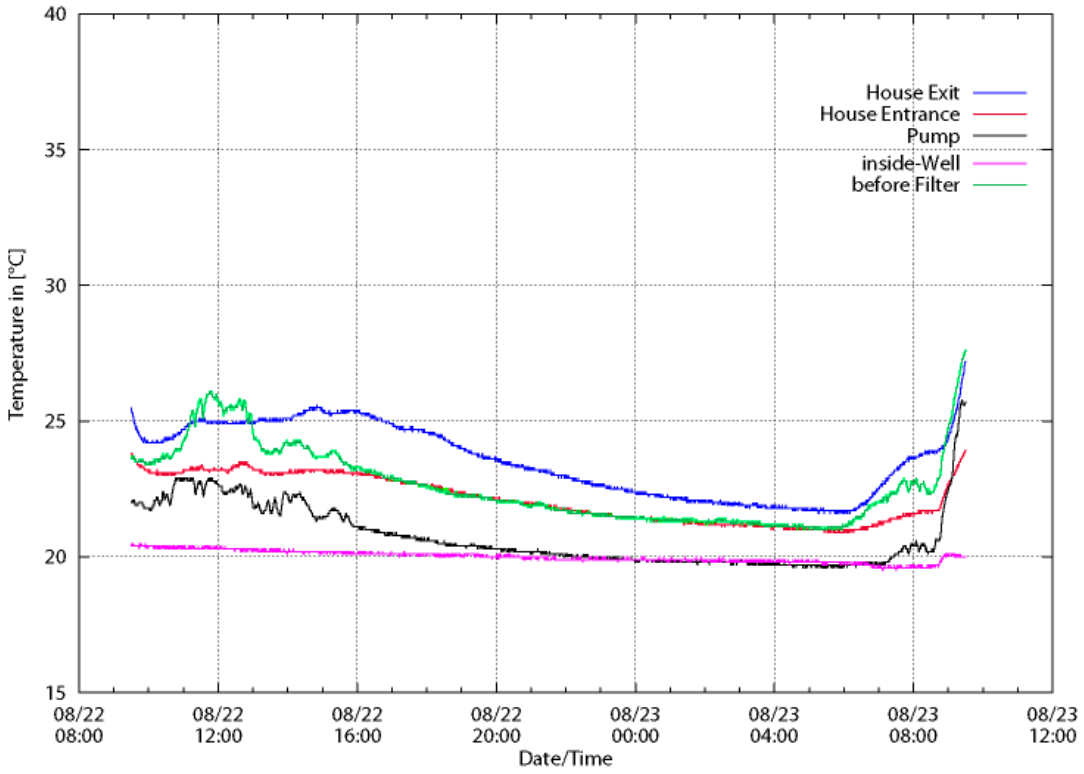

Figure 3.55—Pipe surface and observation well No. 2' temperature for selected sensors during the operation of Scenario A-1.

3.4.3.3.2 Scenario A-2: flow in wall pipes with 7.32 L/min

In the second scenario only the wall pipes of the room were flushed with groundwater with an average flow rate of 7.32 L/min. This flow rate was chosen, as the pressure in the filter did not exceed 100 kPa, but 60 kPa, and was estimated to be safe for the acryl filter case material and the lid. The lid was replaced after scenario one, as it broke when the pressure was raised above 100 kPa. The total operation time was 1430 min. The weather at this time was sunny at the 31st, with showers the evening of the 30th of August. As it can be seen in Figure 3.56, the mean inside temperature was always below the outside temperature. The difference was highest when the outside temperature peaked around noon with about 4 °C difference between outside and inside temperature. The pipe temperature, as shown in Figure 3.57, at the entrance of the house was about 23 °C and 22 °C at night, whereas the groundwater temperature was decreased over 24 hrs from 20.0 °C to 19.0 °C. The water therefore increased its temperature to the house of about 2 °C to 3 °C, probably more as a slight error might have occurred by measuring the temperature in the observation well at a depth of 6 m, as the temperature in the well seems to be layered with 18 °C (-10 m from the well end) at the bottom and 21 °C at the top (- 3.5 m from the well end). However, in the house the temperature only rises about 1 °C to 2 °C as the exit water had a temperature of maximum 25 °C in the afternoon and at night as low as 21.5 °C; therefore a temperature difference to the entrance of only 1 °C during the night. The temperature difference of the exit pipe surface area to the room temperature ranged from 8 °C during the noon and early afternoon time to about 2.5 °C in the night.

The mean energy usage to operate the pump was 429 W. The relatively humidity in the room reached 80 % due to the cooling of the air. Since an appropriate system is missing that dries the air,

the felt temperature in the room, compared to outside, was much higher, even though the mean temperature was below the outside temperature.

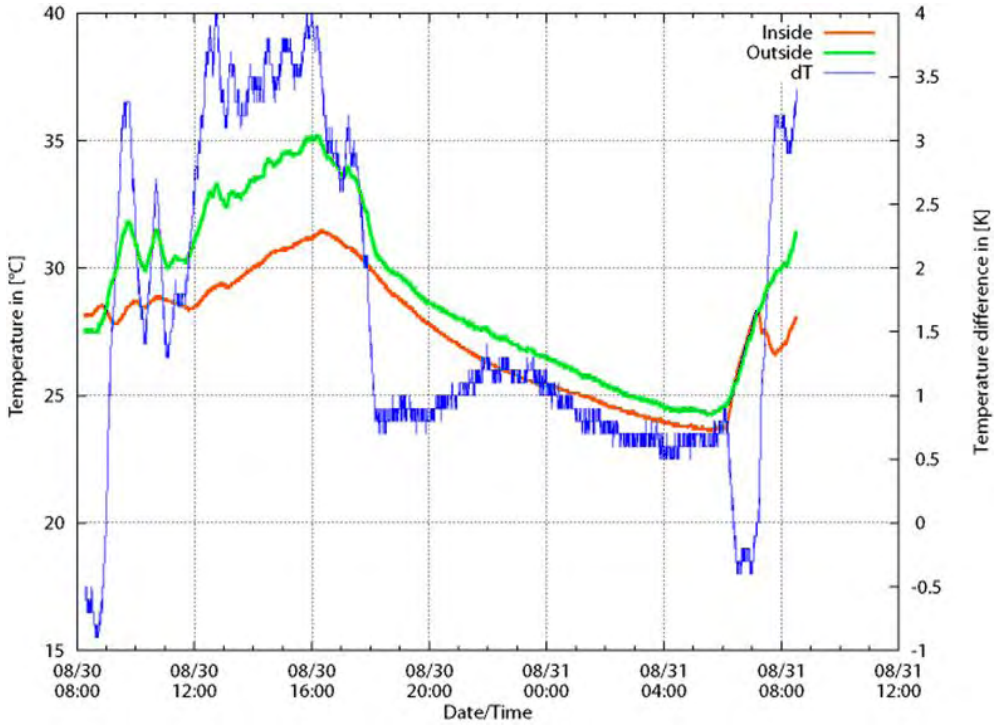

Figure 3.56－Inside and Outside temperature during the operation time (in °C) as well as temperature difference (blue, in K) for Scenario A-2.

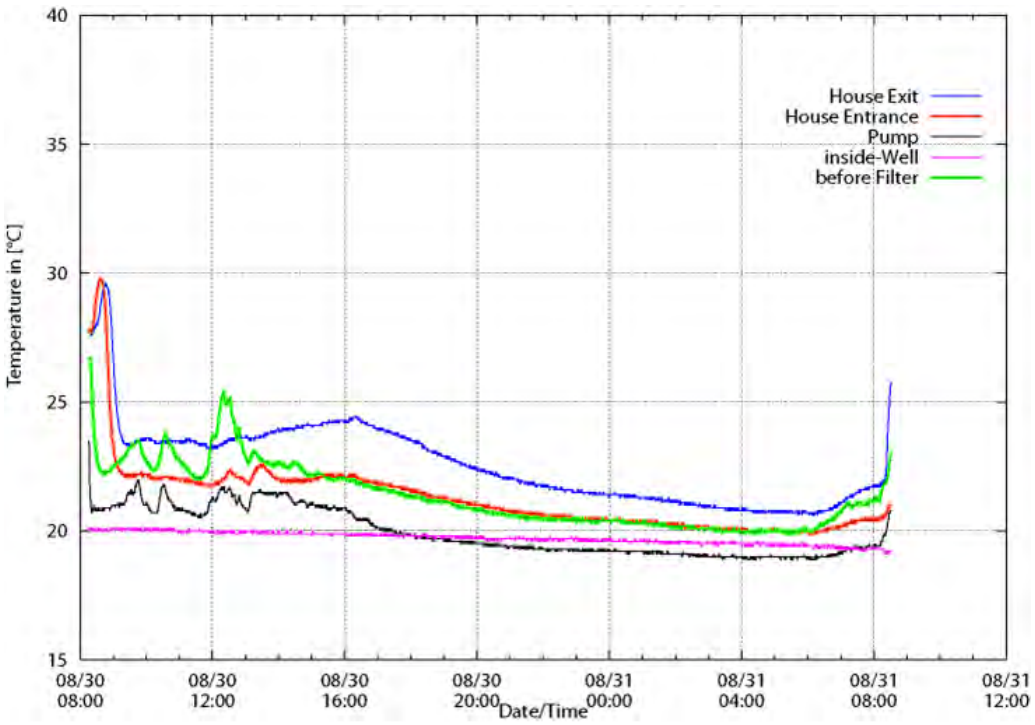

Figure 3.57－Pipe surface and observation well No. 2' temperature for selected sensors during the operation of Scenario A-2.

3.4.3.3.3 Scenario B-1: Flow in ceiling with a flow of 2.46 L/min

In the third scenario only the ceiling pipes of the room were flushed with groundwater with an average flow rate of 2.46 L/min. The pressure in the filter was about 20 kPa. The total operation time was 1340 min. The weather at this time was sunny at the 31st, with strong thunder and rain at the first of September. As it can be seen from Figure 3.58, mean inside temperature was always below the outside temperature. The difference was highest when the outside temperature peaked around noon with about 4 °C difference between outside and inside temperature. The pipe temperature, as shown in Figure 3.59, at the entrance of the house was about 24 °C and 22 °C at night, whereas the groundwater temperature was stable over 24 hrs at 19.0 °C. The water therefore increased its temperature to the house of about 5 °C, probably more as a slight error might occur by measuring the temperature in the observation well at a depth of 6 m, as the temperature in the well seems to be layered with 18°C (-10 m from the well end) at the bottom and 21 °C at the top (- 3.5 m from the well end). However, in the house the temperature only rises about 2 °C as the exit water had a temperature of maximum 26 °C in the afternoon and at night as low as 22.5 °C; therefore a temperature difference to the entrance of only 0.5 °C during the night. The temperature difference of the exit pipe surface area to the room temperature ranged from 5 °C during the noon and early afternoon time to about 1.5 °C in the night. The inside temperature exceeded the outside temperature due to a sudden temperature drop during a thunder storm in the afternoon and night to the first of September.

The mean energy usage to operate the pump was 392.3 W. The relatively humidity in the room reached 90 % due to the cooling of the air. Since an appropriate system is missing that dries the air, the felt temperature in the room, compared to outside, was much higher, even though the mean temperature was below the outside temperature.

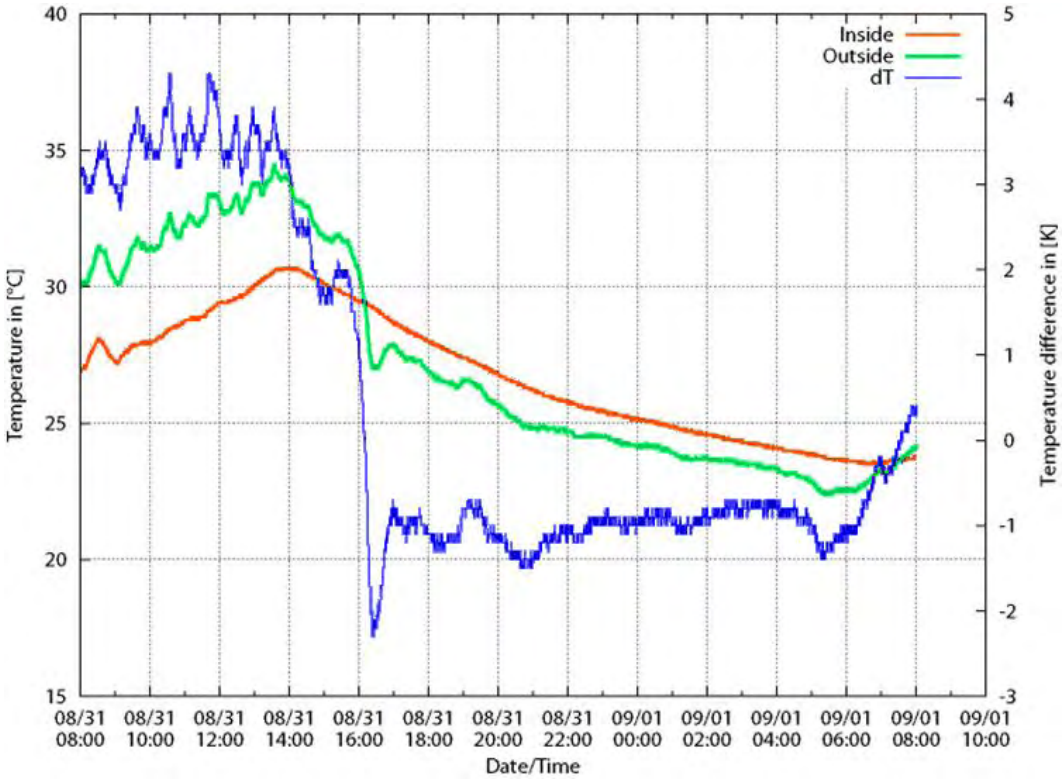

Figure 3.58—Inside and Outside temperature during the operation time (in °C) as well as temperature difference (blue, in K) for Scenario B-1.

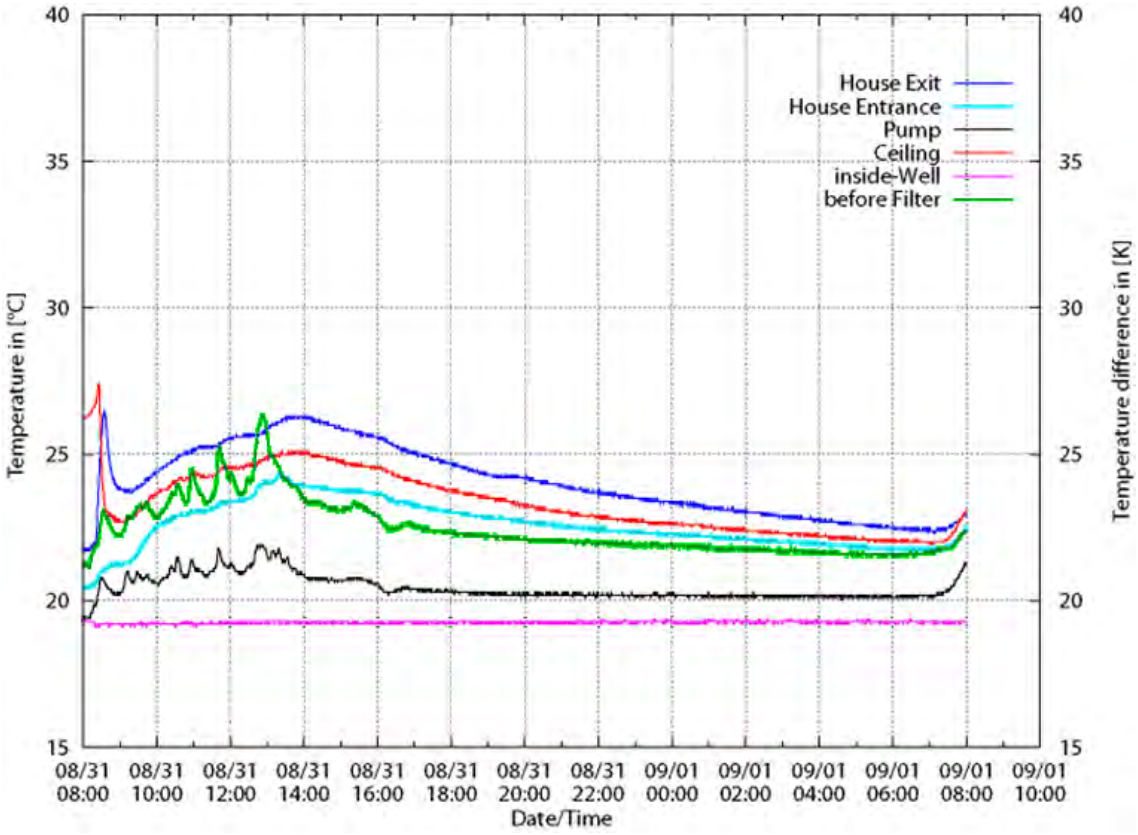

Figure 3.59－Pipe surface and Observation well No. 2' temperature for selected sensors during the operation of Scenario B-1.

3.4.3.3.4 Scenario B-2: flow in ceiling with flow rate of 5.13 L/min

In the fourth scenario only the ceiling pipes of the room were flushed with groundwater with an average flow rate of 5.13 L/min. The pressure in the filter was about 30 kPa. The total operation time was 2860 min, because the weather at the 3rd of September was very unstable, with thunderstorms and rain; whereas the 4th and 5th of September were sunny. It is believed, that the 3rd of September is not representative, as the outside temperature fluctuated with sudden temperature drops. As it can be seen from Figure 3.60, the mean inside temperature was always below the outside temperature for the whole 4th of September. The difference was highest when the outside temperature peaked around noon with about 4 °C difference between outside and inside temperature. The pipe temperature, as shown in Figure 3.61 at the entrance of the house was about 22 °C and 20 °C at night, whereas the groundwater temperature decreased over the time period from 19.0 °C to 18.0 °C. The water therefore increased its temperature to the house of about 4 °C to 3 °C. However, in the house the temperature only rise about 2 °C as the exit water had a temperature of maximum 24°C in the afternoon and at night as low as 21 °C; therefore a temperature difference to the entrance of only 1 °C during the night. The temperature difference of the exit pipe surface area to the room temperature ranged from 6 °C during the noon and early afternoon time to about 2 °C in the night.

The mean energy usage to operate the pump was 409.8 W. The relatively humidity in the room reached 85 % due to the cooling of the air. Since an appropriate system is missing that dries the air, the felt temperature in the room, compared to outside, was much higher, even though the mean temperature was below the outside temperature.

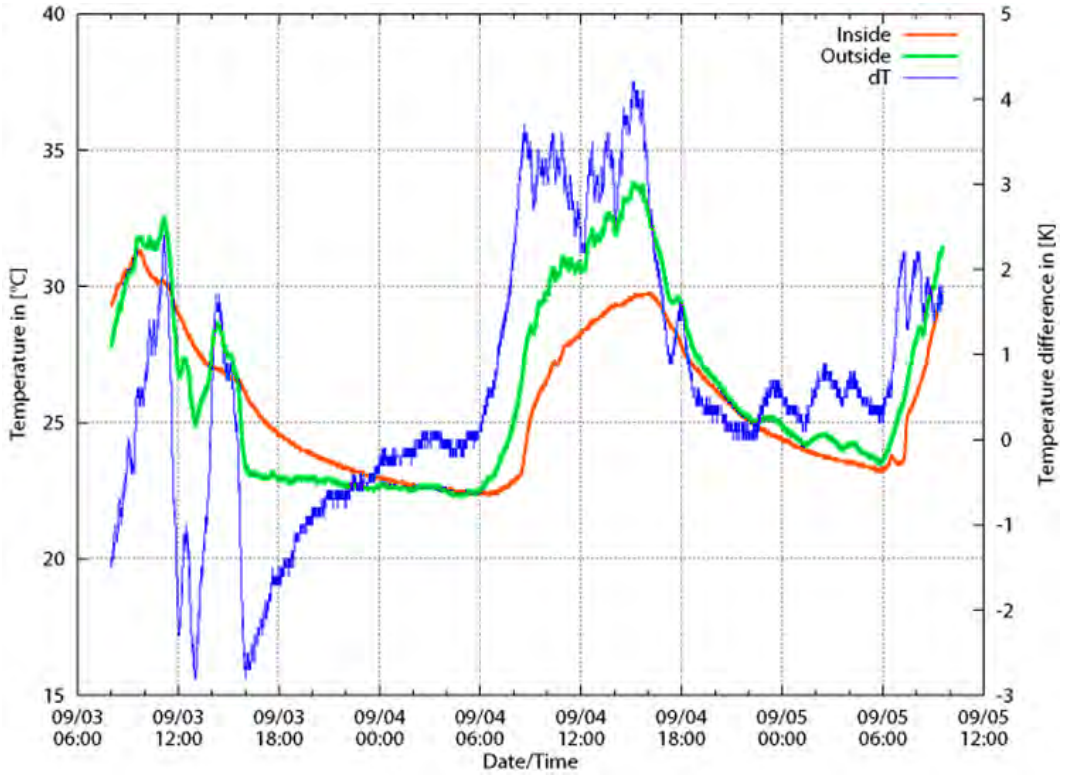

Figure 3.60－Inside and Outside temperature during the operation time (in °C) as well as temperature difference (blue, in K) for Scenario B-2.

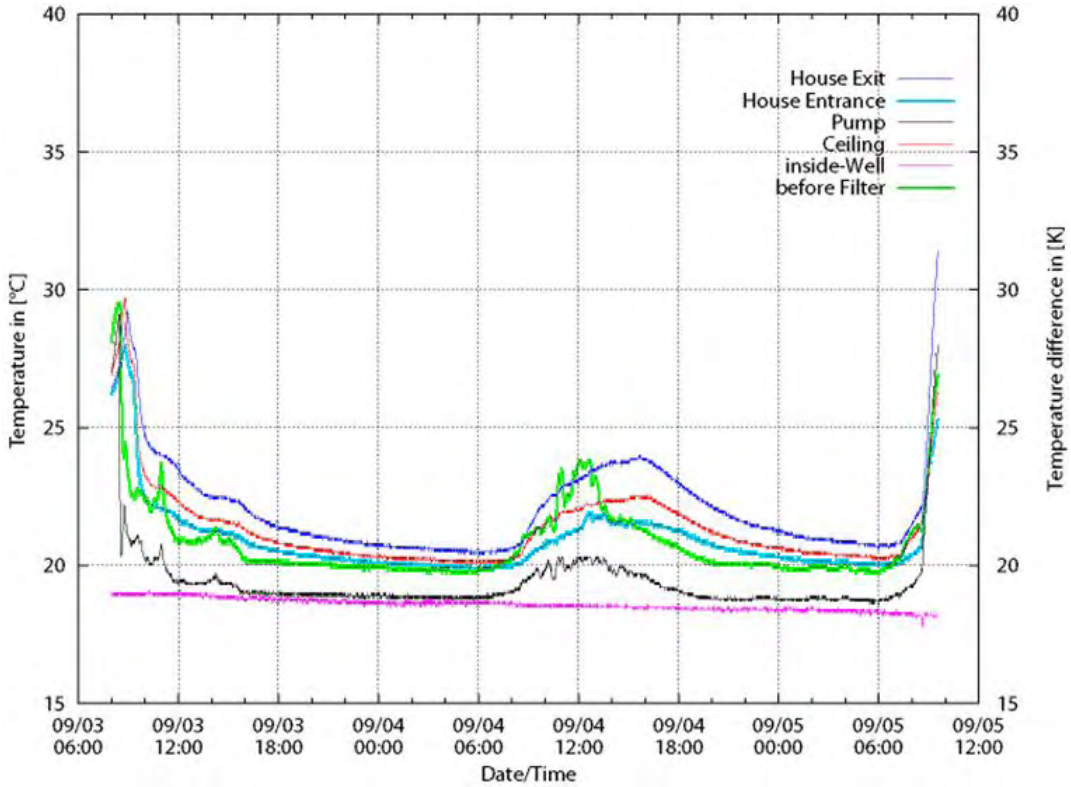

Figure 3.61－Pipe surface and Observation well No.2' temperature for selected sensors during the operation of Scenario B-2.

3.4.3.3.5 Scenario C: low set-up cooler

In Scenario C the in Japan commonly used cooler (MITSUBISHI© MSZ-GXV22P-W) was set on cooling mode, with lowest blow strength and a set temperature of 26 °C. As it can be seen from Figure 3.62, the inside temperature did rapidly decrease to 25 °C. Even though the cooler was set to keep a temperature at about 26 °C the temperature in the room centre increased to 27 °C at noon and decreased with decreasing outside temperature. The outside temperature reached even temperatures about 23 °C during the night. In that time the cooler even heated the room and increased therefore the energy usage, which would be normally lower, as a user wouldn't use the cooler in that time. The maximum temperature difference from outside to inside temperature was reached at noon with about 7 °C difference.

The mean energy usage to operate the cooler was 124.2 W, and would be most likely lower, since the cooler heated the room for about 5 hours. The relatively humidity in the room reached 70%.

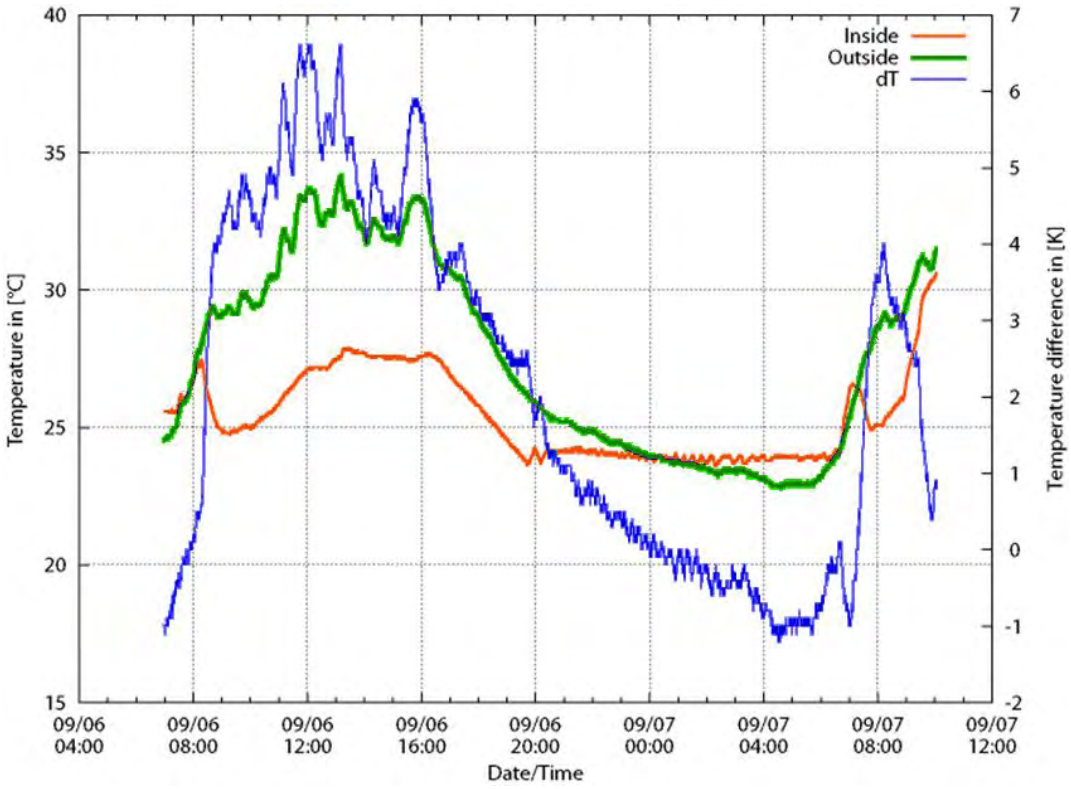

Figure 3.62—Inside and Outside temperature during the operation time (in °C) as well as temperature difference (blue, in K) for Scenario C.

3.4.3.3.6 Scenario D: ceiling and wall flow with flow rate 3.19 L/min and air circulation

In the last scenario the ceiling and wall pipes of the room were flushed with groundwater with an average flow rate of 3.19 L/min. The pressure in the filter ranged between 60 and 110 kPa. The reasons for the rise are unknown, but probably due to air in the pipe system was the flow of the water blocked. An electrical van was used to let the air circulate within in the room and to establish a fast transport of the cooled air from the pipe surface into the free space of the room. The total operation time was 2911 min, because the weather at the 10th of September was very unstable, with thunderstorms and rain; whereas the 11th of September was sunny until the early afternoon. From

then on the temperature dropped due to thunderstorms. It is believed, that the 10th of September is not representative, as the outside temperature fluctuated with sudden temperature drops. As it can be seen from Figure 3.63, the mean inside temperature was always below the outside temperature for the 11th of September until the beginning of the thunderstorm when the temperature suddenly decreased of about 5 °C. The difference was highest when the outside temperature peaked around noon with about 3 °C difference between outside and inside temperature. The pipe temperature, as shown in Figure 3.64, at the entrance of the house was about 22 °C to 20.5 °C at night, whereas the groundwater temperature decreased over the time period from 18.0 °C to 17.6 °C. The water therefore increased its temperature to the house of about 4.4 °C to 2.9 °C. However, in the house the temperature only rose about 2.5 °C as the exit water had a temperature of maximum 24.5 °C in the afternoon and at night as low as 21 °C; therefore a temperature difference to the entrance of only 0.5 °C during the night. The temperature difference of the exit pipe surface area to the room temperature ranged from 3.5 °C during the noon and early afternoon time to about 1 °C in the night. The mean energy usage to operate the pump and van was 431 W. The relatively humidity in the room reached 80-85 % due to the cooling of the air. Since an appropriate system is missing that dries the air, the felt temperature in the room, compared to outside, was much higher, even though the mean temperature was below the outside temperature.

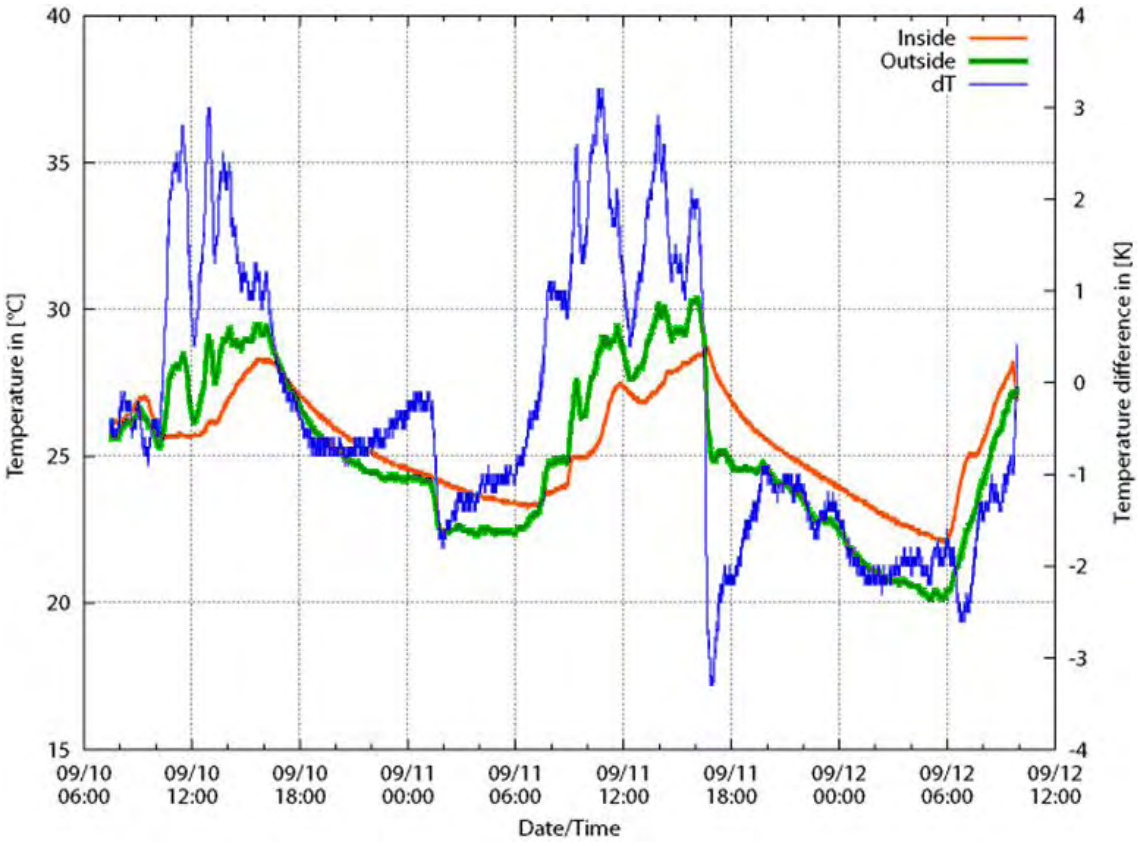

Figure 3.63－Inside and Outside temperature during the operation time (in °C) as well as temperature difference (blue, in K) for Scenario D.

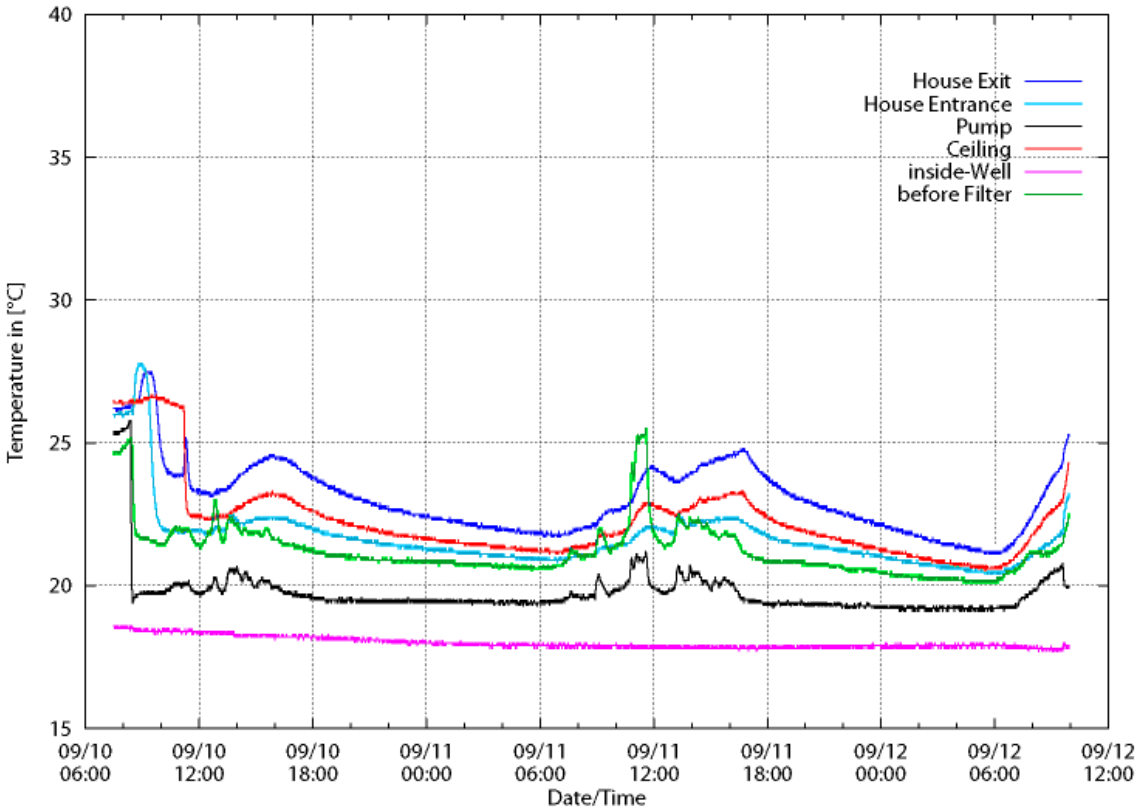

Figure 3.64－ Pipe surface and observation well No 2' temperature for selected sensors during the operation of Scenario D.

3.4.3.4 Discussion

It could be seen from all Scenarios that the pipe system was able to reduce the temperature in the room, compared to the normal temperature curve without a cooling system. However, compared to the cooling system, the geothermal system performed less effective under the given condition. The humidity in the room increased to 85-90 %, because of a missing drying system that is already integrated in a commonly used cooling system. Furthermore, the pump used 3 to 4 times more energy to operate the geothermal system, than the cooler has used. Table 3.16 summarises the above mentioned results.

As it can be seen, the cooler showed a higher performance in terms of energy usage and cooling effect, than the geothermal system. Furthermore, it decreased the humidity in the room to 70 %. However, even though the retention time in the room and contact time with the inner surface area with the groundwater was relatively long, did the exit water temperature still keeps a temperature gradient and hence . The thermal resistance of the used 3 mm PVC-U pipe-wall material is high compared to metal and a heat exchange is lower compared to a metal pipe. Since the used groundwater is corrosive, a metal pipe system made from stainless steel would increase the costs of such a geothermal system dramatically. Nevertheless, a compact metal heat exchanger with a high surface area and relatively long retention time of the water in the heat exchanger will lead to a better usage of the geothermal energy.

Table 3.16－operational parameters of the used Scenarios A to D of the geothermal experiment.

Scenario	Ceiling	Wall	Q [L/ min]	P [W]	p [kPa]	Relative Humidty [%]	dTmax [°C]	dTmin [°C]
A-1		X	4.36	390.0	50	90	5.0	-1.0
A-2		X	7.32	429.0	60	80	4.0	-0.5
B-1	X		2.46	392.3	20	90	4.0	-2.0
B-2	X		5.13	409.8	30	85	4.0	-3.0
C			-	124.2	-	70	6.8	-1.0
D	X	X	3.19	431.0	110 - 60	80 - 85	3.0	-3.3

3.4.3.5 Conclusions

On Tsushima campus, Okayama University, Japan an open loop groundwater heat pump system was developed in order to investigate the charcoal filter performance under field conditions. Furthermore the filtered groundwater was passed through installed pipes of a room at the study site in order to evaluate the cooling capacity of groundwater only by passing the water through PVC-U pipes. In a second experiment a Ferrolite MC3 filter was used for iron and manganese removal with a following injection back to the aquifer. From these experiments the following conclusions were obtained:

(1) Geothermal system was able to reduce the temperature in the room during the night and midday peaks.
(2) The used heat exchanger for the geothermal system didn‘t adjust the rel. humidity in the room that increased by decreasing indoor temperature.
(3) Common cooling system achieved a higher energy efficiency compared to the geothermal system and adjusted the rel. humidity, creating a comfortable indoor climate.
(4) Charcoal filter was able to effectively remove dissolved iron from the used groundwater.
(5) Metal (stainless steel) pipes instead of PVC-U pipes would increase the heat exchange capacity.
(6) If the performance of the on-site wooden charcoal filter with an initial mass of dry coal of 25.27 kg is compared to the laboratory column filter experiment results, the adsorption capacity of this filter was at least double or three times higher.
(7) However, it has to be noticed that the adsorption capacity is highly depended on the initial concentration of ions, the pH of the used groundwater, which will change the charge of active groups on the charcoal surface, and the existence of other ions or affinitive molecules, such as organic substances (Worch, 2012).

REFERENCES

Ahamad, K.U., and Jawed, M., 2010. Kinetics, Equilibrium and Breakthrough Studies for Fe (II) Removal by Wooden Charcoal: A Low-cost Adsorbent. Desalination 251 (1–3):137–145.

Ahfir, N.D., Benamar, A., Alem, A., and Wang, H.Q., 2009. Influence of internal structure and medium length on transport and deposition of suspended particles: A laboratory study. Transport in Porous Media 76, (2): 289–307.

Ampac USA, Advanced water treatment solutions, Iron Removal, URL: http://www.ampac1.com/index.php?_route_=iron_removal.htm: last access: 2013.07.20.

Appelo, C.A.J., Drijver, B., Hekkenberg, R., and de Jonge, M., 1999. Modeling in situ iron removal from ground water. Ground Water 37, (6): 811–817.

Bichara, A. 1988. Redevelopment of clogged recharge wells. Journal of Irrigation and Drainage Engineering 114, (2): 343–350.

Bouwer, H. 2002. Artificial recharge of groundwater: Hydrogeology and Engineering. Hydrogeology Journal 10, (1): 121–142.

Crosta, G., and di Prisco, C., 1999. Onslope instability induced by seepage erosion. Canadian Geotechnical Journal 36, (6): 1056–1073.

Ellis, D., Bouchard, C., and Lantagne, G., 2000. Removal of Iron and Manganese from Groundwater by Oxidation and Microfiltration. Desalination 130, (3):255–264.

Herzig, J.P., Leclerc, D.M., and Goff, P.L., 1970. Flow of suspensions through porous media-Application to deep filtration. Industrial and Engineering Chemistry 62, (5): 8–35.

Hódi, M., Polyák, K., and Hlavay, J., 1995. Removal of Pollutants from Drinking Water by Combined Ion Exchange and Adsorption Methods. Environment International 21, (3): 325–331.

Hokuei Construction corporation, activated charcoal for water purification, URL: http://www.hokuei-k.co.jp/4.jyousuisyorikasseitan.pdf:last access: 2013.07.20.

Igarashi, M., and Saito, K., 2005. Estimation of Impervious Hydraulic Gradient for used Yamasuna Sand, Japanese Society of Civil Engineering (JSCE), 2005 (3): 153 – 154.

Google Inc. 2013, Map of Tsushima Campus, Okayama, Japan retrieved from Google Maps: https://maps.google.de/maps?q=japan&hl=en&ll=34.689982,133.925014&spn=0.002488,0.005284&sll=51.151786,10.415039&sspn=7.776562,21.643066&t=h&hnear=Japan&z=18: last access: 2013.07.15.

H2O Remediation Engineering, URL: www.h2oengineering.com: last access 2013.07.21.

Holländer, H.M., Boochs, P.W., Billib, M., and Panda, S.N., 2005. Labor-Säulenversuche zur Untersuchung von Clogging-Effekten im Grundwasserleiter—Einfluss von physikalischen An- und Ablagerungen, Gasblasen und biologischer Aktivität. Grundwasser 10, (4): 205–215. (in German).

Japanese Geotechnical Society, 1965. Handbook of soil mechanics and foundation engineering, Tokyo, Japanese Geotechnical Society: 93. (in Japanese).

JFE Recycling Management Japan Inc., URL: http://www.jfe-rmj.co.jp: last access 2013.07.22.

JMA – Japan Meteorology Agency, 2012, URL: http://www.jma.go.jp: last access: 2013/01/15.

Jones, J.A.A., 2010. Soil piping and catchment response. Hydrological Processes 24, (1): 1548–1566.

Justin, J.D., 1924. The design of earth dams. Transactions of the American Society of Civil Engineers88, (1): 1–61.

Marsh, H., and Rodríguez-Reinoso, F., 2006. Activated Carbon, 1st ed., Elsevier, Oxford, UK.

McDowell-Boyer, L.M., Hunt, J.R., and Sitar, N., 1986. Particle transport through porous media. Water Resources Research 22, (13): 1901–1921.

Moghadasi, J., Müller-Steinhagen, H., Jamialahmadi, M., and Sharif, A., 2004. Theoretical and experimental study of particle movement and deposition in porous media during water injection. Journal of Petroleum Science and Engineering 43, (3–4): 163–181.

Moreno, J.C., Gómez, R., and Giraldo, L., 2010. Removal of Mn, Fe, Ni and Cu Ions from Wastewater Using Cow Bone Charcoal. Materials 3, (1):452–466.

Mulqueen, J., 2005. The flow of water through gravels. Irish Journal of Agricultural and Food Research 44, (1): 83–94.

Mutschmann, J., and Stimmelmayr, F., 1991. Taschenbuch der Wasserversorgung. Franckh-Kosmos, Stuttgart , Germnay. (in German）

Nakashima, H., Matsubara, M., and Iijima, J., 1986. Observation of the piping phenomenon by x-ray radiography. In Proceedings of the 21st Annual Conference of Japanese Society of Soil Mechanics and Foundation Engineering (JSSMFE), Sapporo, Japan: 1479-1482. (in Japanese)

NLID – National Land and Information Division, National and Regional Policy Bureau, Tokyo, 2011: National Land Agency, Okayama Prefecture, map, URL: http://nrb-www.mlit.go.jp/kokjo/tochimizu/ F3/ZOOMA/3304/index.html: last access 2013.07.01.

Oba, N., Tsuyuki, T., and Ebihara, H., 1967. Mineral and Chemical Composition, and Genesis of the Yamasuna. Gansekikoubutsukoushougakkukaishi, 58(3): 81 – 97. (in Japanese)

Ohno, M., Yamazaki, H., and Tran-Duc, P.O., 1984. Experimental study of piping property of sand. Report of Hazama: 33-40. (in Japanese).

Okajima, K., and Tanaka, T., 2008. Evaluation of analyses of downstream piping of weirs by model experiments and elasto-plastic FEM. Proceedings of Fourth International Conference on Scour and Erosion (ICSE), November 5-7, Tokyo: 460-567. (in Japanese)

Olsthoorn, T.N., 1982. The clogging of recharge wells: Main subjects. Rijswijk, The Netherlands, KeuringsinstituutvoorWaterleidingArtikelen (KIWA).

Pacini, V.A., MaríaIngallinella, A., and Sanguinett,i G., 2005. Removal of Iron and Manganese Using Biological Roughing up Flow Filtration Technology. Water Research 39, (18): 4463–4475.

Pavelic, P., Dillon, P.J., Mucha, M., Nakai, T., Barry, K.E., and Bestland, E., 2011. Laboratory assessment of factors affecting soil clogging of soil aquifer treatment systems. Water Research 45, (10): 3153–3163.

Pérez Paricio, A., 2001. Integrated modelling of clogging processes in artificial groundwater recharge. Ph.D. thesis, Technical University of Catalonia (UPC).

Reddi, L.N., Ming, X., Hajra, M.G., and Lee, I.M., 2000. Permeability reduction of soil filters due to physical clogging. Journal of Geotechnical and Geo-environmental Engineering 126, (3): 236–246.

Saaltink, M.W., Ayora, C., Stuyfzand, P.J., and Timmer, H., 2003. Analysis of a deep well recharge experiment by calibrating a reactive transport model with field data. Journal of Contaminant Hydrology 65, (1–2): 1–18.

Seppánen, H.T., 1992. Experiences of Biological Iron and Manganese Removal in Finland. Water and Environment Journal 6, (4): 333–340.

Shindo, K., 1967. Rock Mechanics, Morikita, Tokyo. (Japanese translation of :Talobre, J.,and D. O. Martin. 1957.La mécanique des roches:appliqué aux travaux publics. Dunod.)

Siemens Water Technologies 2011, Activated Carbon, URL: http://www.water.siemens.com/en/products/activated_carbon/Pages/default.aspx: last accessed: 2013.07.21.

Sichardt, W., 1928. Das Fassungsvermögen von Rohrbrunnen und seine Bedeutung für die Grundwasserabsenkung, insbesondere für größere Absenkungstiefen. Springer. (in German)

Sugii, T., Yamada, K., and Nagura, S., 2009. Critical velocity for progressive seepage failure and change in permeability. Geotecnical Engineering Magazine Japan 57, (9): 26–29. (in Japanese)

Tanaka, T.,1992. Research on artificial Recharge. Master Thesis, Okayama University, Japan. (in Japanese)

Terzaghi, K., Peck, R.B., and Mesri, G., 1996. Soil Mechanics in Engineering Practice. John Wiley and Sons.

Tohkemy Company, 2013, URL: http://www.tohkemy.co.jp/english/item/roka_p6.html: last access: 2013.07.21.

Vigneswaran, S., and Thiyagaram, M., 1984. Application of filtration theories to ground water recharge problems. Water, Air, and Soil Pollution 22, (4): 417–428.

Vigneswaren, S., Jeyaseelan, S., and Gupta. A. D., 1985. A pilot-scale investigation of particle retention during artificial recharge. Water, Air and Soil Pollution 25, (1): 1–13.

Worch, E., 2012. Adsorption Technology in Water Treatment. De Gruyter, Berlin/Boston.

World Health Organisation (WHO), URL: http://www.who.int/en/: last access 2013.06.28.

Ye, X., Du, X., Li, S., and Yang, Y., 2010. Study on clogging mechanism and control methods of artificial recharge. In Proceedings of the 2010 International Conference on Challenges in Environmental Science and Computer Engineering (CESCE), March 6-7, Wuhan, China, Institute of Electrical and Electronics Engineers (IEEE) 2: 29–32.

CHAPTER 4

SOLUBILIZATION AND ACQUISITION OF PHOSPHORUS FROM SPARINGLY SOLUBLE PHOSPHORUS SOURCES AND DIFFERENTIAL GROWTH RESPONSE OF BRASSICA CULTIVARS EXPOSED TO PHOSPHORUS-STRESS ENVIRONMENT

4.1 INTRODUCTION

Phosphorus (P) is essential to sustain life of plants and makes up about 2% of a plant's dry biomass. It is involved in the regulation of numerous physiological and biochemical processes and an essential building block of diverse cell components. It is the key substrate in energy metabolism in the form of adenosine triphosphate (ATP). It is one of the major constituents of nucleic acids in the form of sugar phosphate backbone and membranes in the form of phospholipids bilayer, what means a two-layer membrane that surrounds many types of plants. This membrane consists of phospholipids (molecules) and is like a shield of protection for the cell by keeping unwanted substances out. Furthermore P is required in the transformation of sugar and starch, cell division, membrane construction, signal transduction, genetic information transmission and expression, seed germination, flowering and fruit formation, and almost every phase of plant's vital processes (Hammond et al. 2009, Yuan and Liu 2008, Raghothama and Karthikeyan 2005, Vance, Uhde-Stone, and Allan 2003, Ticconi and Abel 2004, Abel, Ticconi, and Delatorre 2002). Phosphorus, which plants can purchase mostly as phosphate (PO_4^{3-}) anion, is frequently the most limiting macronutrient for plant growth and development. For a typical plant, PO_4^{3-} concentrations are at the ranges of 1 μM in the soil, 10,000 μM in the cells, and 400 μM in the xylem (Fang et al. 2009). The chemistry of P in soils results in very low concentrations of phosphate in the soil solution (2–10 μM). The PO_4^{3-} level in soil solution is regulated mainly with its interaction with organic and inorganic surfaces in the soil and PO_4^{3-} solubility is strongly pH dependent. Nevertheless, many soils have large reserves of total P (1.2 g/ kg on average; Hinsinger et al. 2011), often hundreds of times more than the P available to the crops (Shenoy and Kalagudi 2005). However, P deficiency occurs in soils low innative P or with high P-fixation capacities because it rapidly forms insoluble complexes under acidic and alkaline environments. Humid tropical and subtropical climate with warm, moist conditions result in weathered acidic soils (mostly ultisols and oxisols), in which free iron (Fe) and aluminum (Al) oxides bind native and applied P,

and in the calcareous and alkaline calcareous soils (mostly aridisols), amounts of calcium (Ca) and magnesium (Mg) compounds are usually high, which bind inorganic phosphates into forms highly unavailable to plants (Yan et al. 2006, Panigrahy, Rao, and Sarla 2009). Thus, bioavailable P may constitute less than 0.1% of total soil P. Therefore, in global agriculture, PO_4^{3-} seriously limits plant growth and crop yield.

Concerns about P sustainability in agriculture arise not only from the potential for P scarcity but also from the known effects of agricultural P use beyond the field such as the notorious problem of eutrophication (Gaxiola, Edwards, and Elser 2011). Replenishment of soil P reserves through fertilization is a common practice, but the economic sustainability of this practice is in question, as economically recoverable P reserves are estimated to be 50% depleted by the middle of this century (Abelson 1999).

Global demand for crops will continue to rise over the next half century, increasing the demand for phosphate fertilizers. All modern agriculture is today dependent on regular inputs of P fertilizers derived from rock phosphate (RP) to replenish the P removed from the soil by the growing and harvesting crops. However, P is nonrenewable resource and approximately 50–100 years remain of current known reserves (Steen 1998, Smil 2000, Cordell, Drangert, and White 2009).

Despite the depletion of global P reserves and potential geopolitical tensions, future PO_4^{3-} scarcity and reduced accessibility to farmers is not yet considered by national and international policy and decision makers (Cordell, Drangert, and White 2009). Therefore, there is an urgent need to explore and deploy alternative ecofriendly strategies enhancing P acquisition and P-use efficiency in both low- and high-input sustainable agricultural systems. Plants constantly sense the changes in their environment when mineral elements are scarce, and under PO_4^{3-} deprivation they adapt their physiology and development to efficiently use the lower supply of P (Desnos 2008). Plants respond to PO_4^{3-} starvation by inducing a suite of adaptive responses comprising altered growth behavior, enhanced PO_4^{3-} acquisition, and reduced PO_4^{3-} demand that together define a distinct physiological state (Lai et al. 2007). The adaptation of plants to low P availability is therefore of considerable interest in both basic and applied plant biology. The cultivars efficient in solublizing Ca-P complexes may help to cope with the problem of unavailability of applied fertilizers as the major portion (88–99%) of total P in alkaline calcareous soils exist as Ca phosphates of varying solublities. Under PO_4^{3-} deprivation, plant roots can alter solution PO_4^{3-} availability by rhizosphere acidification through H^+ efflux and carboxylate exudation. In calcareous soils, rhizosphere acidification by H^+ extrusion causes dissolution of poorly available Ca-P minerals. Roots have to acquire PO_4^{3-} against a steep concentration

gradient (100-fold or higher) because of high demand of PO_4^{3-} in the plant. An energy-mediated cotransport process driven by protons generated by plasma membrane H^+ATPase has been proposed for PO_4^{3-} uptake in plants (Sakano, Yazaki, and Mimura, 1992). The PO_4^{3-} absorption is accompanied by H^+ influx with a stoichiometry of 2 to 4 H^+ per $H_2PO_4^-$ transported. Plant species such as buckwheat, oilseed rape, and legumes are quite efficient in utilizing rock P by releasing carboxylates because of changes in cellular metabolism as a PO_4^{3-}-starvation response. Carboxylates can diffuse into the rhizosphere as a result of the high electrochemical potential gradient existing between the cytoplasm of root cells and the soil solution, and can release P from unavailable bound soil P reserves. Differential growth response and P acquisition and P-use efficiency by *Brassica* cultivars grown under P-stress soil conditions is estimated in a pot culture study. Diverse *Brassica* cultivars grown with sparingly soluble P sources [calcium phosphate ($Ca_3(PO_4)_2$ and RP] were used as test plants in solution cultures to elucidate P-stress-induced root-mediated pH changes and carboxylates exudations.

4.2 MATERIALS AND METHODS

4.2.1 Plant Material and Growth Environment

Diverse *Brassica* cultivars (low-P-tolerant and low-P-sensitive) selected in terms of P acquisition and P-use efficiency were used in experiments to investigate relative growth response, P-efficiency characteristics, and the role of P-starvation-induced root-mediated rhizospheric acidification in P solubilization and acquisition from sparingly soluble P sources and low P supply. Uniform and healthy seeds of cultivars were germinated in polyethylene-lined iron trays containing riverbed sand for seed germination and seedling establishment in a dark chamber at 25 ºC for solution culture experiments. Experiment 1 was conducted in glass house having a controlled growth environment, whereas experiments 2 and 3 were conducted in a cultivation chamber (CFH-405; Tomy Seiko Co., Tokyo, Japan) at a cycle of 14 h / 20 ºC night and 10 h / 25 ºC day and a light intensity of 40 μmol/ (m^2 s) (3800 lx). The relative humidity of the chamber was adjusted to 60%. The composition of the used modified Hoffland's solution (Hoffland et al. 1989) was [in mM] potassium nitrate (KNO_3) [2], ammonium nitrate (NH_4NO_3) [1], calcium nitrate [$Ca(NO_3)_2 \cdot 4H_2O$] [2], magnesium sulfate ($MgSO_4 \cdot 7H_2O$) [0.5], and potassium sulfate (K_2SO_4) [0.5] and [in μM] iron [Fe(III)] – ethylenediaminetetraacetic acid (EDTA) [50], boric acid (H_3BO_3) [25], manganese sulfate ($MnSO_4 \cdot H_2O$) [2], zinc sulfate ($ZnSO_4 \cdot 7H_2O$) [2], copper sulfate ($CuSO_4 \cdot 5H_2O$) [0.5], potassium chloride (KCl) [50], and molybdic acid (H_2MoO_4) [0.5]. Solutions

were renovated at 3-day intervals, and sparingly soluble P sources [$Ca_3(PO_4)_2$ (TCP) and Jordan RP finely ground (0.15 mm), 36% total P, 5.5% citrate-soluble (2% citric acid) P, and no water-soluble P] were stirred mechanically twice a day in order to keep close contact with roots.

4.2.2 Phosphorus Acquisition and P-Use Efficiency by Brassica Cultivars Grown in a Low Soil P Environment

By using soil texturally sandy loam and categorized as P deficient [sodium bicarbonate ($NaHCO_3$)–extractable P 3.97 mg/kg, Mehlich 3–extractable P 6.13 mg/kg, electrical conductivity (EC_e) 1.4 dS/m, pH in water (1:5 ratio) 7.8], a pot experiment was conducted in a glasshouse. The soil was air dried and coarsely ground before filling in glazed china clay pots (30 cm deep and 22 cm in diameter) at the rate of 6 kg per pot. To half the pots, P was applied at the rate of 60 mg P/kg soil as ammonium phosphate ($NH_4H_2PO_4$) (+P), whereas no P was applied to the remaining half (0P). In addition, N was applied to all pots at the rate of 175 mgN/kg (in +P pots N was added in addition to N coming from $NH_4H_2PO_4$. Potassium was also added to all pots at the rate of 75 mgK/kg soil. All P, K, and half of N were applied in solution from using enough water to equilibrate with entire soil 2 days before sowing of seeds. The remaining half of N was applied 25 days after sowing. Four seeds of each of the four *Brassica* cultivars were sown per pot. The two-factorial (two P levels, four cultivars) experiment was laid out according to CRD (complete randomized design) with three replicates. All pots were watered daily with demineralized water to maintain 80% field moisture capacity, and plants were harvested 41 days after sowing.

4.2.3 Plant Measurements

4.2.3.1 Biomass Assay

Harvested plants were washed instantly with distilled water (taking care that no grain of TCP or RP was attached with roots), blotted dry with filter paper sheets, and separated into shoots and roots. Leaf area was measured on a leaf area meter (CI- 203 Area Meter, CID, Camas, Wash., USA). The samples were dried at 70 ºC for 48 h in a forced-air-driven oven, and dry mass (g/plant) was recorded. The shoot and root samples were ground to pass through a 0.42-mm screen (40 mesh).

4.2.3.2 Determination of Tissue P Concentration

The plant samples were digested in 2 N hydrochloric acid (HCl) after dry ashing at 550 ºC for 7 h and filtered through Whatman No. 42 filter paper. The first portions of

the filtrate were discarded. The P concentrations ([P]s) in samples were estimated by the vanadate–molybdate yellow method (Chapman and Pratt 1961) using a spectrophotometer (Hitachi, U-1100; Hitachi, Tokyo, Japan). In experiment 1, Ca concentrations ([Ca]) (mg/g) in samples were estimated by using atomic absorption spectrophotometry (Hitachi, Z-6100 polarized Zeeman; Hitachi, Tokyo, Japan). The P uptake (mg/plant) was calculated by multiplying [P]s in the respective tissue with its dry matter:

$$\text{P uptake} = \text{P concentration ([P])}\ (mg/g)\ \times drymatter\ (g/plant) \tag{4.1}$$

4.2.3.3 Estimation of Various Growth Parameters and P-Efficiency Characteristics

The P-stress factor (%PSF) for shoot dry matter (SDM) was calculated as:

$$\text{PSF} = \left(\text{SDM}_{(adequate/Sufficient\ \text{P})} - SDM_{(deficient/stress\ \text{P})}\right) \times 100 \tag{4.2}$$

where SDM is shoot dry matter (g/plant) in the respective treatment. Relative reduction in leaf area/plant (%LA) was calculated by the formula Relative reduction in:

$$\text{LA}\ (\%) = \frac{\left(LA_{(\text{high/+P})} - LA_{(low\ or\ stress/\ \text{0P})}\right)}{LA_{(high/+P)}} \times 100 \tag{4.3}$$

The P-utilization efficiency (PUE) was determined according to Siddiqi and Glass (1981) as:

$$PUE_{(g^2 SDM/mg\ \text{shoot P})} = SDM\ (g/plant)/[\text{P}]\ (\text{mg/g}) \tag{4.4}$$

The P-efficiency ratio (PER) at stress/0P was estimated according to Gerloff and Gabelman (1983):

$$\text{P} - \text{efficiency ratio (g DM/mg } P) = \frac{Total\ dry\ matter\ (g/pant)}{Total\ P{-}uptake\ (g/plant)} \tag{4.5}$$

The P-efficiency (PE) (relative shoot growth) was calculated as described by Ozturk et al. (2005):

$$\text{P} - \text{efficiency (relative shoot growth)} = \frac{SDM_{(low\ or\ stress\ P)}}{SDM_{(adequate/sufficient\ P)}} \times 100 \qquad (4.6)$$

4.2.3.4 Measurement of Root-Induced pH Changes in the Solution Culture Media

In experiment 2, 1-week-old pregerminated healthy and uniform-sized seedlings were transplanted to foam plugged holes in thermopal sheets floating on 3 L of continuously aerated halfstrength modified Hoffland's solution in polyethylene-lined, 3-L-capacity plastic pots, modified to contain no P. Phosphorus was applied to individual pots as KH_2PO_4 as a control treatment (KP) at 200 μM P, and RP at 2 g/L and $Ca_3(PO_4)_2$ (TCP) at 0.2 g/L respectively were applied as sparingly soluble P sources. Solution level in each pot was marked and maintained every day. Initial pH of the solution after addition of RP and TCP was 7 ± 0.1. pH changes were monitored regularly in all pots on 0, 4, 8, 12, 16, and 20 days after transplanting (DAT). Nitrogen was supplied as nitrate (NO_3) and ammonium (NH_4) at a 3:1 ratio. Treatments were performed in triplicate according to a completely randomized design (CRD), and each set of experiments was repeated at least twice.

4.2.3.5 Determination of Exuded Carboxylates by Tested Cultivars

One-week-old uniformly sized seedlings of four cultivars were transferred to a complete nutrient solution for 7 days using KH_2PO_4 as a P source in experiment 3. The pH of the solution was monitored daily and maintained at 5.5 ± 0.5. The nutrient solution was refilled every 3 days. After 7 days in a complete nutrient solution, the seedlings were transferred to an aerated nutrient solution containing 200 μM P (+P) using KH_2PO_4, without P (–P), RP (2 g/L), and $Ca_3(PO_4)_2$ at 0.2 g/L, respectively in 3.5 L pots. Each cultivar was transplanted in three pots maintaining three plants per pot using factorial CRD, and each set of experiments was repeated at least twice. The plants were grown for an additional 12 days in the cultivation chamber. Plant roots were washed with deionized water and then submerged in 300 mL of aerated solution with 0.5 mM calcium chloride ($CaCl_2$; pH = 5.5) for 4 and 8 h, respectively, and root exudates were collected for carboxylates. The solution was evaporated to about 5 ml under reduced pressure at 45 ºC on a rotary evaporator (Vacuum controller NVC-1100, Eyela, Tokyo Rikakikai Co., Ltd., Japan). The solution containing root exudates was allowed to pass first through a cation exchange column (16 mm × 14 cm) filled with 5 g Dowex 50 W × 8 (100–200, H^+ form) resin (Muromachi Kagaku Kogyo Co., Ltd, Tokyo, Japan) and then through an anion exchange column filled with 2 g Dowex 1 × 8

resin (0.15–0.06 mm, Cl^- form) without adjusting the pH. This procedure was carried out under nonsterile conditions and the carboxylates (citrate, malate, and succinate) retained in the anion exchange resin were eluted with 8N formic acid. The eluent was concentrated to dryness under reduced pressure using a rotary evaporator. The residue was redissolved in 1 ml ultrapure water adjusted to pH 2.1 with perchloric acid ($HClO_4$) and filtered with a 0.45-μM filter. The carboxylates were detected by high-performance liquid chromatography [HPLC; LC-6A, Shimadzu, Kyoto, Japan equipped with the ion-exclusion column Chemoo-pack Nucleosil 5C18, 4.6 × 250 (6 A), Japan].

4.2.3.6 Statistical Analysis

Data were subjected to statistical analyses according to standard procedures (Steel and Torrie 1980) using the MSTAT-C program (MSTAT, East Lansing, Mich.) and the methods described by Gomez and Gomez (1984). Factorial CRD was employed for analysis of variance (ANOVA). Treatment means were separated using DMRT (Duncan's multiple range test) and presented with standard errors. Correlation coefficient (*r*) values were determined among various parameters using treatment means. $P < 0.05$ was considered statistically significant.

4.3 RESULTS

4.3.1 Growth Response and P Acquisition under Soil P-Stress Environment

Brassica cultivars and P supply had a significant ($P < 0.001$) main and interactive effect on shoot growth, root development, and total dry matter (TDM) production. Averaged over cultivars, SDM, RDM, and TDM were more than two-fold higher at +P (control) compared to 0P treatment (Figure 4.1; Table 4.1). Leaf area per plant was also doubled at +P compared to 0P treatment (Table 4.1)

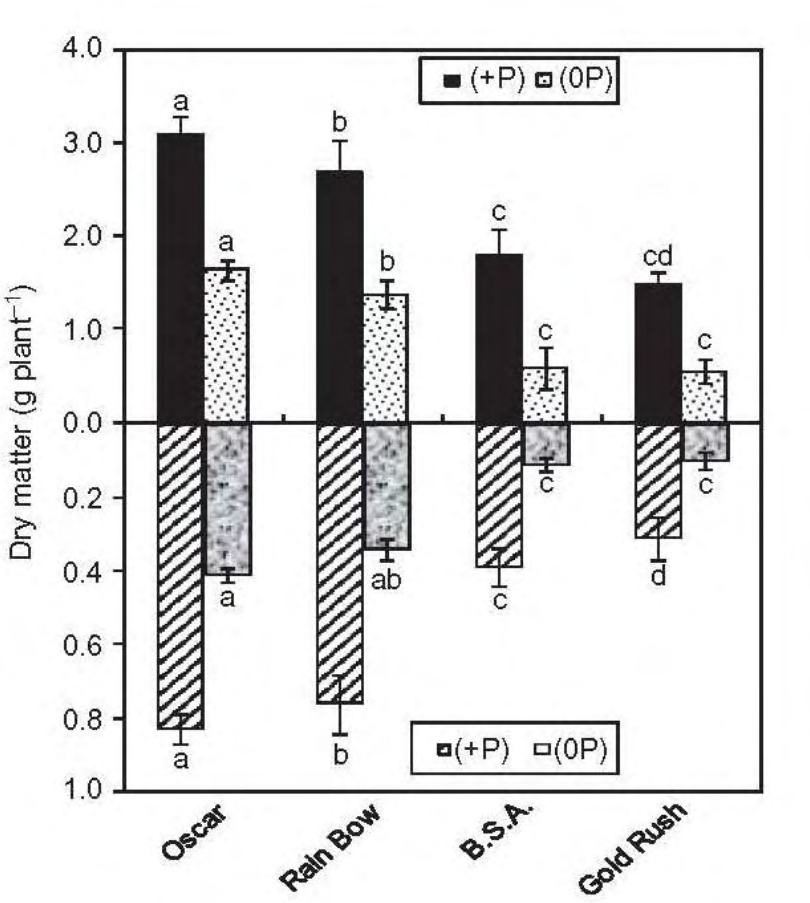

Figure 4.1—Biomass accumulation by four *Brassica* cultivars at low (0P) and high (+P) supply (experiment 1).

Table 4.1—Various growth parameters of *Brassica* cultivars at high (+P) and low P (0P) supply

		Cultivar				
Parameter	P level	Oscar	Rainbow	BSA	Gold Rush	Mean
P concentration, shoot	+P	7.21 c	6.96 d	8.33 ab	8.61 a	7.78 A
(mg g−1 DM)	0P	1.90 c	1.97 bc	2.13 ab	2.26 a	2.07 B
P concentration, root	+P	3.50NS	3.98	3.57	3.62	3.67 *B*
(mg g−1 DM)	0P	4.57 c	4.38 cd	9.10 a	8.55 b	6.65 A
Shoot P uptake (mg	+P	22.21 a	18.58 b	14.83 c	12.66 d	17.07 A
plant−1)	OP	3.10 a	2.70 b	1.24 cde	1.24 cde	2.07 B
Root P uptake (mg	+P	3.05 ab	3.18 a	1.46 c	1.19 cd	2.22 A

plant−1)	OP	1.97 a	1.58 b	1.08 c	0.86 d	1.37 B
Total P uptake (mg	+P	25.25 a	21.77 b	16.29 c	13.85 d	19.29 A
plant−1)	OP	5.06 a	4.28 b	2.33 c	2.10 c	3.44 B
Ca concentration,	+P	16.29 ab	16.82 a	15.52 c	16.72 ab	16.34 B
shoot (mg g−1 DM[1)])	OP	24.32 ab	25.47 a	23.74 b	20.39 cd	23.48 A
Ca concentration, root	+P	9.20 b	9.74 a	8.41 cd	9.66 ab	9.25 B
(mg g−1 DM)	OP	9.74 e	11.76 cd	18.64 b	20.70 a	15.21 A
Shoot Ca uptake (mg	+P	50.17 a	44.91 b	27.63 cde	24.58 e	36.82 A
plant−1)	0P	39.64 a	34.89 b	13.77 cd	11.21 ef	24.88 B
Root Ca uptake (mg	+P	8.00 a	7.79 ab	3.45 c	3.19 cd	5.61 A
plant−1)	OP	4.19 ab	4.23 a	2.24 cd	2.07 e	3.18 B
Total Ca uptake (mg	+P	58.18 a	52.70 b	31.07 cd	27.77 de	42.43 A
plant−1)	OP	43.83 a	39.13 b	16.01 de	13.28 e	28.06 B
Total dry matter (g	+P	3.95 a	3.47 ab	2.19 c	1.80 d	2.85 A
plant−1)	OP	2.06 a	1.73 b	0.70 d	0.65 de	1.29 B
Root–shoot ratio	+P	0.28 b	0.30 a	0.23 c	0.22 cd	0.26 A
	OP	0.26 a	0.26 a	0.21 c	0.18 d	0.23 B
Leaf area (cm2	+P	304 a	275 b	177 de	181 cd	234 A
plant−1)		189 a	161 b	60 cd	56 de	117 B

[1)]. Means followed by different letter(s) differed significantly according to Duncan's multiplerange test (P = 0.05). NS, nonsignificant; and DM, dry matter (experiment 1).

4.3.2 Phosphorus Acquisition and P Efficiency of Brassica Cultivars

Phosphorus supply and cultivars had significant main and interactive effects on plant [P] and P contents of tested cultivars (Table 4.1). On an average, [P] was approximately 3.75 times lower in shoots of plants grown with 0P compared with +P. Nevertheless, [P] in roots of cultivars grown with 0P was greater than the cultivars grown with +P, and cultivar differences were statistically important only at 0P (Table 4.1). Cultivars having lower root [P] produced greater SDM (r= –0.95**) at 0P. Averaged over all cultivars, total P contents increased 5.58 times with P supply (Table 4.1). Low P caused invariable decrease in P contents of tested cultivars. The magnitude of decrease, however, was relatively greater in the case of the aboveground parts than roots. Total P uptake had a highly significant positive correlation with RDM and SDM at 0P, suggesting that the cultivars with greater RDM accumulated greater amounts of P.

4.3.3 Phosphorus Efficiency of Brassica Cultivars

Cultivars and P levels had a significant main and interactive effect on PUE in cultivars calculated according to Siddiqi and Glass (1981) (Figure 4.2a). On average, about a 1.7 times decrease in PUE was observed with +P compared to 0P implying that less dry matter was produced for each additional unit of P absorbed. There was significant variation in PE among the cultivars, ranging from 33% (BSA) to 53% (Oscar) (Figure 4.2b). Cultivars showing greater PE had greater SDM at 0P. The PER (reciprocal of tissue-[P]) decreased at +P indicating a decline in the internal utilization of P to produce dry mass (Figure 4.2c).

The cultivars that had taken up more Ca also showed greater P uptake (Figure 4.2d) and were able to produce more biomass (Figure 4.1). Consequently, the correlations between PE and SDM (r= 0.94**) and between PER and SDM (r= 0.96**) were highly significant at 0P (Figures 4.3a and 4.3b). The correlation between shoot [P] and PE was statistically not significant.

Shoot P content showed a very significant correlation with PE (r= 0.96**). This may indicate a greater role of P uptake in expression of high PE in cultivars. There were highly significant negative correlations between PSF and PUE (Figure 4.3c) and between PSF and PE (Figure 4.3d), implying that the cultivars showing greater PUE and PE and low PSF values were more tolerant under a P-stress environment.

SDM (r= 0.94**) and between PER and SDM (r= 0.96**) were highly significant at 0P (Figures 4.3a and 4.3b). The correlation between shoot [P] and PE was statistically not significant. Shoot P content showed a very significant correlation with PE (r= 0.96**). This may indicate a greater role of P uptake in expression of high PE in cultivars. There were highly significant negative correlations between PSF and PUE (Figure 4.3c) and between PSF and PE (Figure 4.3d), implying that the cultivars showing greater PUE and PE and low PSF values were more tolerant under a P-stress environment.

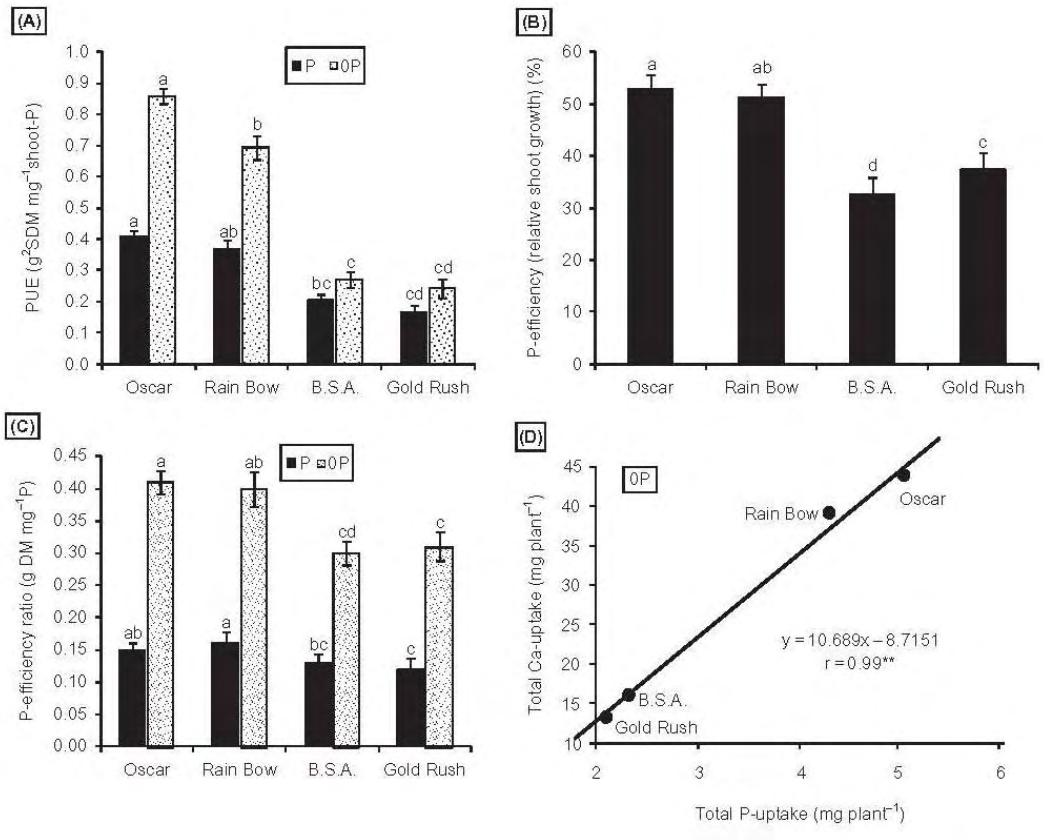

Figure 4.2－ (A) P-utilization efficiency (PUE), (B) P efficiency, (C) P-efficiency ratio, and (D) relationship between total Ca uptake and P uptake at low P by *Brassica* cultivars grown with low (0P) and high (+P) supply (experiment 1).

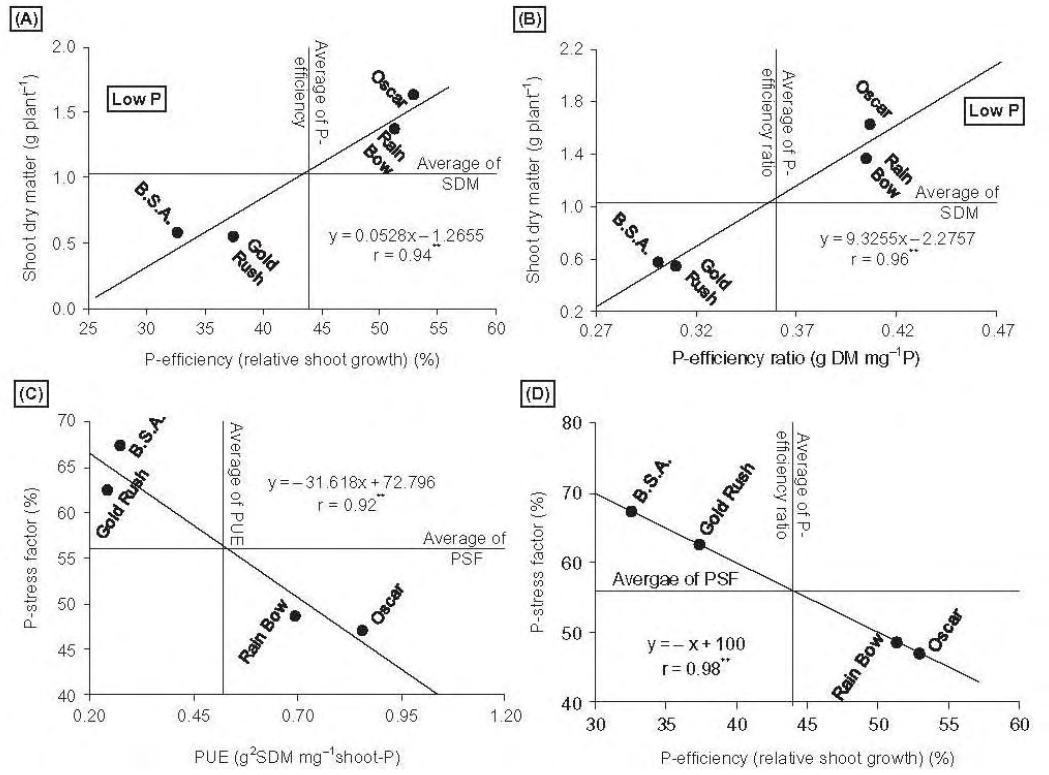

Figure 4.3－ Relationship between biomass accumulation and various growth parameters of four *Brassica* cultivars at low soil P. ∗∗Significant at *P* = 0.01 (experiment 1).

4.3.4 Relative Reduction in Plant Biomass

Variation in low-P-stress tolerance of tested cultivars was obvious from their PSF values, ranging from 47% (Oscar) to 67% (BSA) in experiment 1 (Figure 4a). Leaf area per plant (LA) of tested cultivars was lower in 0P pots than in P-treated pots (Table 4.1). The magnitude of reduction, however, was variable among cultivars, ranging from 38% (Oscar) to 69% (Gold Rush) with a mean value of 54% (Figure 4.4b). Relative reduction in leaf area per plant and shoot biomass (PSF) as a function of PE and RDM, respectively, at 0P revealed that P-tolerant cultivars presented lower PSF and greater RDM and PE values, and are considered to be more P tolerant than P-sensitive cultivars (Figures 4.4c and 4.4d).

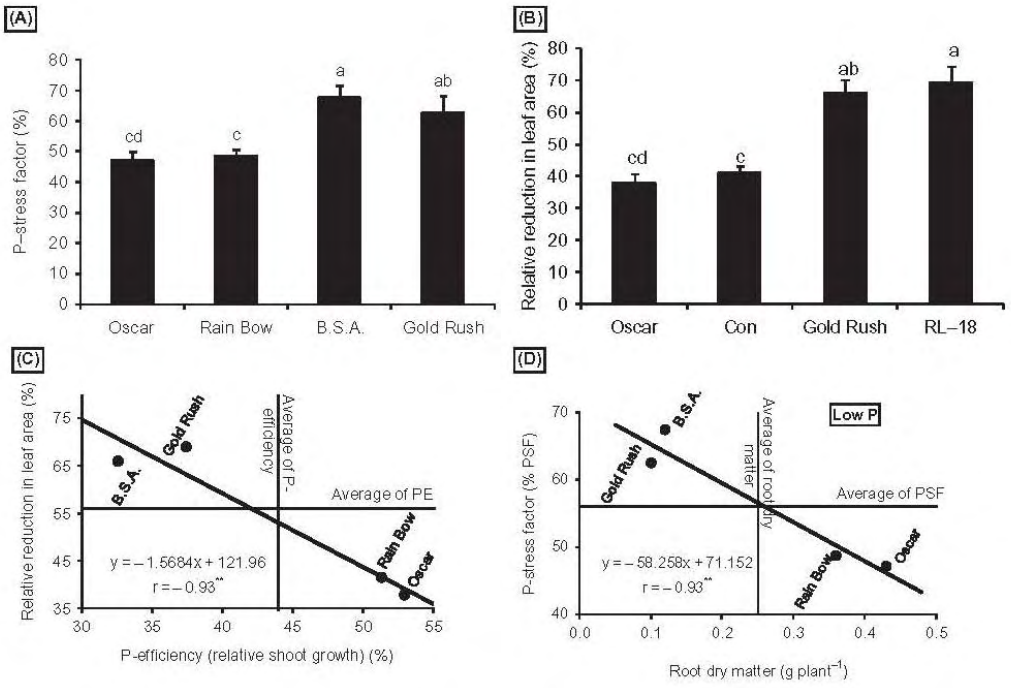

Figure 4.4－ (a) P-stress factor (PSF), (b) relative reduction in leaf area due to P stress, and ordination plots between (c) relative reduction in leaf area and P efficiency and (d) PSF and root dry matter of *Brassica* cultivars grown with low (0P) and high (+P) supply. ⁎⁎Significant at *P* = 0.01 (experiment 1).

4.3.5 Phosphorus Starvation Induced Roots to Mediate pH Changes and P Contents of Brassica Cultivars

Phosphorus-starvation-induced root-mediated pH changes and total P contents of cultivars grown with sparingly soluble P sources are depicted in Figure 5. Phosphorus-starvation induced pH changes were compared in hydroponically grown cultivars with differing ability to mobilize sparingly soluble P sources (TCP and RP). Compared with the control, a substantial decrease in solution media pH was observed among cultivars grown with sparingly soluble TCP and RP. Figures 4.5a–c depict the changes in culture media pH with time, and cultivars can be categorized into two classes. Class I (P-efficient) cultivars showed a greater decrease in pH than class II (P inefficient) cultivars. Cultivars accumulating a greater amount of total P in plants had a lower pH in the rooting media and vice versa. Total P contents of the plants also had a significantly ($P < 0.001$) negative correlation ($r = –0.97^{**}$ and $–0.92^{**}$ at RP and TCP, respectively) with pH of solutions measured at 20 days after transplant (DAT; Figure 4.5d).

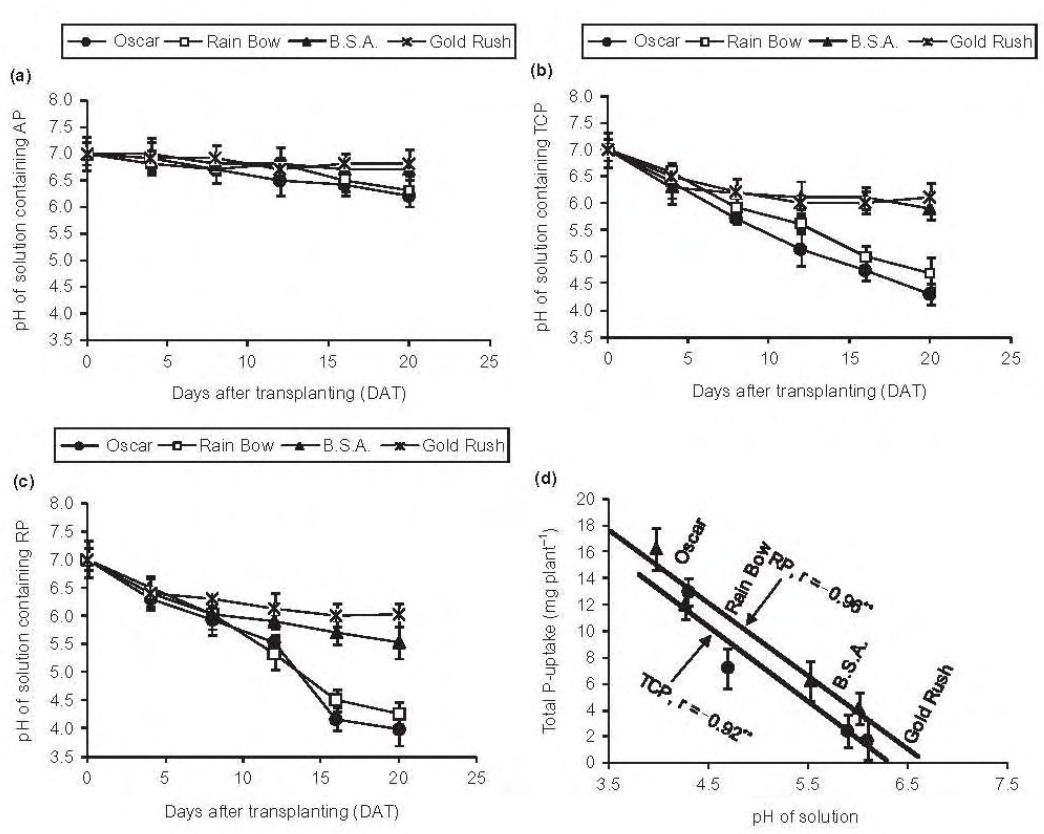

Figure 4.5－Panels (a)–(c) Changes in pH of the solutions by cultivars measured at 0, 4, 8, 12, 16, and 20 DAT containing KH_2PO_4 (KP), $Ca_3(PO_4)_2$, and rock P (RP) in solutions, and (d) total P uptake by cultivars in relation to pH of solutions measured at 20 DAT containing $Ca_3(PO_4)_2$ and rock P as P sources in the rooting media; error bars show ± SE.

****Significant at $P < 0.01$ (experiment 2).**

4.3.6 Phosphorus-Starvation-Induced Carboxylates Exudation by Brassica Cultivars

Carboxylates were measured in the root exudates of class I (Oscar and Rainbow) and class II (BSA and Gold Rush) cultivars grown with or without P and sparingly soluble TCP and RP. Class I cultivars are relatively well adapted to low P conditions and accumulating greater biomass than class II cultivars, when both are exposed to P-stress environment. Carboxylates (citric, malic, fumaric, and succinic acids) were measured in the root exudates of 26-day-old plants. Total amount of carboxylates exuded from the roots of P-stressed plants differed from those of plants grown under adequate P supply (Figure 4.6). Apparently, when plants were supplied with sufficient P, carboxylates were released in low amounts by all cultivars. On the other hand, carboxylates were released in greater amounts, when plants were recultured for 12 days

under P stress. The amounts of total carboxylates extruded by the roots differed among cultivars, and class I cultivars exuded 2- and 3-times more carboxylates than class II cultivars. Nevertheless, amounts of exuded carboxylates appeared to be specific to cultivar and time. However, the exudation rate of cultivars of both classes decreased with time. The greatest exudation rate was found after the first 4 h of collection and then tended to decrease (Figure 4.6).

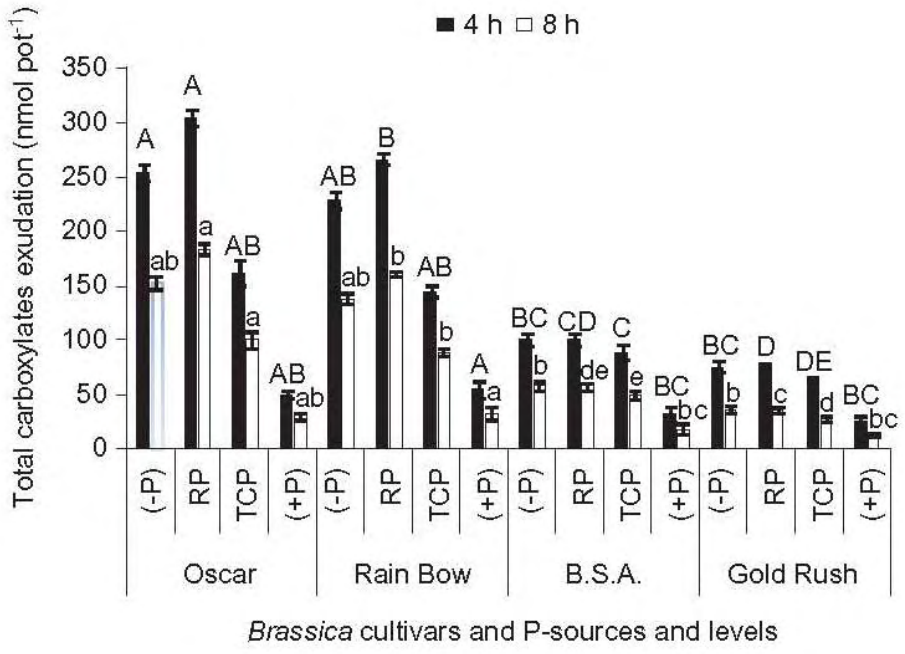

Figure 4.6 － Total carboxylates exudation by the roots of four diverse *Brassica* cultivars. Seedlings raised on moist sand for 7 days. They were cultured in complete nutrient solution for 7 days. The seedlings then transferred to the solutions with or without 0.20 mM P using KH_2PO_4, TCP at 0.2 g/L or RP at 2 g/L for 12 days. Root exudates were collected for 4 and 8 hrs, respectively, to evaluate time course effect and analyzed by using HPLC. Means with different letter(s) on top of the bars differed significantly according to DMRT (*P* = 0.05); error bars show ±SE (experiment 3).

4.4 DISCUSSION

The response of plant growth and yield to P fertilization differs among crops. *Brassica* and cereal crops achieve their maximum yields on soils with relatively little available P. Downloaded by whereas the yields of other crops, such as common bean, spinach, and especially potato, tomato, carrot, onion, and lettuce, respond to larger inputs of P fertilizer (Greenwood et al. 2005).

The genetic potential for improving the response of yield to P inputs may also differ among crops. Comparison of cultivars relative to mineral nutrition has been judged mostly on the basis of biomass accumulation, and tolerance to low P stress based on evaluation of biomass can be regarded as the product of the plant mechanisms involving acquisition, translocation, and utilization of P from ambient environment. Repeated measurements of biomass are the basis for the calculations of net primary production and growth rates (Poschlod et al. 2003, Cornelissen et al. 2003), and thus, a basis for quantifying physiological responses of plants to environmental conditions and their developmental processes.

Tested *Brassica* cultivars presented substantial genetic diversity for biomass and differed significantly in growth behavior at stress P and in response to P fertilization in experiment 1. Accumulation of shoot biomass is a good indicator of ultimate economic yield (Römer and Schenk 1998), and selection of cultivars for SDM production under P stress may provide the best estimate of productivity in low-P soils.

Averaged over all cultivars, a difference of more than 2-times in the cases of SDM and RDM of the cultivars at stress P (0P) indicated considerable genetic diversity among tested cultivars that allowed them to exploit a P-stressed environment for biomass accumulation (Figure 4.1). Root growth is a key trait for optimizing the efficiency of P acquisition and use in plants. To benefit from applied as well as native fixed P, the plant root system can be targeted to enhance P acquisition from soil.

The RDM of the cultivars grown under P stress was positively correlated to their total P uptake ($r = 0.96^{**}$), which in turn was related positively to SDM ($r = 0.93^{**}$) and TDM ($r = 0.94^{**}$) and negatively related to PSF ($r = -0.96^{**}$). It highlights the importance of RDM on low P-stress tolerance of tested cultivars, without imparting any drainful effects on the aboveground plant parts. Nutrient-efficient plants are defined as plants that could produce greater yields per unit of nutrient applied or absorbed compared with other plants grown under similar agro-ecological conditions (Fageria, Baligar, and Li 2008).

The PUE, calculated for each cultivar, decreased with high P level, as was expected (Figure 4.2a). This index evaluates the amount of dry matter produced for a given [P] in the plant dry tissue, and maximum PUE are usually found at low P levels. Low-P-tolerant cultivars also presented greater PE and PER values under a P-stress environment (Figures 4.2b and 4.2c). A strong positive correlation existed between total Ca uptake and total P uptake of cultivars at 0P (Figure 4.2d); hence, it can be assumed that greater P acquisition of efficient cultivars was because of their high Ca uptake. By the principal of mass action, high Ca uptake by plants caused an increase in P solubility

from Ca-bound P sources; a phenomenon that can increase availability of indigenous P in calcareous soils. Cultivars that are efficient accumulators of Ca are desirable as they can acquire greater amounts of P from otherwise P-deficient soils. A better relationship between the amount of P in shoot and PE of cultivars, and a highly significant correlation (r = 0.94**) between PE and SDM at stress P (Figure 4.3a), indicate that shoot growth at low P supply can be an appropriate parameter for PE. Low-P-tolerant cultivars are desirable when the combination of high PE and high biomass is considered for plants.

Significant correlation between SDM and PER (Figure 4.3b) also indicates that differences in P-use efficiency were largely due to differences in yields. It is possible to conceive from the data that SDM production and total amount of P per shoot at stress P are the most reliable parameters in assessing *Brassica* cultivars for their P efficiency at the vegetative stage. Ordination plots of PSF (relative reduction in shoot biomass due to P stress), PUE, and PER revealed that cultivars having high PUE and PER and low PSF values are desirable choices under P-starved environments (Figures 4.3c and 4.3d).

Phosphorus starvation is reported to inhibit leaf expansion via their inhibitory effects on hydraulic conductance of roots. Radin and Eidenbock (1984) reported that suboptimal application levels of P strongly inhibited leaf expansion in young plants through significantly decreasing hydraulic conductance, and the negative effect of P stress was primarily on cell expansion.

Phosphorus-starvation-induced repressing effect on plant growth is considered to be a result of decrease in photosynthetic (leaf) surface area, and P stress reduces the leaf area by limiting the cell division at the meristematic apex of the shoot. Another possibility is that the effect of P stress on leaf expansion may be mediated by growth hormones.

Cultivars representing more decreases in leaf area due to P starvation depicting greater sensitivity to P stress in terms of relative reduction in SDM (PSF; a relative stress tolerance index) and LA, and vice versa (Figures 4.4a and 4.4b). Radin and Eidenbock (1984) assumed that reduced leaf area per plant due to P stress was related to the accumulation of total dry matter (TDM) per plant.

Therefore, it can be assumed that cultivars that can resist P stress on leaf area development per plant can better adapt to low-P conditions. Relative reduction in leaf area and P-stress factor as functions of PE and RDM, respectively, at 0P revealed that class I cultivars presented lower PSF and greater RDM and PE values, and are considered to be more P tolerant than class II cultivars (Figures 4.4c and 4.4d). Acquisition of PO_4^{3-} from sparse extracellular P sources or unavailable bound P

reserves can be enhanced by biochemical rescue mechanisms such copious H^+ efflux and/or carboxylates exudation into rhizosphere by roots via plasmalemma H^+ ATPase and anion channels triggered by P starvation. Plant roots are responsible for considerable changes in rhizospheric pH. Various origins of pH changes are (i) cation–anion balance, (ii) carboxylate release, (iii) root exudation and respiration, and (iv) redox-coupled processes (Hinsinger et al. 2003). Several plant-induced factors may be responsible for changes in pH such as release of H^+, OH^-, or HCO_3^- to balance the excess cations or anions absorbed by the roots, respectively, and/or carboxylate exudation. Quantitatively, net ion fluxes such as uptake of inorganic cations and anions, extrusion or (sometimes) uptake of H^+ and carboxylates exudation are involved in plant growth. Extracellular pH changes and intracellular pH stabilization is affected by cation–anion uptake, and internal charge balance involves the accumulation of inorganic and organic (carboxylates) anions. Solution pH influenced by P supply and cultivar types is presented in experiment 2. The pH of the culture solutions showed substantial decrease over starting adjusted value of 7 (Figures 4.5a–c). Low P-tolerant cultivars (Oscar and Rainbow) that were efficient accumulators of biomass showed more decrease in pH of the solutions containing sparingly soluble P sources (RP and TCP) than low-P-sensitive cultivars (Gold Rush and BSA). Decrease in pH measured at 20 DAT correlated significantly with plant total P contents (Figure 4.5d). The amounts of P taken up by cultivars increased linearly with decreasing pH. The P-tolerant cultivars effluxed more H^+ than sensitive cultivars, and accumulated more biomass by utilizing more P from RP and TCP applied in the solution.

The P-starvation-induced rootmediated rhizosphere acidification was more pronounced because of enhanced H^+ efflux in P-tolerant cultivar Oscar than P-sensitive Gold Rush. The H^+ release into the rhizosphere is a common response of plant cells to counter intracellular acidity. The driving force for nutrient uptake by root cells is H^+ extrusion, mediated by the activity of a plasma-membrane-bound H^+ pumping ATPase, which creates an outward positive gradient in electropotential and pH between the cytosol (pH 7–7.5) and the apoplast (pH 5–6) (Neumann and Römheld 2002). Yan et al. (2002) reported that enhanced catalytic activity of a plasma membrane H^+-ATPase of P-stressed cluster roots in white lupin that might be responsible for the increase of H^+ extrusion. Sakano (2001) pointed out that active H^+ extrusion is a possible response of the plant cell to prevent the inhibiting effect of cytosolic acidification. Because most PO_4^{3-} is transported as $H_2PO_4^-$, cotransport involves a cation. Acidification of cytoplasm that occurs upon PO_4^{3-} addition to P-deficient cells suggests H^+ is the cotransport product for the vast majority of plants (Neumann and Römheld 1999). In

alkaline calcareous soils, rhizosphere acidification by H^+ efflux causes dissolution of poorly available bound P forms. Most RPs are made of apatite like Ca-phosphates and thus exhibit an increasing solubility with decreasing pH. The H^+ released by ATPase pumps located in plasmalemma during nutrient uptake attack RP to solubilize P for meeting plant growth requirements.

All these processes collectively form the basis of internal electric charge balance and biophysical (membrane transport) and biochemical pH state. Superimposed on them, there can also be an extrusion of carboxylates plus H^+ extrusion (Marschner 1995).

The reactions controlling the amounts of PO_4^{3-} in solution include dissolution–precipitation of P-bearing minerals, adsorption–desorption of phosphate on soil surfaces, and the hydrolysis of organic matter (Hinsinger 2001). Along with the types and amounts of clay and metal oxides, P availability is also controlled by soil solution pH, ionic strength, concentrations of P and metals (Fe, Al, and Ca), and the presence of competing anions, including organic acids (OAs) (Hinsinger et al. 2003).

Total amount of carboxylates exuded from the roots of P-stressed plants differed from those of plants grown under adequate P supply (Figure 6). Apparently, when plants were supplied with sufficient P, carboxylates were released in low amounts by all cultivars. On the other hand, carboxylates were released in greater amounts when plants were recultured for 12 days under P starvation. Low-P-tolerant cultivars exuded 2- to 3-fold more carboxylates than class II cultivars. Nevertheless, the amounts of extruded carboxylates appeared to be specific to P supply and cultivar. However, the exudation rate of the cultivars of both classes (low-P-tolerant and low-P-sensitive) decreased with time. The greatest exudation rate was observed after the first 4 hrs of collection and then tended to decrease (Figure 4.6).

Reactions of carboxylates in soils are extremely complex (Jones et al., 2003). Once released, carboxylates can almost instantly sorb to anion exchange sites in acidic soils and rapidly biodegrade in calcareous soils (Wang et al. 2010). Carboxylates release P from strongly sorbed forms by replacing P bound to Al or Fe in acidic soils or P bound to Ca in alkaline soils (Veneklaas et al. 2003), or by locally reducing pH in highly alkaline soils (Dinkelaker, Römheld, and Marschner 1989).

Analysis of expressed sequence tags from PO_4^{3-}-starved proteoid roots of white lupin identified a putative protein exhibiting homology to a transmembrane protein belonging to the MATE protein family. This PO_4^{3-}-starvation induced MATE gene has been suggested as a potential candidate for carboxylates exudation during PO_4^{3-} starvation (Vance, Uhde-Stone, and Allan, 2003). Carboxylates can diffuse into the rhizosphere because of the high electrochemical potential gradient existing between the

cytoplasm of root cells and the soil solution (Ryan, Delhaize, and Jones 2001) and can release P from unavailable bound soil P reserves.

These classical rescue strategies collectively provided the basis of P solubilization and acquisition from sparingly soluble P sources by *Brassica* cultivars to thrive in a typically stressful environment.

Conclusively, *Brassica* cultivars presented considerable genetic variability and differential growth potential in accessing, mobilizing, acquiring, and efficiently using P in a low-P environment. Low-P-tolerant cultivars expressing better P-efficiency characteristic values were better adaptable to P-starved environments. Greater P acquisition depicted by efficient cultivars at 0P might be a result of their high Ca uptake. Phosphorus starvation- induced rhizospheric acidification due to H^+ efflux and carboxylates exudation by P-efficient/tolerant cultivars were important plant biochemical rescue traits for mobilization and acquisition of PO_4^{3-} from extracellular sparingly soluble P forms such as RP and TCP or bound soil P reserves. Systematic understanding and better combination of these natural occurring plant adaptive traits involved in mobilization, acquisition, and efficient utilization will open new avenue to bring more P in cropping systems from different sparingly soluble P reserves.

REFERENCES

Abel, S., Ticconi, C. A., and Delatorre, C. A., 2002. Phosphate sensing in higher plants. Physiologia Plantarum, 115:1–8.

Abelson, P. H., 1999. A potential phosphate crisis. Science, 238:2015.

Chapman, H. D., and Pratt, P. F., 1961. Phosphorus, In Methods of analysis for soils. plants, and waters, 160–170, Berkeley: University of California.

Cordell, D., Drangert, J. O., and White, S., 2009. The story of phosphorus: Global food security and food for thought. Global Environmental Change 19:292–305.

Cornelissen, J. H. C., Lavorel, S., Garnier, E., Díaz, S., Buchmann, N., Gurvich, D. E. et al., 2003. A handbook of protocols for standardized and easy measurement of plant functional traits worldwide. Australian Journal of Botany 51:335–380.

Desnos, T., 2008. Root branching responses to phosphate and nitrate. Current Opinion in Plant Biology 11:82–87.

Dinkelaker, B., Römheld, V., and Marschner, H., 1989. Citric acid excretion and precipitation of calcium citrate in the rhizosphere of white lupin (Lupinus albus L.). Plant Cell and Environment 12:285–92.

Fageria N. K., Baligar, V. C., and Li, Y. C., 2008. The role of nutrient efficient plants in improving crop yields in the twenty first century. Journal of Plant Nutrition 31:1121–1157.

Fang, Z., Shao, C., Meng, Y., Wu, P., and Chen, M., 2009. Phosphate signaling in Arabidopsis and Oryza sativa. Plant Science 176:170–180.

Gaxiola, R. A., Edwards, M., and Elser, J. J., 2011. A transgenic approach to enhance phosphorus use efficiency in crops as part of a comprehensive strategy for sustainable agriculture. Chemosphere 84: 840–845.

Gerloff, G. C., and Gabelman, W. H., 1983. Genetic basis of inorganic plant nutrition. In Encyclopedia of plant physiology, ed. Läuchli, A., and Bieleski, R. L., 453–480, New York: Springer Verlag.

Gomez, K. A., and Gomez, A. A., 1984. Statistical procedures for agricultural research. New York: John Wiley and Sons.

Greenwood, D. J., Stellacci, A. M., Meacham, M. C., Broadley, M. R., and White, P. J., 2005. Components of P response of different Brassica oleracea genotypes are reproducible in different environments. Crop Science 45:1728–1735.

Hammond, J. P., Broadley, M. R., White, P. J., King, G. J., Bowen, H. C., Hayden, R., Meacham, M. C., Mead, A., Overs, T., Spracklen, W. P., and Greenwood, D. J., 2009. Shoot yield drives phosphorus use efficiency in Brassica oleracea and

correlates with root architecture traits. Journal of Experimental Botany 60:1953–1968.

Hinsinger, P., 2001. Bioavailability of soil inorganic P in the rhizosphere as affected by root-induced chemical changes. Plant and Soil 273:173–195.

Hinsinger, P., Plassard, C., Tang, C., and Jaillard, B., 2003. Origins of root-induced pH changes in the rhizosphere and their responses to environmental constraints. Plant and Soil, 258:43–59.

Hinsinger, P., Betencourt, E., Bernard, L., Bruman, A., Plassard, C., Shen, J., Tang, X., and Zhang, F., 2011. P for two, sharing a scarce resource: Soil phosphorus acquisition in the rhizosphere of intercropped species, Plant Physiology. 156: 1078–1086.

Hoffland, E., Findenegg, G. R., and Nelemans, J. A., 1989. Solubilization of rock phosphate by rape, I: Evaluation of the role of the nutrient uptake pattern. Plant and Soil. 113:155–160.

Jones, D. L., Dennis, P. G., Owen, A. G., and van Hees, P. A. W., 2003. Organic acid behavior in soils: Misconceptions and knowledge gaps. Plant and Soil 248:31–41.

Lai, F., Thacker, J., Li, Y., and Doerner, P., 2007. Cell division activity determines the magnitude of phosphate starvation responses in Arabidopsis. Plant Journal 50:545–556.

Marschner, H., 1995, Mineral nutrition of higher plants. London: Academic Press,

Neumann, G., and Römheld, V., 2002. Root-induced changes in the availability of nutrients in the rhizosphere, In Plant roots: The hidden half , ed. Waisel, Y., Eshel, A., and Kafkaf, U., 617–649. New York: Marcel Dekker.

Neumann, G., and Römheld, V., 1999. Root excretion of carboxylic acids and protons in phosphorus deficient plants. Plant and Soil 211:121–130.

Ozturk, L., Eker, S., Bulent, T., and Cakmak, I., 2005. Variation in phosphorus efficiency among 73 bread and durum wheat genotypes grown in a phosphorus-deficient calcareous soil, Plant and Soil. 269:69–80.

Panigrahy, M., Rao, D. N., and Sarla, N., 2009. Molecular mechanisms in response to phosphate starvation in rice. Biotechnology Advances 27:389–397.

Poschlod, P., Kleyer, M., Jackel, A. K., Dannemann, A., and Tackenberg, O., 2003. BIOPOP, a database of plant traits and Internet application for nature conservation. Folia Geobotanica 38:263–271.

Radin, J. W., and Eidenbock, M. P., 1984. Hydraulic conductance as a factor limiting leaf expansion of phosphorus-deficient cotton plants. Plant Physiology 75:372–377.

Raghothama, K. G., and Karthikeyan, A. S., 2005. Phosphate acquisition, Plant and Soil 274:37–49.

Römer, W., and Schenk, H., 1998. Influence of genotype on phosphate uptake and utilization efficiencies in spring barley. European Journal of Agronomy. 8:215–224.

Ryan, P. R., Delhaize, E., and Jones, D. L., 2001. Function and mechanism of organic anion exudation from plant roots. Annual Review of Plant Physiology and Plant Molecular Biology 52:527–560.

Sakano, K., 2001. Metabolic regulation of pH in plant cells: Role of cytoplasmic pH in defense reaction and secondary metabolism. International Review of Cytology 206:1–44.

Sakano, K., Yazaki, Y., and Mimura, T., 1992. Cytoplasmic acidification induced by inorganic phosphate uptake in suspension cultured Catharanthus roseus cells. Plant Physiology 99:672–680.

Shenoy, V. V., and Kalagudi, G. M., 2005. Enhancing plant phosphorus use efficiency for sustainable cropping. Biotechnology Advances 23:501–513.

Siddiqi, M. Y., and Glass, A. D. M., 1981. Utilization index: A modified approach to the estimation and comparison of nutrient utilization efficiency in plant. Journal of Plant Nutrition 4:289–302.

Smil, V., 2000. Phosphorus in the environment: Natural flows and human interferences. Annual Review of Energy and the Environment 25:53–88.

Steel, R. G. D., and Torrie, J. H., 1980. Principles and procedures of statistics. 2nd ed. New York: McGraw Hill

Steen, I., 1998. Phosphorus management in the 21st century: Management of a non-renewable resource. Phosphorus and Potassium 217:25–31.

Ticconi, C., and Abel S., 2004. Short on phosphate: Surveillance and countermeasures. Trends in Plant Science 9:548–555.

Vance, C. P., Uhde-Stone, C., and Allan, D. L., 2003. Phosphorus acquisition and use: Critical adaptations by plants securing a nonrenewable resource. New Phytologist 157:423–457.

Veneklaas, E. J., Stevens, J., Cawthray, G. R., Turner, S., Grigg, A. M., and Lambers, H., 2003. Chickpea and white lupin rhizosphere carboxylates vary with soil properties and enhance phosphorus uptake. Plant and Soil 248:187–197.

Wang, X., Yan, X., and Liao, H., 2010. Genetic improvement for phosphorus efficiency in soybean: A radical approach. Annals of Botany 106:215–222.

Yan, F., Zhu, Y., Mueller, C., and Schubert, S., 2002. Adaptation of H^+ pumping and plasma membrane H^+ ATPase activity in proteoid roots of white lupin under phosphate deficiency. Plant Physiology 12:50–63.

Yan, X., Wu, P., Ling, H., Xu, G., Xu, F., and Zhang, Q., 2006. Plant nutriomics in China: An overview. Annals of Botany 98:473–482.

Yuan, H., and Liu, D., 2008. Signaling components involved in plant responses to phosphate

Starvation. Journal of Integrative Plant Biology 50:849–859.

CHAPTER 5

GENERAL CONCLUSIONS AND RECOMMENDATIONS

5.1 OVERALL OBJECTIVES

Injection of water, whether in case of open-loop heat pump systems or in case of artificial recharge, will become an important practice in order to augment groundwater problems. There is urgent need to investigate clogging issues in order to ensure good construction guidelines and maintenance for those systems. In this research, chemical and physical clogging were investigated (1) in order to obtain more deep understanding in the detailed processes regarding particle mobilization during water injection, (2) in order to propose an eco-friendly and cheap filter material for dissolved iron ion removal from groundwater in open-loop heat pump systems and (3) in order to understand the processes in soil chemistry regarding plant survival in low phosphorus soils. Furthermore an open-loop heat pump system was applied at Okayama University, Japan in order to test the filter material in practice with accompanied cooling of a room and also compare to a common Ferrolite MC3 filter. This thesis aims to be a contribution in order gain advantages in groundwater sustainability.

This chapter will give an overview of the obtained conclusions of each chapter summarized a general conclusions and recommendations for future research.

5.2 GENERAL CONCLUSIONS

In chapter one a general background was given which points out why groundwater research is needed especially advantages of artificial groundwater recharge. It was obtained that due to population growth an increase in fresh water demand as well as energy demand will become a serious issue in future. Open-loop heat pump systems and also artificial groundwater recharge a practicable countermeasure for those problems. Clogging often is reported to be the main limiting factor in the practicability of injection of water into an aquifer. Hence, detailed understanding of the processes leading to clogging occurrence is direly needed. Furthermore guidelines for use in practice are necessary in order to reduce installation and maintenance costs and make it applicable also in developing countries where water scarcity is the most serious.

In chapter two a review of chemical and physical clogging and their prevention methods was given. The following points could be concluded:

(1) The precipitation of ions present in the groundwater is depending on pH, pε and also E(h) of the groundwater.

(2) Precipitation because of iron and manganese is not only a problem when pumping groundwater, but also when the injection water has different values of E(h) or pH or DO, precipitation may occur in the aquifer during injection.

(3) To date, studies on physical clogging were conducted almost considering suspended particles in the recharge water. However, research on particle mobilization of soil particles initially present in the aquifer should not be neglected, especially its influence it is not well known.

(4) Although, it is to prove how the theories of particle mobilization regarding the piping effect is adoptable for clogging problems.

(5) Pretreatment of the injection water with filters accompanied with chemical treatment is often applied.

(6) After clogging has occurred back flushing is the most applied method in order to redevelop the system.

(7) Aquifer conditions, chemical composition of the groundwater and geological characteristics have to be investigated when planning an injection project.

(8) General construction guidelines, operation methods, adequate pre-treatment methods and early regeneration methods are direly needed.

In chapter 3, experimental studies regarding physical clogging, chemical clogging and field tests were conducted.

(1) The one-dimensional horizontal-flow column experiments, in order to investigate particle mobilization, showed that not only the fine colloidal particles of the soil were mobilized, but also the larger particle ranging between 0.25 and 2 mm were moved by velocity forces. Experimental results showed that when the bigger particles were mobilized by velocity forces, the finer particles were pushed aside and thus fine particles deposited in the areas near the injection port.

(2) Results from a two dimensional experiment (Tanaka, 1992) two types of soils with different distribution curves were used in order to investigate the problem of fine particle movement, and to determine the critical water level rise in the injection well. From the results of the axisymmetric experiments, it is plausible to conclude that at a critical hydraulic gradient of 0.3, for a content of fine particles in the aquifer below 0.104 mm, was determined for injection in the field indicating that clogging might occur below hydraulic gradient of 0.3.

(3) When comparing the results from axisymmetric groundwater model with the previous studies on critical velocity, a good agreement with the data of Ohno et al. (1984) and Koslova (Shindo, 1967) was obtained. A comparison of the

critical hydraulic gradient approaches from Terzaghi (1996) and Sichardt (1928) showed that for the one-dimensional experimental data both equations do not agree with the results. For the two- dimensional axisymmetric groundwater model, Terzaghi's equation again results in too high value of hydraulic gradients. But for Sichardt's equation, the resulting hydraulic gradients agree with the experimental data what indicates that the two dimensional experiment gives more realistic results and is more capable for field application.

(4) The laboratory experiments investigating an eco-friendly and cheap filter material for iron removal, experimental results showed that the proposed wooden charcoal is capable of adsorbing and removing dissolved iron from groundwater under anoxic condition.

(5) Fine sand was also able to remove iron from groundwater, however, the hydraulic conductivity of the material was already reduced by the order of one to two after 1.4 days of operation and was not recoverable due to backflushing, hence, the efficiency of this filter material is assumed to be very low because of clogging occurrence within the column caused by fine particles blocking the pores.

(6) Because of iron flakes already grew during pumping the groundwater, temporary back flushing of the filter columns was necessary in order to regenerate the flow rate of the columns.

(7) In the Laboratory a adsorption capacity of wooden charcoal showed the highest adsorption capacity for dissolved iron with an average $b_{eq} \approx 3.5$ g/(kg dry mass of charcoal) compared to fine sand and volcanic ash.

(8) The charcoal filter in the field test showed higher two to three times higher adsorption potential than obtained from the laboratory column experimental data. These results showed that the aquifer characteristics and conditions like temperature, pH, DO, initial concentration of the dissolved iron are of great influence on the adsorption.

(9) The Ferrolite MC3 filter showed the best performance in removing iron and manganese from groundwater. Nevertheless, the price of the Ferrolite filter is much more expensive than charcoal material.

(10) Cooling the room by passing the groundwater through PVC-U pipes in a room at the field study site, the energy consumption compared to common cooler (energy safe mode) showed that the PVC-U pipes are less effective.

(11) It is necessary prior to the operation of the filter, that the adsorbent material is flushed with a volume of one to two filter pore volumes, as found in the washing

experiment of charcoal material.

(12) On the basis of the adsorption capacity obtained from the column experiments (b_{eq}), the time of use, the initial concentration of dissolved iron ion and the flow rate, appropriate filter design could be carried out. But since the chemistry of the groundwater can differ so much and hence, the adsorption capacity may differ from place to place it is suggested to (1) add a safety factor of about 30 % and (2) also determine the b_{eq}- value of each study site referring to the different groundwater composition.

(13) The injection experiment showed that no clogging occurred as long as the filter was effective in removing dissolved iron from the groundwater. After the filter broke through, hence iron containing groundwater was injected, soon clogging was observed.

In chapter four, an excursus was done in order to understand the soil chemistry and its interactions with plants and their growth. Because it is suggested to apply the charcoal containing adsorbed iron for agricultural use, the growth response of Brassica cultivars has been investigated under P-stress soil conditions.

(1) The importance of P-availability was confirmed because the shoot growth, root development and biomass production was two-times higher when P was applied to the soils in form of ammonium phosphate ($NH_4H_2PO_4$) compared the growth of Brassica cultivars grown in soils without P-supply.

(2) Statistical correlations showed that cultivars, having greater phosphorus-utilization efficiency and P-efficiency, and also were low in P-stress factor, were more tolerant under a P-stress environment.

(3) Plant survival and reproduction rely on efficient strategies enhanced by biochemical rescue strategies such as plentiful H^+ efflux and/or carboxylates exudation into the root zone by roots. This biochemical process is called plasmalemma H^+- ATPase.

5.3 RECOMMENDATIONS

Because of the fact that many processes are depending on various parameters, also the results of this research have to be commented with some recommendations for further adoption. The results gained in this work should be adopted, linked, compared and contributed. For this purpose the following recommendations are given:

(1) In the one-dimensional physical clogging experiments, packing of the columns may have been of great influence to the particle mobilization; hence, it is recommended to investigate with glass bead experiments the influence of

packing.

(2) The data obtained from the two-dimensional experiment showed a very good fit with experimental data obtained from research regarding the piping effect of earth fill dams. From this conclusion it is evident that research should not be only focused on the problem and its name itself, rather more an understanding and investigation from all different kind of perspectives of the involved processes causing this problem and deriving possible relations to other field of science should be considered.

(3) The physical clogging investigations in this research showed that particle mobilization is of great influence for clogging occurrence. But determining the critical hydraulic gradient or critical velocity can also be useful for recover methods like backflushing of a clogged aquifer. Thus, it is recommended for further research to develop a field test method in order to determine the critical hydraulic gradient to verify experimental laboratory results.

(4) Chemical clogging experiments were conducted by using available groundwater on Tsushima Campus, Okayama University, the results conducted in the laboratory and the results conducted at field site showed some difference in adsorption capacity. Unfortunately no detailed information on the groundwater composition was available, thus it is recommended in every case to analyze the groundwater especially on carbon and ions.

(5) Because the adsorption is influenced by a couple of parameters (Worch, 2012), it is recommended that for every new study site column experiments like proposed in this study should be conducted in order to determine the maximum amount of iron what can be adsorbed (b_{eq}) by the charcoal.

(6) For the filter design the experimental data should be used as input data and in this study a safety factor of 30 % is applied. This 30 % are derived from several engineering experiences in Europe for planning of treatment plants and other water management facilities. Hence, when designing a charcoal filter a safety factor is highly recommended just to make sure that the calculated filter size is really valid under real conditions.

(7) The charcoal filter applied in the field in this study was composed with a mesh at the bottom and several layers of gravel with different particle sizes, the charcoal in the middle and some coarse gravel on the top. This composition is recommended to adapt also for future filter designs, especially some gravel on the top because the charcoal has the characterization of swelling and thus the porosity may be changed due to filtering and this may result in less filtering

ability.

(8) Because of too high pressures in the charcoal filter at the field site, it is recommended to install a pressure relieve valve on the top of the filter.

(9) For maintaining the charcoal filter it is highly recommended to backflush the filter frequently in order to wash out iron precipitates in the inlet and first centimeters of the filter what reduces the filter velocity.

(10) Because the pumped groundwater was measured to include 0.5 mg/L dissolved oxygen (DO), and we know that iron already can precipitate when 0.14 mg/L oxygen is present, investigations are recommended in order avoid mixing with oxygen during pumping of groundwater. Even the application of a packer in the pumping well resulted in the same DO level of 0.5 mg/L.

REFERENCES

Ohno, M., Yamazaki, H., and Tran-Duc, P.O., 1984. Experimental study of piping property of sand. Report of Hazama: 33-40. (in Japanese)

Shindo, K., 1967. Rock Mechanics. Morikita, Tokyo. (Japanese translation of : Talobre, J.,and D. O. Martin. 1957. La mécanique des roches:appliqué aux travaux publics. Dunod.)

Sichardt, W., 1928. Das Fassungsvermögen von Rohrbrunnen und seine Bedeutung für die Grundwasserabsenkung, insbesondere für größere Absenkungstiefen. Springer. (in German)

Tanaka, T., 1992. Research on artificial Recharge. Master Thesis, Okayama University, Japan.

Terzaghi, K., Peck, R.B., and Mesri, G., 1996. Soil Mechanics in Engineering Practice. John Wiley and Sons.

Worch, E., 2012. Adsorption Technology in Water Treatment. 1st ed., Walter de Gruyter, Bonn/Bosten, Germany/USA.

APPENDIX

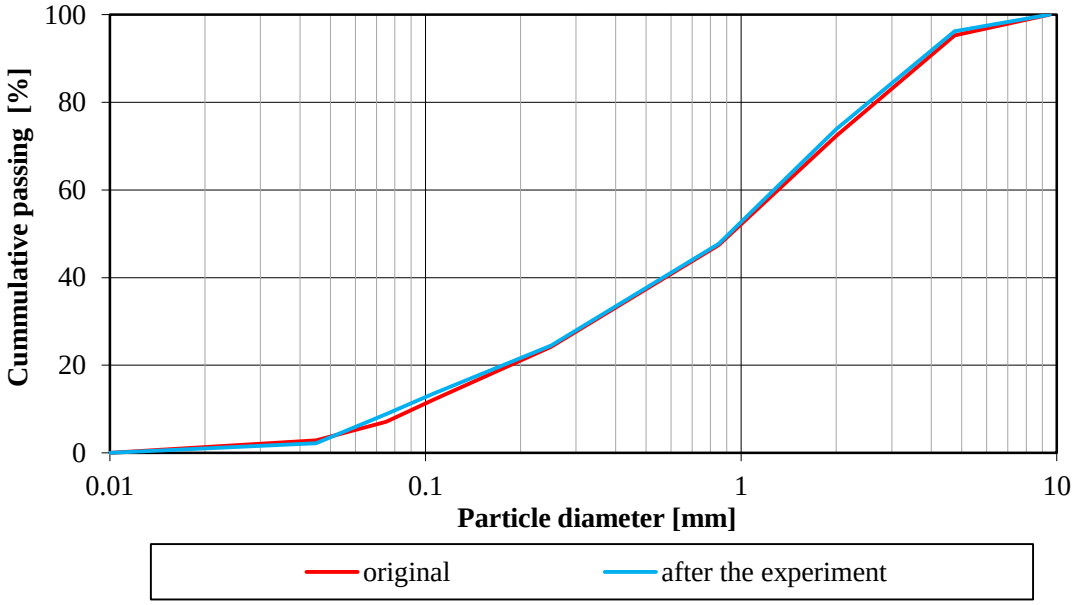

A 1－Comparison of soil distribution curves for test A with i=0.02 (Layer 0-10 cm).

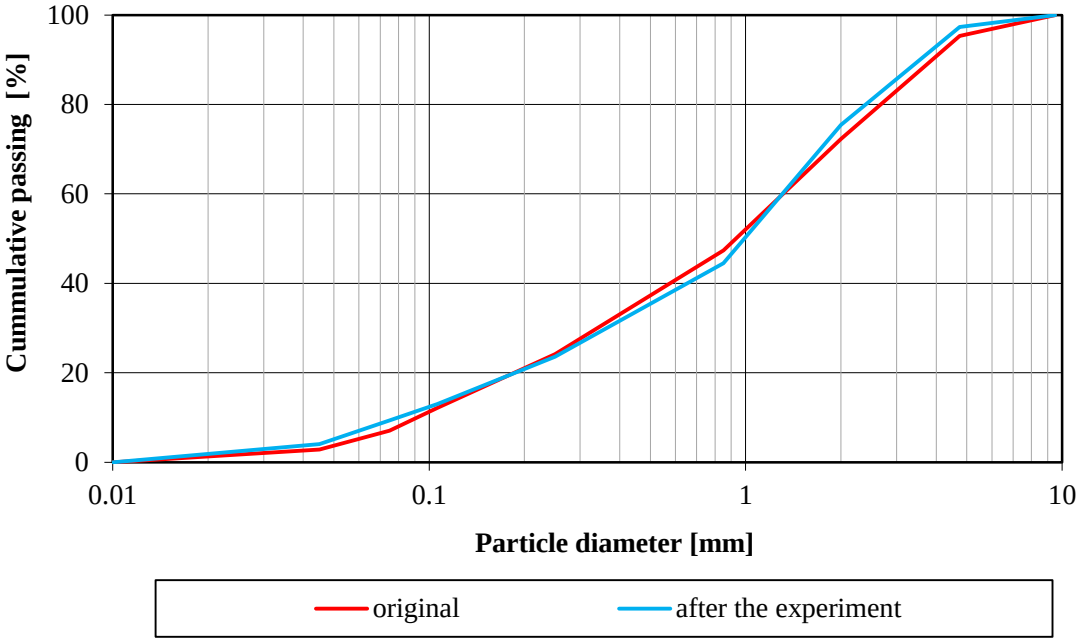

A 2－Comparison of soil distribution curves for test A with i=0.02 (Layer 10-20 cm). Particles between 2 and 4.75 mm moved away from the injection point within 10-30 cm column length.

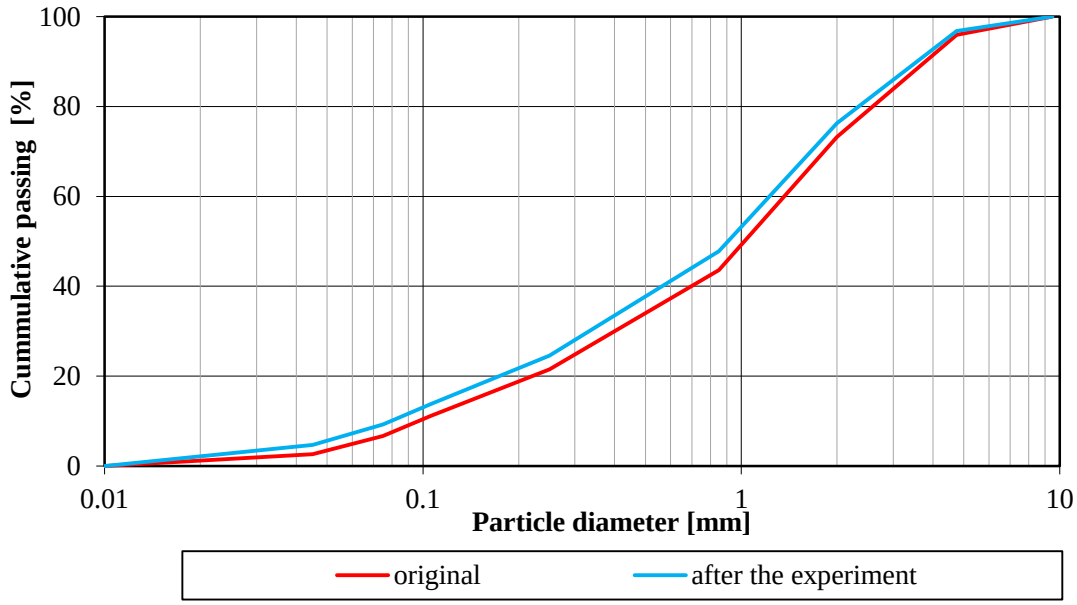

A 3－Comparison of soil distribution curves for test A with i=0.02 (Layer 20-30 cm).

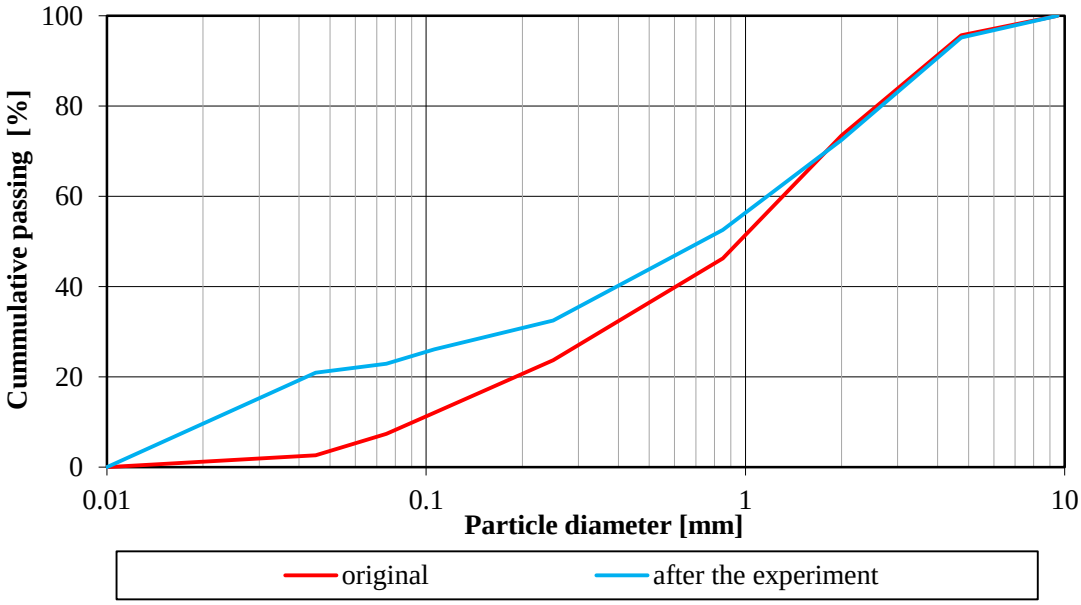

A 4－Comparison of soil distribution curves for test A with i=0.02 (Layer 30-40 cm). Particles between 2 and 4.75 mm moved away from the injection point within 10-30 cm column length.

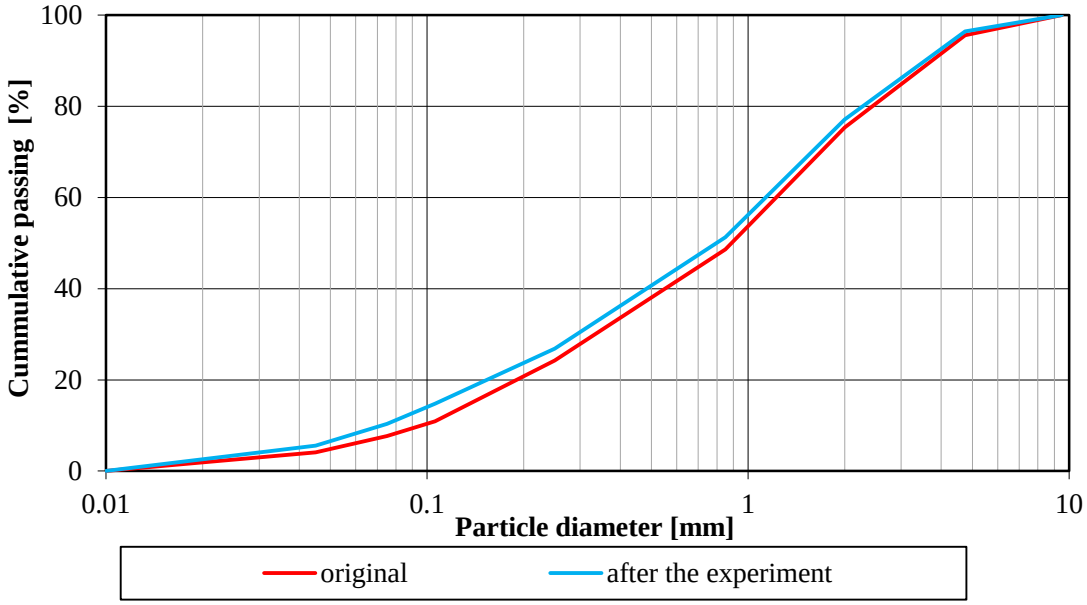

A 5－Comparison of soil distribution curves for test A with i=0.02 (Layer 40-50 cm). Particles between 2 and 4.75 mm moved away from the injection point within 10-30 cm column length.

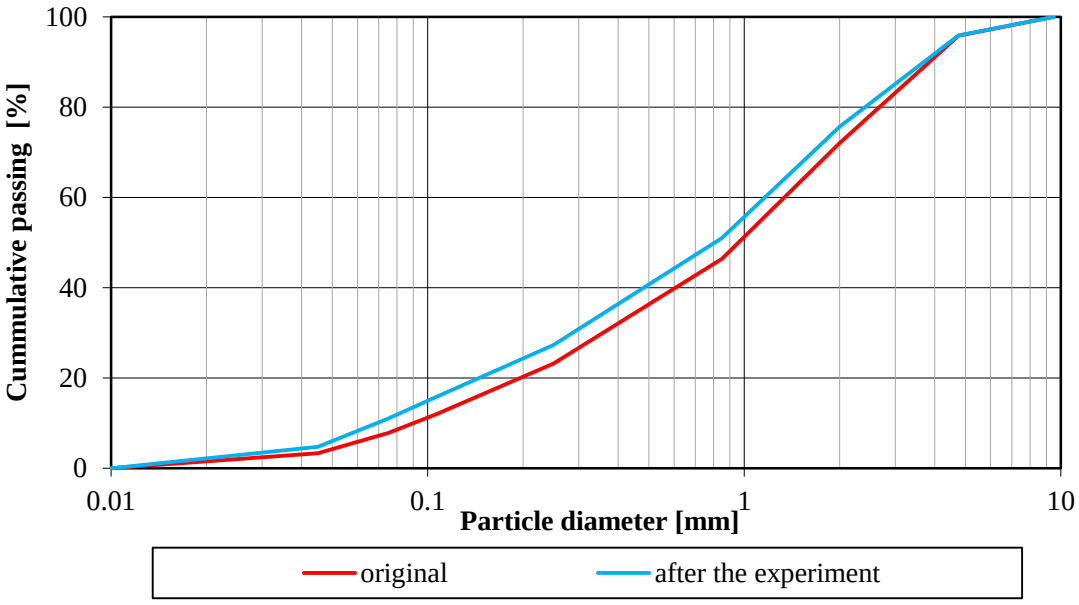

A 6－Comparison of soil distribution curves for test B with i=0.1 (0-10 cm).

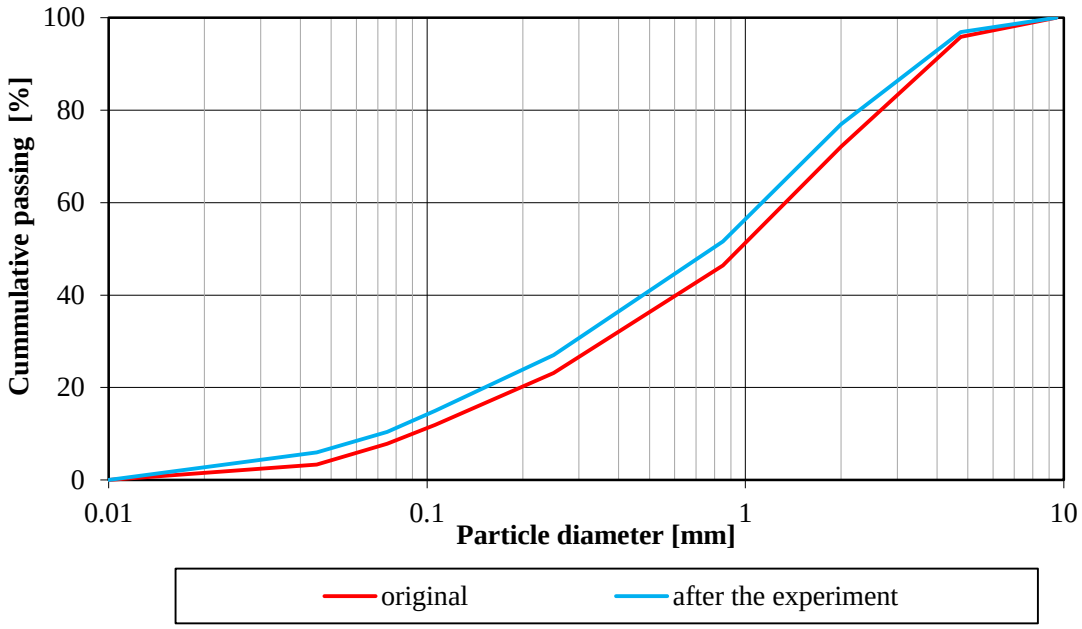

A 7－Comparison of soil distribution curves for test B with i=0.1 (10-20 cm).

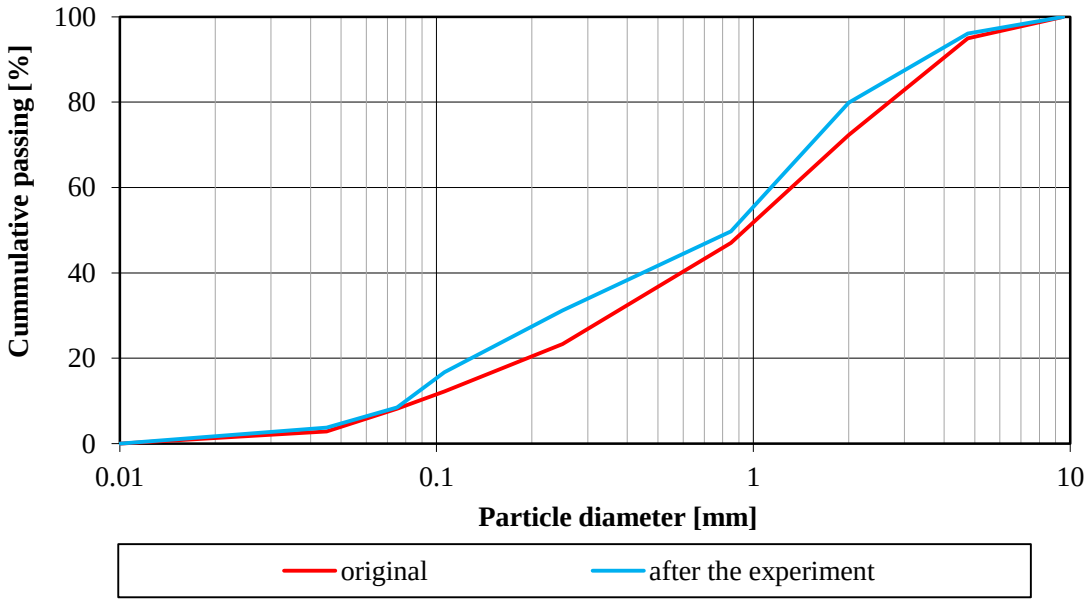

A 8－Comparison of soil distribution curves for test B with i=0.1 (20-30 cm). Particles between 0.85 and 2 mm moved from the 30-40 cm layer into the 20-30 cm layer.

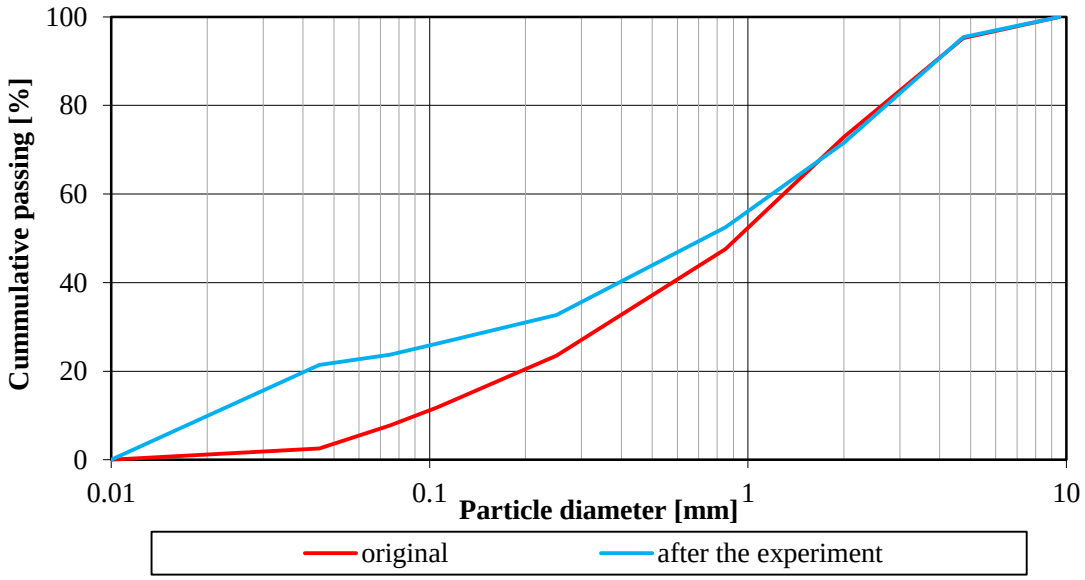

A 9－Comparison of soil distribution curves for test B with i=0.1 (30-40 cm).

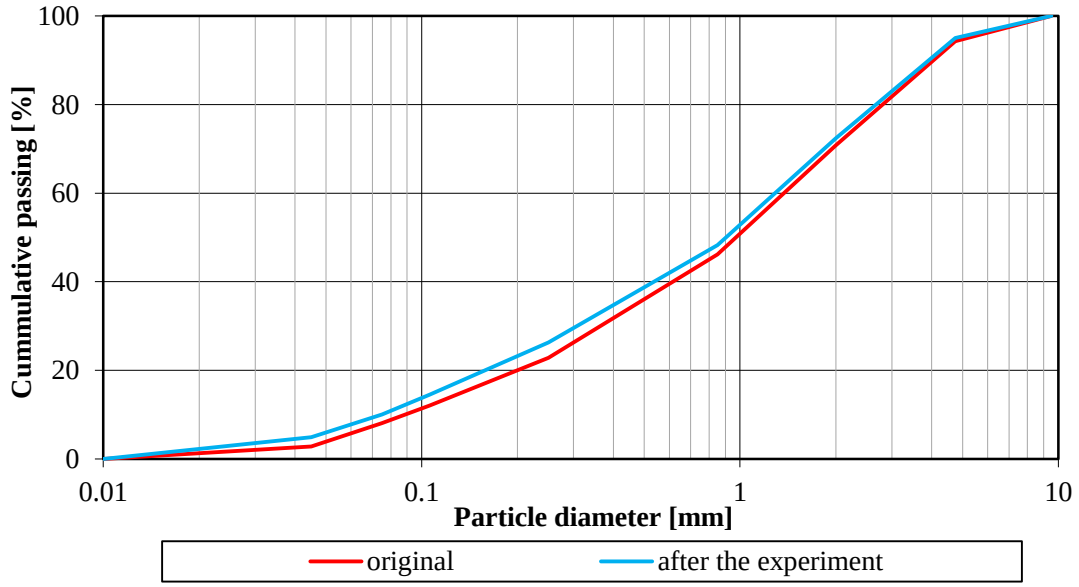

A 10－Comparison of soil distribution curves for test B with i=0.1 (40-50 cm).

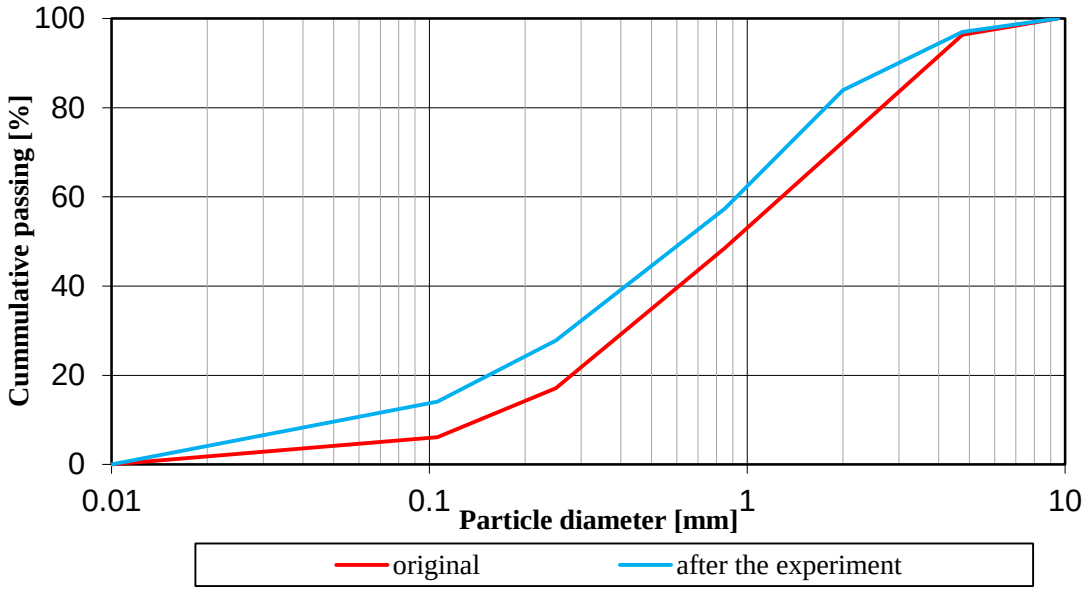

A 11－Comparison of soil distribution curves for test C with i=0.2 (0-10 cm).

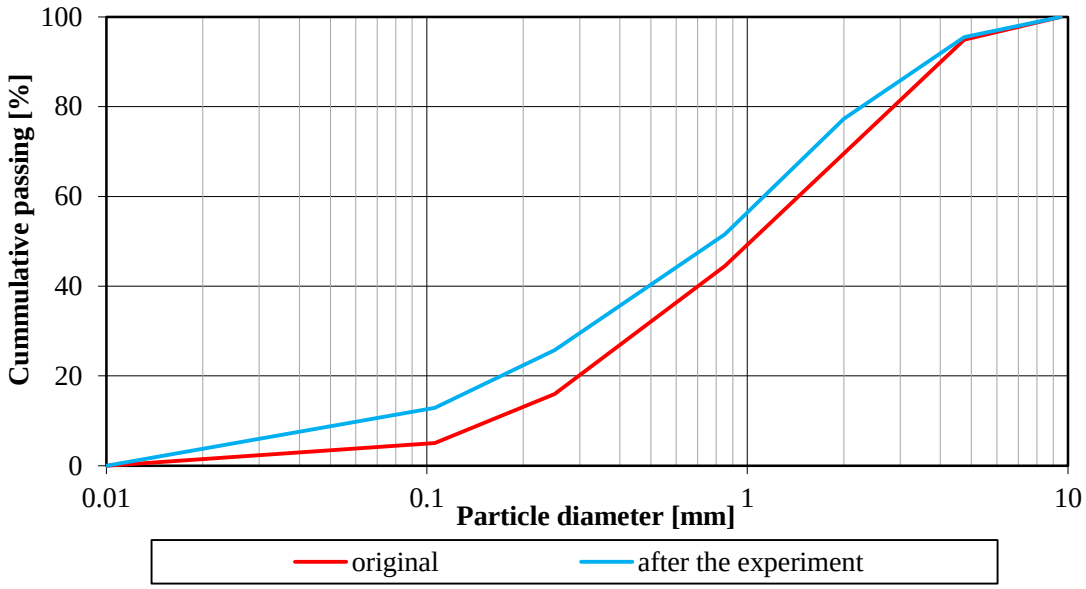

A 12－Comparison of soil distribution curves for test C with i=0.2 (10-20 cm).

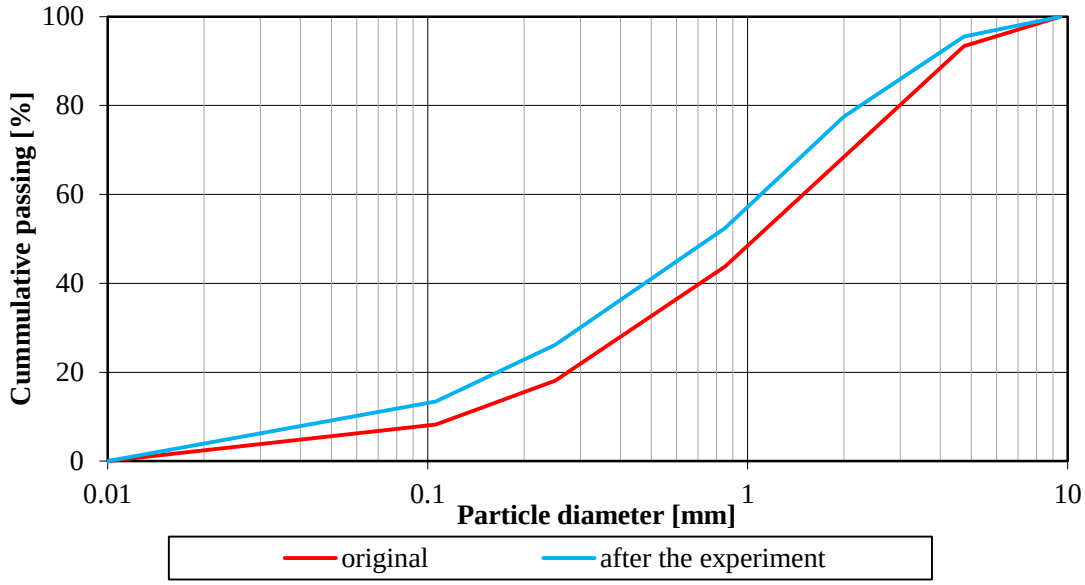

A 13－Comparison of soil distribution curves for test C with i=0.2 (20-30 cm).

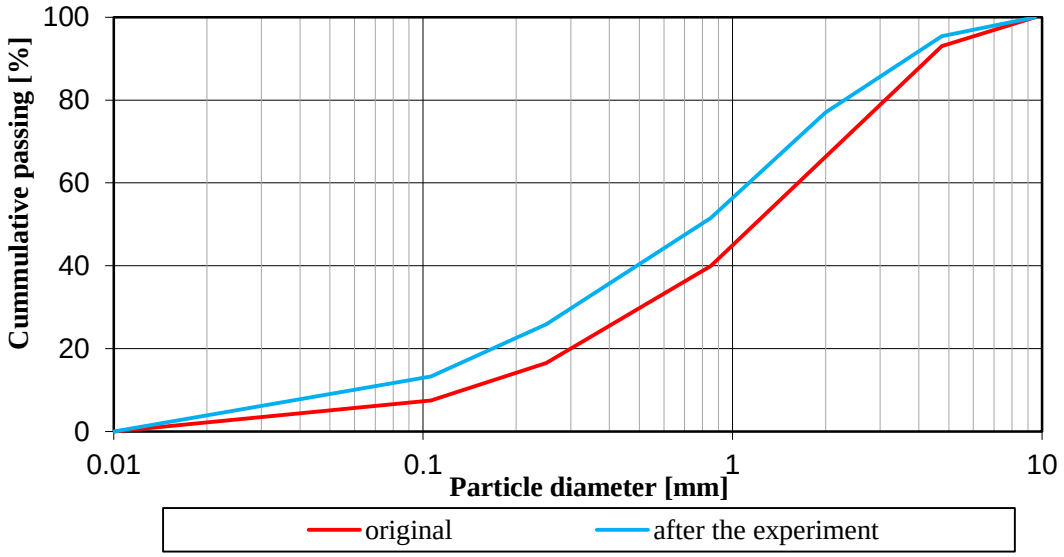

A 14－Comparison of soil distribution curves for test C with i=0.2 (30-40 cm). Particles below 0.85 mm settled down, and particles below 0.106 mm doubled in this zone.

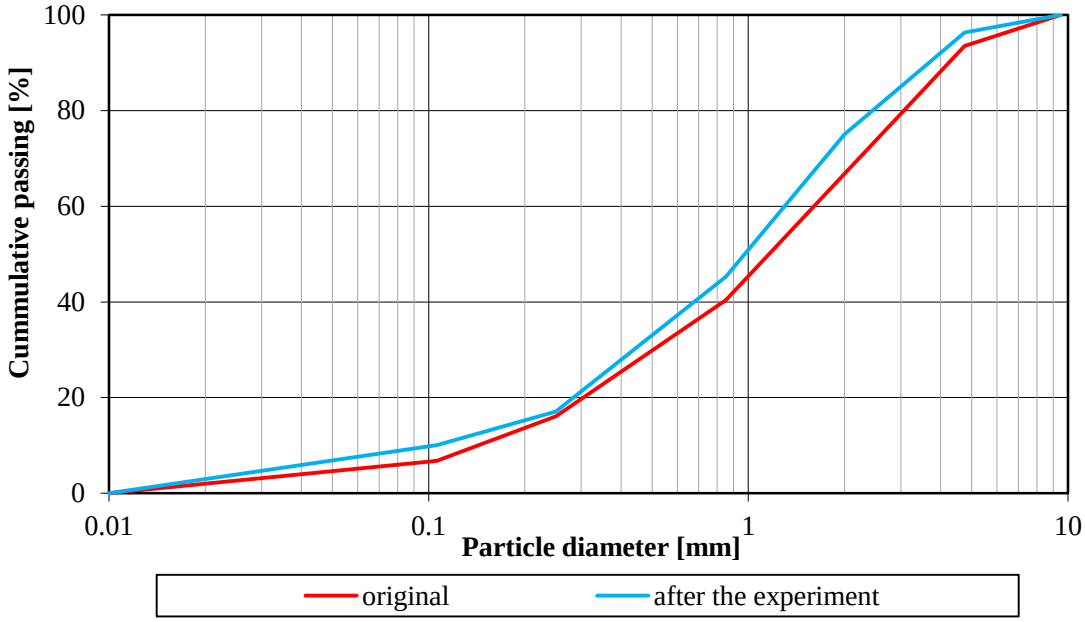

A 15—Comparison of soil distribution curves for test C with i=0.2 (40-50 cm).

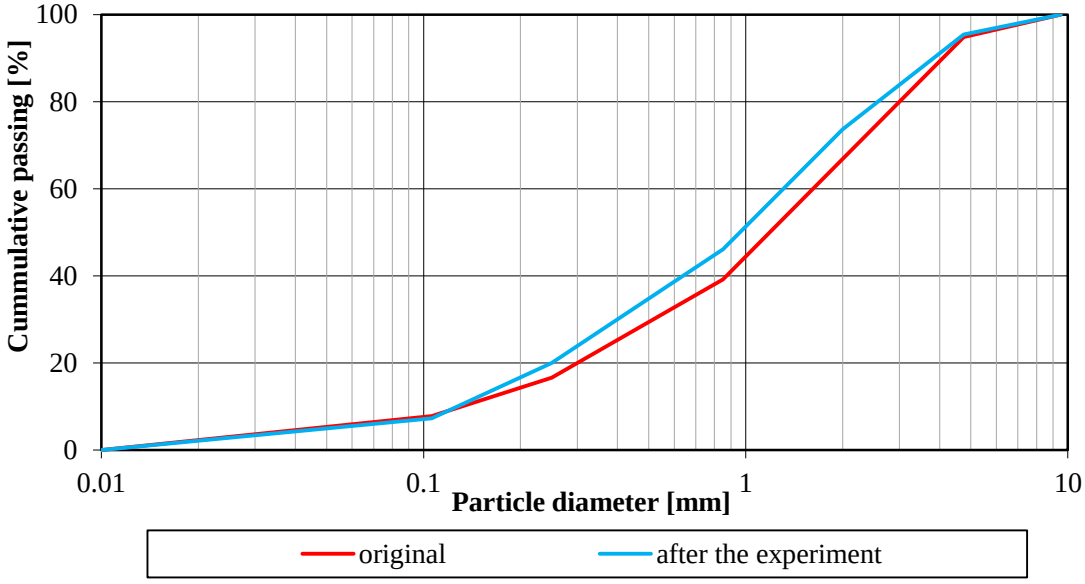

A 16—Comparison of soil distribution curves for test C with i=0.2 (50-60 cm). Deposition of particles between 0.25 and 4.75 mm within 50 -80 cm of column length.

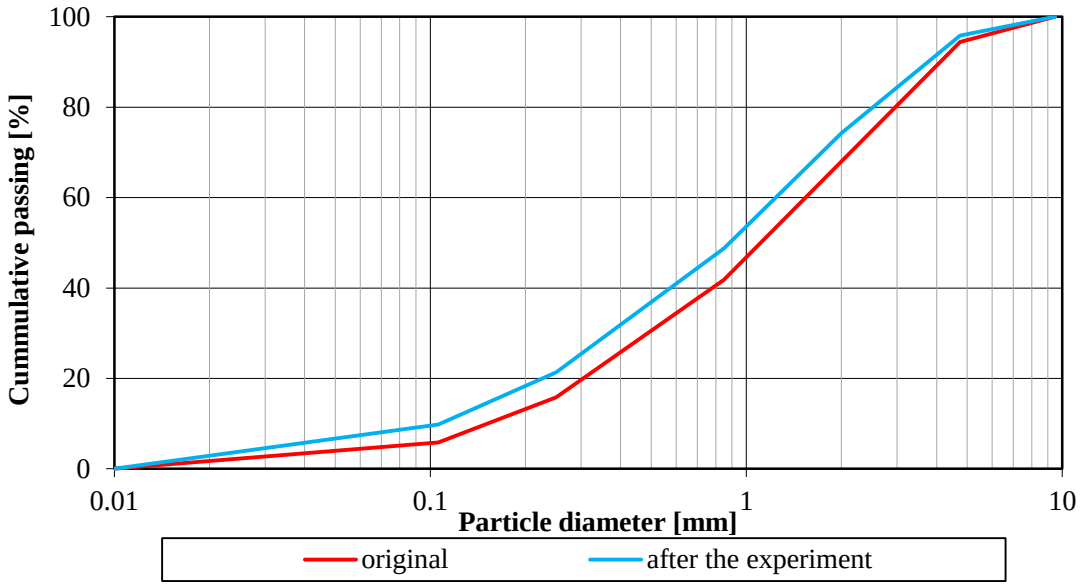

A 17－Comparison of soil distribution curves for test C with i=0.2 (60-70 cm).

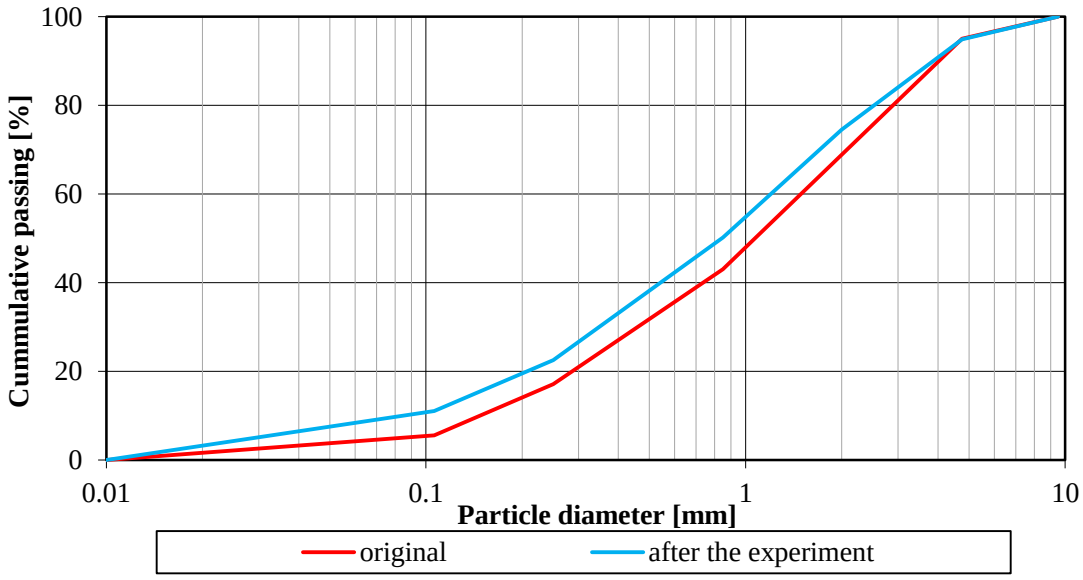

A 18－Comparison of soil distribution curves for test C with i=0.2 (70-80 cm).

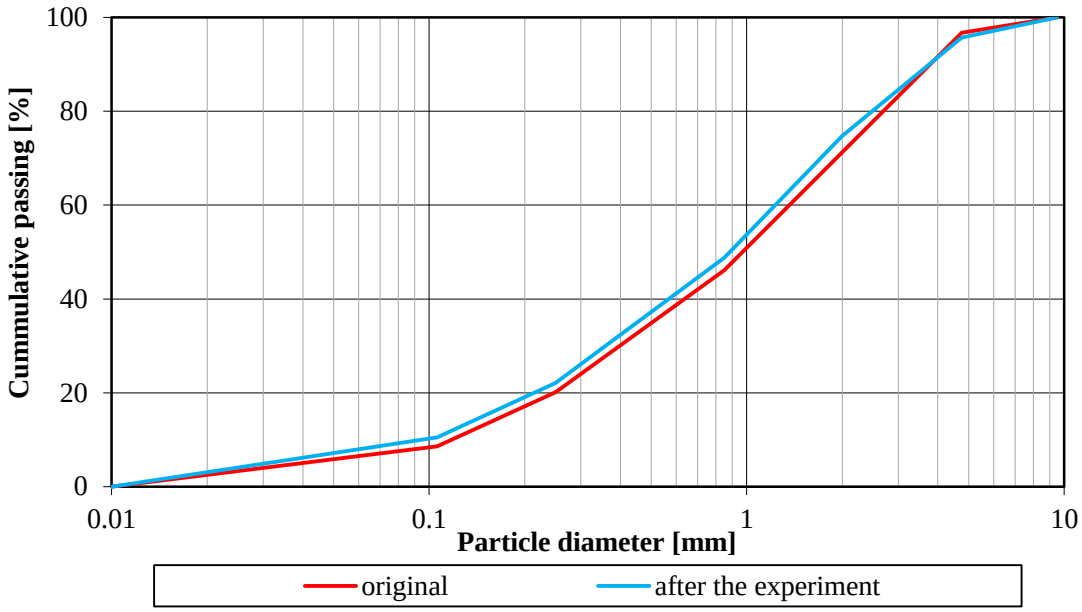

A 19－Comparison of soil distribution curves for test C with i=0.2 (80-90 cm).

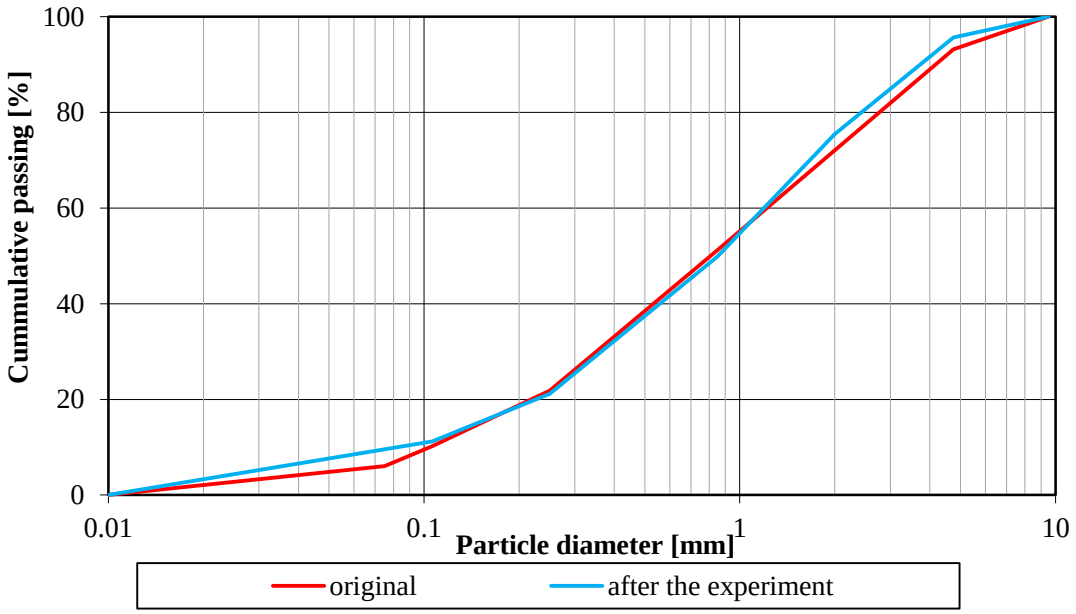

A 20－Comparison of soil distribution curves for test C with i=0.2 (90-100 cm).

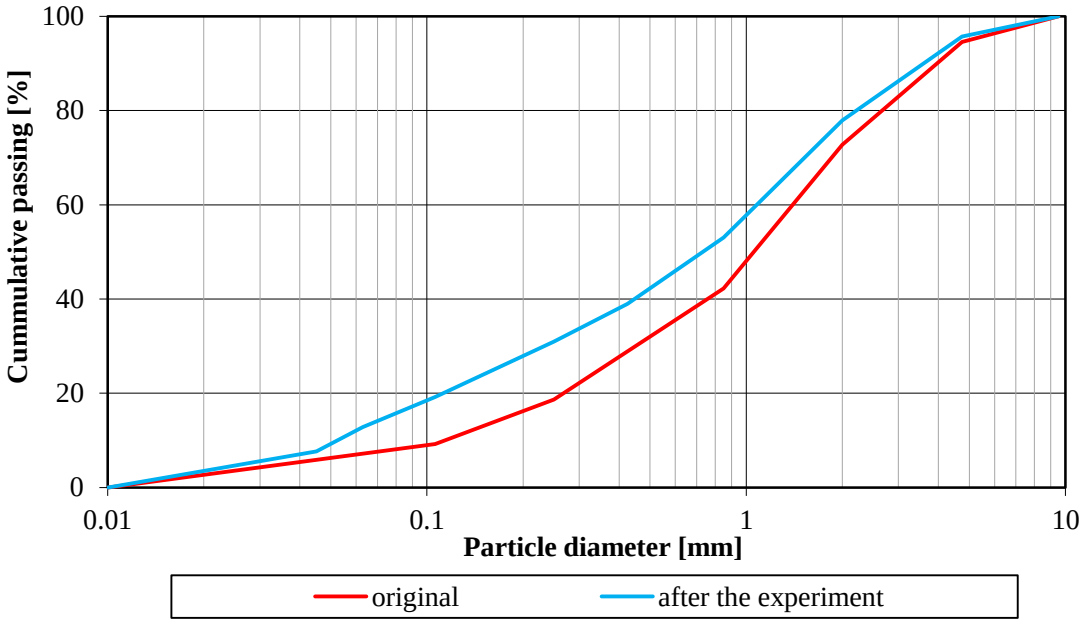

A 21－Comparison of soil distribution curves for test B with i=0.3 (0-10 cm).

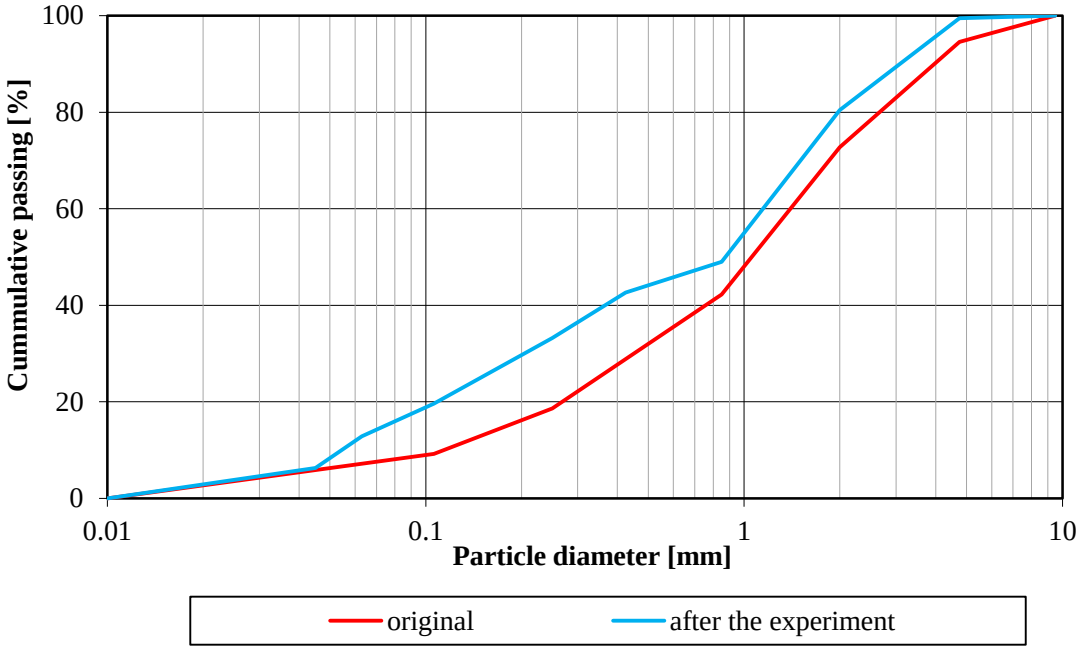

A 22－Comparison of soil distribution curves for test B with i=0.3 (10-20 cm).

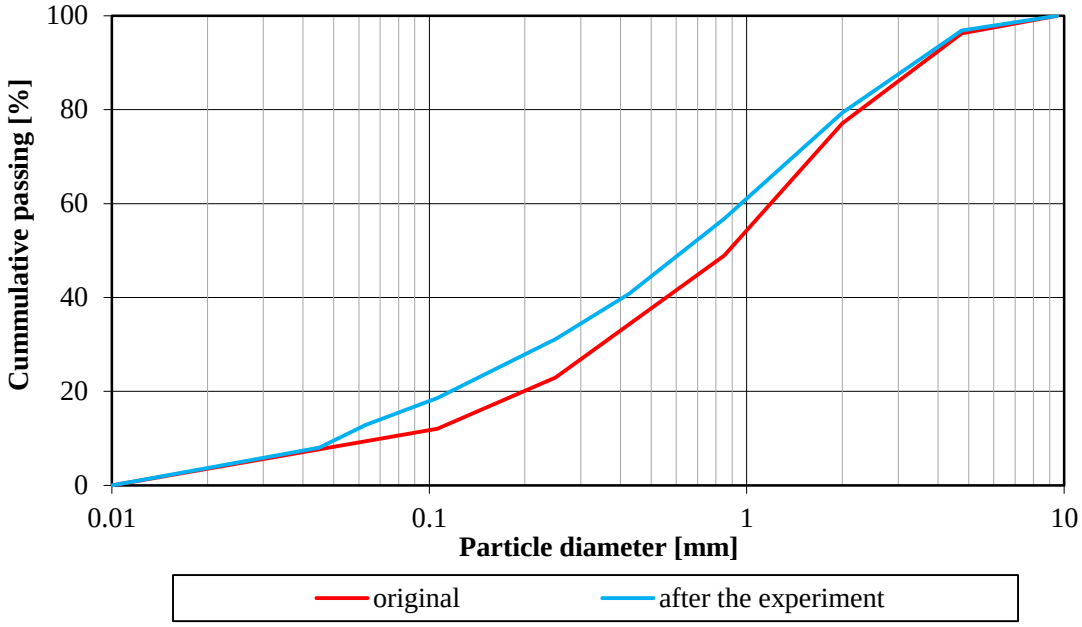

A 23—Comparison of soil distribution curves for test B with i=0.3 (20-30 cm).

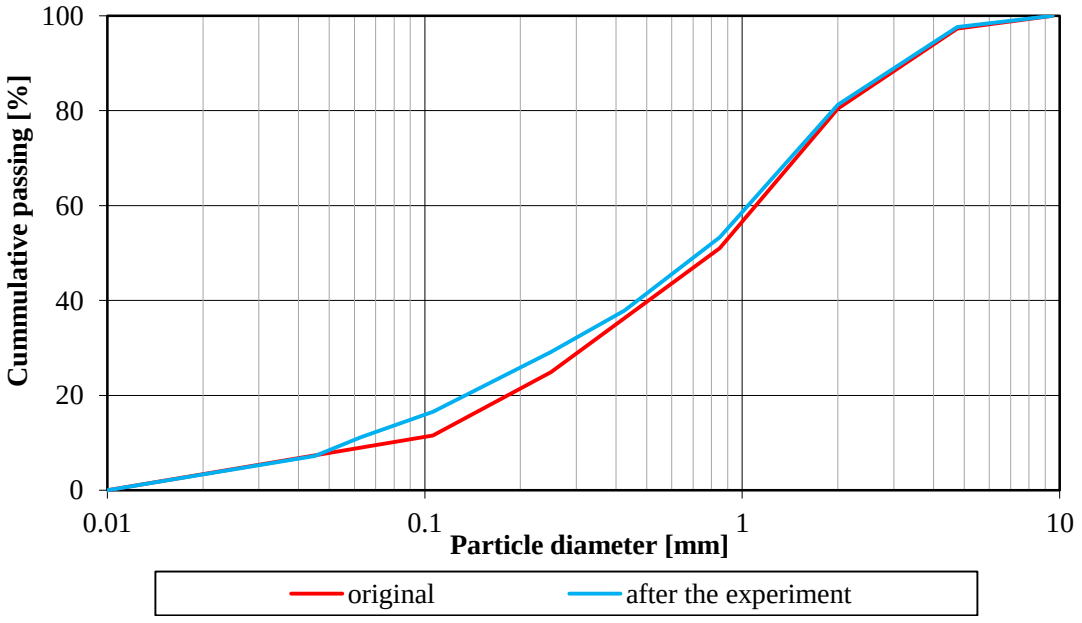

A 24—Comparison of soil distribution curves for test B with i=0.3 (30-40 cm).

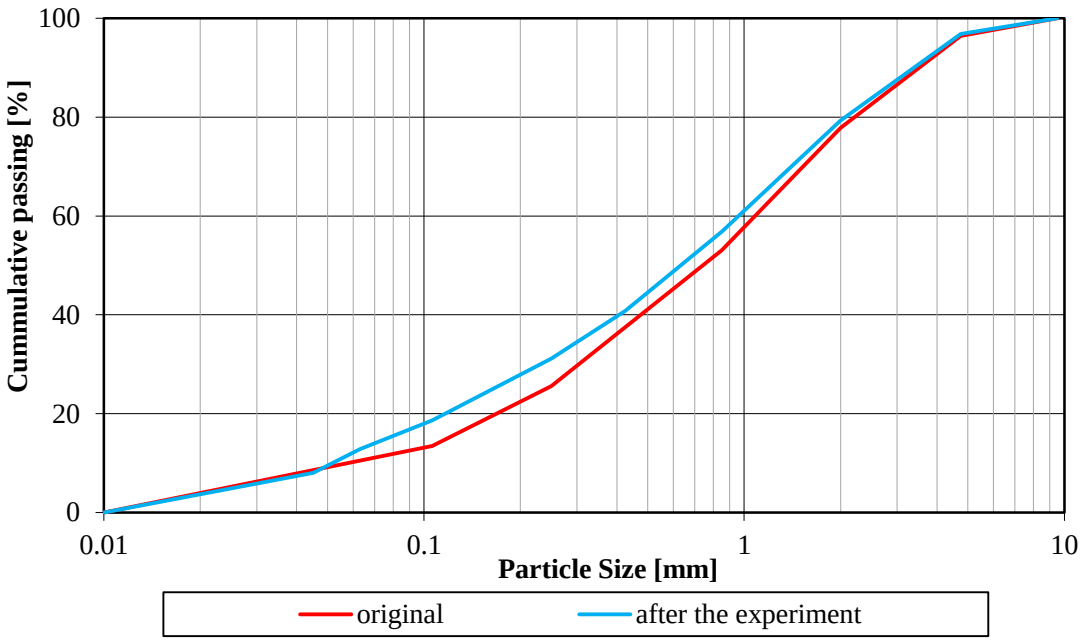

A 25—Comparison of soil distribution curves for test C with i=0.3 (40-50 cm).

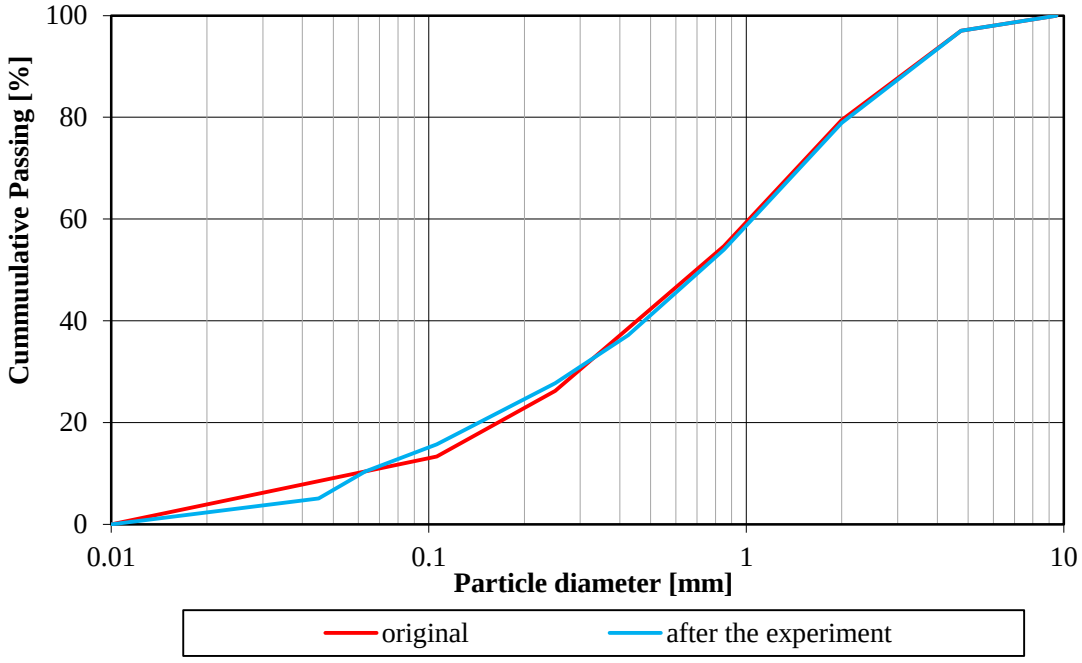

A 26—Comparison of soil distribution curves for test C with i=0.3 (50-60 cm).

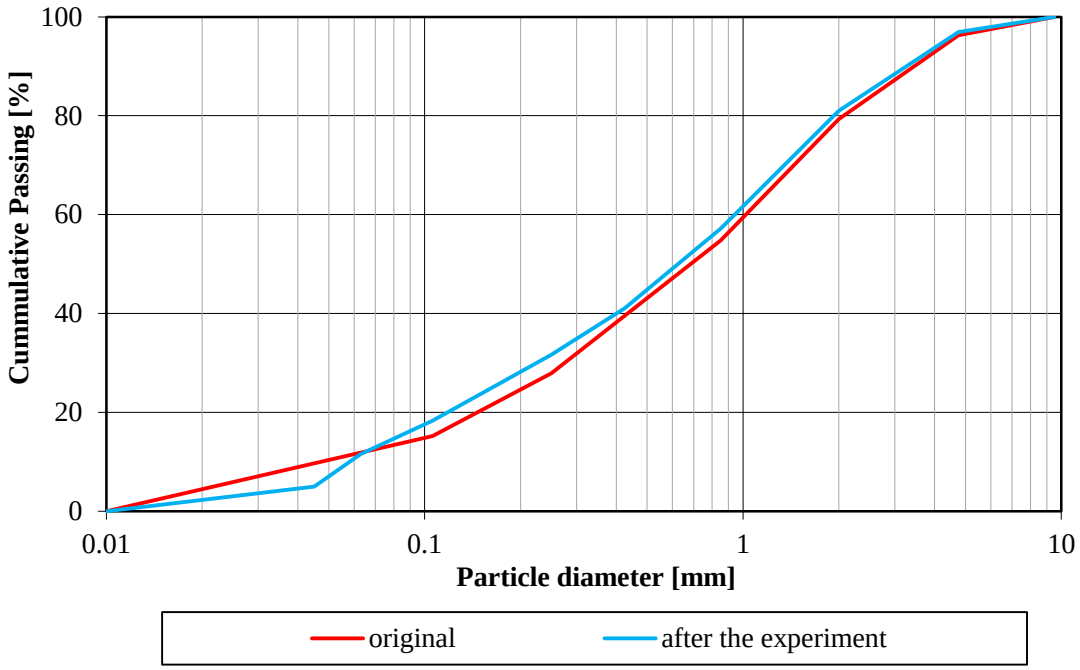

A 27—Comparison of soil distribution curves for test C with i=0.3 (60-70 cm).

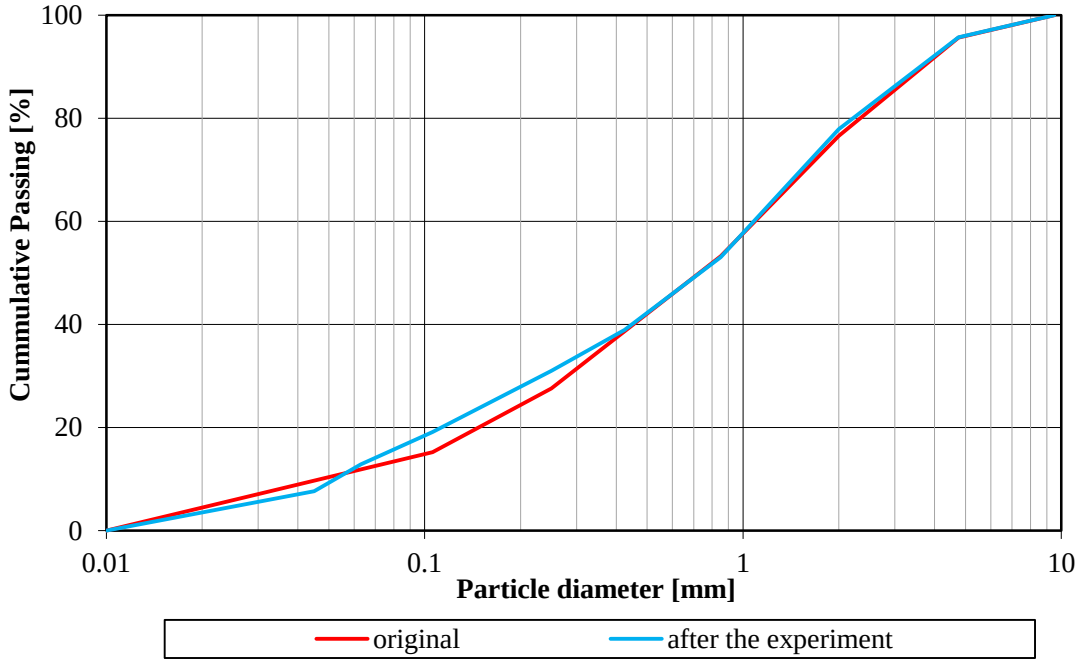

A 28—Comparison of soil distribution curves for test C with i=0.3 (70-80 cm).

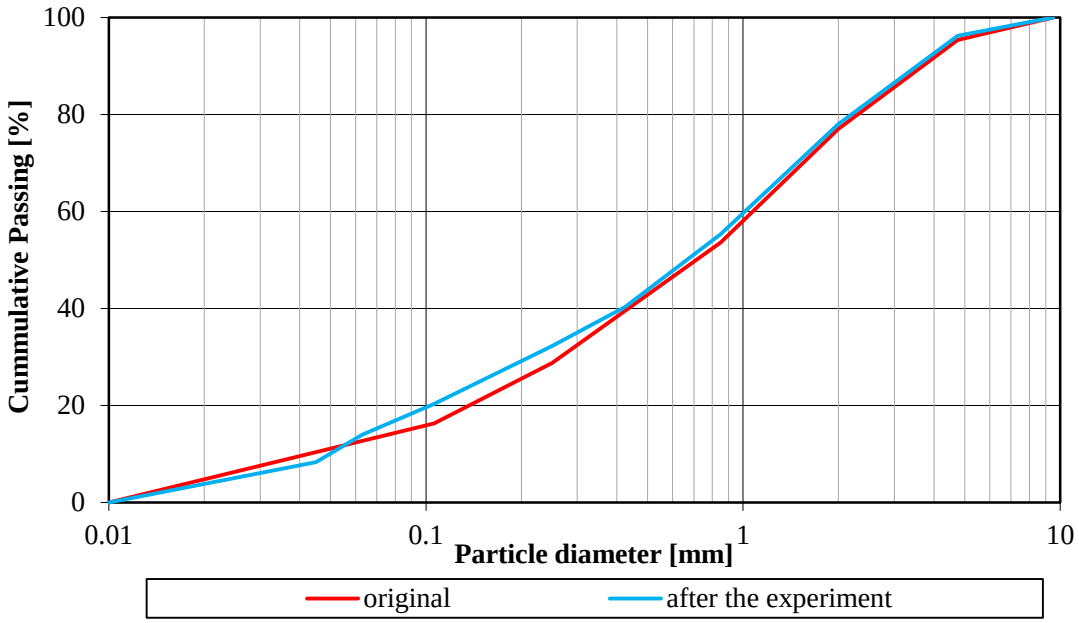

A 29－Comparison of soil distribution curves for test C with i=0.3 (80-90 cm).

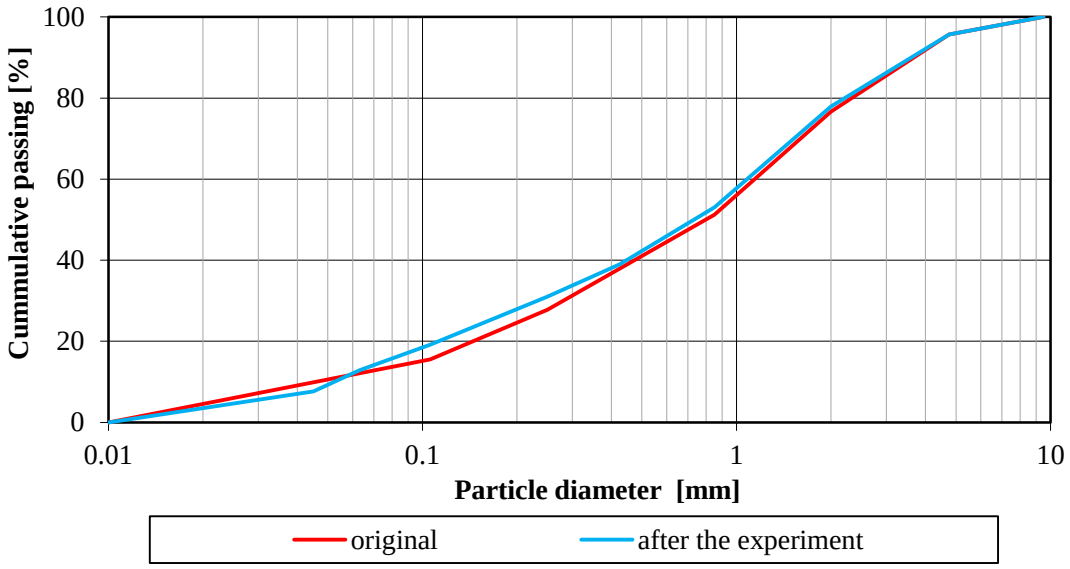

A 30－Comparison of soil distribution curves for test D with i=0.3 (90-100 cm). Almost no change in particle distribution was observed from 80 to 100 cm column length. The same results was obtained from test C with i=0.2.

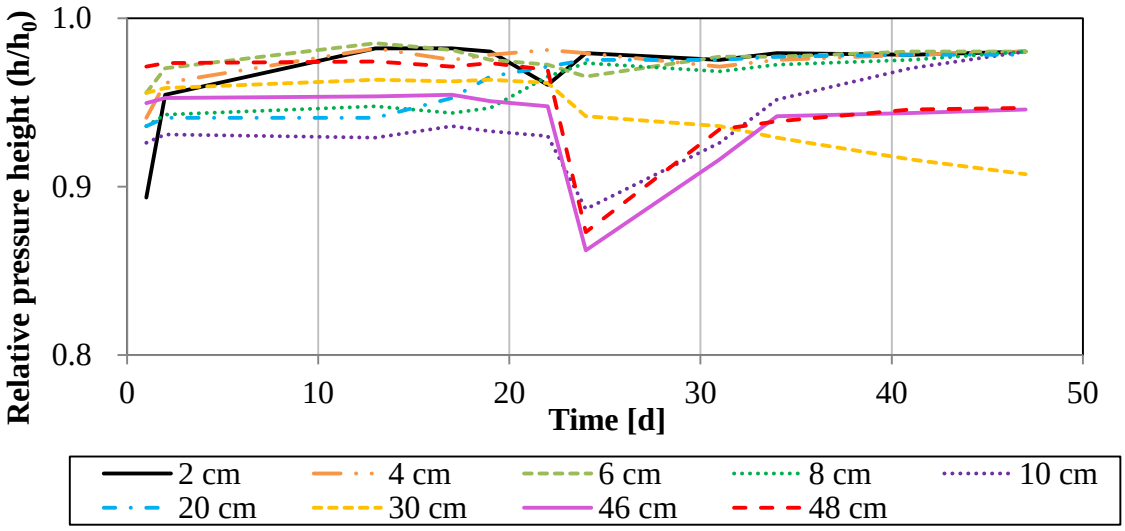

A 31—Change of the pressure heads over time at different points of the column length, measured by manometer for i=0.02 (test A).

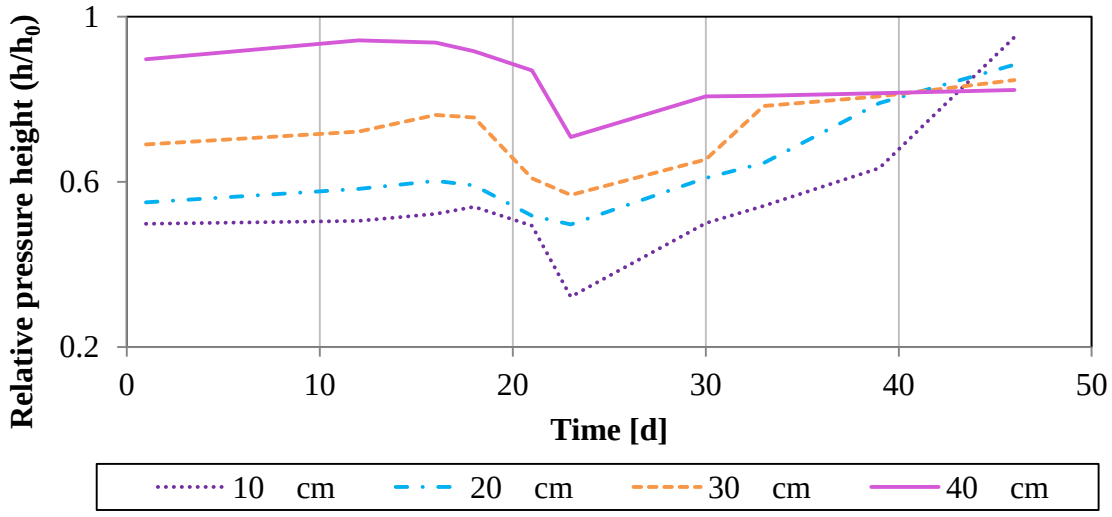

A 32—Change of the pressure heads over time at different points of the column length, measured by manometer for i=0.1 (test B).

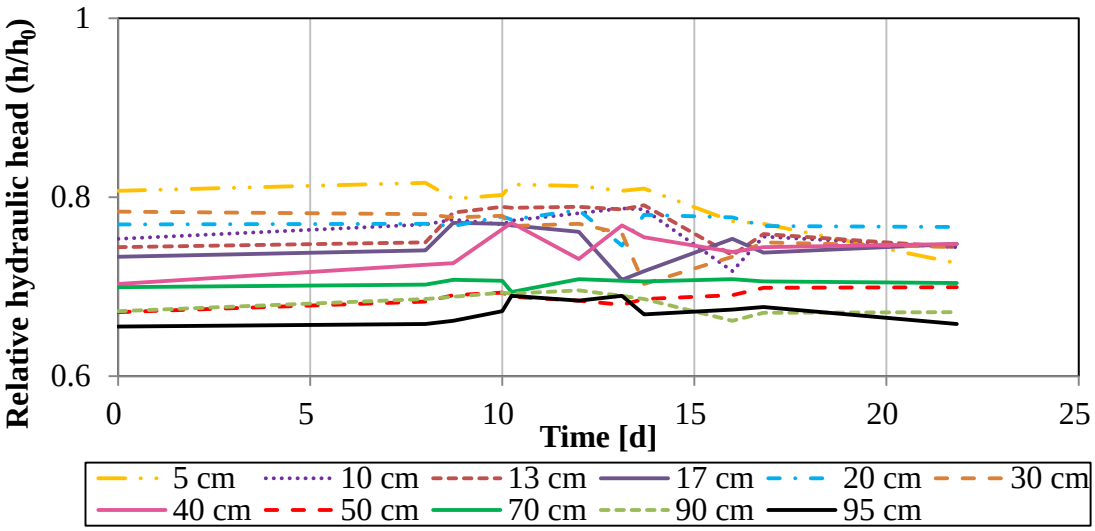

A 33－Change of the pressure heads over time at different points of the column length, measured by manometer for i=0.3 (test D).

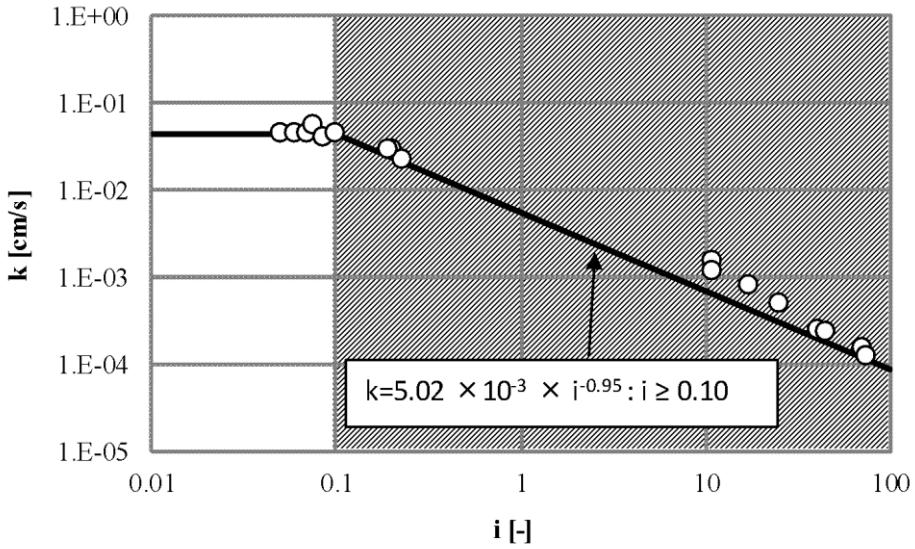

A 34－Relationship between permeability (k) and hydraulic gradient (i) for River sand No. 2. The shaded parts in the graphs indicate the above mentioned relations between hydraulic gradient and permeability in the areas of flow rate reduction. The non-shaded areas in the graphs represent the relations between hydraulic gradient and permeability outside the areas of permeability reduction at the termination of the experiment.

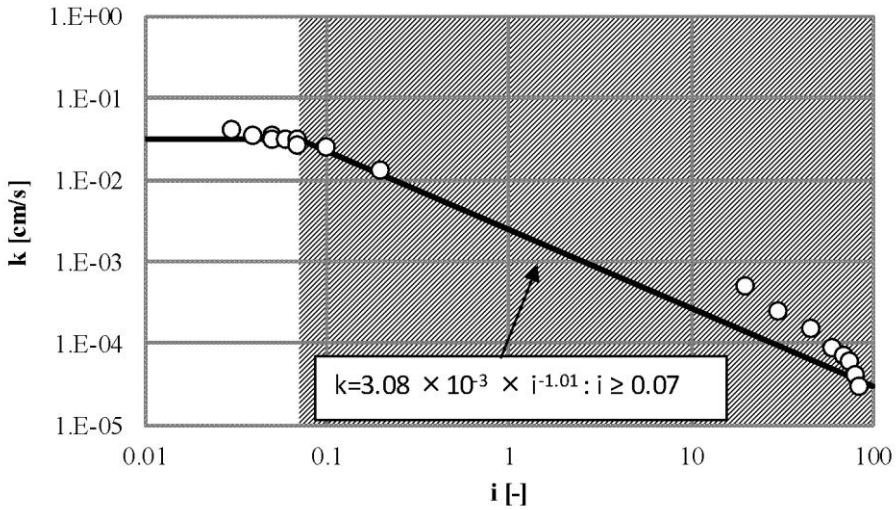

A 35—Relationship between permeability (k) and hydraulic gradient (i) for River sand No. 3. The shaded parts in the graphs indicate the above mentioned relations between hydraulic gradient and permeability in the areas of flow rate reduction. The non-shaded areas in the graphs represent the relations between hydraulic gradient and permeability outside the areas of permeability reduction at the termination of the experiment.

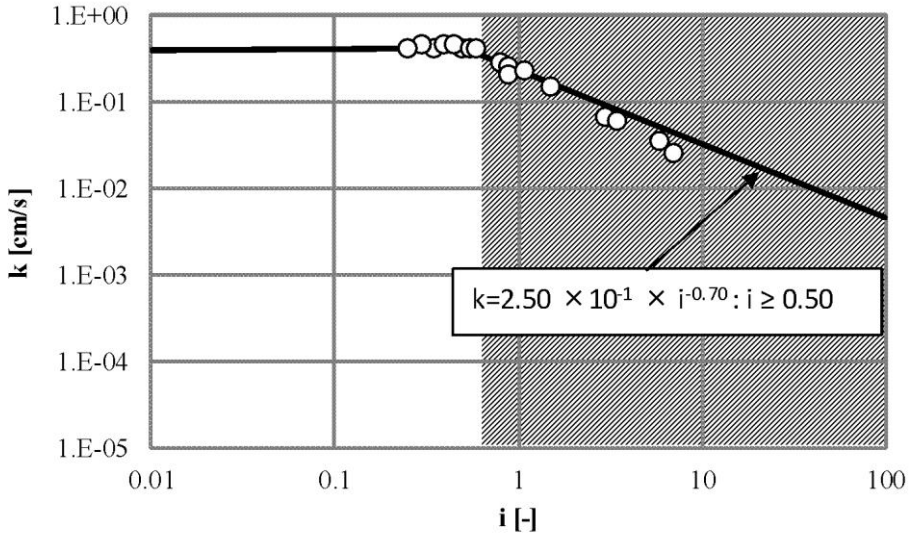

A 36—Relationship between permeability (k) and hydraulic gradient (i) for River sand No. 4. The shaded parts in the graphs indicate the above mentioned relations between hydraulic gradient and permeability in the areas of flow rate reduction. The non-shaded areas in the graphs represent the relations between hydraulic gradient and permeability outside the areas of permeability reduction at the termination of the experiment.

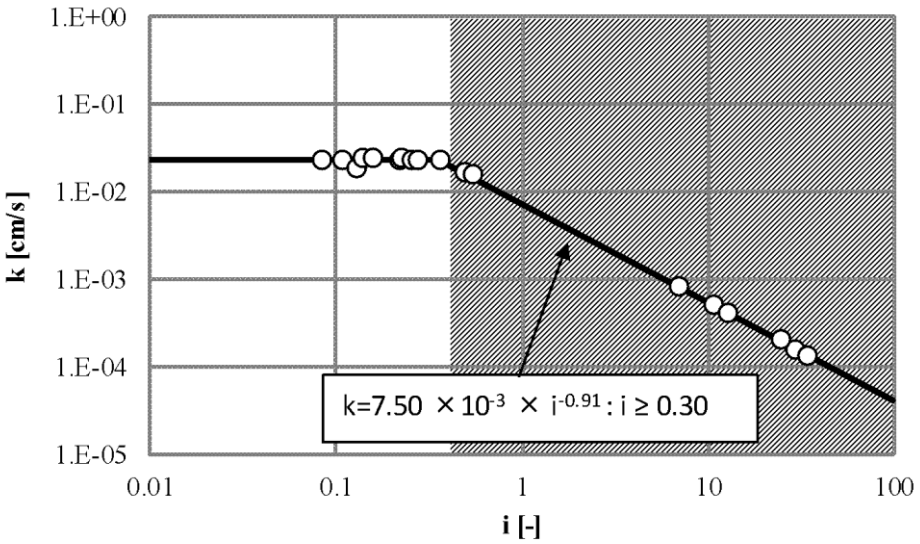

A 37－Relationship between permeability (k) and hydraulic gradient (i) for Narita sand No. 1. The shaded parts in the graphs indicate the above mentioned relations between hydraulic gradient and permeability in the areas of flow rate reduction. The non-shaded areas in the graphs represent the relations between hydraulic gradient and permeability outside the areas of permeability reduction at the termination of the experiment.

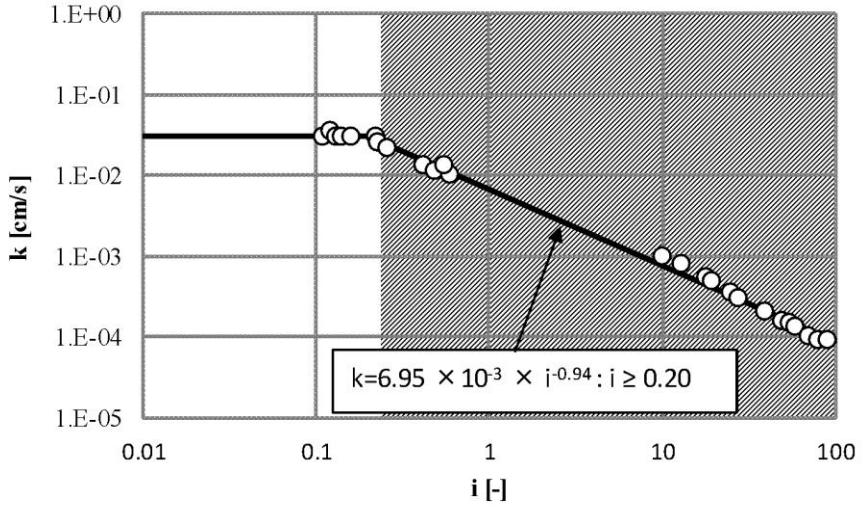

A 38－Relationship between permeability (k) and hydraulic gradient (i) for Narita sand No. 2. The shaded parts in the graphs indicate the above mentioned relations between hydraulic gradient and permeability in the areas of flow rate reduction. The non-shaded areas in the graphs represent the relations between hydraulic gradient and permeability outside the areas of permeability reduction at the termination of the experiment.

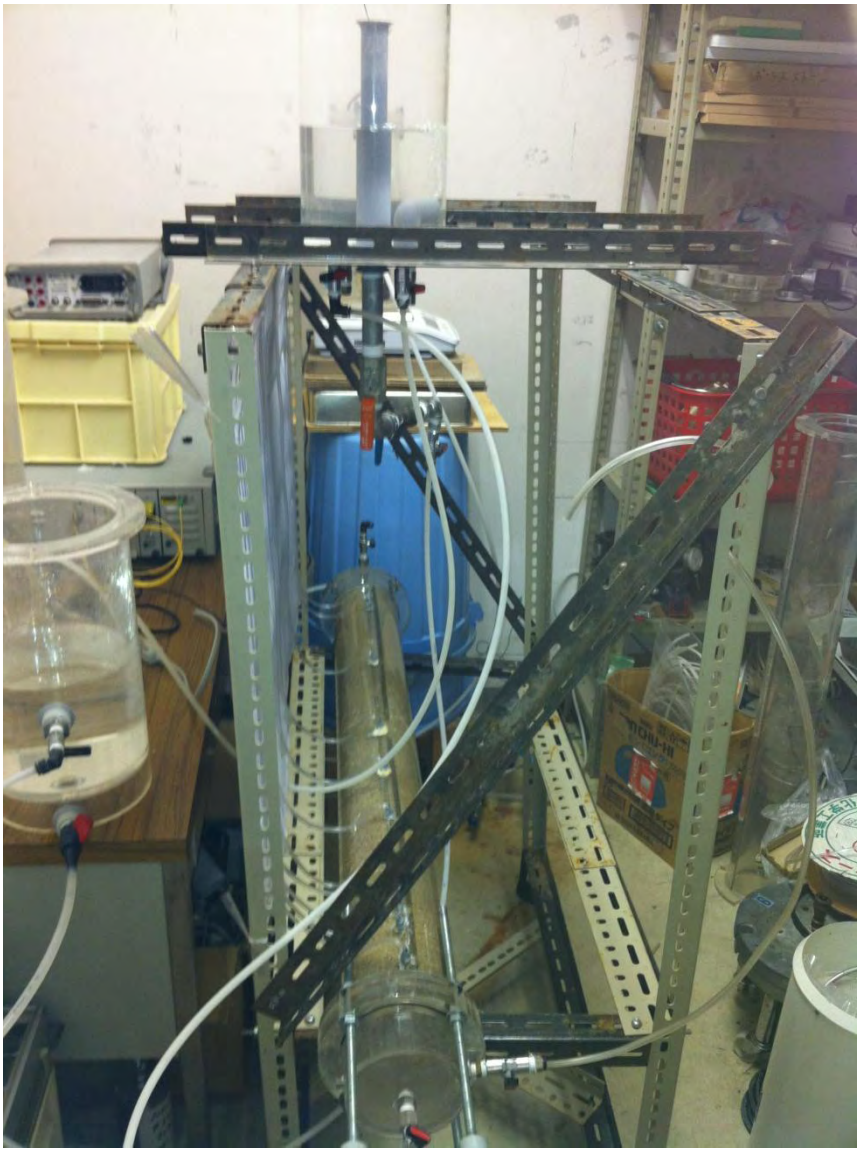

A 39－Experimental setup of the one-dimensional particle mobilization experiment regarding physical clogging in the laboratory.

A 40—Picture of the charcoal in the column after the experiment was stopped (1). The charcoal were taken out in 2-3 cm layers and the total iron content was measured.

A 41—Picture of the charcoal in the column after the experiment was stopped (2). The charcoal were taken out in 2-3 cm layers and the total iron content was measured.

A 42－Installation of observation well No. 3'.

A 43－Installation of injection well No.1.

A 44－Installation of pumping well No.2.

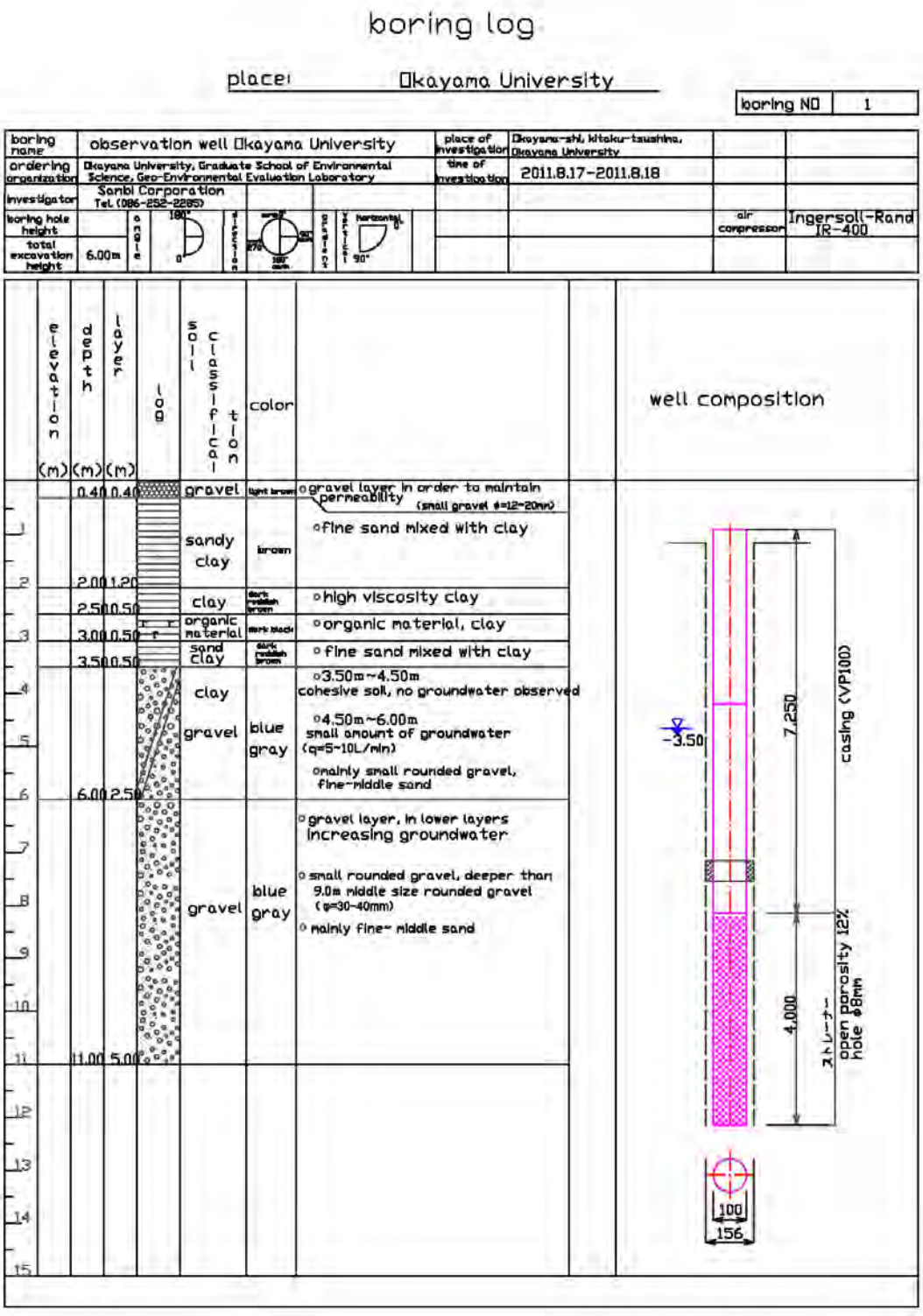

A 44－Boring log for observation well No.1'.

boring log

place: Okayama University

boring NO 2

boring name	observation well Okayama University	place of investigation	Okayama-shi, kitaku-tsushima, Okayama University		
ordering organization	Okayama University, Graduate School of Environmental Science, Geo-Environmental Evaluation Laboratory	time of investigation	2011.8.17-2011.8.18		
investigator	Sanbi Corporation Tel. (086-252-2285)				
boring hole height / total excavation height	6.00m			air compressor	Ingersoll-Rand IR-400

road (m)	elevation (m)	depth (m)	layer thickness (m)	log	soil classification	color	consistency / granularity	remarks
1								
2		2.00	2.00		sandy clay loam	brown		○fine sand, fine gravelly cohesive soil
3					clay	brown		○ loose clay ○ partially high viscosity
4		4.00	2.00					
5		5.00	1.00		clayey sand	brown		○loose clay, mainly fine sand ○ high moisture content, very loose
6		6.00	1.00		gravelly sand	brown		○ sand layer with high moisture content, very loose ○ mixed small gravel
7								○ rounded and sub-angular gravel mainly ϕ=10~20mm deeper than 8.0msmall amount of rounded gravel ϕ=40mm
8					pebbles	brown	granularity	○mainly fine sand, in deeper layers middle sand increases
9		9.00	3.00					
		9.50	0.50		gravelly sand	griseous		○rounded gravel, ϕ25~40mm, fine~middle sand
10		10.00	0.50		clay	griseous		○sedimented clay, gravel
11								
12								
13								
14								
15								

well composition

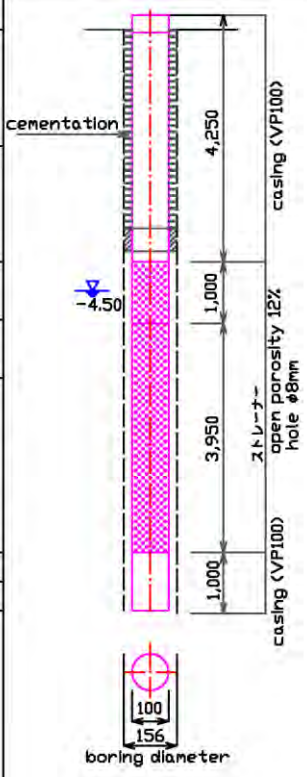

A 45－Boring log for observation well No.2'.

boring log

place: Okayama University

boring NO	3

boring name	observation well Okayama University	place of investigation	Okayama-shi, Kitaku-tsushima, Okayama University
ordering organization	Okayama University, Graduate School of Environmental Science, Geo-Environmental Evaluation Laboratory	time of investigation	2011.8.17-2011.8.18
investigator	Sanbi Corporation Tel. (086-252-2285)		
boring hole height / total excavation height	6.00m	air compressor	Ingersoll-Rand IR-400

road elevation (m)	depth (m)	layer (m)	log	soil classification	color	relative consistency		well composition
1	1.00	1.00		sandy clay	dark gray		○ fine sand, fine gravel	
2				clay	blue green gray		○ loose clay, high viscosity	
3	3.00	2.00						
4	4.00	1.00		clay	blue gray			
5				clayey pebble	blue gray		○ high content of rounded gravel ○ small amount of groundwater	
6	6.00	2.00						
7				pebble	dark blue grey		○ aquifer ○ mainly rounded small gravel, in lower layers more middle size gravel main grain size φ=15~20mm middle size gravel φ=30mm ○ mainly fine~middle sand	
8								
9	9.00	3.00						
10	9.80	0.80		clay pebbel	faint blue gray		○ high content of cohesive soil ○ rounded small~middle size gravel, ○ groundwater rarely seen	
	10.20	0.40		pebble clay	faint blue gray		○ cemented clay, rounded gravel gravel size φ=20~30mm	
11								
12								
13								
14								
15								

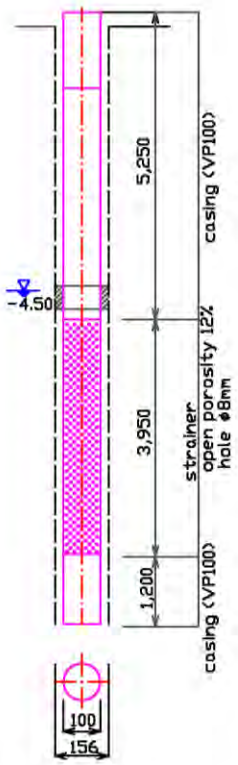

A 46－Boring log for observation well No.3'.

A 47－Charcoal filter column infront of the house at the study site on Tsushima campus, Okayama University.

A 48－Gravel layer at the bottom of the charcoal filter at the field site.

A 51－Picture of filling the charcoal into the filter column. It is also one sampling port shown, reaching to the middle of the column.

A 52－Picture of the charcoal filter at the field site showing the top with the fine gravel packed abouve the charcoal material, the lid and the connection for the pipe.

A 53－Small filter (100 mesh) installed HITACHI© (GF-25V) before the charcoal filter in order to avoid clogging through fine particle and also to keep already build up iron flakes out of the filter inlet.

A 54－Ferrolite MC3 filter setup.

A 55－Piping network of the room at the study site on Tsushima campus, Okayama University (1).

A 56－Piping network of the room at the study site on Tsushima campus, Okayama University (2).

A 57－Set up of Temperature and head sensores in Injection well No. 1 (infront) and observation well No. 1'.

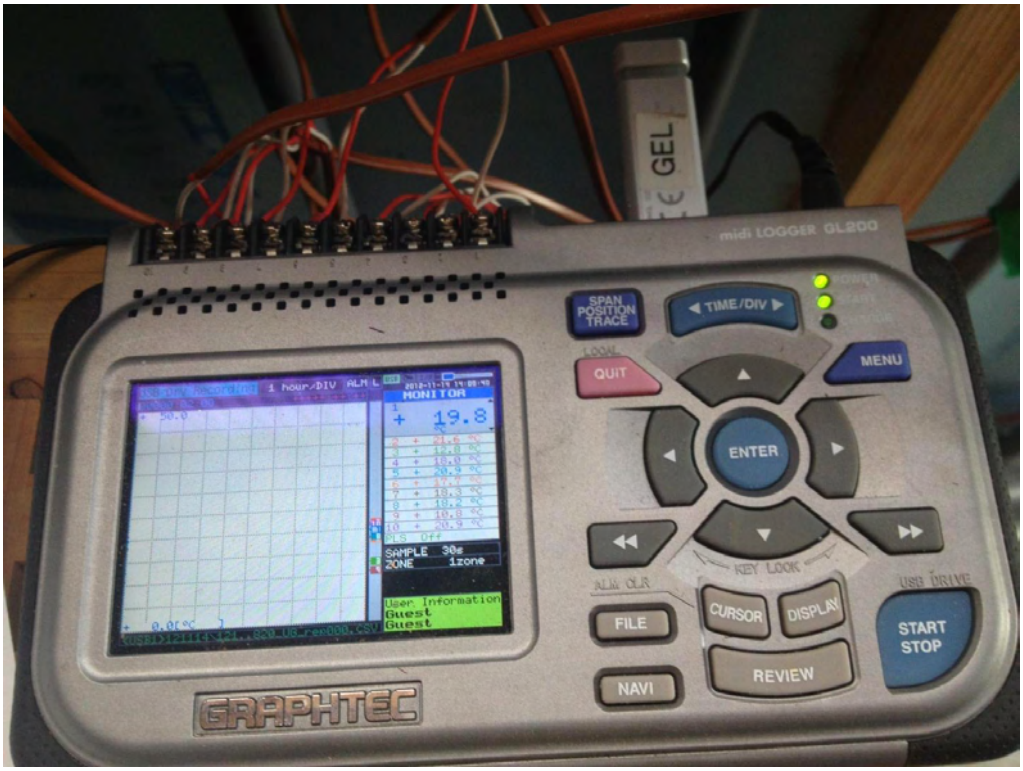

A 58－Live temperature measurement [interval 30s] with Data Logger Graphtec©.